Investigating the Pharmacology, Dimerisation and Receptor-Dependent Toxicology of Metabotropic Glutamate Receptor 5

Thesis Submitted for the Degree of Doctor of Philosophy at the University of Leicester

By Andrew Daniel Weaver

MRC Toxicology Unit

University of Leicester

March 2017

Investigating the Pharmacology, Dimerisation and Receptor-Dependent Toxicology of Metabotropic Glutamate Receptor 5

Andrew Weaver

ABSTRACT

G protein-coupled receptors represent the largest family of druggable targets in the human genome, with over half of drugs currently on the market acting at these receptors. Metabotropic glutamate receptor 5 is one such receptor, thought to be involved in several neurological diseases such as schizophrenia, anxiety, and depression as well as many neurodegenerative disorders. Allosteric modulators, ligands which act at a site topographically different from that of the endogenous ligand, have shown promise in overcoming many of the problems associated with previous drug development efforts targeting this receptor. Understanding the mechanistic action of these compounds is fundamental to driving further drug discovery, and as such the way in which compounds interact with metabotropic receptor 5 both *in vitro* and *ex vivo* is a key focus of this thesis.

In this thesis, previous studies of the allosteric mechanism of action of two allosteric modulators, CDPPB and ADX-47273, are extended to the human metabotropic glutamate receptor 5 using recombinant cell lines and show that the action of these compounds is preserved across species. Furthermore, the allosteric mode of action of LSN-2814617 and VU0430644 is demonstrated and shown to be efficacy driven at both the human and rat receptor homologues. The pharmacological consequences of heterodimerisation between group I metabotropic glutamate receptors is explored using mutant receptors which constitutively dimerise. Data herein demonstrates that metabotropic glutamate receptor 1 inhibits the action of compounds acting at metabotropic glutamate receptor 5 in a non-reciprocal manner. Finally, the receptor-dependent neurotoxicity of LSN-2814617 is demonstrated in *ex vivo* tissue samples with chronic, high-dose administration of LSN-2814617 inducing neuronal cell death in the anterior cortex of the rodent brain. Understanding the interactions between metabotropic glutamate receptor 5, compounds acting at this receptor, and other receptors will be key in the development of compounds for progression to the clinic.

Publications

Abstracts

Weaver A.D., Broad L.M., and Tobin A.B. Understanding the Mechanisms of Toxicology of a Positive Allosteric Modulator acting on Metabotropic Glutamate Receptor 5. *3rd Lilly Case Day 1st July 2013. Oral Communication.*

Weaver A.D. and Tobin A.B. Adapting an in vitro neuronal excitotoxicity model to elucidate the novel toxic mechanism of a positive allosteric modulator of the metabotropic glutamate receptor 5. *4th Focused Meeting Cell Signalling 28rd-29th April 2014. Poster Presentation.*

Weaver A.D., Broad L.M., and Tobin A.B. Delineation of the mechanism of allosteric action of three positive allosteric modulators with differential toxicological profiles acting at the metabotropic glutamate receptor subtype 5. *4th Lilly Case Day 4th October 2014. Poster Presentation.*

Weaver A.D., Broad L.M., and Tobin A.B. Understanding the mechanism of action of mGlu5 PAMs. *5th Lilly Case Day 21st October 2015. Oral Communication.*

Weaver A.D., Colvin E.M., Broad L.M. and Tobin A.B. Investigating pharmacological interactions between mGlu1 and mGlu5 using a constitutive heterodimer construct. *6th Focused Meeting Cell Signalling 18rd-19th April 2016. Poster Presentation.*

Acknowledgements

First and foremost I would like to thank my group leader Professor Andrew Tobin for countless hours of advice, debate, and guidance in pursuit of this thesis. Without your help this project would be a tenth of what it is today. Furthermore, I'd like to thank Dr. Lisa Broad of Eli Lilly for her support, guidance, critique, and infectious enthusiasm for the mGlu5 project at Lilly and presented herein. Your help has been critical for delivering this project and expanding its horizons beyond the initial scope. Special thanks to Dr. Sophie Bradley for insight, criticism, and morale-boosting talks over the last 4 years: You have a shining career ahead of you.

I'd also like to thank all of the Tobin group senior research staff, Dr. Adrian Butcher, Dr. Lev Solyakov, Dr. Mahmood Alam, Dr. Deborah Mitchesson, Dr. Ana Sanchez, and Dr. Catherine Moss for providing a great atmosphere conducive to collaboration, the pursuit of knowledge, and laughs along the way. Special thanks to my friend and colleague Dr. Rudi Prihandoko for many years of entertaining discussions and thoughtful debates regarding both pharmacology and fantasy football. I will miss you all. Thank you to my fellow PhD student, now Dr. Sajjad Riaz: You were a great influence on my PhD and I'm sure you will go on to achieve great things. Best of luck to Simon and Omar, my fellow PhD students whose company I have enjoyed greatly. Thanks also to Timothy Macedo-Hatch for his boundless wit and appreciation of wordplay which has provided much needed relief in times of hardship.

Thank you to Ellen, Helen, Adrian, Richard, Liz, and Amy at Lilly for your help and support during my brief internship with your company: I cannot express how much I appreciated all you have done to help me. Thanks to my mum for her tireless support and enthusiasm as she followed my career from nursery to academia. Thank you to my partner Amy Brooks for listening to me talk about science for 4 years and I promise I will not pursue any further university study. Finally, thanks to the BBSRC and Eli Lilly for funding my PhD studentship.

Table of Contents

Abbreviations

AC	Adenylyl cyclase
3D	Three dimensional
7TM	Seven Transmembrane
AKT	Protein kinase B
AMPA	α-amino-3-hydroxy-5-methyl-4-isoxazolepropionic acid
BHK	Baby hamster kidney
BSA	Bovine serum albumin
CA	*Cornus ammonis*
cAMP	Cyclic adenosine monophosphate
cDNA	Complimentary DNA
CNS	Central nervous system
CRD	Cystine-rich domain
CREB	cAMP response element-binding protein
DAG	Diacylglycerol
DAPI	4',6-diamidino-2-phenylindole
DIV	Days *in vitro*
DMEM	Dulbecco's modified eagle medium
DMSO	Dimethyl sulfoxide
EAAT1	Excitatory amino acid transporter 1
ECL	Extracellular loop
ELISA	Enzyme-linked immunosorbent assay
EPSC	Excitatory post-synaptic current

ERK	Extracellular signal-regulated kinase
FLIPR	Fluorescence imaging plater reader
FRET	Fluorescence resonance energy transfer
FZD	Frizzled receptor
GABA	γ-aminobutyric acid
GDP	Guanosine-diphosphate
GEF	Guanine-nucleotide-exchange factor
GEP	Guanine-nucleotide exchange protein
GIRK	G protein-gated inwardly rectifying potassium channels
GPCR	G protein-coupled receptor
GRK	G protein-coupled receptor kinase
GTP	Guanosine-triphosphate
GTPγS	Guanosine 5'-O-[gamma-thio]triphosphate
HBSS	Hanks balanced salt solution
HEK293	Human embryonic kidney cells
HEPES	4-(2-hydroxyethyl)-1-piperazineethanesulfonic acid
ICL	Intracellular loop
iGluR	Ionotropic glutamate receptor
IP_3	Inositol trisphosphate
IPSC	Inhibitory post-synaptic current
LBD	Ligand-binding domain
LDH	Lactate dehydrogenase
LTD	Long-term depression
LTP	Long-term potentiation

MAPK	Mitogen-activated protein kinase
mGluR/mGlu#	Metabotropic Glutamate Receptor (#)
mRNA	Messenger ribonucleic acid
NAM	Negative allosteric modulator
NMDA	N-methyl-D-aspartate
NSB	Non-specific binding
PAM	Positive allosteric modulator
PBS	Phosphate-buffered saline
PDE	Phospho-diesterase
PIP_2	Phosphatidylinositol 4,5-bisphosphate
PKA	Protein kinase A
PLC	Phospholipase C
PTX	Pertussis toxin
RGS	Regulators of G protein signalling
RIPA	Radioimmunoprecipitation assay buffer
SAM	Silent allosteric modulator
SMO	Smoothened receptor
TMD	Transmembrane domain
TRP	Transient receptor potential
VFD	Venus flytrap domain

CHAPTER 1. Introduction

1.1 The G protein-coupled receptor superfamily

The G protein-coupled receptor (GPCR) protein superfamily is large, diverse, and responsible for a large proportion of signal transduction across the cell membrane in eukaryotes (De Mendoza et al., 2014). These receptors respond to many different stimuli from photons, small organic molecules, amino acids, proteins and fatty acids to name but a few. Stimulation causes a change in conformation of the receptor from an inactive to an active state and results in a cascade of intracellular signalling, often mediated through heterotrimeric G proteins, which ultimately evokes a cellular response (Kobilka, 2007). The GPCRs have a common structure in a broad sense: they all contain an extracellular N-terminal tail, 7 transmembrane α-helical domains (TMDs) which are connected serially by intracellular loops (ICLs) and extracellular loops (ECLs), and an intracellular C-terminal tail (Rosenbaum et al., 2009). Despite this commonality there is a rich diversity of primary structure within the superfamily, with some members displaying next to no homology with any other members (Pin and Bockaert, 1999). In the human genome, GPCRs represent the largest group of transmembrane proteins with over 800 distinct GPCRs, and of these, 92 receptors have no known ligand (Davenport et al., 2013; Fredriksson et al., 2003). They are involved in the regulation of many physiological processes, such as blood pressure, neurotransmission, and metabolism (Pierce et al., 2002). It is perhaps unsurprising, given their widespread physiological relevance, that they are implicated in many diseases. Indeed, it is estimated that more than 50% of all prescribed drugs target GPCRs, though currently less than 20% of GPCRs have been exploited (Allen and Roth, 2011; Schöneberg et al., 2004). Given this, and the fact they are so diverse in structure, it is clear that further research into the molecular mechanisms of this important receptor type has the potential to lead to further therapeutic knowledge and invention.

1.2 The five GPCR families

The derivation of the primary sequences of the bovine rhodopsin and the human ß$_2$-adrenergic receptor, over 3 decades ago, gave credence to the idea that there were a large number of such 7TM receptors (Dixon et al., 1986; Nathans and Hogness, 1983). With the publication of the human genome (Lander et al., 2001; Venter et al., 2001), and the wealth of newly discovered GPCRs within, the receptors were grouped into five families based on residue conservation in primary sequence (a so-called 'fingerprint') and tertiary structure (Attwood and Findlay, 1994; Fredriksson et al., 2003). Commonly referred to as the GRAFS system, these five groups are: family A ('rhodopsin-like'), family B ('secretin-like'), family C ('metabotropic glutamate-like'), the Adhesion family, and the Frizzled family (see Figure 1.2.1).

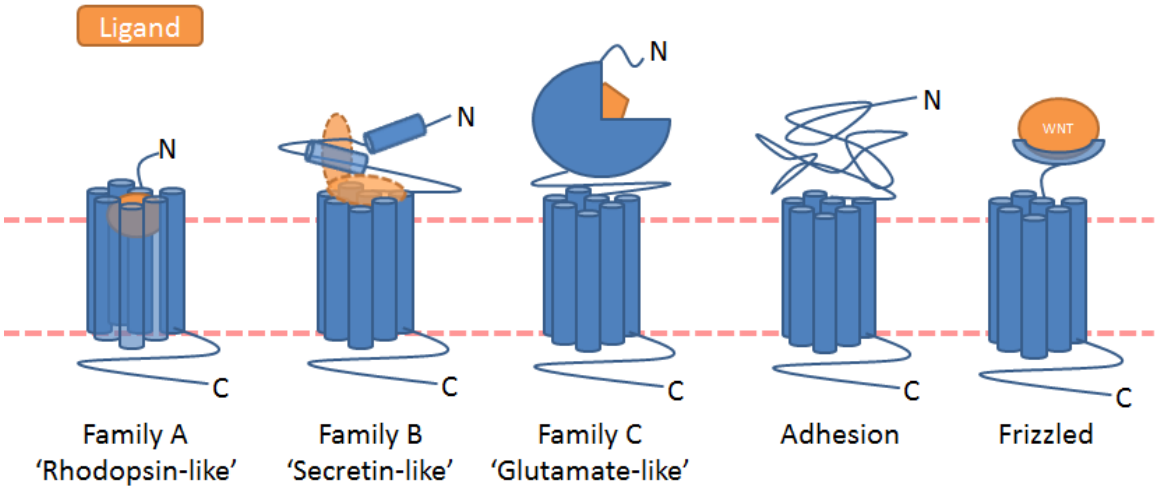

Figure 1.2.1 A diagram showing the tertiary structure of all five receptor families of the GPCR superfamily according to the GRAFS classification system. The receptor is shown in blue, the plasma membrane in red, and the position of ligand binding is denoted by an orange shape. Though all 5 families have a 7TM structure with an extracellular N-terminus and an intracellular C-terminus, the N-terminal domains are strikingly different in a tertiary sense.

1.2.1 Family A: Structure and activation

Family A, the rhodopsin-like receptors, is the largest family of GPCRs with 249 non-olfactory members and an estimated 460 olfactory receptors (Fredriksson et al., 2003; Lander et al., 2001; Takeda et al., 2002). These receptors typically have a short N-terminal domain with the ligand binding pocket located within the TMD. Despite this shared tertiary structure the primary sequence homology in this family is low, and though the binding site for the endogenous ligands is in a similar location with respect to the tertiary structure, there are large differences in the ligand binding domains on a molecular level.

In the case of rhodopsin, an 11-*cis*-retinal moiety is covalently bound within the transmembrane domains by linkage to a lysine sidechain on the 7th TMD. 11-*cis*-retinal is a chromophore which acts as an inverse agonist in the absence of light, holding the receptor in an inactive state (R). Absorption of light causes a photoisomerisation of the chromophore to an all-*trans*-retinylidene which ultimately pushes the receptor into an active state (R*) (Palczewski, 2006). Other family A receptors do not hold their ligand in the binding pocket in this way. For instance, the ß-adrenergic receptors exist in an equilibrium between the inactive and active states, with a certain proportion of the receptor pool being constitutively active (Engelhardt et al., 2001). The catecholamine agonists of this receptor bind transiently to the receptor, interacting with two serine residues in the 5th TMD, and an asparagine residue on the 3rd TMD. This transient interaction pushes the receptor equilibrium towards the active state and increases the signalling activity (Strader et al., 1989; Warne et al., 2011). Given the lack of primary sequence homology between the family A receptors, and the variety of ligands which interact with them, it may come as no surprise that the binding domains are highly varied. For example, the proteinase-activated receptors (PAR) contain a protease cleavage site in the N-terminus, which is cleaved to release a peptide ligand which interacts with the receptor through the 2nd ECL (Macfarlane et al., 2001). This heterogeneity is

undoubtedly key to the wide variety of roles these receptors play throughout the body.

Despite the differences throughout the rhodopsin-like family, primary sequence alignment showed several conserved residues across the family A receptors. There is a conserved disulphide bridge between cysteine residues on ECL1 and ECL2 which has homologues across all GPCR families and is thought to be important for the tertiary structure of the helical bundle of TMDs (Peeters et al., 2011; Wheatley et al., 2012). There is a highly conserved E/DRY motif close to the cytoplasmic end of the 3rd TMD within all family A receptors, though only the arginine residue therein was fully conserved (Oliveira et al., 1993; Probst et al., 1992). It is perhaps unsurprising that such a highly conserved sequence of amino acids proved to be important to the function of the receptor. This motif appears in the third intracellular loop of the majority of family A GPCRs, and mutational studies across several receptors within this family have shown that it plays an important role in receptor activation (Rovati et al., 2007). Mutation of these residues in the gonadotrophin-releasing hormone receptor hinted that the glutamatic/aspartic acid residue interacted with the fully conserved asparagine residue, and this interaction stabilises the receptor in the inactive state (Ballesteros et al., 1998). Further examples of this interaction were demonstrated across a number of family A receptors, and a charged residue on the 6th TMD was also implicated in this so-called 'ionic-lock' (Ballesteros et al., 2001; Greasley et al., 2002; Li et al., 2001; Shapiro et al., 2002).

Mutations at these residues had a variety of effects depending on the receptor. In some receptors, such as the β_2-adrenergic receptor, histamine H_2 receptor, and the vasopressin II receptor, mutations to the E/D residue resulted in an increase in constitutive activity displayed by these receptors (Alewijnse et al., 2000; Morin et al., 1998; Rasmussen et al., 1999). Interestingly, for other family A receptors, such as the muscarinic M_1 receptor and the cannabinoid 2 receptor, a mutation at this residue did not

lead to an increase in constitutive activity (Feng and Song, 2003; Lu et al., 1997). Similarly mutation of the fully conserved arginine residue leads to a variety of effects dependent on receptor; clearly the role of this moiety does not translate to all family A receptors (Rovati et al., 2007). The crystal structure of rhodopsin gave the first insight into the 3D arrangement of any GPCR (Palczewski et al., 2000). It confirmed beyond doubt the 7 transmembrane domain nature of these receptors, and showed the presence of a 'salt bridge' interaction between the glutamic acid and the arginine residues of the E/DRY motif on the 3rd TMD, corroborating the mutagenesis studies discussed previously. The crystal structure also showed evidence of interactions between the arginine of the E/DRY and a glutamate and threonine residue on the 6th TMD, which is key to the receptor ground state. Following advances in crystallographic methods, the crystal structures of the inactive adenosine$_{A2A}$ receptor, the β_1, and the β_2-adrenergic receptor were derived. Though the 'salt bridge' between the glutamate/aspartate and the arginine in the E/DRY motif was present in all four crystal structures, the ligand activated receptors did not appear to have the strong 'ionic lock' present between TM3 and TM6 in rhodopsin (Kobilka, 2007; Rosenbaum et al., 2009). In family A, there is also a highly conserved NPxxY motif on the 7th TMD, which may act as an 'activation switch' whereupon the binding of a ligand pushes the receptor into the R* state, and the asparagine residue of the NPxxY breaks its stabilising interactions with asparagine/threonine residues on the 6th TMD, and forms a new interaction with an asparagine residue on the 2nd TMD (Urizar et al., 2005). The proline in this motif is thought to induce an inwards kink at the intracellular end of the 7th TMD.

The crystal structure for opsin, the active state form of rhodopsin, gave great insight into the conformational changes the receptor undergoes as it transfers from the inactive to active state (Park et al., 2008). Upon the photoisomerisation of the 11-*cis*-retinal the 6th TMD tilts outwards, the 5th TMD shifts sideways, and the ionic lock between the 3rd and 6th TMDs is broken. These changes open up a pocket in the core of the receptor helix bundle, which allows the binding and activation of the G protein (Scheerer

et al., 2008). Crystal structures of active ligand-binding family A GPCRs, such as the agonist-bound $ß_2$-adrenergic receptor and the $adenosine_{A2A}$ receptor, revealed that these changes were perhaps common determinants of receptor activity in this family (Lebon et al., 2011; Rasmussen et al., 2011a; Xu et al., 2011). Since the year 2000, over 20 family A GPCR crystal structures have been published. Interestingly, it is now thought that there are approximately 24 important interactions within the TMDs of family A receptors, mediated by 36 amino acids which, although differing, play the same structural role in each (Venkatakrishnan et al., 2013).

1.2.2 Family B: Structure and comparison

Family B, the secretin-like receptors, are the second smallest family of GPCRs. Encoded by just 15 genes in the human, each receptor has a relatively long N-terminal tail of approximately 100-160 amino acids which, along with the extracellular portion of the TMDs, is thought to be involved in ligand binding in many of these receptors (Harmar, 2001). Endogenous ligands at this family tend to be peptides, for example secretin, glucagon-like peptide (GLP), and parathyroid hormone (PTH). The receptors of this family have 21-67% sequence homology with most of the variation occurring in the large N-terminus. Despite the high variation, there is a network of 3 disulphide bridges between highly conserved cysteine residues in the N-terminus across the family (Lagerstrom and Schioth, 2008). Crystal structures of the N-terminus of various family B receptors gave rise to a proposed model of ligand binding and receptor activation named the 'two-domain' model. In brief, the C-terminal of the large peptide ligand binds to the large N-terminus of the GPCR with high affinity, whilst the N-terminal domain of the ligand binds within the ECLs/TMDs of the receptor (Hoare, 2005). This was deftly demonstrated using a chimeric peptide ligand consisting of the N-terminal portion of calcitonin combined with the C-terminal portion of PTH activating a chimeric receptor with the N-terminal domain of the PTH1 receptor and the transmembrane portion of the calcitonin receptor (Bergwitz et al., 1996).

The crystal structure of the TMDs of the corticotrophin-releasing factor receptor subtype 1 (CRF_1R) gave insight into the similarities and differences that may exist between the family A and family B receptors (Hollenstein et al., 2013). The receptor has a crucible-like tertiary structure, with a wide aperture at the extra-cellular portion, perhaps allowing binding of the large peptide between the ECL regions, which narrows towards the cytoplasmic end. Interestingly, the shape of the cytoplasmic section of the receptor, specifically of the 3rd and 5th TMDs, overlay quite well with that of the family A dopamine receptor subtype 3 (D_3R). Given that these two GPCRs couple to the same effector G protein, a common structure at the cytoplasmic end is unsurprising, and may be important for the coupling of the G protein. Though the crystal structure revealed a lack of structural homologues present at family A receptors, a conserved GWGxP motif on the 4th TMD of family B receptors was shown to have several strong interactions linking the 4th TMD to the rest of the receptor, which may be important for the tertiary structure of these receptors.

The absence of an agonist bound family B receptor crystal structure makes understanding the conformational change from inactive to active states difficult to determine. Mutational studies have shown perhaps an interaction between a histidine residue on the 2nd TMD (His155) and a glutamate residue on the 3rd TMD (Glu209) are important for family B activation and this has been demonstrated on several receptors such as the GLP-1 receptor and calcitonin receptor (Heller et al., 1996; Vohra et al., 2013). Given that the family B receptors lack the E/DRY motif as well as the ionic lock which are common features of the members of family A, it is likely that, despite the intracellular portions of the TMDs overlaying well with family A, the activation of this family involves different molecular machinations.

1.2.3 Family C: Structure and comparison

Family C, the metabotropic glutamate receptor (mGluR)-like receptors, are the third largest family of GPCRs, with 22 distinct members (Bräuner-

Osborne et al., 2007). These receptors have a characteristically large N-terminal domain (known as the venus flytrap domain (VFD)) which is the binding site of this family's native ligands, which tend to be ions, amino acids, or sugar molecules. The metabotropic glutamate receptors were the first to be cloned, followed by the calcium-sensing receptors (CaRs), the $GABA_B$ receptors, and various others (Lagerstrom and Schioth, 2008; Masu et al., 1991). The LBD is a large, two-lobed structure stabilised by conserved cysteine residues which form disulphide bridges (Kunishima et al., 2000). This domain is highly conserved across the Family C receptors and, interestingly, it shares high homology with a bacterial periplasmic-binding protein LIVBP (O'Hara et al., 1993). The binding site within the LBD is also highly conserved, and studies show that it has comparable structure between the subfamilies (Brown et al., 1995; Kuang et al., 2003; Silve et al., 2005).

These receptors, with the exception of the $GABA_B$ receptors, also have a cysteine-rich domain (CRD) with 9 highly conserved cysteine residues, which is responsible for linking the LBD to the 7 TMDs and plays a critical role in transferring the conformational change of the LBD to the TMDs to alter the receptor confirmation and activate the receptors. For example, the lower lobe of the LBD of the mGlu2-receptor subtype was recently shown to form a disulphide bond with the CRD, and this interaction was crucial for receptor activation (Rondard et al., 2006). This interaction was also shown, via a crystal structure, to happen in the mGlu3-receptor subtype (Muto et al., 2007).

Recent crystal structures of the TMDs of mGlu1 and mGlu5 have revealed some commonality between family A, B, and C. The first 4 TMDs of mGlu1 overlaid well with those of family A and B, however, the 7^{th} TMD has a proline-induced kink which pushes the cytoplasmic end of this helix away from the helix bundle, whereas in the family A receptors have a proline-induced kink that pushes this helix towards the centre of the bundle (Wu et al., 2014). As a consequence, the extracellular end of the 7^{th} TMD is pushed

towards the centre of the helix bundle, which makes sense given that the endogenous ligands do not bind here in the family C receptors like they do in family A. Although the family C receptors lack the E/DRY motif common to the family A receptors, the mGlu1 crystal structure showed that an equivalent salt-bridge to the family A discussed previously exists between a lysine on the 3rd TMD and a glutamate residue on the 6th TMD. This bridge was also present in the mGlu5 crystal structure and is well conserved across family C (Doré et al., 2014). It likely plays a similar role to that of the highly conserved salt bridge in family A in stabilising the inactive conformation of these receptors, and the breakage of this bridge may be important in activation of the receptor allowing G protein access to the helical bundle.

An interesting feature of the family C receptors is that they exist as dimers, a phenomenon which has been demonstrated with the mGlu5 and the CaR (Bai et al., 1998; Romano et al., 1996b). These initial studies showed that the dimerisation was probably mediated primarily by the VFD, within 17 kDa from the N-terminus. Further study showed that these dimers were stabilised by both disulphide bridges between conserved cysteine residues as well as non-covalent bonds between the protomers (Romano et al., 2001). Perhaps the most striking dimerisation in family C is that the of the $GABA_B$ receptors. When the $GABA_{B1}$ monomer was first cloned it was noted that when expressed alone it had agonist affinity 3 orders of magnitude lower than the wild-type receptor. Not only that, its coupling to G proteins was relatively weak (Kaupmann et al., 1998). Studies revealed that when $GABA_{B1}$ was expressed as a monomer it did not traffic past the endoplasmic reticulum, and it was only when dimerised with the $GABA_{B2}$ subunit that it is successfully transported to the cell membrane (Marshall et al., 2016). It was subsequently shown that $GABA_{B1}$ was responsible for the binding of an agonist which caused a conformational change in both protomers, allowing $GABA_{B2}$ to activate the effector G protein (Bowery et al., 2002; White et al., 1998).

1.2.4 The Adhesion family

The adhesion receptors are the second largest GPCR family, with 33 members. They share primary sequence homology with the family B receptors (Stacey et al., 2016), though they are classified in their own family due to large differences in the N-terminal domain and the fact they bind extracellular matrix molecules rather than peptide hormones (Fredriksson et al., 2003; Lagerstrom and Schioth, 2008). The large N-terminus of all adhesion class receptors contains a GPCR proteolytic (GPS) domain which is a motif that causes the receptor to be cleaved in the golgi apparatus, allowing correct folding and trafficking to the cell membrane (Krasnoperov et al., 2002). The TMDs of these receptors contain structural cysteines in ECL1 and 2 which are highly conserved among all GPCRs and stabilise the helical bundle (Harmar, 2001). Three of these receptors have known ligands (Hamann et al., 1996; Liu et al., 1999; Stacey et al., 2016), and it has been demonstrated that members of this family can couple to the Gq/11 G protein (Little et al., 2004), however, little is known of the signalling pathways and pharmacological characteristics of these receptors.

1.2.5 The Frizzled family

The final family consists of 10 frizzled receptors (FZD1-10) and the smoothened receptor (SMO). The 10 frizzled receptors have a large N-terminal domain (200-320 amino acids) where there is a set of 9 conserved cysteines which form a binding pocket alongside residues of the ECLs for Wnt glycoproteins (Chen et al., 2004; Dann et al., 2001). Comparisons with other GPCR families showed that the FZDs have some similarity to other GPCR families: They possess the conserved structural cysteine-mediated disulphide bridge between ECL1 and ECL2 (Barnes et al., 2016). They also possess a tyrosine in the 7th TMD which may be analogous to the tyrosine residue in the highly conserved NPxxY motif found on family A GPCRs (Robitaille et al., 2002), and they may form homodimers mediated by a disulphide bridge much like the family C receptors (Carron et al., 2003). The SMO receptor is homologous to the Frizzled receptors, but interestingly it

appears to function in a ligand-independent fashion as part of a transcription factor complex (Murone et al., 1999).

1.3 Signal transduction in GPCRs

G protein-coupled receptors, as discussed in brief previously, have a remarkable range of ligands which initiate a conformational change and subsequent cellular response. Within this diverse array, there are sub-families which bind the same endogenous ligand. For example, the family A muscarinic acetylcholine receptors have 5 members which all bind acetylcholine, a neurotransmitter. Despite having the same ligand, these receptors influence a wide array of processes within the body, from heart rate and smooth muscle contraction to learning and memory (Felder, 1995). Obviously, the localisation of GPCRs is an important determinant in their action on a systemic level, but on a cellular level different GPCRs can have remarkably diverse effects too, and a range of cellular machinery is responsible. In a simplistic sense the pathways by which GPCRs affect cellular processes can be divided into two types: G protein dependent signalling, and G protein independent signalling (Marinissen and Gutkind, 2001).

1.3.1 G protein-dependent signalling

Guanine nucleotide-binding proteins, commonly referred to as G proteins, are responsible for linking the receptor to cellular effector proteins. They function as a heterotrimeric complex consisting of a combination of 3 subunits, an α subunit, a ß subunit, and a γ subunit, tethered to the cell membrane by a hydrophobic motif on the Gγ subunit. The shift of a receptor into the active R* state, particularly a tilting of the 6th TMD allows the binding of the G protein heterotrimer to residues on the 1st and 2nd ICLs. The GPCR then acts as a guanine-nucleotide-exchange factor (GEF) which causes a guanosine-diphosphate (GDP) molecule bound within the Gα subunit to be exchanged for guanosine-triphosphate (GTP) (Willars, 2006). The binding of GTP causes the dissociation of the G protein heterotrimer

into the Gα subunit with GTP bound, and a Gβγ dimer. These subunits go on to regulate/modulate effector mechanisms such as the cyclic adenosine monophosphate (cAMP) pathway, the inositol phosphate pathway, protein kinases or ion channels within the cell (Figure 1.3.1) (Simon et al., 1991).

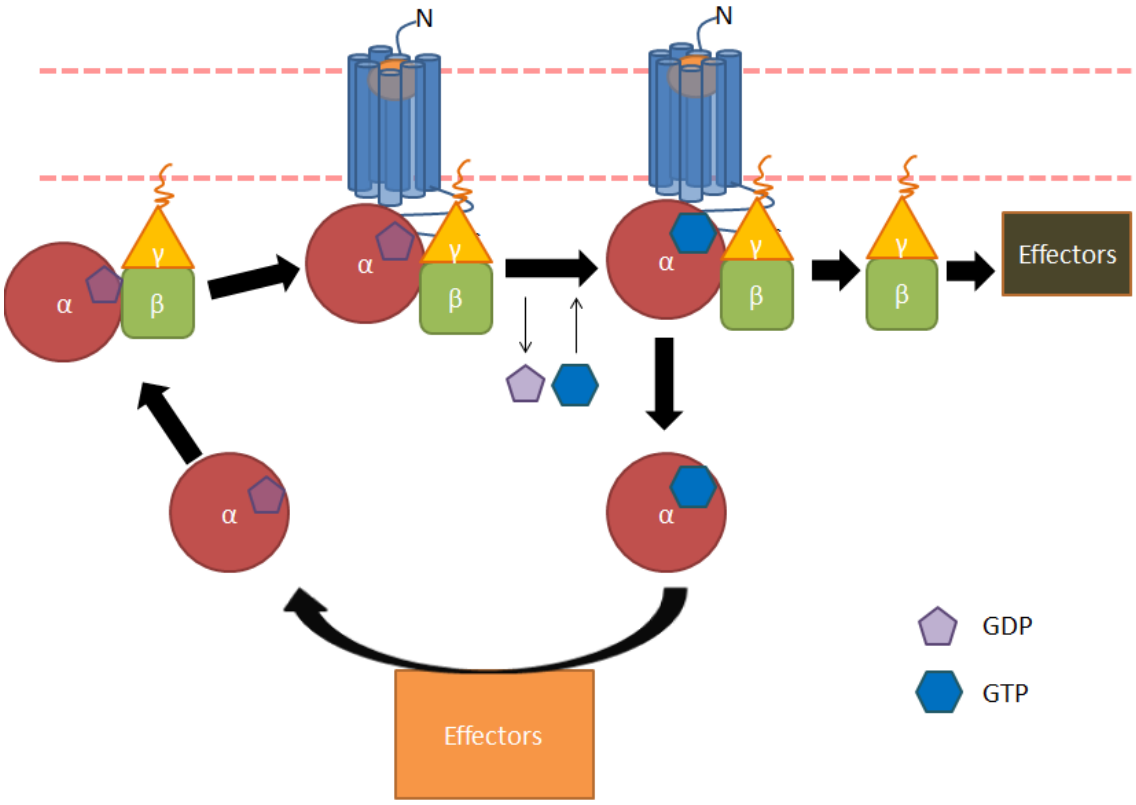

Figure 1.3.1 A diagram illustrating the association/dissociation of the heterotrimeric G protein complex with the active receptor. Several key features of the cycle are shown, with the exchange of GDP (purple pentagon) for GTP (blue hexagon) upon receptor binding, and the subsequent dissociation of the Gα subunit and the Gβγ complex.

The cDNA cloning showed that there are at least 41 G protein subunits in the human genome: 23 Gα subunits, 5 Gβ subunits, and 12 Gγ subunits (Clapham and Neer, 1997; Neves et al., 2002). All Gα subunits have some commonality in structure revealed by the publication of several crystal structures (Lambright et al., 1996; Sondek et al., 1996, 1994). The α subunit provides the residues responsible for GDP/GTP binding, as well as Gβγ, GPCR, and effector protein association sites (Oldham and Hamm, 2008). All α subunits contain a conserved GTPase domain linked with a protein fold to

a helical domain which is made up of 6 α-helical domains which cap the GTPase domain to hold the guanine nucleotides within. There are also 3 amino acid loops , known as switches I-III, which were shown to have different orientations in the active GTPγS-bound (a non-hydrolyzable nucleotide) when compared to the inactive GDP-bound state, suggesting an important role for these loops (Coleman et al., 1994; Noel et al., 1993). The GTPase activity of the α subunit can be modulated by other proteins, for example, a class of >37 proteins known as regulators of G protein signalling (RGS) proteins have been demonstrated in eukaryotes (Willars, 2006). The structure of these proteins is varied and as such they have a diverse range of actions on G proteins.

Though the α subunits have these common structural features, there are key differences and as such they are subdivided into 4 groups based on sequence similarity: $G\alpha_s$, $G\alpha_{i/o}$, $G\alpha_{q/11}$, and $G\alpha_{12}$. Historically, the $G\alpha_s$ signalling pathway was the first to be delineated in a study about so called 'liver phosphorylase' and was further understood in subsequent studies (Rall et al., 1956; Ross and Gilman, 1977; Sutherland and Wosilait, 1955). This group primarily acts by modulating adenylyl-cyclase (AC) which increases cAMP production which subsequently activates other cellular machinery such as protein kinase A (PKA), phospho-diesterase (PDE) and cAMP response element–binding protein (CREB). $G\alpha_{i/o}$ generally have an inhibitory effect on adenylyl-cyclase and as such is inhibitory on the cAMP pathways. $G\alpha_{q/11}$ proteins activate phospholipase C (PLC) which causes the conversion of phosphatidylinositol 4,5-bisphosphate (PIP_2) to inositol trisphosphate (IP_3) and diacylglycerol (DAG). IP_3 causes the release of calcium from cellular stores through the IP_3 receptors, and DAG activates the protein kinase C pathway and further downstream effectors (Neves et al., 2002). Perhaps the least studied G protein group is that of the $G\alpha_{12/13}$, and assays for the study of this family are a relatively recent development (Siehler, 2008). These G proteins interact mainly with Rho-GTPase nucleotide exchange factors (RhoGEFs) which modulate downstream signalling through RhoA and associated proteins (Siehler, 2009).

Subfamilies of GPCR can act on any number of these effectors, and as such the same ligand can have different cellular effects. For example the muscarinic M_1 acetylcholine receptor, found mainly in the brain, preferentially signals through the Gq/11 family proteins, whereas the M_2 receptor, found mainly in the heart, signals primarily through the Gi/o family proteins (Griffin et al., 2007; Ross and Berstein, 1993). Interestingly, it is increasingly apparent that GPCRs are promiscuous in terms of G protein signalling. To use a previous example, the M_2 receptor has also been shown to transduce signals through Gs and Gq/11 family G proteins, though perhaps less favourably than through Gi/o (Michal et al., 2007). Given that less than 30 Gα proteins associate with over 700 GPCRs it seems probable that there are common determinants of G protein coupling. Studies with rhodopsin have shown that there is an area with several hydrophobic residues which bind the C-terminal portion of a Gα protein (in this case transducin) and an 11 amino acid peptide corresponding to the C-terminal tail of this protein can compete with the full length protein binding to the receptor, implying a shared binding site (Hamm et al., 1988; Janz and Farrens, 2004). Similarly, modification of a cysteine residue on the C-terminus of $G\alpha_i$ by pertussis toxin (PTX) inhibited the activation of this Gα subunit by the receptor (West et al., 1985).

Perhaps the most detailed view of G protein coupling came from the crystal structure of the β_2-adrenergic receptor in complex with $G\alpha_s$ for which Brian Kobilka shared the Nobel prize for chemistry in 2012 (Rasmussen et al., 2011b). It showed several important interactions between the 2nd ICL and the 5th and 6th TMDs of the receptor with several residues across the $G\alpha_s$ structure. They also noted that the C-terminus of $G\alpha_s$ shares 5 conserved residues with $G\alpha_i$, and that the coupling of certain Gα subunits must be conferred by more subtle secondary and tertiary characteristics. Despite this, one important interaction for all $G\alpha_s$-coupled receptors has been postulated to form between a highly conserved phenylalanine residue (position 149) present on the 2nd ICL and a hydrophobic pocket in $G\alpha_s$. Perhaps the publication of the crystal structure of another Gα subtype in

complex with its receptor will shed some light on the structural determinants of G protein specificity.

The Gß subunit is always associated with a Gγ subunit, except under denaturing conditions (Clapham and Neer, 1997). The Gß subunit has two distinct structural domains: an α-helical sequence of 20 amino acids towards the N-terminus, and a propeller like repeated structure of amino acids known as a WD repeat due to 7 tryptophan-aspartate repeats. These structural elements were confirmed with the publication of crystal structures of the G protein heterotrimer (Lambright et al., 1996; Wall et al., 1995). The α-helical domain forms a coiled-coil interaction with the N-terminus of the Gγ protein, and further interactions between the rest of the Gγ protein and domains 5, 6, and 7, which perhaps explains why the dimer interface is so strong. The γ subunits contain a so-called 'CAAX-box' at the C-terminus which is a putative site of lipid modification which is key for anchoring the Gßγ complex to the cell membrane, as shown in mutagenesis studies (Simonds et al., 1991). Though there are approximately 72 combinations of ßγ subunits, not all of these are found to form. For example, $G\gamma_1$ will associate with $G\beta_2$, but $G\gamma_2$ will not (Yan et al., 1996). This specificity is thought to be mediated by 5 important residues in the middle of the γ subunit, and the 5th WD repeat/N-terminus of the ß subunit (Lee et al., 1995; Meister et al., 1995).

It was initially assumed that the role of the Gßγ complex was simply to bind to inactivated GDP-Gα subunits and promote reinsertion into the membrane until further activation for GPCRs (Clapham and Neer, 1997). This assumption was challenged when the Gßγ complex was shown to directly affect potassium channels in the heart (Logothetis et al., 1987). Several more interactions like these were observed, such as the weaver potassium channel in the brain, and as such the subunits that make up these ion channels are known as G protein-gated inwardly rectifying potassium (GIRK) channels (Luscher et al., 2010; Navarro et al., 1996). We now know that Gßγ complexes can influence several effectors such as voltage-gated

calcium channels, phospholipase A and C isoforms, and adenylyl-cyclase to name a few (Herlitze et al., 1996; Jelsema and Axelrod, 1987; Park et al., 1993; Tang and Gilman, 1991).

1.3.2 Receptor desensitisation and G protein-independent signalling

Further signalling acuity is gained through two methods of receptor desensitisation, heterologous or homologous desensitisation, which allow further spatio-temporal control of GPCR signalling. Heterologous desensitisation describes when the activation of a receptor leads to the inhibition of another which has not necessarily been activated itself (Hosey, 1999). Increased secondary messenger activity (e.g. cAMP, DAG, or Ca^{2+}) leads to the phosphorylation of receptors by kinases from the activated pathway, such as PKA or PKC, which inhibits the association of the G protein heterotrimer to the receptor and prevents further signalling (Pierce et al., 2002). Interestingly, not all GPCRs share this ability, for example, the activation of M_3 muscarinic receptors can cause the desensitisation of bradykinin B_2 receptors, but the reverse does not occur, at least *in vitro*. Furthermore, the desensitisation of B_2 receptors by M_3 receptors in this study does not appear to be phosphorylation dependent either (Willars et al., 1999).

Homologous desensitisation involves two steps in which, firstly, the agonist-bound receptor is phosphorylated by a G protein-coupled receptor kinase (GRK) and, secondly, a large arrestin-type protein binds to the intracellular face of the receptor, preventing G protein accession (Lefkowitz, 1998). The desensitising action of GRKs was first shown with rhodopsin, and subsequently with the β_2-adrenergic receptor. The subsequent members of this family were discovered by cDNA cloning due to their homology with GRK1 and GRK2. The GRK protein family, which has 7 members, phosphorylate serine/threonine residues on the 3rd ICL and C-terminus of active-state GPCRs (Pitcher et al., 1998) . The phosphorylation increases the likelihood of the binding of arrestin type proteins, and it has been demonstrated that arrestin binds an order of magnitude better compared to

the agonist occupied receptor alone (Gurevich et al., 1995; Lohse et al., 1992).

The arrestins are a family of at least 4 proteins, though only ß-arrestin 1 and 2 are known to be expressed outside of the retina (Smith and Rajagopal, 2016). Initially, the only known function of the ß-arrestins was as mediators of GPCR desensitisation. As mentioned previously they sterically inhibit the binding of G proteins to the GPCR thus inhibiting continued signal transduction through these receptors (Ferguson et al., 1996). Secondly they act as adapters, facilitating the trafficking of GPCRs from the cell membrane into clathrin-coated pits from where the receptors are either recycled to the membrane, or degraded (Kang et al., 2013; Laporte et al., 1999). It is now increasingly apparent that ß-arrestins play a larger role than simply shutting-down GPCR signalling. The emerging role of ß-arrestins as signal mediators was shown *in vitro* where ß-arrestin appeared to co-localise with Src kinases after stimulation of the $ß_2$-adrenergic receptor (Luttrell et al., 1999a). Mutation of ß-arrestin such that it no longer binds to the receptor or Src appeared inhibitory to ERK signalling after stimulation of the $ß_2$-adrenoceptor (Miller et al., 2000), therefore it seems likely the ß-arrestin is acting as a signalling scaffold linking the active receptor to Src kinase and ERK, a mitogen-activated protein kinase (MAPK) pathway. This ground-breaking finding showed that GPCR signalling is multifaceted, with the G protein-coupled transduction being relatively transient (<1h), and the ß-arrestin signalling events lasting longer (Ahn et al., 2004; Gesty-Palmer et al., 2006). Though the ERK pathway is perhaps the best studied with respect to ß-arrestin signalling, it has been shown to activate other MAPKs, such as JNK3 and p38, as well as other families of kinases such as AKT (protein kinase B) and RhoA (DeWire et al., 2007). Since the discovery that ß-arrestins can act as signal mediators several other G protein-independent signalling pathways have been postulated, such as the PDZ, SH2 and SH3 pathways, though these are not as thoroughly characterised (Marinissen and Gutkind, 2001).

1.4 The metabotropic glutamate receptors

The amino acid glutamate plays the largest role as an excitatory neurotransmitter in the mammalian central nervous system (CNS). Receptors that respond to glutamate are found ubiquitously within the CNS, and they exert their effect, broadly speaking, through two types of receptor: The ionotropic receptors, which are ligand gated ion channels (LGICs); or the metabotropic receptors, which are ligand activated GPCRs (Meldrum, 2000). In brief, the ionotropic glutamate receptors are divided into three groups named after their preferential synthetic ligands: the N-methyl-D-aspartate (NMDA) receptors, the α-amino-3-hydroxy-5-methyl-4-isoxazolepropionic acid (AMPA) receptors, and the kainate receptors. These receptors are comprised of 4 or more subunits in complex and the composition of each oligomer dictates many aspects of their function (reviewed in detail in Traynelis et al. 2010). In general terms, the binding of glutamate opens the ion channel to allow cations (mainly Na^+ and Ca^{2+}) into the cytosol, causing depolarisation and the initiation of an action potential in the neuron. These receptors are responsible for the fast excitatory transmission in the glutamatergic system. The metabotropic glutamate receptors, as previously discussed, are prototypical family C GPCRs which activate a variety of signalling cascades upon ligand binding, and mediate slower responses in the glutamatergic system, as well as regulating other pathways within this system. It is these receptors which are the focus of this thesis.

The metabotropic glutamate receptors were first discovered when it was shown that glutamate was coupled to the formation of inositol phosphates via a mechanism that was unrelated to the ionotropic glutamate receptors (Sladeczek et al., 1985; Sugiyama et al., 1987). This discovery lead to the identification by two independent groups of the first metabotropic glutamate receptor, metabotropic glutamate receptor 1 (mGlu1, splice variant a) (Houamed et al., 1991; Masu et al., 1991). Pharmacological investigations following this discovery hinted at the possibility of the existence of several

subtypes, and cDNA analysis revealed 7 further members of the metabotropic glutamate receptor family, labelled mGlu1-8 (Schoepp et al. 1990; reviewed in Conn & Pin 1997).

1.4.1 Structure of the metabotropic glutamate receptors in detail

The delineation of the primary sequence of mGlu1a showed a GPCR unlike any other known at the time (Figure 1.4.1.1). The mGlu1a receptor is 1199 amino acids in length which is far larger than the family A GPCRs. The large N-terminal domain of approximately 590, which was to become characteristic of the family C GPCRs, bore resemblance to bacterial periplasmic binding proteins, such as LIVBP. At the very N-terminal end of the LBD, there is a sequence of approximately 20 amino acids with a hydrophobic profile which may serve as a signalling peptide (Abe et al., 1992). By comparing the structures of the mGluRs with LIVBP a glutamate binding site was proposed. This binding site involved two residues (Ser165 and Thr188) on the lower of the two lobes of the LBD, as the binding of glutamate was markedly reduced when these were mutated to alanine residues (O'Hara et al., 1993). These two lobes are connected by three short amino acid loops which create a 'Venus fly-trap' hinged structure (Jingami et al., 2003). Analysis of several crystal structures of the ligand binding domains of various mGluRs lead to several revelations about glutamate binding in the LBD. Firstly, glutamate binds in a cleft formed by the lower and upper lobes of the LBD, there are several residues which form the binding pocket for glutamate (Acher and Bertrand, 2005). Seven polar residues are conserved across all mGluRs and they serve as principal interacting motifs for glutamate binding, alongside a Tyrosine residue (74) which forms a significant hydrogen bond with glutamate (Kunishima et al., 2000). Where glutamate and other agonists cause a closing of the cleft which leads to receptor activation, antagonists prevent activation by holding the cleft open (Muto et al., 2007; Tsuchiya et al., 2002). The binding of an agonist induces a closing of the hinge between the two LBD lobes of approximately 31° (Jingami et al., 2003). Indeed, mutations which stabilise

the open state of the LBD can switch antagonists to agonists in $mGlu_8$, showing the importance of these LBD conformations (Bessis et al., 2002). The crystal structure of the mGlu1 LBD showed that this portion of the receptor homodimerises via a disulphide bridge in which Cys140 was thought to be critical for increasing the number of mGluR homodimers at the cell surface (Jingami et al., 2003; Ray and Hauschild, 2000). Mutation of this residue to an alanine did not disrupt the dimerisation of the LBD and so the dimeric interaction is perhaps more complex than first assumed (Tsuji et al., 2000). The dimer interface is proposed to form between the N-terminal side lobe of the LBD where two α-helices from each protomer form an area of hydrophobicity (Jingami et al., 2003). Given that this area is well conserved across the mGluR family it is likely a dimeric interface for other subtypes these receptors. It has been proposed that dimerisation of the LBDs has profound implications for the activation of the receptor (Niswender and Conn, 2010). For instance, a homodimer formed of a wild-type mGlu1 receptor and an mutant mGlu1 was not activated by glutamate, showing that both LBDs need to be occupied in order to transduce a signal (Kammermeier and Yun, 2005). In contrast, a lone molecule of glutamate was able to activate mGlu5 homodimers, though ligand binding at both produced a more robust response (Kniazeff et al., 2004).

The LBD is connected to the TMDs by the cysteine-rich domain (CRD), and is thought to be responsible for transducing the conformational change of the LBD from open to closed into a conformational change in the TMDs from inactive to active (Niswender and Conn, 2010). Within this region there are 9 cysteine residues which are highly conserved in the family C receptors, and are thought to be critical for signal transduction from the LBD to the TMD in this family (Hu et al., 2000). Studies have shown that a cysteine in the lower lobe of the LBD (Cys234 in $mGlu_2$) cross-links with cysteine in the CRD (Cys518 in $mGlu_2$), and that this interaction is critical for receptor activation (Rondard et al., 2006). The exact role of the other conserved cysteines remains to be delineated, though it is likely that they are responsible for structural arrangement of the protein in a tertiary sense.

Indeed, mutation of the 9 conserved family C residues in the calcium-sensing receptor resulted in a loss of expression at the cell surface (Fan et al., 1998). It is possible, due to incorrect protein folding, that the receptor is retained and degraded in the endoplasmic reticulum and this is likely to happen across family C GPCRs mutated in such a way.

For a long time a crystal structure of a family C GPCR remained elusive. Many comparisons have been made with family A crystal structures, though the sequence homology between family C and either family A or B receptors is only 10-15% (Hermans and Challiss, 2001). Several key motifs present in the family A receptors are indeed missing in the mGluR family. For instance, the mGluR family lacks the E/DRY motif important for receptor activation in family A receptors (Conn and Pin, 1997). Truncated forms of mGlu5 which do not possess the LBD or the CRD can be activated by allosteric modulators which do not activate the full length receptor (Goudet et al., 2004). This implies that perhaps the N-terminal domain in its unbound, open state holds the TMDs in an inactive conformation and the binding of glutamate allows the movement of the TMDs in such a way to activate the receptor, suggesting that the LBD is contributing to stabilising the inactive conformation of the receptor.

With the advancement of protein-crystallographic techniques crystal structures of the TMDs (581-860) of mGlu1, shortly followed by mGlu5 (569-836), were published (Doré et al., 2014; Wu et al., 2014). The structure of the mGlu1 structure provided valuable insight into the potential role of the TMDs in the dimerisation typical of these receptors. There is a hydrophobic dimer interface that forms between the 1st TMD helix of each protomer. Additionally, 6 cholesterol molecules packed between the 1st and 2nd TMD of each protomer were robustly observed and these may be involved in mediating the dimerisation of the TMDs. This hydrophobic, cholesterol rich region was not noted in the published mGlu5 TMD structure. The disulphide bond between ECL2 and the extracellular side of the 3rd TMD,

which is highly conserved across all GPCR families, was present in mGlu1 between Cys657 and Cys746, and mGlu5, between Cys644 and Cys733.

The 'ionic lock' E/DRY motif present in family A, which stabilises the inactive conformation of the TMDs, is absent in both the mGlu1 and mGlu5 structures. Instead in mGlu1 there is a similar salt bridge formed between Lys678 on the intracellular portion of the 3rd TMD and Glu783 on the 6th TMD, and Lys665 and Glu770 in mGlu5. As mGlu5 can be activated by transmembrane binding ligands when the LBD is removed (Goudet et al., 2004), it appears that stabilisation and activation of family C GPCRs occur via a similar mechanism to that of family A. The highly conserved NPxxY motif from family A, which undergoes large changes during activation, is absent in the mGlu1 and mGlu5 structure. The crystal structure of the mGlu1 and mGlu5 TMDs showed that Pro833 (mGlu1) and Pro 820 (mGlu5) are in a similar position on the 7th TMD to the NPxxY proline in family A receptors but it is on the other side of the helix resulting in an outwards kink at the C-terminal end as opposed to the inward kink observed in family A. The exact mechanism of activation of these receptors remains to be determined with an agonist-bound crystal structure of the TMDs.

Extensive study of mGlu1 revealed several residues thought to be critical in mediating the interaction of the receptor with specific G protein subunits (Francesconi and Duvoisin, 1998). Mutation of Cys694 and Thr695 in the 2nd ICL completely abolished signalling through Gq/11 proteins showing them as important residues for this interaction. These two residues are only conserved in mGlu1 and mGlu5, and these two receptors are consequently the only two of the mGluRs which activate this pathway. Mutation of the Lys690 showed a receptor with a markedly reduced ability to activate the Gq/11 pathway also. Chimaeric forms of mGlu1 and mGlu3, where the ICLs were exchanged, showed that the 2nd and 3rd ICL were important determinants in G protein specificity and activation and 3 key residues in the 2nd ICL, Pro698, Cys694 and Thr695, were responsible for Gs coupling (Francesconi and Duvoisin, 1998; Gomeza et al., 1996). Two residues in the

3rd ICL, Arg775 and Phe781, were critical for G protein activation (Hermans and Challiss, 2001).

The C-terminal tails of mGluRs are highly variable in length and sequence, which is true across the GPCR superfamily. Even at the same subtype of receptor, there are many examples of splice modifications creating differing C-terminal tails. The mGlu1 receptor has 4 splice variants, a-d, which have variable C terminal tails, with mGlu1a having the longest (318 amino acids in the rat isoform), followed by mGlu1d (26 amino acids), mGlu1b (20 amino acids), and mGlu1c (11 amino acids) (Conn and Pin, 1997; Pin et al., 1992; Tanabe et al., 1992). The impact of these splice variants is unclear, but it has been suggested that they may differ in trafficking, signalling kinetics, and oligomerisation profiles (Techlovská et al. 2014; reviewed in detail in Hermans & Challiss 2001). The mGlu5 receptor has two splice variants, a and b, where the b variant has 32 extra amino acids residues approximately 50 amino acids downstream of the cytosolic end of the 7th TMD (Minakami et al., 1994). These splice variants appear to have no discernible differences in pharmacology or signal transduction, so the unique function of each remains a mystery, though the expression of each subtype in astrocytes has been shown to differ over time (Cai et al., 2000; Joly et al., 1995). C-terminal tail splice variants of mGlu7 and mGlu8 receptor subtypes have also been demonstrated (Corti et al., 1998).

The functional role of the C-terminal tails of GPCRs is multifaceted and complex. For instance, mGlu1a and mGlu5 isoforms C-terminal tails possess a PPxxF motif which is thought to bind Homer proteins (Brakeman et al., 1997; Niswender and Conn, 2010). These proteins have been shown to influence the receptor localisation in both primary cells as well as transfected, recombinant systems (Shiraishi-Yamaguchi and Furuichi, 2007). They may also be involved in a variety of higher-order complex formations with varying roles such as linking mGlu1 and mGlu5 to ionotropic glutamate receptors, as well as kinases (Hermans and Challiss, 2001; Mao et al., 2005b). Tamalin, a scaffold protein with a PDZ domain,

like those found in homer proteins, can also bind mGlu1a and mGlu5 isoforms, at the SSSSL motif conserved at these receptors (Kitano et al., 2002). It appears to play a role in linking these mGluRs to other proteins in complex such as cytohesins, which are involved in trafficking and have some activity as a guanine-nucleotide exchange protein (GEP) (Meacci et al., 1997).

As well as the formation of protein complexes, a role for the C-terminal tail in G protein specificity has been reported in mGlu1 receptors. Essentially, an RRKK site on the C-terminal tail is inhibitory towards Gq/11 activity (Mary et al., 1998; Tateyama and Kubo, 2008). When the site is completely abolished with a C-terminal truncation, the mGlu1 receptor loses its ability to signal through Gq/11, instead signalling through the Gi/o pathway (Kammermeier, 2010). Interestingly, mGlu5 isoforms lack the RRKK motif, and little study has been performed to see whether there is a similar motif contained in the large C-terminal tail of this receptor subtype.

Though the metabotropic glutamate receptors share several common structural features, such as the large N-terminal ligand binding domain, the 7 transmembrane domains linked by extra and intracellular loops, and a variable C terminal tail, they display a variety of pharmacological properties, and as such are divided into three groups based on sequence homology, preferential G protein coupling, and agonist efficacy: Group I consists of the mGlu1 and mGlu5 isoforms and these receptors are the focus of this thesis. Group II consists of the $mGlu_2$ and $mGlu_3$ receptors, and group III consists of $mGlu_4$, $mGlu_6$, $mGlu_7$, and $mGlu_8$ (reviewed in Conn & Pin 1997).

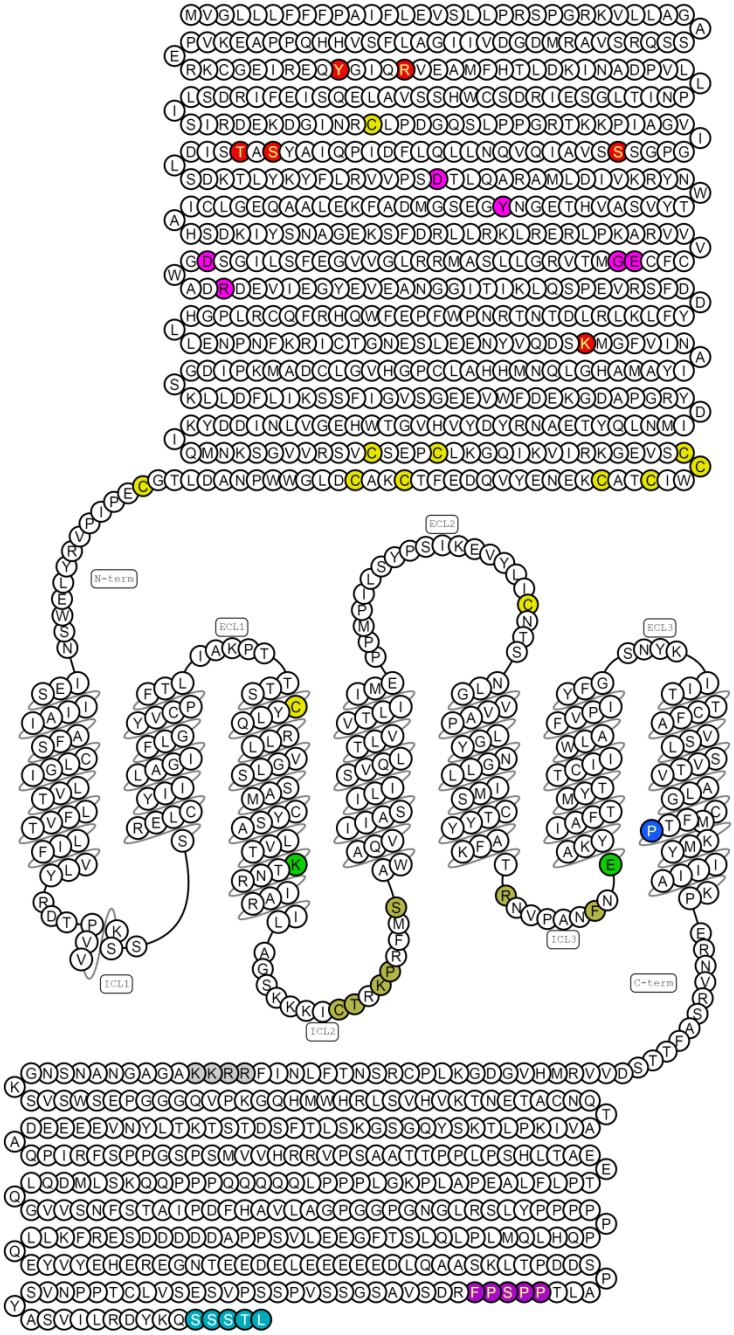

Figure 1.4.1.1 A snake plot of mGlu1a, highlighting several important structural features of the receptor. Cysteines which play key roles in receptor structure, activation, and dimerisation are highlighted in yellow. The residues of the ligand binding domain responsible for the binding of glutamate are highlighted in red (for the upper lobe) and pink (for the lower lobe). The 'salt-bridge' residues are highlighted in green. The proline which is involved in the critical inward kink at this receptor is highlighted in blue. Residues in the 2nd and 3rd ICLs responsible for G protein specificity are highlighted in dark yellow. The residues in the C-terminal tail responsible for Gq association are highlighted in grey. The PDZ domains responsible for homer and other PDZ domains are highlighted in purple and sky blue, respectively. Snakeplot created using tools provided by Horn et al., 2003.

1.4.2 Signal transduction of the group I metabotropic glutamate receptors

Group I consists of mGlu1 and mGlu5, which share between 60 and 70% sequence homology between them, compared to 30 and 40% with the other mGluRs. Perhaps the most striking difference between group I and the other groups is that both mGlu1 and mGlu5 couple preferentially to the Gq/11 pathway, as opposed to the Gi/o pathway preferred by group II and III mGluRs (Masu et al., 1991; Minakami et al., 1994). Upon the binding of an agonist, the Gq/11 protein activates the phospholipase C (PLC) isozyme PLC-ß, which converts PIP_2 to IP_3, which diffuses into the cytosol and stimulates calcium release from intracellular stores. Interestingly, there is a divergence of calcium signal characteristics between mGlu1 and mGlu5 receptors (Kawabata et al., 1998).

When expressed in recombinant HEK293 cells, the stimulation of mGlu1 results in a single peak of calcium release from intracellular stores, with a steady plateau or oscillatory Ca^{2+} signal mediated by the influx of extracellular calcium through an mGlu1 mediated Ca^{2+} channel. After the initial Ca^{2+}signal induced by activation of mGlu1, an extracellular buffer treated with EGTA to chelate Ca^{2+} ions prevented the plateau/oscillatory signalling, however, stimulation with carbachol activating the Gq/11 pathways through endogenous muscarinic receptors produced a calcium response. This showed that the intracellular stores were not depleted, but their release through mGlu1 was attenuated after the initial activation of the receptor. In contrast, mGlu5 expressed in HEK293 cells produced robust oscillations which were not alleviated by chelation of extracellular Ca^{2+} chelation. Chelation did affect the frequency of mGlu5 induced oscillations, but these oscillations were undoubtedly through Ca^{2+} release from intracellular stores through the IP_3 pathway. Remarkably, mutation of an aspartate to threonine at position 850 of mGlu1 allowed it to cause oscillations in much the same way as those of mGlu5. Conversely, mutation of Thr840 to aspartate in mGlu5 made its signalling profile more like that of mGlu1. Further study has shown that the Ca^{2+} oscillations caused by

mGlu5 stimulation are regulated by PKC. Inhibition of PKC results in a loss of oscillation via mGlu5, whereas activation of PKC abolishes the Ca^{2+} response of mGlu5 completely (Kawabata et al., 1996).

Further study has shown that the initial activation of PKC by mGlu5 stimulated Ca^{2+} signalling actually results in phosphorylation of a single residue on the mGlu5 receptor, Ser839, and not Thr840 as previously thought. The phosphorylation of Ser839 inhibits the activity of the receptor, and the oscillations are due to rapid phosphorylation/dephosphorylation cycles mediated by PKC (Kim et al., 2005). This study further showed that, rather than being directly phosphorylated by PKC, Thr840 plays a permissive but critical role in the phosphorylation of Ser839. This activity is not an artefact of recombinant cell expression systems, and it has been shown to occur in native preparations such as astrocytes and neurons (Flint et al., 1999; Nakahara et al., 1997). A recent study, where different isoforms of PKC were knocked down using siRNA techniques, showed that in astrocytes this cyclic phosphorylation of Ser839 was likely mediated by the PKC isoform PKCε (Bradley and Challiss, 2011). Given that mGlu5, but not mGlu1, is highly expressed in astrocytes it is probable that these oscillations play important roles in astrocyte function. One such function of mGlu5 is reducing the expression of the glutamate transporters GLAST and GLT-1 in astrocytes, which may act to increase glutamate concentration at the synapse and increase neuronal excitability (Aronica et al., 2003). The formation of DAG by group I mGluRs, which remains localised to the membrane due to its hydrophobic structure, is important in the activation of PKC isoforms (Klein et al., 1997).

mGlu1 has shown the ability to couple to cAMP formation by stimulation of AC through Gs G proteins (Aramori and Nakanishi, 1992). Interestingly, the homodimerisation of this receptor has been implicated in this functional response: When only one subunit of the dimer is in the active conformation, G protein coupling is split between G_s and Gq/11. In contrast, when both subunits are in the active conformation Gq/11 is the preferential coupler

(Tateyama and Kubo, 2006). This coupling is disputed, with at least one study showing a failure of any splice variants of mGlu1 to couple to the cAMP signalling pathway (Hiltscher et al., 1998). It is possible that this coupling is dependent on the recombinant system in which it is expressed, though there is evidence of mGlu1 mediated cAMP signalling in neurons (Sugiyama et al., 2008). There is some evidence of mGlu1 coupling to Gi/o proteins in the baby hamster kidney (BHK) recombinant cell line, but whether this has any physiological relevance *in vivo* is debatable (Selkirk et al., 2001). No such promiscuity with respect to mGlu5-G protein coupling has been robustly reported to date, and indeed the initial evidence is in concurrence (Abe et al., 1992).

Group I mGluRs have also shown the ability to signal through mechanisms independent of G proteins. In neurons from the CA3 region of the rat hippocampus it was shown that, despite blockage of G protein signalling using inhibitors such as GDPβS, EPSCs could be invoked by a mechanism in which Src, a tyrosine kinase, was activated by mGlu1 (Heuss et al., 1999). It has since been additionally shown that activation of mGlu1, not mGlu5, results in activation of ERK1/2 which is dependent on Src activation by mGlu1, at least in rat CA1 hippocampal neurons. This ERK activation pathway leads to an influx in cellular Ca^{2+} in these neurons whereby ERK potentiates the transient receptor potential (TRP) cation channels. A recent report suggested that EPSCs in CA3 neurons were mediated through the ERK1/2 pathway by the β-arrestin 2 isoform (Eng et al., 2015). In their study, CA3 neurons in hippocampal neurons from β-arrestin 2 knockout mice did not display EPSCs after mGlu1 activation, but β-arrestin 1 knockout neurons were unaffected. Given that the β-arrestins are involved in complexing other GPCRs, such as the β-adrenoceptor 2, to the SRC and ERK pathways, it's possible that this is true for mGluRs as well (Luttrell et al., 1999b; Miller and Lefkowitz, 2001).

In the case of mGlu5 the role of β arrestins is unclear, though they do display a variety of G protein-independent signalling. For instance, mGlu5

has been shown to interact with protein phosphatase 2A, which is involved in the ability of the receptor to interact with the ERK pathway (Mao et al., 2005a). mGlu1 and mGlu5 also interact with proline-rich tyrosine kinase 2 (Pyk2) which results in phosphorylation of ERK1/2 (Nicodemo et al., 2010). A recent study has implicated mGlu5, specifically, in the action of amyloid-ß proteins at neurons (Um et al., 2013). Essentially, it has been shown to transduce a signal when activated by amyloid-ß in complex with cellular prion proteins through the tyrosine-kinase Fyn. Given the involvement of amyloid-ß in the progression of Alzheimer's disease, it is interesting to speculate whether this interaction will one day prove to be key in the pathophysiology of this neurodegenerative disease and indeed, in a mouse model of Alzheimer's disease, mGlu5 knockout has been shown to reduce the cognitive impairment and pathogenesis which are hallmarks of this disease (Hamilton et al., 2014).

1.4.3 Dimerisation of the metabotropic glutamate receptors

As discussed previously, the mGluRs are homodimeric in nature. This homodimerisation has consequences for mGluR function. Replacing the C-terminal tails of the mGluRs with those of the $GABA_B$ receptors drives constitutive dimerisation of the receptor at the cell membrane, and studies using this technique have given great insight into the functional consequences of dimerisation. For instance, the use of a heterodimer comprising of an mGluR1 construct with the $GABA_{B1}$ C-terminal tail coupled to an mGluR1 construct with the $GABA_{B2}$ C-terminal tail and point mutations to allow the non-competitive mGluR5 antagonist MPEP to bind showed that the inhibition of one protomer is not sufficient to prevent activation of the receptor dimer (Hlavackova et al., 2005). Furthermore, the activation of just one protomer was sufficient to induce the full activation of the receptor dimer in this model. Further study, using this model to create mGlu1 and mGlu5 heterodimers, demonstrated that the binding of a compound in the TMDs of either protomer was sufficient to induce the full activation of the dimer complex further adding to the theory that in the

active dimer only a single protomer is activated (Goudet et al., 2005). Given that the wild-type homodimers are symmetrical in nature, the asymmetric activation of the receptor is a surprising finding. Considering the evidence that for full activation both LBDs of the dimer must be occupied by agonist, this finding is even more peculiar. The constitutive heterodimers demonstrated in these studies are used in this thesis to model the pharmacology of allosteric modulators acting at mGlu1 and mGlu5 in order to further demonstrate the pharmacological interaction of this dimer.

Inter-mGluR heterodimerisation has been demonstrated in the literature. For example, recent studies have shown that mGlu2 and mGlu4 can form heterodimers in native systems (Kammermeier, 2012). This heterodimerisation has effects on the pharmacological characteristics of compounds acting at these receptors, with the mGlu2 and mGlu4 ligands unable to potentiate the response of the heterodimer to glutamate. Furthermore, studies using radioligand binding techniques have shown the existence of mGlu2 and $5HT_{2A}$ heterodimers *in vivo* (Moreno et al., 2011). This heterodimerisation alters the affinity of compounds acting at these receptors, and has functional consequences *in vivo*. Recent evidence has emerged that suggests that group I mGluRs can heterodimerise. For instance, recombinant cells co-transfected mGlu1 and mGlu5 receptors with fluorescent tags displayed fluorescence resonance energy transfer (FRET) which implied they were heterodimerising (Doumazane et al., 2011). Furthermore, co-transfecting the mGlu1 and mGlu5 receptor altered the pharmacology of ligands acting at either receptor, demonstrating that they were functionally interdependent (Sevastyanova and Kammermeier, 2014). Clearly, heterodimerisation of mGluRs has implications for the action of ligands and the function of these receptors. If mGlu1 and mGlu5 do heterodimerise *in vivo* then understanding how the pharmacology of ligands acting at these receptors is affected will be key to future therapeutic development. In this thesis the mutant, constitutive mGlu1 and mGlu5 heterodimer is used as a model for radioligand interaction, and these

interactions may provide evidence of heterodimerisation *in vivo* if demonstrated in native tissues.

1.4.4 Expression and functional roles of the group I metabotropic glutamate receptors in the synapse

When mGlu1 was first discovered, the expression profile in the brain was established through mRNA blotting and *in situ* hybridisation (Masu et al., 1991). This early study showed that this receptor was expressed throughout the brain, with particularly high expression in the cerebellum and the olfactory bulb. It was also noted that there was high expression in the hippocampus, particularly the dentate gyrus and CA2-CA3 regions of the hippocampus, as well as in Purkinje cells in the cerebellum. For mGlu5, a similar technique was used and it showed expression across the CNS, with a particular emphasis in the dentate gyrus and CA1-CA4 region of the hippocampus, the cerebellum, areas of the olfactory bulb and anterior olfactory nucleus, as well as the striatum, accumbens nucleus, lateral septal nucleus, as well as further regions of the thalamic nuclei and inferior colliculus (Abe et al., 1992). In stark contrast to the expression of mGlu1, little expression of mGlu5 was noted in the Purkinje cells of the cerebellum. As a general guide, on the synaptic level group I mGluRs are thought to be expressed mostly on the postsynaptic neuron, where they act to increase the excitability of the synapse through depolarisation and ion channel modulation, though there are exceptions (Lujan et al., 1996; Niswender and Conn, 2010).

(S)-3,5-DHPG stimulation of group I mGluRs results in increased neuronal excitability in a number of neuronal populations, such as the hippocampus and the cortex (Davies et al., 1995; Libri et al., 1997). As an example, in hippocampal CA1 pyramidal neurons, stimulation of group I mGluRs by DHPG caused an increase in postsynaptic neuronal depolarisation, and in guinea pig olfactory cortical neurons the administration of (S)-3,5-DHPG induced a similar increase in postsynaptic neuron excitability. The effect of group I mGluR stimulation on voltage gated ion channels are numerous,

diverse, and complex (for a detailed review see Anwyl 1999). As an example, N-type Ca^{2+} channels could be blocked by group I agonists in the cortex (Choi and Lovinger, 1996), and this inhibition was modulated in some way by PKC, a major downstream signalling pathway utilised by group I mGluRs (Swartz et al., 1993). In cerebellar granule cells, stimulation with group I selective agonists resulted in a slow inhibition of these channels (Chavis et al., 1995). Blockage of intracellular calcium release in retinal ganglion cells using IP_3 and ryanodine receptor blockers prevented this inhibition upon mGluR agonist stimulation (Shen and Slaughter, 1998). In contrast, one of the groups who noted slow inhibition of these channels by group I cells in cerebellar granule cells later noted facilitation of these channels as a result of mGlu1 or mGlu5 signalling (Cellulaire and It, 1995). There are even more examples of mGluR influenced mechanisms which act to increase the excitability of the synapse through a variety of other Ca^{2+}, K^+, and non-specific cation channels (see Anwyl 1999).

Another function of the mGluRs is to regulate the release of various neurotransmitters into the synapse (Cartmell and Schoepp, 2000). Interestingly, the mGluRs can alter the amount of their own endogenous agonist, glutamate, into the synapse: they act as autoreceptors. Stimulation of group I mGluRs with (S)-3,5-DHPG enhanced K^+ channel blockage evoked glutamate release from cortical synaptosomes (Reid et al., 1999). Electrophysiological studies on CA1 pyramidal cells showed this to be something of a 'one-shot' facilitation: a synaptic transmission resulted in a short-term facilitation of glutamate signalling in the synapse which is rapidly desensitised, and this desensitisation prevented further potentiation of glutamatergic transmission by (S)-3,5-DHPG in the short term (Rodríguez-Moreno et al., 2016). It is thought that perhaps this rapid desensitisation is important for preventing a feedback loop whereby the release of glutamate leads to increased glutamatergic transmission *ad infinitum* which could cause excitotoxicity at the synapse (Cartmell and Schoepp, 2000). The specific receptor originally thought to be responsible for this is mGlu5, as in mGlu1 knockout mice this effect of (S)-3,5-DHPG was

still observed (Sistiaga et al., 1998). It is now known that both mGlu1 and mGlu5 presynaptic receptors are expressed, and it has been demonstrated that their stimulation lead to exocytosis of aspartate and glutamate from the presynaptic terminal with mGlu5 being the 'high-affinity' target relative to mGlu1 (Musante et al., 2008; Raiteri, 2008). The release of other neurotransmitters such as GABA, dopamine, and serotonin, to name but a few examples, are also thought to be facilitated by group I mGluRs (reviewed in Cartmell & Schoepp 2000). Along with the role of mGlu5 in astrocytes discussed in the previous section, mGlu5 control of neurotransmitter levels appears multifaceted and nuanced.

The excitatory action of group I mGluRs can also be enacted through interactions with ligand-gated ion channels including, but not limited to, the iGluRs. The excitotoxic action of NMDA in cultured cortical neurons with astrocytes was enhanced by the addition of the group I selective agonist (S)-3,5-DHPG, suggesting that somehow NMDA receptor action is being potentiated by these receptors (Bruno et al., 1995). This potentiation was further demonstrated in other neuronal cell types, such as striatal and hippocampal cells (Pisani et al. 1997; Doherty et al. 1997). In the case of mGlu1, this potentiation was initially attributed to the actions of PKC as a downstream signal of the receptor (Skeberdis et al., 2001). It is now known to involve activation of the Src kinase family discussed in the previous section (Heidinger et al., 2002). In brief, stimulation of mGlu1 leads to activation of Src kinase which phosphorylates the NR2A subunit of the NMDARs, leading to a potentiation of NMDA mediated Ca^{2+} responses (Chen and Roche, 2007). This has also been reported for mGlu5 receptors (Takagi et al., 2012). The signalling between NMDARs and mGlu5 is interesting as it appears that cross-talk occurs between these receptors: the activation of mGlu5 causes the direct potentiation of NMDAR mediated Ca^{2+} currents (Awad et al., 2000). This potentiation has been shown to occur when both mGlu5 and NMDARs are activated together, and it is dependent on Gq/11/PKC/Src kinase activation, and can be blocked using the mGlu5 selective negative allosteric modulator MPEP (Huang et al., 2001; Kotecha

et al., 2003). The activation of the NMDARs causes the dephosphorylation of mGlu5 receptors that have been desensitised by PKC through calcineurin (Alagarsamy et al., 2005). With high NMDAR activity, mGlu5 is phosphorylated by PKC signalling induced by NMDAR signalling activity (Alagarsamy et al., 2002; Challiss et al., 1994). Taken together, these studies suggest that the specific mGluR subtype involved in potentiating NMDAR responses varies based on which neuronal population is studied, with mGlu5 being implicated in the hippocampus and subthalmic nucleus, for example, and mGlu1 being implicated in cortical neurons, though it is not necessarily without exception (Doherty et al. 1997; Mannaioni et al. 2001; Awad et al. 2000; Heidinger et al. 2002; Alagarsamy et al. 2005). Modulation of the AMPARs by group I mGluRs is similarly complex with stimulation of mGluRs leading to changes in the function and regulation of AMPARs in the brain through events mediated by protein kinases, Ca^{2+} channels, and phosphatases (see Ahn & Choe 2009; Gladding et al. 2009).

1.4.5 Physiological function and role in disease

The production of mGlu1 and mGlu5 knockout mice gave a great insight into the potential role of these receptors on a systemic level. In the first mGlu1 knockout study by Conquet et al. (1994), perhaps the most obvious phenotype was that of a severe motor deficit. It is perhaps not surprising to learn that mGlu1 is involved in motor control given the high expression of mGlu1 in the cerebellum. This has been attributed to a distinct impairment of long-term depression (LTD), a mechanism of learning at the neuronal level by which synaptic transmission is reduced due to distinct signalling inputs at the synapse (Aiba et al., 1994b). Further study indicated that mGlu1 is important for the regression of the multiple innervations of so called 'climbing fibers' to Purkinje cells. Where usually multiple inputs to the Purkinje cells would be 'pruned' until a single, dominant innervation pattern appears, in mGlu1 deficient mice this pruning process is impaired, and could be rescued by induced-expression of mGlu1 (Ichise, 2000).

The high expression of mGlu1 in certain areas of the hippocampus hinted that the receptor may be important in learning and memory events. Indeed, mGlu1 knockout mice show an impaired ability to induce long-term potentiation (LTP) in hippocampal neurons (Aiba et al., 1994a). mGlu1 knockout mice had an impaired ability to induce context-specific learning and LTP in the CA1-3 region, where synaptic enhancement through mGlu1 associated Ca^{2+} signalling was implicated (Galván et al., 2015; Gil-Sanz et al., 2008). Interestingly, recent study has suggested that mGlu1 induced LTD, mediated through interactions with NMDA receptors, is important for learning and memory processes and synaptic plasticity in the CA1 region of the hippocampus, showing the nuanced and varied function of these receptors, even within the same brain structures (Bhouri et al., 2014).

Knockout of the mGlu5 receptor revealed a role for this receptor in a multitude of CNS functions (Niswender and Conn, 2010). For instance, mice lacking mGlu5 receptors show lower indicators of cocaine addiction than their wild-type counterparts. These mice do not self-administer cocaine or even respond to it in the same way that a wild-type mouse does (Chiamulera et al., 2001). Further study of the mGlu5 receptor has shown it to be an important factor in multiple addictions, such as alcohol, nicotine, and methamphetamine (Cozzoli et al., 2009; Olive et al., 2005; Osborne and Olive, 2008; Tronci et al., 2010). Remarkably, smokers and ex-smokers showed a reduced ability to bind an mGlu5 ligand used in an positron emission topography study which perhaps shows that nicotine can significantly alter the expression levels of this receptor *in vivo* (Akkus et al., 2013). Pharmacological study has also implicated mGlu5 as a key player in anxiety disorders, pain, depression, and, as mentioned previously, neurodegenerative disorders such as Alzheimer's disease (reviewed in Niswender & Conn 2010). mGlu5 may also play a key role in Fragile X syndrome, with mGlu5 signalling being significantly more pronounced in this disease (Bear et al., 2004). Indeed, pharmacological blockade of mGlu5 receptors in mouse models of Fragile X leads to the attenuation of two phenotypes of disease models in the mouse (Yan et al., 2005).

Both mGlu1 and mGlu5 are potentially involved in schizophrenia, and knockouts of mGlu1 and mGlu5 show reduced prepulse inhibition, a measure of schizophrenia-like in animal models (Brody et al., 2004, 2003). As with mGlu1, mGlu5 is known to be involved in memory formation through synaptic plasticity mechanisms, with a key role in LTD and LTP in the brain, and the exact role is highly location dependent. For instance, studies have shown that mGlu5 is critical for types of LTP induction in the CA1 region of the hippocampus (Lanté et al., 2006). Conversely, administration of the mGlu5 selective agonist (R,S)-2-chloro-5-hydroxyphenylglycine (CHPG) could also enhance LTD at these neurons (Neyman and Manahan-Vaughan, 2008). This follows the trend of LTP and LTD induction by group I mGluRs being highly dependent on context and location.

1.4.6 Ligand development at group I metabotropic glutamate receptors

Despite the fact that drugs targeting the GPCR superfamily account for an estimated 50% of all prescribed drugs, it is the minority of these receptors for which drugs are available (Conn et al., 2009). Historically, ligand development at GPCRs focused on drugs binding at the same site as the endogenous receptor, such as the discovery of isoprenaline as an adrenoceptor agonist in the treatment of asthma, or the use of atropine purified from *atropa belladonna* to dilate the pupils by antagonising muscarinic acetylcholine receptor action in the muscles of the eye (Gay and Long, 1949; Moulton and Fryer, 2011). To some extent these early ligands, which were largely non-selective between similar receptor subtypes, were harbingers for drug development of competitive agonists and antagonists at group I mGluRs.

Competitive ligands bind to the same site as the endogenous ligand, and this site is termed the 'orthosteric' site. In the case of mGluRs, the first group I selective agonist to be discovered was L-quisqualate (Aramori and Nakanishi, 1992). Though L-quisqualate activates group I receptors with at least 10-fold selectivity over other mGluRs (Conn and Pin, 1997), it also

activates other types of glutamate receptor such as the AMPA iGluRs (Schoepp et al., 1999). The first truly selective group I mGluR agonist to be discovered was (S)-3,5-dihydroxyphenylglycine ((S)-3,5-DHPG), which binds to and activates mGlu1 and mGlu5 isoforms (Schoepp et al., 1994). This compound and other orthosteric compounds, including antagonists, developed for the group I mGluRs were not ideal for therapeutic use due to their lack of subtype specificity which is perhaps unsurprising given the high homology of the LBD between the mGluRs as a whole. Indeed, the lack of specificity of orthosteric compounds such as these is a common characteristic across the GPCR superfamily; this is a direct consequence of the fact that these receptors bind the same engodenous ligand, and so there must be structural commonality within this binding pocket. Unfortunately, the orthosteric mGluR agonists lack bioavailability and CNS penetration characteristics necessary for drugs of therapeutic relevance (Kew, 2004). With the recent shift in focus away from radioligand binding towards functional assays in high-throughput compound screening technology another class of ligand has come to the fore: the allosteric modulator.

Allosteric (from the greek for 'other site') modulators are defined as compounds which 'act at a site that is topographically distinct from the orthosteric site' (Conn et al., 2009). Though they do not compete with the orthosteric site they can potentiate a signal through the receptor, inhibit the signal, or bind but have no effect on the function of the receptor; as such they are known as positive (PAMs), negative (NAMs), or silent allosteric modulators (SAMs), respectively. The first specific mGluR allosteric modulator to be discovered was CPCCOEt, an mGlu1 specific NAM (Annoura et al., 1996; Litschig et al., 1999). Since the discovery of this NAM, many other examples have subsequently been identified with a variety of properties which have allowed for *in vivo* investigations into the function of this receptor (Sheffler et al., 2011). In particular, [4-[1-(2-fluoropyridine-3-yl)-5-methyl-1H-1,2,3-triazol-4-yl]-N-isopropyl-N-methyl-3,6-dihydropyridine-1(2H)-carboxamide] (FTIDC, for simplicity) has shown efficacy in animal models of pain (Satow et al., 2008; Suzuki et al., 2007).

These NAMs have also shown efficacy as an anxiolytic, an anti-psychotic, and in the treatment of addiction (Satow et al., 2008; Xie et al., 2010). PAMs for mGlu1 have also been reported with Ro 01-6128, Ro 67-4853, and Ro 67-7476 being the prototypes of these compounds (Knoflach et al., 2001). Interestingly, PAMs of mGlu1 have shown efficacy in ameliorating addiction to cocaine in rats (Loweth et al., 2014).

Mutagenesis studies of mGlu1 showed that the action of the PAMs Ro 01-6128 and Ro 67-7476 is dependent on Val757 in the 5th TMD. The inhibition induced by CPCCOEt was mediated by two residues on the 7th TMD, Thr815 and Ala818 (Litschig et al., 1999). The publication of the crystal structure of mGlu1, discussed previously, showed several interacting residues with the mGlu1 NAM 4-fluoro-*N*-(4-(6-(isopropylamino)pyrimidin-4-yl)thiazol-2-yl)-*N*-methylbenzamide (FITM) (Wu et al., 2014). The binding of this compound was found to involve residues Gln660, Leu648, and Thr815 on the 3rd, 2nd, and 7th TMDs, respectively. Other mutagenesis studies have shown the large diversity of interactors which other allosteric modulators of mGlu1 are dependent on. For example, Val757 (5th TMD), Trp798, Phe801, Tyr805 (6th TMD), and the critical Val815 (7th TMD) were vital for the binding of 1-ethyl-2-methyl-6-oxo-4-(1,2,4,5-tetrahydro-benzo[d]azepin-3-yl)-1,6-dihydro-pyrimidine-5-carbonitrile (EM-TBPC), a negative allosteric modulator of mGlu1. This serves as a good example of the exploitability of these binding pockets for the discovery of multiple allosteric modulators.

Obviously the term allosteric implies that a ligand can potentially bind at any site on the receptor distinct from the orthosteric site. In reality these allosteric sites must have a permissive structure which allows space for the ligand as well as interaction sites on the receptor which encourage interaction of the ligand and the protein. The family C receptors, especially the metabotropic glutamate receptors, have a wealth of allosteric ligands available for study. CPCCOEt, a negative allosteric modulator at mGlu1, is dependent on two residues at the extracellular surface of the 7th TMD, though residues in the 5th and 6th TMD have also been shown to be

important for the formation of the binding pocket (Malherbe et al., 2003). It was shown that this was likely to be a common binding site for multiple negative allosteric modulators of mGlu1, as they all inhibited the binding of the radiolabelled allosteric compound [^{3}H]-R214127 (Lavreysen et al., 2003). The binding mGlu1 PAMs may happen in the same tertiary region of mGlu1, but interact with different individual residues (Knoflach et al., 2001). It was shown through studies of mGlu1 and mGlu5 receptor mutants that NAMs occupy a similar tertiary binding pocket in both receptor subtypes: Mutating two residues in the 3rd TMD and one in the 7th TMD of mGlu5 with their equivalents from mGlu1 collectively abolished the binding of the radiolabelled mGlu5 NAM [^{3}H]M-MPEP, and the mutagenesis of hmGlu1 with the equivalent residues for mGlu5 gave the receptor a high affinity for the radioligand, the binding of which could be competitively inhibited by CPCCOEt (Pagano et al., 2000). Furthermore, by altering a few key chemical moieties on a compound it was shown that an mGlu5 NAM could be changed to a PAM, highlighting how important interactions with individual residues are not only for subtype selectivity, but also for the nature of the interaction (Wood et al., 2011). These studies serve as examples of how allosteric modulators allow increasingly nuanced control of GPCRs for therapeutic benefit.

Allosteric modulators of all three classes, NAMs, PAMs, and SAMs, have been discovered for mGlu5 (O'Brien et al., 2003; Rodriguez et al., 2005; Varney et al., 1999), and those used in this thesis are summarised in Tables 1.4.6.1 and 1.4.6.2. The first allosteric modulators of mGlu5, SIB-1757 and SIB-1893, were found by high throughput functional screening, with a focus on small molecules dissimilar from amino acids (Spooren et al., 2001; Varney et al., 1999). These results showed that in recombant cells expressing human mGluRs, SIB-1757 was a specific, potent antagonist of mGlu5 by a non-competitive mechanism. SIB-1893 was a specific, potent antagonist of mGlu5, also acting by a non-competitive mechanism, however, it had some agonist activity at hmGlu4 receptors. These compounds also proved potent inhibitors of (S)-3,5-DHPG evoked calcium responses in

cultured primary cortical neurons of the rat. This showed that these compounds were not species specific, perhaps unsurprising given the high homology (95.4%) between the rat and human receptor. The discovery of these compounds lead to the rapid development of many specific allosteric modulators of mGlu5. MPEP, a derivative of SIB-1893, has a potency up to two orders of magnitude higher than that of the previous NAMs of mGlu5 (Gasparini et al., 1999). MPEP is perhaps the most well characterised NAM of mGlu5. Due to its high potency, good oral bioavailability, and CNS penetration, MPEP has been used to investigate the action of NAMs in the CNS across an array of diseases (See Lea & Faden 2006). mGlu5 NAMs are known to be clinically validated anxiolytics as demonstrated by fenobam (Porter et al., 2005). They have also demonstrated potency in rodent models of depression and Fragile X Syndrome, as discussed previously (Tatarczyńska et al., 2001; Yan et al., 2005). Mutagenesis studies of MPEP binding to the mGlu5 receptor showed that 8 residues are critical for the action of MPEP: Pro654, Tyr658 (3rd TMD), Leu743 (5th TMD), Thr780, Trp784, Phe787, Tyr791(6th TMD), and Ala809 (7th TMD) (Malherbe et al., 2003). Publication of the crystal structure of the mGlu5 TMDs in complex with mavoglurant, a derivative of MPEP-like NAMs, revealed important interactions between this drug and the receptor (Doré et al., 2014). Three hydrogen bonds between Asp747 (5th TMD), Ser805, and Ser809 (7th TMD) residues and the compound were critical though many more residues were involved (See figure 6a, Doré et al. 2014). Remarkably, the exchange of just 4 amino acids (V664I, S668P, C671S, V823A) between mGlu5 and mGlu1 results in the ability of mGlu1 to bind tritiated MPEP in a manner which can be competitively inhibited by the mGlu1 NAM CPCCOEt, showing that these binding pockets are in topographically similar locations on the two receptor subtypes.

Several series of PAMs have been described for the mGlu5 receptor. The first, 3,3′-difluorobenzaldazine (DFB), binds at an overlapping site with the NAM MPEP (O'Brien et al., 2003). Unfortunately, this compound displayed low potency, a poor solubility profile and low CNS penetration and so lacks

therapeutic potential (Cleva and Olive, 2011). The second, *N*-[5-chloro-2-[(-1,3-dioxoisoindolin-2-yl)methyl]phenyl]-2-hydroxybenzamide (CPPHA), binds at a site distinct from MPEP, but despite having a greater potency than DFB, it showed poor CNS penetration and therefore is not suitable for therapeutic intervention (O'Brien et al., 2004). Remarkably, CPPHA acts as a PAM of mGlu1 and mGlu5, but does not competitively displace ligands binding at either the MPEP pocket or the CPCCOEt pocket (Chen et al., 2008). The great breakthrough in mGlu5 PAMS came with the discovery of 3-cyano-*N*-(1,3-diphenyl-1*H*-pyrazol-5-yl)benzamide (CDPPB), a highly potent compound which binds in the same pocket as MPEP, and displays good CNS penetration (Chen et al., 2007; Lindsley et al., 2004). This compound has displayed the potential antipsychotic nature of mGlu5 activators, discussed previously, in rodent models (Kinney et al., 2005).

Several studies have begun to delineate the residues responsible for the action of PAMs at the MPEP binding site (Gregory et al., 2013; Turlington et al., 2013). Of particular interest was the finding that three mutations in the 5th TMD of mGlu5, P742S, L743V, and N746A, resulted in a sharp decline in the affinity of PAMs binding at the MPEP site, but their potentiation of the receptor response was unaffected. This highlights the complex structure-activity relationships at play and the decoupled nature of allosteric modulator affinity and allosteric action. There are now a wealth of mGlu5 NAMs and PAMs which display various properties, but the way these allosteric modulators interact with the receptor requires new modelling paradigms.

1.4.6.1 Extending the operational model to allosterism

A seminal paper by Black & Leff (1983) described the operational model of agonism to quantify the link between ligand binding and receptor function (See Equation 4). Wherein E is the response, E_{MAX} is the maximum response of the system, [A] is the concentration of agonist (A), K_A is the equilibrium dissociation constant (or affinity) of A, and τ is the function linking the

ability of the agonist to induce a response (efficacy) and the ability of the receptor stimulus to elicit a response from the system (see Equation 4b).

$$E = \frac{E_{MAX}\tau[A]}{[A](1+\tau)+K_A)} \qquad \textit{(Equation 4)}$$

This model was derived based on the observation that the relationship between agonist concentration and tissue response is commonly hyperbolic in nature. If receptor and drug interactions obey the law of mass action, then the function that links receptor occupancy to agonist action must also be hyperbolic.

$$\tau = \frac{[R_0]}{K_E} \qquad \textit{(Equation 4b)}$$

To clarify, τ is derived as the ratio of the receptor density [R_0] and a function (K_E) expressing the ability of the system to elicit a response from the agonist/receptor complex combined with the intrinsic efficacy of the agonist. As such, the operational model takes into account all the features of agonism with 'three necessary and sufficient parameters' (Black and Leff, 1983): The equilibrium dissociation constant of an agonist, K_A; receptor density, [R_0]; and the concentration of the AR complex that elicits 50% of the maximal response of a given system as a measure of efficacy, K_E. It is worth noting that this model assumes that the agonist binding is at equilibrium in the system, and this is often not the case when functional assays are performed. For instance, the Fluorescence Imaging Plate Reader (FLIPR) technique used as a measure of agonist response in this thesis is taken immediately upon addition of agonist, a time frame in which the system is unlikely to have reached equilibrium. Therefore caution must be taken when interpreting functional data from methods with different sampling timepoints.

The operational model was extended to model the interactions of allosteric modulators (Leach et al., 2007). In this extended model, the ability of an allosteric modulator to modify the affinity of an orthosteric compound is described. This co-operativity of binding (α) is a reciprocal effect, where any

change on an orthosteric ligand also reflects an equal change in affinity for the allosteric ligand. The ability of an allosteric modulator to modify the functional response is also described. This co-operativity of function (ß) reflects an increase in the ability of the receptor to transduce the binding of an orthosteric agonist to a functional response. Finally, the intrinsic efficacy of an allosteric modulator is described by this model (τ_B). Logically, τ_B as described by the original operational model of agonism (*Equation 4b*) cannot account for allosteric modulators with no efficacy, as the only way to achieve that value would be by accepting the receptor density is zero. In order to allow for this, τ_B is redefined as follows (*Equation 4c,* Leach et al., 2007):

$$\tau_B = \frac{\varepsilon[R_0]}{K_E} \qquad \textit{(Equation 4c)}$$

The addition of the intrinsic efficacy parameter (ε) is a logical basis for the use of the model for allosteric modulators without intrinsic efficacy, where ε = 0.

1.4.6.2 Modelling allosteric interactions

As described earlier, there are three ways in which the binding of a ligand at an allosteric site can influence the receptor: they can alter the receptor conformation such that the ability of the orthosteric ligand to bind to the receptor is altered, known as co-cooperativity of binding (α); they can affect the ability of the receptor to activate downstream signalling effectors upon ligand binding, known as co-cooperativity of function (ß); finally, they can activate the receptor in their own right, so-called ago-allosteric compounds. These properties of an orthosteric and allosteric compound binding at a receptor are described mathematically by the allosteric ternary complex model (Figure 1.4.6.1) (Stockton et al., 1983).

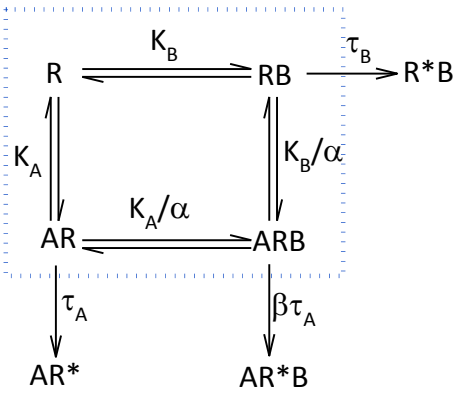

Figure 1.4.6.1 Diagram illustrating both the allosteric ternary complex model and operational model of allosterism. The classic allosteric ternary complex model of the binding of one orthosteric ligand (A), and one allosteric modulator (B) is shown within the blue box. K_A and K_B represent the equilibrium dissociation constants of ligand (A) and ligand (B) respectively. The reciprocal change in affinity for the receptor (the cooperativity of binding) caused by the interaction between the binding of A and B is denoted by α. In the Operational Ternary Complex Model the receptor has two states: active (R*) and inactive (R). The relative efficacy of A and B is represented by τ_A and τ_B, respectively. The change in the ability of A to activate the receptor induced by the binding of B (cooperativity of function) is denoted by ß. (reviewed in Leach et al. 2007).

The effect of the allosteric modulator on the affinity of the orthosteric compound is a reciprocal effect; an allosteric modulator which increases or decreases the affinity of an orthosteric compound will have its affinity for the receptor increased or decreased by the binding of the orthosteric compound in kind. This effect is probe-dependent, so the effect of an allosteric modulator on one orthosteric compound may differ for another, and vice versa. The effect of an allosteric modulator on the activation of the receptor is described by an extended ternary complex model which incorporates the operational model described previously (Black and Leff, 1983; Leach et al., 2007). This incorporates the ability of an allosteric modulator to alter the efficacy of an orthosteric compound, whilst also allowing for the ability of the allosteric modulator to activate the receptor by itself. Interestingly, the co-cooperativity of binding and of function are independent of each other: a positive modulator with respect to binding is not necessarily a positive modulator of function. Perhaps the most striking example of this to date is the ligand Org27569 which has a positive co-

cooperativity of binding with agonist CP 55940 at the CB_1 receptor, but has negative co-cooperativity with respect to function (Price et al., 2005). In this thesis, the allosteric mode of action of two previously uncharacterised mGluR5 PAMs, LSN-2814617 and VU0430644, will be characterised using the models described herein to interpret data from radioligand binding and functional assays.

There are many potential therapeutic advantages which allosteric modulators possess due to their mode of action. Firstly, because they do not bind in the highly conserved orthosteric site, they may bind in an area of low homology which allows for the development of subtype specific ligands. Secondly, where orthosteric ligands activate or deactivate the receptor, allosteric modulators without intrinsic efficacy only alter receptor signalling when the orthosteric ligand is present which preserves the spatiotemporal aspects of natural receptor function. Finally, the effect of an allosteric modulator is saturable: there is a limit to which they will alter the receptors activity even if the local concentration is increased further, and this may act to prevent excessive activation or inhibition of the receptor and ameliorate dose-dependent adverse events (Conn et al., 2009). The ago-allosterics, allosteric compounds with intrinsic efficacy, could provide an increased level of background signalling whilst also amplifying the natural ligand-mediated activation of the receptor. They may also provide a unique avenue for producing subtype-selective agonists at receptor subfamilies (May et al., 2007). The silent allosteric modulators also have the potential for a niche role in therapeutic use. As they can compete for an allosteric site, but their binding will not cause any change of the receptor function, they could act to ameliorate the effect of a PAM or NAM if receptor-dependent adverse events were to occur once administered.

1.4.7 mGlu5 positive allosteric modulators: neuroprotective?

The role that mGlu5 plays in neuronal cell death is complex and heavily debated (Flor et al., 2002). Given that, as discussed previously, group I agonists such as (S)-3,5-DHPG potentiate the excitotoxic action of NMDA

receptors *in vitro* (Bruno et al., 1995), one would perhaps expect NAMs of mGlu5 to be neuroprotective. Indeed, the early negative allosteric modulators SIB-1757, SIB-1893, and MPEP reduced excitotoxic cell death in mixed cortical cultures and in mouse-brains injected with NMDA (Bruno et al., 2000). Initially, it was commonly accepted that this neuroprotection is mediated by mGlu5, however, evidence is emerging that these NAMs can interact directly with the NMDA receptor at concentrations at which their neuroprotective qualities become apparent, usually much higher a concentration than is required for the inhibition of phosphoinositide hydrolysis (Movsesyan et al., 2001; O'Leary et al., 2000). Indeed, *in vitro* characterisation of the neuroprotective effect of a newer, more selective mGlu5 NAM MTEP showed that the majority of neuroprotection is mediated through non-mGlu5 mechanisms(Lea et al., 2005). Intriguingly, group I mGluR inhibition with the group I selective antagonist AIDA has been shown to exacerbated neuronal cell death induced by amyloid-beta oligomers, but only in the presence of the iGluR antagonists MK-801 and NBQX (Allen et al., 1999). However, in a later study the inhibition of mGlu5 with MPEP prevented cell-death induced by amyloid-beta oligomers at concentrations at which off target effects do not occur, showing that perhaps mGluR5 inhibition is neuroprotective against certain types of cell death (Bruno et al., 2000).

Early studies into the role of mGlu5 activation in cell death were mired by a lack of subtype selective agonists, producing a complex picture on the role of group I receptors in neurodegeneration (Nicoletti et al., 1999). For instance, injection of (S)-3,5-DHPG induced seizures and neuronal cell death in the mouse hippocampus (Camón et al., 1998). In contrast, activation of group I mGluRs in hippocampal slices with (S)-3,5-DHPG prior to the induction of exctitotoxic cell death with NMDA showed group I activation to be neuroprotective (Blaabjerg et al., 2003). *In vitro* studies using the mGlu5 selective agonist CHPG showed that mGlu5 activation could reduce amyloid-beta induced lactate dehydrogenase (LDH) release, indicative of cell-death (Movsesyan et al., 2004).

Positive allosteric modulators of mGlu5 play similarly complex roles in neuroprotection and neurotoxicity. CDPPB has been shown *in vitro* to be protective against neuronal injury, inhibiting LDH release in cultured neurons (Chen et al., 2012). CDPPB also decreases striatal cell death *in vivo* in a mouse model of Huntington's disease via an AKT-related mechanism (Doria et al., 2015). In contrast, reports have recently emerged of mGlu5 PAMs with an intrinsically neurotoxic profile. Chronic administration of a high-dose of the mGlu5 PAMs 5PAM523, 5PAM000, 5PAM413, and 5PAM916 caused seizures and neuronal cell loss in the hippocampus and auditory cortex of treated mice (Parmentier-Batteur et al., 2014). This neurotoxicity was not observed in mGlu5 knock-out mice, indicating that it is mGlu5-dependent. Furthermore, PAMs from diverse chemical series, such as VU0424465, have also been shown to induce this mGlu5 dependent neurotoxicity, further reinforcing the theory that it is mGlu5-dependent, and not metabolite or compound related (Conde-Ceide et al., 2015). In house data from Lilly has shown that chronic, high-dose administration of LSN-2814617 leads to seizures and neuronal cell death in mice, providing further evidence of mGlu5-dependent neurotoxicity. In this thesis the *in vivo* action of chronic, high-dose administration of LSN-2814617 is assessed using immunohistochemical methods. The neuronal toxicity induced by LSN-2814617 is then evaluated *in vitro* using the primary cortical cultures discussed previously.

Table 1.4.6.1: Summary of positive allosteric modulators used.

Abbreviation	Target	Structure	IUPAC Name
CDPPB	mGlu5	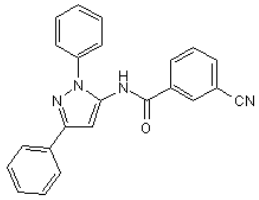	3-Cyano-*N*-(1,3-diphenyl-1*H*-pyrazol-5-yl)benzamide
CPPHA	mGlu1/mGlu5	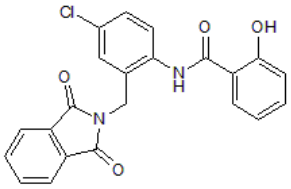	*N*-[4-Chloro-2-[(1,3-dihydro-1,3-dioxo-2*H*-isoindol-2-yl)methyl]phenyl]-2-hydroxybenzamide
ADX47273	mGlu5	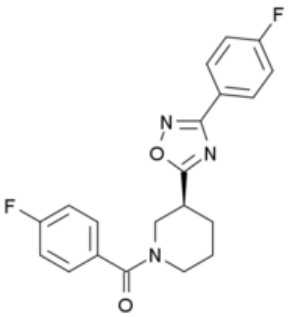	(S)-(4-fluorophenyl)-(3-[3-(4-fluoro-phenyl)-[1,2,4]-oxadiazol-5-yl]piperidin-1-yl)methanone
Ro-67 4853	mGlu1	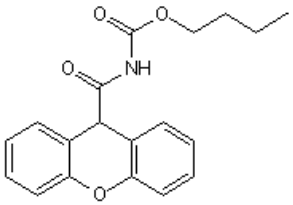	(9*H*-Xanthen-9-ylcarbonyl)-carbamic acid butyl ester
LY2814617	mGlu5	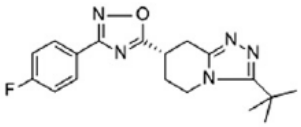	5-[(7S)-3-tert-butyl-5H,6H,7H,8H-[1,2,4]triazolo[4,3-a]pyridin-7-yl]-3-(4-fluorophenyl)-1,2,4-oxadiazole
VU0430644	mGlu5	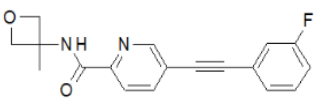	5-[2-(3-fluorophenyl)ethynyl]-N-(3-methyloxetan-3-yl)pyridine-2-carboxamide

Table 1.4.6.2: Summary of negative allosteric modulators used.

Abbreviation	Target	Structure	IUPAC Name
MPEP	mGlu5	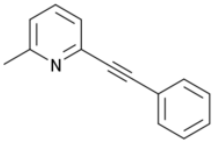	2-Methyl-6-(phenylethynyl)pyridine
M-MPEP	mGlu5	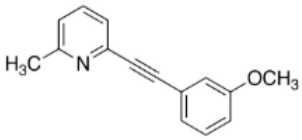	2-Methyl-6-[(3-methoxyphenyl)ethynyl]-pyridine
JNJ 1625985	mGlu1 selective	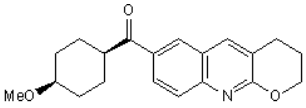	(3,4-dihydro-2H-pyrano-[2,3-b]quinolin-7-yl)-(cis-4-methoxycyclohexyl)-methanone

1.5 *Thesis aims*

1. To characterise the allosteric mode of action of two reference compounds, CDPPB and ADX-47273, and two previously uncharacterised compounds, LSN-2814617 and VU0430644, using pharmacological techniques to delineate cooperativity of binding (α) and cooperativity of function (ß) of each compound at both the human and the rat mGlu5 receptor.
2. To investigate pharmacological consequences of heterodimerisation between mGlu1 and mGlu5 receptors using chimeras wherein the C-terminal tail is replaced with that of modified $GABA_B$ receptors. Furthermore to assess whether pharmacological characteristics of these mutants can provide evidence of this heterodimerisation in native tissues.
3. To evaluate the toxic action of LSN-2814617 administration *in vivo*, and then model this toxicity using primary tissue culture methods.

Chapter 2. Materials and methods

2.1 Materials

2.1.1 Reagents, consumables, and compounds

Standard reagents for buffers and solutions were purchased from Sigma-Aldrich (Poole, UK) or Fisher Scientific (Loughborough, UK) unless otherwise stated. Buffers and solutions were made in-house, unless otherwise stated, using de-ionised water filtered through a PURELAB Ultra filtration system from ElgaVeolia (Marlow, UK). Any sterilisation for bacterial or mammalian cell culture was performed by autoclaving at 121°C for at least 20 minutes or, where applicable, through filtration using SteriCup filter units or Sterile Millex syringe filters, depending on volume, from EMD Millipore (Watford, UK). Media for cell culture, including serum, trypsin solution (10x), hygromicin B, zeocin, and Hank's balanced salt solution (HBSS), were obtained from Thermo Fisher Scientific (Paisley, UK). The transfection reagent Genejuice was obtained from EMD Millipore (Watford, UK). The transfection reagent PEI (1 mg/ml in PBS) was kindly made in house by Dr. Adrian Butcher at the MRC Toxicology Unit (Leicester, UK). DNAase for using cortical cell preparations was obtained from Thermo Fisher Scientific (Paisley, UK). c0mplete protease inhibitor tablets and G418 solution were obtained from Roche (Hertfordshire, UK). DNA purification kits were obtained from Qiagen (California, USA). Restriction enzymes and buffers were from New England Biolabs (Hitchin, UK). CytoTox 96 Non-radioacitve Cytotoxicity Assay kits were purchased from Promega (Wisconsin, USA). Solutions used in SDS-PAGE and Western-blotting procedures, including molecular weight markers, were purchased from Bio-Rad (Hertfordshire, UK). Nitrocellulose membrane and Hyperfilm ECL film was obtained from GE Healthcare Life Sciences (Amersham, UK). Bradford assay reagents were purchased from Thermo Fisher Scientific (Paisley, UK). Fluo4-AM for FLIPR assays was purchased from Thermo Fisher Scientific (Paisley, UK). L-glutamic acid monosodium salt monohydrate (L-glu) and M-MPEP hydrochloride were obtained from

Santa Cruz Biotechnology (Texas, USA). L-quisqualic acid, MPEP hydrochloride, (S)-3,5-DHPG, CDPPB, CPPHA, Ro 67-4853, and JNJ 16259685 were obtained from Tocris Bioscience (Bristol, UK). LSN-2814617, VU0430644, and ADX-47273 were synthesised in-house by Lilly (Surrey, UK). [^{3}H]-M-MPEP was donated kindly by Lilly, but originally synthesised by ViTrax (California, USA). Ultima Gold F scintillation cocktail was purchased from PerkinElmer (Beaconsfield, UK). GF/B glass-fiber filters were purchased from GE Healthcare Life Sciences (Amersham, UK). The monoclonal anti-mGluR5 rabbit antibody, which was raised against a synthetic peptide corresponding to a C-terminal portion (beginning at amino acid 1150) of the human metabotropic glutamate receptor 5a was purchased from Abcam (Massachusetts, USA). The monoclonal anti-mGluR1 rabbit antibody, which was raised against a synthetic peptide corresponding to a C-terminal portion (disclosed as 'residues surrounding Leu1105') of the human metabotropic glutamate receptor 1 was purchased from Cell Signalling Technologies (Massachusetts, USA). The monoclonal anti-GFAP mouse antibody, raised against GFAP protein from the pig spinal cord, was purchased from Sigma-Aldrich (Poole, UK). The polyclonal anti-c fos rabbit antibody, raised against a synthetic peptide corresponding to an N-terminal portion (amino acids 3-16) of the human c fos proto-oncogene, was purchased from Sigma-Aldrich (Poole, UK). The monoclonal anti-ß tubulin mouse antibody, which was raised against purified bovine tubulin (as disclosed), was purchased from Sigma-Aldrich (Poole, UK). The monoclonal anti-GAPDH rabbit antibody, which was raised against a synthetic peptide corresponding to the C-terminal portion of the human GAPDH protein (epitope not disclosed), was purchased from Cell Signalling Technologies (Massachusetts, USA). The polyclonal anti-NeuN rabbit antibody, raised against the N terminus (as disclosed by the manufacturer), was purchased from EMD Millipore (Watford, UK). All other antibodies were purchased as disclosed in Tables 2.6.4.1, 2.6.6.1, and 2.6.7.1.

2.1.2 cDNA constructs for transfection

Plasmid pcDNA3.1 containing the following cDNA constructs were kindly provided by Lilly (Surrey, UK):

hmGlu5: The full length human $mGlu5_b$ receptor cDNA.

HA-hmGlu1/hmGlu5-C2-KKTN: A mutant receptor comprising of either the human $mGlu1_a$ or human $mGlu5_b$ receptor with an N-terminal hemagglutinin (HA) tag (-YPYDVPDYA-) inserted downstream of the signal peptide after Ser22 (outlined in Ango et al. 1999), and the C-terminal tail replaced with that of the human $GABA_{B2}$ receptor (Gln761-E821), followed by the retention motif KKTN prior to a stop codon (based on Brock et al., 2007). In the case of $mGlu1_a$, the $GABA_{B2\text{-}KKTN}$ tail was inserted in place of the $mGlu1_a$ C-terminal tail after Met858. In the case of $mGlu5_a$, the $GABA_{B2\text{-}KKTN}$ tail was inserted in place of the $mGlu5_a$ C-terminal tail after Met845.

FLAG-hmGlu5-C1: A mutant receptor comprising of the human $mGlu5_b$ receptor with an N-terminal FLAG (-DYKDDDDK-) tag inserted downstream of the signal peptide after Ser22, and the C-terminal tail replaced with that of the human $GABA_{B1}$ receptor (Lys875-Stop962) after Met845 (Based on mutants disclosed in Brock et al., 2007)..

The full sequence data and pcDNA vectors used for these constructs are disclosed in Appendix 1. Figure A1 shows the full sequence of the hmGlu5b used. Figure A2 shows the vector used for the hmGlu5b receptor. Figure A3 shows HA-hmGlu1-C2-KKTN sequence, and figure A4 shows the vector used. Figure A5 shows the full sequence of the HA-hmGlu5-C2-KKTN construct, and figure A6 shows the vector used. Figure A7 shows the FLAG-hmGlu5-C1 sequence in full, and figure A8 shows the vector used.

2.1.3 Mammalian recombinant cell lines

Human Embryonic Kidney 293 (HEK293) cells were used to generate cells transiently expressing cDNAs for binding studies. AV12 cell lines stably expressing the full length human $mGlu1_a$ or $mGlu5_b$ receptor, co-transfected with excitatory amino acid transporter 1(EAAT1) were kindly created, validated, and provided by Lilly (Surrey, UK) for use in functional assays. AV12 cell lines stably expressing constitutive heterodimer constructs, either HA-hmGlu1-C2-KKTN and FLAG-hmGlu5-C1 or HA-hmGlu5-C2-KKTN and FLAG-hmGlu5-C1, co-expressing EAAT1 were kindly created, validated, and provided by Lilly (Surrey, UK) for use in functional assays.

2.1.4 Tissue samples from rodent

The following tissue samples were kindly provided by Lilly (Surrey, UK):

Cortices from wild-type, mGlu5 and mGlu1 knockout mice.

Perfusion-fixed cortices from wild-type mice either treated with vehicle or with 100 $mg.kg^{-1}$ of LSN2814617 per day for a total of 7 days.

Prior ethical approval was sought from the local Lilly oversight committee for the use of animals in these studies.

2.2 Bacterial culture, transformation, and purification

XL-1 Blue competent *Escherichia Coli (E. Coli)* from New England Biolabs (Massachusetts, USA) were used for the purpose of plasmid cDNA amplification according to manufacturer's instructions.

2.2.1 Creation of an N-terminally HA-tagged full length hmGlu5 receptor cDNA construct in pcDNA3.1

A restriction digest of the full length hmGlu5 cDNA in pcDNA3.1 and the HA-hmGlu5-C1 construct in pcDNA3.1 was performed using a BamHI restriction site present in the N-terminus of each construct according to a protocol provided, kindly, by Dr. Adrian Butcher (MRC Toxicology Unit,

Leicester, UK). In brief, plasmid cDNA was incubated in a 50 µl reaction volume containing 2.5 µg of purified plasmid cDNA, 5 µl of BamHI specific reaction buffer (10x), 10 units of BamHI restriction enzyme, and deionised water at 37 °C for 1 hour. Following digest, fragments were separated by electrophoresis through agarose gel as follows. Agarose gel was dissolved in TAE buffer (Tris/Acetate 40 mM, EDTA 1 mM, pH 8.0, 0.7% agarose (w/v)) and ethidium bromide was added to a concentration of 0.5 $\mu g.ml^{-1}$ prior to being poured into a cast. After the addition of TAE buffer to the tray, DNA ladder (0.1 to 10 kb) from New England Biolabs (Massachusetts, USA) was added along with DNA fragment solutions mixed with loading buffer (Ficoll-400 2.5% (v/v), EDTA 11mM, Tris-HCl 3.3mM, SDS 0.017% (w/v), bromophenol blue 0.015% (w/v), pH 8.0) prior to electrophoresis at 100V for 90 minutes. DNA bands were then visualised using UV light, and the bands were cut out and purified using the Nucleospin® Gel and PCR Clean-up kit from Macherey Nagel (Düren, Germany) according to manufacturer's instructions. In brief, 200 µl of buffer NTI was added for every 100 mg of agarose gel prior to incubation at 50 °C for 10 minutes until gel is dissolved. The sample was then loaded into a spin column and collecting tube and centrifuged at 11,000 x g for 30 seconds. Bound cDNA is then washed with 700 µl of buffer NT3 and centrifuged at 11,000 x g for 30 seconds. The column is then dried by further centrifugation at 11,000 x g for 30 seconds before the addition of 15-30 µl of buffer NE and incubation at room temperature for 1 minutes. After another centrifugation at 11,000 x g, the flow through containing cDNA is retained in the collecting tube. The small fragment containing the N-terminus of hmGlu5 with an HA tag is mixed with the large fragment containing the rest of the full receptor construct for ligation as follows. 7 parts of large fragment to 1 part of small fragment is incubated with 1 unit of T4 DNA ligase and 1 µl ligation buffer made up to a 10 µl reaction volume with deionised water at 25 °C for 5 hours. After ligation, cDNA constructs were transformed into competent *E. Coli,* amplified, and purified as described in sections *2.2.2-2.2.5.* Correct orientation of the insert was determined by sequencing carried out by

Protein and Nucleic Acid Chemistry Laboratory (PNACL) at the University of Leicester (Leicestershire, UK).

2.2.2 Transformation of competent bacteria

Competent bacterial cells were transformed according to the manufacturer's instructions. In brief, 50 µl of competent bacterial cells were placed into a pre-chilled falcon tube and mixed with 1 µg of plasmid cDNA before incubation, on ice, for 30 minutes. The mixture was then 'heat-shocked' by incubation in a water bath at 42°C for 45 seconds, before immediate transfer and incubation on ice for 5 minutes. 450 µl of SOC medium (2% w/v tryptone, 0.5% w/v yeast extract, 10 mM NaCl, 2.5 mM KCl, 10 mM MgCl2, 10 mM MgSO4, and 20 mM glucose) was added before incubation in a shaking incubator at 220 rpm, 37 °C for 1 hour. Following this incubation, 20-200ul of the bacterial culture was spread evenly onto 10 cm dishes containing a layer of LB Agar (1% w/v tryptone, 0.5% w/v yeast extract, 1% w/v NaCl, and 1.5% w/v bacteriological agar) infused with 50 $mg.ml^{-1}$ of ampicillin and incubated overnight at 37 °C.

2.2.3 Amplification of plasmid cDNA using competent bacteria

A single colony of bacterial culture expressing plasmid was picked and placed into a 1 L conical flask containing 250 mls of LB broth (1% w/v tryptone, 0.5% w/v yeast extract, and 1% w/v NaCl) infused with 50 $mg.ml^{-1}$ of ampicillin. This was then incubated overnight at 220 rpm and 37 °C.

2.2.4 Isolation and purification of plasmid cDNA

Plasmid cDNAs were isolated using a MaxiPrep kit from Qiagen according to manufacturer's instructions (California, USA). In brief, bacterial cultures were pelleted by centrifugation at 6000 x g at 4 °C for 15 minutes. Following centrifugation, the bacterial pellet was mixed thoroughly until homogenous with 10 ml of buffer P1 (resuspension buffer) before the addition of 10 ml of buffer P2 (lysis buffer). The mixture was inverted 6 times and then incubated at room temperature for 5 minutes. 10 mls of buffer P3

(neutralisation buffer), pre-chilled, was then added to the mixture which was then inverted 6 times to ensure mixing before incubation on ice for 20 minutes. The mixture was then centrifuged at 20,000 x g, at 4 °C for 30 minutes. Following centrifugation the supernatant was taken from the mixture and centrifuged for a further 15 minutes at 20,000 x g at 4 °C. During centrifugation the Qiagen-tip was equilibriated with 10 ml of buffer QBT, before the supernatant from the mixture was run through the column. The Qiagen-tip was then washed twice with 30 ml of buffer QC. Once filtration was complete, the plasmid cDNA was eluted using 15 ml of buffer QF, before the addition of 10.5 ml of isopropanol to precipitate the cDNA. The mixture was then centrifuged at 15000 x g at 4 °C for 30 minutes, and then the supernatant was carefully decanted leaving a plasmid cDNA pellet in the falcon tube. The pellet was washed with 5 ml of 70% ethanol, 30% deionised water before further centrifugation at 15000 x g for 10 minutes. The supernatant was removed, and then the pellet was resuspended in 0.5 ml of TE buffer (10 mM Tris, 1 mM EDTA, pH 8.0).

2.2.5 Plasmid cDNA quantification

The plasmid cDNA was measured using a Nanodrop spectrophotometer from Thermo Fisher Scientific according to manufacturer's instructions (Paisley, UK). In brief, 1 µl sample of plasmid cDNA in TE buffer was loaded into the machine, which gives out a concentration of the DNA, as well as a ratio of absorption at the wavelengths 260 nm over 280 nm. A ratio between 1.70 and 1.90 is considered pure enough for use in transfection.

2.3 Tissue culture, transfection, and membrane harvesting

2.3.1 Maintenance of HEK293 cells

HEK293 cells were maintained in Dulbecco's Modified Eagle Medium (DMEM) with 10% foetal bovine serum (FBS) in a humidified incubator (37°C, 95% air, 5% CO_2) according to a standard tissue culture protocols. At 90% confluency, cells were washed twice with sterile phosphate-buffered saline (PBS) and then trypsinised for 5 mins at 37°C using 0.25% w/v

Trypsin in PBS with 0.5 mM EDTA. Cells were mechanically dissociated from the tissue culture flask before dilution in DMEM with 10% foetal bovine serum. After centrifugation for 5 mins at 250 x g at room temperature, the supernatant was discarded and the cell pellet was triturated in media before being placed in a tissue culture flask. These cells were then incubated in the humidified incubator (37°C, 95% air, 5% CO_2) until use or further passage.

2.3.2 Transient transfection of HEK293 cells

HEK293 cells were transfected using GeneJuice from Millipore (Massachusetts, USA) as per manufacturers' instructions. In brief, HEK293 cells were seeded into T175 tissue culture flasks, and transfected at 60% confluency. 500 µl of reduced serum OptiMEM from Thermo Fisher Scientific (Paisley, UK) was mixed with 30 µl of GeneJuice and incubated for 5 minutes at room temperature before the addition, dropwise, of 10 µg of plasmid cDNA. After 15 minutes of incubation at room temperature the mixture was added dropwise into the T175 flasks containing the HEK293 cells. Cells were then incubated in a humidified incubator for 48 hours (37°C, 95% air, 5% CO_2) before use.

2.3.3 Membrane preparation from HEK293 cells

Membrane preparation was performed using a standard laboratory membrane preparation protocol. In brief, 48 hours post transfection, HEK293 cells expressing constructs of interest were washed twice with an excess of PBS before mechanically dissociation from their flasks and centrifuged at 500 x g for 10 mins at 4 °C. They were then resuspended in 10 ml of pre-chilled homogenisation buffer (20 mM HEPES, 10 mM EDTA and 1 x c0mplete protease cocktail inhibitor tablet per 50 ml). The cell suspension was homogenised at 20,000 rpm in 5 second bursts for 30 seconds before centrifugation at 350 x g at 4 °C for 5 minutes. The supernatant was retained before the pellet was resuspended and homogenised as before. After 3 homogenisation cycles, the supernatant was

centrifuged at 40000 x g at 4 °C for 45 minutes. The supernatant was discarded and then the cell pellet was resuspended in 10ml of storage buffer (20 mM HEPES, 1 mM EDTA and 1 x c0mplete protease cocktail inhibitor tablet per 50 ml). The protein concentration was determined using the Bradford assay (Bradford, 1976), and then the membranes were diluted in storage buffer to a concentration of 1 $mg.ml^{-1}$ and stored at -80 °C until use.

2.3.4 Maintenance of AV12 stable cell lines

AV12 cell lines were maintained in Dulbecco's Modified Eagle Medium (DMEM) with 10% foetal bovine serum (FBS) in a humidified incubator (37°C, 95% air, 5% CO_2) according to an in-house Lilly protocol. In brief, At 90% confluency, cells were washed twice with sterile phosphate-buffered saline (PBS) and then trypsinised for 5 mins at 37°C using 0.25% w/v Trypsin in PBS with 0.5 mM EDTA. Cells were mechanically dissociated from the tissue culture flask before dilution in DMEM with 10% foetal bovine serum. After centrifugation for 5 mins at 250 x g at room temperature, the supernatant was discarded and the cell pellet was triturated in media before being placed in a tissue culture vessel. These cells were then incubated in the humidified incubator (37°C, 95% air, 5% CO_2) until use or further passage. Selection of cells stably expressing constructs of interest was maintained by infusing the media with 0.75 $mg.ml^{-1}$ of geneticin (G418) and 0.25 $mg.ml^{-1}$ of hygromycin B and/or 0.5$mg.ml^{-1}$ of zeocin, as appropriate.

2.3.5 Membrane preparation from rat cortex samples

Brains were taken from adult Wistar rats and both hemispheres of the cortex were isolated before storage at -80 °C. Once thawed, adult rat cortical membranes were prepared as described in section *2.3.3*.

2.3.6 Membrane Preparation from Mouse Cortex Samples from mGlu5 or mGlu1 knockouts

Once thawed, mouse cortical membranes from mGlu5 or mGlu1 knockout samples were prepared as described in section *2.3.3.*

2.3.7 Culture of rat cortical neurons and astrocytes

Cortices from E18 (embryos 18 days post-gestation) Sprague-Dawley rats were purchased, already dissected and stored at 4 °C in Hibernate-E® media, from Charles River (London, UK). Pregnant females were killed by rising CO_2 followed by cervical dislocation prior to removal of embryos). The cortices were trypsinised for 15 mins at 37°C using 0.25% w/v Trypsin in PBS with 0.5 mM EDTA, with mixing every 5 minutes. The trypsin was removed, 5ml of Neurobasal medium from Invitrogen (California, USA) containing 10 % FBS was added then removed 5x to neutralise any remaining trypsin, and then 10 ml of HBSS with 1mg.ml^{-1} DNAase was added. The mixture was then triturated 15x with a fine pipette. After centrifugation at 200 x g at 15 °C for 5 minutes, the pelleted cells were resuspended in 10 ml of HBSS before being triturated 15x. The mixture was then centrifuged at 200 x g at 15 °C for 5 minutes before being resuspended in 10 ml of Neurobasal media containing B-27 Serum-free supplement from Thermo Fisher Scientific (Paisley, UK) and passed through a 100 µm filter mesh. Cells were then counted and plated on poly-D-lysine coated culture plates. For pure neuronal cultures, arabinose C was added at a final concentration of 1 µM at 2 days *in vitro (*DIV) to inhibit glial growth. Half of the media was removed every 4 days and replaced with the same volume of fresh media until use.

2.4 Radioligand binding

Radioligand binding studies were carried out based on methods disclosed in Bradley et al. (2011) using the membranes prepared from recombinant HEK293 cells transiently expressing hmGlu5, HA-hmGlu1-C1 and FLAG-hmGlu5-C2, or HA-hmGlu5-C1 and FLAG-hmGlu5-C2, as described in

section *2.3.3*, using 30 μg.well^{-1} of membranes. Radioligand binding studies were also carried out using membranes prepared from the cortices of adult Wistar rats, as described in section *2.3.4,* using 50 μg.well^{-1} of membranes. Finally, studies were also carried out using membranes prepared from the cortices of wild-type and mGlu1 knockout mice, as described in section *2.3.5,* using 50 μg.well^{-1} of membranes. The final assay volume for all experiments was 1 ml per well, with constituents made up in assay buffer (50 mM HEPES, 2 mM $MgCl_2$, pH 7.4). The mGlu5 specific negative allosteric modulator [^{3}H]-M-MPEP was used as the probe in all experiments, and non-specific binding was established using MPEP at a final assay concentration of 1 μM. After 90 minutes of incubation at room temperature, radioligand bound to membranes was separated from free radioligand by rapid vacuum filtration through GF/B glass fibre filters pre-soaked in ice-cold wash buffer (20 mM HEPES, 2 mM $CaCl_2$, 2 mM $MgCl_2$, pH 7.2) before being washed with 5 mls of pre-chilled, ice cold wash buffer. Once dried, membrane samples captured in the glass fibre filters were placed into scintillation tubes with an excess of Ultima Gold F scintillation cocktail and incubated overnight. Radioactivity was determined using a scintillation counter. DMSO concentration for all experiments was >0.05% (v/v). Radioligand binding experiments using [^{3}H]-M-MPEP carried out in this thesis are based on methods disclosed by Bradley et al., (2011).

2.4.1 Saturation binding of [^{3}H]-M-MPEP

Increasing concentrations of [^{3}H]-M-MPEP (0.15 to 20 nM) were incubated with membrane, as described in section *2.4* in assay buffer (50 mM HEPES, 2 mM $MgCl_2$, pH 7.4).

2.4.2 Inhibition binding

1 nM of [^{3}H]-M-MPEP was incubated with membrane in assay buffer with a range of concentrations of MPEP (100 pM to 1 μM), LSN2814617 (1 nM to 10 μM), VU0430644 (1 nM to 10 μM), CDPPB (1 nM to 10 μM), (S)-3,5-

DHPG (1 nM to 10 μM), ADX-47273 (1 nM to 10 μM), JNJ16259685 (100 pM to 1 μM), Ro-67 4853, or M-MPEP (10 pM to 1 μM).

In order to assess the cooperativity of binding (α) between the allosteric and orthosteric binding sites of mGlu5, a range of concentrations of allosteric modulators as described above were incubated with a single concentration of [^{3}H]-M-MPEP (1 nM) with (S)-3,5-DHPG (10 μM) or L-quisqualic acid (10 μM). For the binding of ADX-47273, where the lower asymptote was not well defined, the analysis was constrained such that the lower asymptote is greater than zero and shared between the curves generated in the absence and presence of (S)-3,5-DHPG. This constraint means the resulting pKi values can only represent an estimate, and as such should be viewed with caution.

In order to assess pharmacological interactions between the HA-hmGlu1-C1 and FLAG-hmGlu5-C2 or HA-hmGlu5-C1 and FLAG-hmGlu5-C2 constructs, a range of concentrations of mGlu5 allosteric modulators, as described above, were incubated with a single concentration of [^{3}H]-M-MPEP (1 nM) and a single concentration of (S)-3.5-DHPG (10 μM), Ro-67 4853 (10 μM), or JNJ16259685 (100 nM).

2.5 Measurement of intracellular calcium mobilisation using a Fluorescent Imaging Plate Reader (FLIPR)

2.5.1 Measurement of intracellular calcium release in AV12 stable cell lines

The use of FLIPR for quantification of calcium signalling was first disclosed by Schroeder, (1996). FLIPR functional assays were carried out according to an in-house Lilly protocol. AV12 cells were seeded at 60,000 cells per well into poly-D-lysine coated clear-bottomed black 96 well assay plates 48 hours prior to experiments. On the day of the experiment the growth media was removed and the fluorescent, calcium-sensitive dye Fluo4-AM from Invitrogen (California, USA) was dissolved with pluronic F127 at a final concentration of 1 μM/0.05% (v/v), respectively, into assay buffer (HBSS, 20

mM HEPES, pH 7.2). Cells were incubated with the Fluo4-AM/assay buffer mixture for 1 hour in the dark before being washed once with 50 µl of assay buffer. Following the addition of 100 µl of assay buffer, plates were transferred to the FLIPR^2 from Molecular Devices (California, USA) for imaging. Images were collected before and after the addition of compounds of interest at a rate of 1 image per second. Intracellular calcium release was measured as the peak height of fluorescence measured at (excitation at a wavelength of 488 nm, emission at 520 nm), expressed as Relative Fluorescent Units (RFU). This value was baseline corrected using the fluorescence in the absence of agonist.

For the measurement of intracellular calcium release induced by agonist, a range of concentrations of (S)-3,5-DHPG (100 nM to 25 µM) were added to the cells after baseline counting. For the measurement of the effect of the MPEP on agonist response, a set concentration of MPEP (1 µM), diluted in assay buffer, was pre-incubated for 3 minutes before the addition of a range of concentrations of (S)-3,5-DHPG (100 nM to 25 µM). For the measurement of the effect of positive allosteric modulators on the response of these receptors to agonist, a range of concentrations of LSN-2814617 (10 nM to 10 µM), VU0430644 (100 pM to 10 µM), CDPPB (1 nM to 3 µM), ADX-47273 (1 nM to 10 µM), CPPHA (1 nM to 10 µM), or Ro-67 4853 (1 nM to 10 µM), diluted in assay buffer, were pre-incubated for 3 minutes before the addition of a range of concentrations of (S)-3,5-DHPG (25 nM to 10 µM). For the measurement of the concentration-dependent ability of allosteric modulators to inhibit intracellular calcium release induced by receptor, a range of concentrations of MPEP (3 pM to 100 nM) or JNJ 16259685 (30 pM to 1 µM), diluted in assay buffer, were pre-incubated for 3 minutes before the addition of a single concentration of (S)-3,5-DHPG (10 µM). DMSO concentration for all experiments was > 0.05%.

2.5.2 Measurement of intracellular calcium release in rat cortical neurons

Primary cortical neurons were seeded at 66,000 cells per well into poly-D-lysine coated clear-bottomed black 96 well assay plates after preparation as

described in section *2.3.7*. At 7 DIV the growth media was removed and the fluorescent, calcium-sensitive dye Fluo4-AM from Invitrogen (California, USA) was dissolved with pluronic F127 at a final concentration of 1 μM/0.05% (v/v), respectively, into assay buffer (HBSS, 20 mM HEPES, pH 7.2, 1 μM tetrodotoxin). Cells were incubated with the Fluo4-AM/assay buffer mixture for 1 hour in the dark before being washed once with 50 μl of assay buffer. Following the addition of 100 μl of assay buffer, plates were transferred to the FLIPR^2 from Molecular Devices (California, USA) for imaging. Images were collected before and after the addition of compounds of interest at a rate of 1 image per second. Intracellular calcium release was measured as the peak height of fluorescence measured at (excitation at a wavelength of 488 nm, emission at 520 nm), expressed as Relative Fluorescent Units (RFU). This value was baseline corrected using the fluorescence in the absence of agonist.

For the measurement of intracellular calcium release induced by agonist, a range of concentrations of (S)-3,5-DHPG (100 nM to 25 μM) were added to the cells after baseline counting. For the measurement of the effect of the MPEP on agonist response, a set concentration of MPEP (1 μM), diluted in assay buffer, was pre-incubated for 3 minutes before the addition of a range of concentrations of (S)-3,5-DHPG (100 nM to 25 μM). For the measurement of the effect of positive allosteric modulators on the response of these receptors to agonist, a range of concentrations of LSN-2814617 (10 nM to 10 μM), VU0430644 (100 pM to 10 μM), or CDPPB (1 nM to 3 μM), diluted in assay buffer, were pre-incubated for 3 minutes before the addition of a range of concentrations of (S)-3,5-DHPG (25 nM to 10 μM). DMSO concentration for all experiments was less than 0.05%.

2.6 Sample preparation and immunoassays

2.6.1 Preparation of whole cell lysates from AV12 stable cell lines

AV12 cells stably expressing hmGlu5 were grown in 6-well plates prior to preparation by a standard laboratory protocol. At 90% confluency, cell

media was removed and the cells were washed twice with ice-cold PBS. After washing, 250 µl of ice-cold RIPA buffer (20 mM Tris, 3 mM EDTA, 150 mM NaCl, 1% Nonidet P-40, 0.5% Na deoxycholate, pH 7.4, one c0mplete protease inhibitor cocktail tablet per 50ml) was added and then the samples were incubated on ice for 30 minutes. After incubation, samples were centrifuged at 14000 x g at 4 ° C for 20 minutes, then the supernatant was removed and assayed for protein concentration using the Bradford method (Bradford, 1976). Samples were stored at -30 °C until use.

2.6.2 Preparation of whole cell lysates from cultured primary tissues

Primary cortical neurons, prepared as described in section *2.3.7*, were plated at a cell density of 300,000 cells per well in a poly-D-lysine coated 6-well plate. Whole cell lysates were prepared according to a standard laboratory protocol. In brief, Samples were taken at DIV1, 7, 14, and 21 as follows. Cell media was removed and the cells were washed twice with ice-cold PBS. After washing, 250 µl of ice-cold RIPA buffer (20 mM Tris, 3 mM EDTA, 150 mM NaCl, 1% Nonidet P-40, 0.5% Na deoxycholate, pH 7.4, one c0mplete protease inhibitor cocktail tablet per 50ml) was added and then the samples were incubated on ice for 30 minutes. After incubation, samples were centrifuged at 14000 x g at 4 ° C for 20 minutes, then the supernatant was removed and assayed for protein concentration using the Bradford method (Bradford, 1976). Samples were stored at -30 °C until use.

2.6.3 Preparation of mouse cortex samples treated with vehicle, LSN2814617, or VU0430644

Samples of cortices from mice treated with vehicle, 100 $mg.kg^{-1}$ LSN2814617, or 100 $mg.kg^{-1}$ VU0430644 daily for seven days were kindly provided, snap-frozen, by Lilly (Surrey, UK). Samples were thawed before the addition of 500 µl of pre-chilled RIPA buffer per cortex. Samples were triturated until homogenous and then incubated on ice for 30 minutes. After incubation, samples were centrifuged at 14,000 x g at 4 °C for 20 minutes.

The supernatant was removed and assayed for protein concentration using the Bradford method (Bradford, 1976) before storage at -80 °C prior to use.

2.6.4 Sample loading, SDS-PAGE (Sodium Dodecyl Sulfate-Polyacrylamide Gel Electrophoresis), and Western blotting

Seperation of proteins using SDS-PAGE and detection of proteins using specific antibodies was performed based on a standard laboratory protocol. The original description of SDS-PAGE separation and Western blotting are described in Towbin et al. (1979) Burnette (1981). Samples of lysates (outlined in sections *2.6.1* to *2.6.3)* or membranes (outlined in sections *2.3.3*, *2.3.5*, and *2.3.6*) were added to 5x concentrated loading buffer (125mM Tris, 200mM dithiothreitol, 4% SDS, 20% glycerol, and 0.05% bromophenol blue, pH 6.8) at a ratio of 4 parts sample to 1 part buffer, mixed, and then incubated for 5 minutes at room temperature. Samples were then loaded onto SDS-PAGE gels, alongside molecular weight markers from Bio-Rad (Hertfordshire, UK) and electrophoresis was conducted at 200 V for 45 to 55 minutes. Once complete, the gels containing sample proteins were incubated in semi-dry transfer buffer (25mM Tris, 192mM Glycine, 0.5% sodium dodecyl sulfate (SDS), 20% methanol). Protein samples were then transferred to nitrocellulose membranes, pre-soaked in transfer buffer, by electrophoresis at 400 mV for 1 hour using a semi-dry transfer cell from Bio-Rad (Hertfordshire, UK). The protein samples immobilised on nitrocellulose membranes were then incubated in PBS (pH 7.4) with 5 % non-fat milk powder (w/v) and 0.1% Tween-20 (v/v) for 30 minutes at room temperature to block non-specific antibody binding sites. Samples were then incubated with primary antibodies of interest (outlined in Table 2.6.4.1) diluted in PBS (pH 7.4) with 5 % non-fat milk powder (w/v) and 0.1% Tween-20 (v/v) overnight at 4 °C. Samples were then washed 3 times with 15 ml of PBS (pH 7.4) with 0.1 % Tween-20 (v/v) before incubation with their relevant secondary antibodies (outlined in Table 2.6.4.1) diluted in PBS (pH 7.4) with 5 % non-fat milk powder (w/v) and 0.1% Tween-20 (v/v) for 1 hour at room temperature. After incubation, samples were again washed as before prior

to the addition of standard ECL reagents and photographic development using Hyperfilm ECL film from GE Healthcare Life Sciences (Amersham, UK).

2.6.5 Immunocytochemistry

Immunocytochemistry experiments were performed according to a standard laboratory protocol based upon a manufacterer's protocol (Abcam, Massachusetts, USA). Recombinant cell lines of interest were seeded onto poly-D-lysine coated 10 mm glass coverslips in 24-well tissue culture plates at a low density at least 24 hours before experimental use. On the day of the experiment, cells were washed three times with 500 µl of PBS prior to fixation with 4 % paraformaldehyde diluted in PBS. Coverslips bearing cells were incubated in fixative for 10 minutes to allow crosslinking of cellular proteins. For the permeabilisation of cells, coverslips bearing cells were incubated for 10 minutes at room temperature in PBS containing 0.2 % Triton X-100 (v/v). Following fixation (and permeabilisation, where applicable), coverslips were washed 3 times with 500 µl of PBS before incubation in blocking buffer (PBS, pH 7.4, 1% Bovine Serum Albumin (BSA) (w/v)) for an hour at room temperature. Coverslips were then incubated in primary antibody diluted in blocking buffer (see Table 2.6.6.1) for 1 hour at room temperature. Coverslips were then washed a further three times with 500 µl of PBS prior to the addition of the relevant fluorescent secondary antibody (see Table 2.6.6.1). Coverslips were incubated with the appropriate fluorescent secondary antibody, diluted in blocking buffer, for 1 hour at room temperature in darkness prior to washing as before. Coverslips were then mounted using VECTASHIELD HardSet Antifade Mounting Medium with DAPI from Vector Laboratories (California, USA). Once set, mounted coverslips were stored in the dark at 4 °C until imaging.

2.6.6 Histochemistry and immunohistochemistry

Perfusion-fixed mouse brain samples (outlined in section 2.1.4) were processed in paraffin wax and 5 μM slices were taken coronally. Sections were prepared and stained, where appropriate, with haemotoxylin and eosin in house by Dr. Jennifer Edwards at the MRC Toxicology Unit (Leicester, UK). Immunohistochemistry using antibodies was performed according to a protocol kindly provided by Dr. Sophie Bradley (MRC Toxicology Unit, Leicester, UK). After antigen retrieval the samples were washed in PBS with 0.25% Triton X-100 (v/v) three times for 15 minutes per wash prior to incubation with blocking buffer (PBS, pH 7.4, with 0.1% Triton X-100 (v/v), 10 % goat serum (v/v), and 5% BSA (w/v)) for 2 hours at room temperature. After blocking, samples were incubated with primary antibodies diluted in blocking buffer (outlined in Table 2.6.7.1) overnight at 4 °C. After washing as before, samples were incubated with fluorescent secondary antibodies (outlined in Table 2.6.7.1). After three further washes as before, samples were mounted using VECTASHIELD HardSet Antifade Mounting Medium with DAPI from Vector Laboratories (California, USA). Once set, mounted coverslips were stored in the dark at 4 °C until imaging.

2.6.7 Whole cell ELISA

HEK293 cells were transfected with constructs of interest as described in section 2.3.2. Whole Cell ELISA experiments were performed according to a protocol kindly provided by Dr. Adrian Butcher (MRC Toxicology Unit, Leicester). In brief, 24 hours post-transfection, cells plated into poly-D-lysine coated black 96-well tissue culture plates at a cell density of 40,000 cells.well^{-1} and then incubated for a further 24 hours in a humidified incubator, as described previously, prior to experimental use. The cells were washed once with 200 μl of PBS (pH 7.4) followed by the addition of 100 μl of 4 % PFA diluted in PBS (pH 7.4) for 10 minutes at room temperature for fixation. For the permeabilisation of cells, wells were incubated for 10

minutes at room temperature in PBS containing 0.2 % Triton X-100 (v/v). Following fixation (and permeabilisation, where applicable), wells were washed 3 times with 100 µl of PBS before incubation in blocking buffer (PBS, pH 7.4, 1% Bovine Serum Albumin (BSA) (w/v)) for an hour at room temperature. Coverslips were then incubated in HRP-conjugated primary antibody diluted in blocking buffer (outlined in table 2.6.6.1) for 1 hour at room temperature in prior to washing as before. 50 µl of ECL reagent was then added to each well, and chemiluminesence was assessed using a CLARIOstar plate reader from BMG Labtech (Offenburg, Germany).

2.7 Assessment of cell death in primary cultures

Cell death was assessed by measuring the activity of extracellular lactate dehydrogenase (LDH) activity (Decker and Lohmann-Matthes, 1988). In the following experiments, LDH activity was measured using a CytoTox 96® Non-Radioactive Cytotoxicity Assay from Promega (Wisconsin, USA), according to manufacturer's instructions. In brief, a sample of 50 µl of media was taken from each well and frozen until use. On the day of experiment, the 50 µl media samples were thawed and placed into a clear-bottom black 96-well plate along with 50 µl of CytoTox 96® Reagent and incubated in the dark for 30 minutes at room temperature. After 30 minutes, 50 µl of stop solution was added, and absorbance of light at a wavelength of 490 nm was measured using a CLARIOstar plate reader from BMG Labtech (Offenburg, Germany).

2.7.1 Cell death measurement in primary cortical neurons

Primary cortical neurons were plated into poly-D-lysine coated 96-well plates at a cell density of 100,000 cells.well^{-1}, prior to use in this assay, and arabinose C at 1 µM was included in the media from 2 DIV to inhibit glial growth. At 7 DIV, 50 % of the media was removed, then the cells were pre-incubated for 30 minutes with a set concentration of either LSN-2814617 (100 µM) or MPEP (100 µM). After incubation, a range of concentrations of L-glutamate (1 µM to 10 mM), dissolved in cell media, was added to the

primary cortical cultures. The cultures were then returned to the humidified incubator for 24 hours before the assessment of LDH activity as described above. The concentration-dependent effect of MPEP on excitotoxic cell death was further assessed as before, but with a range of concentrations of MPEP (100 nM to 100 μM).

2.7.2 The Effect of allosteric modulators of mGlu5 on the time course of excitotoxic cell death induced by L-glutamate in primary cortical neurons

Primary cortical neurons were plated into poly-D-lysine coated 96-well plates at a cell density of 100,000 cells.well^{-1}, prior to use in this assay, and arabinose C at 1 μM was included in the media from 2 DIV to inhibit glial growth. At 7 DIV, 50 % of the media was removed, then the cells were pre-incubated for 30 minutes with a set concentration of either LSN-2814617 (100 μM) or MPEP (100 μM). Following this, a set concentration of L-glutamate (316 μM) was added to each well, and media samples were taken at a range of timepoints (1 minute to 24 hours) and frozen prior to the assessment of LDH activity as described above.

2.7.3 The effect of LSN2814617 of mGlu5 on the excitotoxic cell death induced by L-glutamate in mixed primary cortical neurons and astrocytes

Primary cortical neurons were plated into poly-D-lysine coated 96-well plates at a cell density of 100,000 cells.well^{-1}, prior to use in this assay. At 14 DIV, 50 % of the media was removed, then the cells were pre-incubated for 30 minutes with a set concentration of LSN-2814617 (10 μM) dissolved in cell media. After incubation, a range of concentrations of L-glutamate (10 nM to 1 mM), dissolved in cell media, was added to the primary cultures. The cultures were then returned to the humidified incubator for 24 hours before the assessment of LDH activity as described above.

2.8 Data analysis

2.8.1 Analysis of radioligand binding data

Radioligand binding data was analysed using Prism v6.07 from GraphPad (California, USA). For the saturation binding of [^{3}H]-M-MPEP, total binding and non-specific binding data was globally fitted using equation 1, where Y is radioligand binding (fmol.mg protein^{-1}), B_{max} is the maximal binding capacity of the available receptors, [A] is the radioligand concentration, K_A is the equilibrium dissociation constant of the radioligand and NS is the fraction of non-specific radioligand binding.

(*Equation 1*)

$$Y = \frac{B_{max} \cdot [A]}{[A] + K_A} + NS \cdot [A]$$

For inhibition of the binding of [^{3}H]-M-MPEP, the specific binding data from each compound was fitted to equation 2, where Emax and Basal are the maximal and minimal asymptotes of the curve, respectively, Log [B] is the concentration of inhibitor, Log IC_{50} is the logarithm of the concentration of inhibitor that reduces half the maximal radioligand binding for each binding site and n_H is the Hill slope (constrained to unity). IC_{50} values were converted to K_I values (equilibrium dissociation constant) using equations described by Cheng & Prusoff (1973).

(*Equation 2*)

$$Y = Basal + \frac{(E_{MAX} - Basal)}{1 + 10^{(Log[B] - LogIC_{50}) \cdot n_H}}$$

Where an third compound, acting at a different binding site to [^{3}H]-M-MPEP, was added to the inhibition binding reaction between [^{3}H]-M-MPEP and an allosteric compound, the cooperativity of binding (α) was calculated as a ratio between the K_A of the allosteric modulator in the presence of the third compound, and the K_A of the allosteric modulator in the absence of the third compound, based upon the allosteric ternary complex model outlined

in Lazareno & Birdsall (1995). This method assumes that the third ligand has no cooperative effect on the radioligand. For ADX-47273 data, the lower asymptote was constrained such that, whether (S)-3,5-DHPG was present or not, the lower asymptotes are shared and above zero. These are logical assumptions that allow an estimation of the co-operativity between the allosteric and orthosteric sites, but the pKi values should be viewed with caution.

2.8.2 Analysis of functional data

Analysis of agonist stimulated dose-response data was fitting using a four parameter equation (equation 3) with the operational model of agonism described by Black & Leff (1983) (equation 4) where Y represents the response of the agonist, Emax is the maximum system response, basal is the basal activity of the system, [A] is the concentration of the agonist, EC_{50} is the concentration of agonist required to elicit 50 % of its maximal response, n is the slope factor of the transducer function that links occupancy to response, E_{MAX} is the maximum reponse of the system under measure, τ is an index of the efficacy of the agonist, and K_A is the dissociation constant of the agonist. The operational model assumes that the affinity of the agonist remains unchanged regardless of the system being measured, and that the agonist obeys the law of mass action.

(*Equation 3*)

$$Y = Basal + \frac{(E_{MAX} - Basal)}{1 + 10(logEC_{50} + log[A])^n}$$

(*Equation 4*)

$$E = \frac{E_{MAX}\tau[A]}{[A](1+\tau) + K_A}$$

The ability of the allosteric modulators to inhibit agonist response in constructs of interest was analysed using the four parameter dose-response model (equation 3) where $logEC_{50}$ is replaced with $logIC_{50}$, the concentration

of antagonist required to elicit 50 % of the maximum inhibition of agonist activity.

Comparisons between ligands and constructs, where appropriate, were analysed using an unpaired, two-tailed t-test, with a p-value <0.05 considered statistically significant.

The ability of positive allosteric modulators to potentiate the action of an orthosteric agonist were analysed globally using the full operational model of allosterism. This model accounts for the ability of allosteric modulators to modulate orthosteric agonist affinity and efficacy as well as activating the receptor in their own right (Black and Leff (1983); discussed in Leach et al., 2007):

(*Equation 5*)

$$Y = Basal + \frac{(E_M - Basal)\cdot\left(\left(\tau_A[A](K_B + \alpha\beta[B])\right) + \tau_B[B]\cdot K_B\right)^n}{([A]K_B + K_A K_B + K_A[B] + \alpha[A][B])^n + [\![(\tau]\!]_A[A](K_B + \alpha\beta[B]) + \tau_B[B]\cdot K_B)^n}$$

This model estimates the equilibrium dissociation constants and relative efficacies of orthosteric and allosteric (K_A, τ_A or K_B, τ_B, respectively) ligands, as well as the cooperativity of binding and function between the two (α and ß, respectively). *Basal* is the response of the system in the absence of ligand and the terms E_M and n denote the maximal possible system response and the slope factor of the transducer function that links occupancy to response respectively. For Chapter 3 data, this model was fit by constraining τ_B to zero, K_B and α were constrained to the values of the equilibrium dissociation constant and binding co-operativity (α) derived in corresponding radioligand binding studies. For Chapter 4, data was fit to a four parameter logistic equation (Equation 3), and the change in pEC50 of (S)-3,5-DHPG in the absence and presence of the highest concentration of positive allosteric modulator was used to compare constructs as appropriate.

2.8.3 Estimating the total number of neurons in a coronal section of the anterior cortex

In order to estimate the number of neurons present in a coronal section, stained with eosin and haematoxylin in house, the total area of the cortical hemisphere of each coronal sample from three mice was calculated using an Axiovert 200M microscope. The total number of neurons was counted manually from 3 portions of each hemisphere and then an estimate of the total number of neurons was made by multiplying the average by the scaling factor of the sample area vs. the full cortical area.

2.8.4 Densitometric analysis of immunoblot data

AUC values were generated from each band of interest from Western blot data using ImageJ from the National Institutes for Health (Maryland, USA).

2.8.5 Statistical analyses

Any comparisons between a pair of data sets were made using an unpaired, one-tailed t-test with a p-value less than 0.05 considered statistically significant. Multiple data sets were compared using a one-way analysis of variance (ANOVA) test where a p value less than 0.05 was considered statistically significant. Further multiple comparisons were performed using Tukey's Honest Significant Difference (HSD) post-hoc analysis with a p-value of less than 0.05 considered statistically significant.

Details of statistical analyses performed can be found in the figure legend or accompanying table, as appropriate.

Table 2.6.4.1: Summary of antibodies and their use in Western blotting.

Antibody	Species	Dilution	Company	Catalogue No.
Monoclonal anti-mGluR5	Rabbit	1:5000	Abcam	ab76316
Monoclonal anti-ß tubulin	Mouse	1:1000	Sigma-Aldrich	T8328
Monoclonal anti-mGluR1	Rabbit	1:1000	Cell Signalling Technology	#12551
Monoclonal anti-GAPDH	Rabbit	1:2000	Cell Signalling Technology	#2118
HRP-conjugated anti-rabbit	Goat	3:10,000	Bio-Rad	1706515
HRP-conjugated anti-mouse	Goat	3:10,000	Bio-Rad	1706516

Table 2.6.6.1: Summary of antibodies and their use in immunocytochemistry and whole cell ELISA.

Antibody	Species	Dilution	Company	Catalogue No.
Monoclonal anti-mGluR5	Rabbit	1:300	Abcam	ab76316
Monoclonal anti-HA	Rat	1:1000	Roche	11867423001
Monoclonal anti-FLAG	Mouse	1:1000	Sigma-Aldrich	F3165
Monoclonal anti-HA-Peroxidase	Rat	1:1000	Roche	12013819001
Alexafluor ® 488-conjugated anti-rabbit	Donkey	1:1000	Thermo Fisher Scientific	R37118
Alexafluor ® 488-conjugated anti-rat	Donkey	1:1000	Thermo Fisher Scientific	A-21208
Alexafluor ® 488-conjugated anti-mouse	Donkey	1:1000	Thermo Fisher Scientific	R37115

Table 2.6.7.1: Summary of antibodies and their use in immunohistochemistry.

Antibody	Species	Dilution	Company	Catalogue No.
Monoclonal anti-mGluR5	Rabbit	1:300	Abcam	ab76316
Monoclonal anti-GFAP	Mouse	1:400	Sigma-Aldrich	G3893
Monoclonal anti-NeuN	Rabbit	1:500	Millipore	ABN78
Polyclonal anti-c fos	Rabbit	1:5000	Sigma-Aldrich	F7799
Alexafluor ® 488-conjugated anti-rabbit	Donkey	1:1000	Thermo Fisher Scientific	R37118
Alexafluor ® 488-conjugated anti-mouse	Donkey	1:1000	Thermo Fisher Scientific	R37115

Chapter 3. Pharmacological characterisation of allosteric modulators acting at the mGlu5 receptor

3.1 Introduction

The pharmacological manipulation of the mGlu5 receptor may provide a way to intervene in addiction, anxiety, depression, schizophrenia, fragile X syndrome, Parkinson's disease and Alzheimer's disease (Dekundy et al., 2006; Kumar et al., 2015; Niswender and Conn, 2010). The development of ligands binding at the orthosteric site yielded the Group I selective agonist (S)-3,5-DHPG, a derivative of phenylglycine with micromolar affinity at these receptors (Brabet et al., 1995). Further development yielded an mGlu5 specific orthosteric agonist, CHPG, though neither compound has progressed to the clinic due to the lack of subtype selectivity and poor blood-brain barrier permeability typical of the amino acid derivative ligands (Doherty et al., 1997; Spooren et al., 2001). Recently, the development of ligands acting outside of the orthosteric site, so-called 'allosteric modulators', has allowed the development of highly subtype-specific ligands with favourable pharmacokinetic properties (Conn et al., 2009).

The development of the mGlu5 specific PAMs DFB, CPPHA, and CDPPB showed the potential of exploiting the TMDs for drug development. CDPPB, for example, binds at the same site as MPEP, and has a micromolar potency for the mGlu5 receptor and is reported to be a partial agonist in its own right (Kinney et al., 2005; Lindsley et al., 2004). The fact that these allosteric modulators bind at an alternative site to the endogenous ligand is a great advantage for the development of subtype specific compounds as it is thought that there is less evolutionary pressure for conservation of the allosteric sites and so these sites have a more diverse, exploitable range of residues (Lewis et al., 2008). Interestingly, in the case of mGlu5, small changes to allosteric ligands can change their activity entirely, and this has been demonstrated for several structural chemotypes of mGlu5 allosteric modulator (Wood et al., 2011). For example, the prototypical PAM DFB can

be modified to exhibit NAM activity by substitution of the fluoro groups with methoxy groups (O'Brien et al., 2003). Furthermore, substitution of the same groups with chloro moieties yields a silent allosteric modulator (SAM). Similarly, MPEP can be modified to produce NAMs which do not fully block receptor activity, M5-MPEP and Br-5MPEPy, as well as the SAM 5MPEP (Rodriguez et al., 2005). The mGlu5 ago-PAM (a PAM with intrinsic agonist activity) ADX-47372 has proven to be similarly malleable: alterations of chemical groups on this compound resulted in PAMs lacking agonist activity, as well as NAMs of various inhibitory strength (Engers et al., 2009; Lamb et al., 2011). These 'molecular switches' are useful in understanding structure-activity relationships, and may yield further unique compounds at mGlu5 and many other GPCRs.

As well as the effect of molecular switches on compound activity, another important consideration for compound action is their individual interaction with the receptor. Given that allosteric modulators have cooperativity of binding (α) and of function (ß), it is possible that there are examples of mGlu5 compounds which operate via differing modes of action. It has been previously demonstrated that MPEP and 5MPEP do not alter the binding of L-quisqualic acid at the orthosteric site, and so their inhibitory action must be through cooperativity of function (Bradley et al., 2011). The same study showed that many of the PAMs developed for mGlu5 act in a mechanistically different way. DFB displays approximately equal cooperativity of function and binding, CDPPB has a greater cooperativity of binding, and ADX-47273 having a greater cooperativity of function. Understanding these properties of allosteric modulators is vital in order to develop structure activity relationships and expand the pharmacological toolbox available for this receptor.

In this chapter, I use pharmacological methods to delineate the characteristics of one recently reported PAM, LSN-2814617, and a previously unpublished PAM, VU0430644, both binding at the MPEP binding site (Gilmour et al., 2013). I then go on to characterise their

allosteric interaction with the orthosteric agonist (S)-3,5-DHPG in order to delineate the mechanism by which they exert their influence on receptor signalling. Finally, I investigate these properties in rat brain samples and primary rat cortical neurons in culture in order to delineate any species-specific actions of these compounds and validate the study of the action of mGlu5 PAMs in recombinant cell lines.

3.2 Results

3.2.1 HEK293 cells express transiently transfected hmGlu5 constructs at a level sufficient for radioligand binding studies

HEK293 cell lines are well established as a vehicle for the production of recombinant proteins (Thomas and Smart, 2005). With that in mind, the expression of hmGlu5 in membranes prepared from transiently transfected HEK293 cells was assayed using immunoblot and immunocytochemical techniques (Figure 3.2.1.1). Western blotting using an mGlu5 specific antibody showed the presence of a protein band with a molecular weight of approximately 150 kDa in the membranes derived from transfected cells, with no band present in the untransfected cells (Figure 3.2.1.1A). Equal protein loading was confirmed by immunoassaying the levels of glyceraldehyde 3-phosphate dehydrogenase (GAPDH), a housekeeping gene expressed in many tissue types (Barber et al., 2005). Immunocytochemical analysis of untransfected cells (Figure 3.2.1.1B) and cell transiently transfected with hmGlu5 cDNA (Figure 3.2.1.1C) was performed by immunostaining with an mGlu5 specific antibody and DAPI, a fluorescent nuclear-staining agent. In untransfected and hmGlu5 transfected cells, nuclear staining with DAPI was clear, however, mGlu5 staining was only visible in hmGlu5 transfected cells.

To assess the expression of hmGlu5 in membranes prepared from HEK293 cells, a membrane titration was performed, and based on that 30 $\mu g.well^{-1}$ was chosen for radioligand binding experiments due to a high signal window and a depletion value less than 10 % (*data not shown*). To further investigate the expression of hmGlu5 in our membrane preparations, a [^{3}H]-M-MPEP saturation analysis was performed (Figure 3.2.1.2).

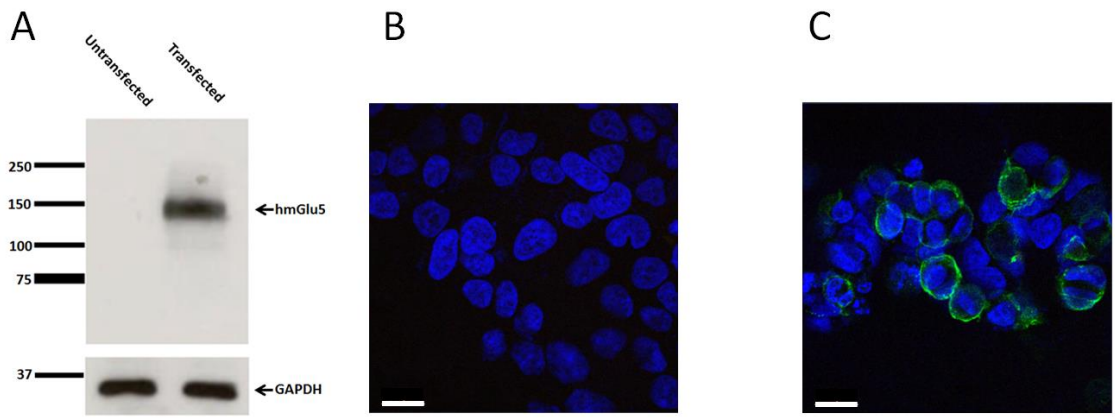

Figure 3.2.1.1 The transient transfection of HEK293 cells with an hmGlu5 construct was assessed using immunochemical methods. An immunoblot analysis of membranes from either unstransfected HEK293 cells or HEK293 cells transiently transfected with hmGlu5 was performed with an anti-mGlu5 primary antibody, and an anti-GAPDH antibody to assess protein loading (A). Immunocytochemical analysis was performed on paraformaldehyde-fixed HEK cells which were either untransfected (B), or transiently transfected with hmGlu5 (C). The data shown are single representative images from three independent experiments. The images represent 40x magnification with the scale bar representing 20 μm.

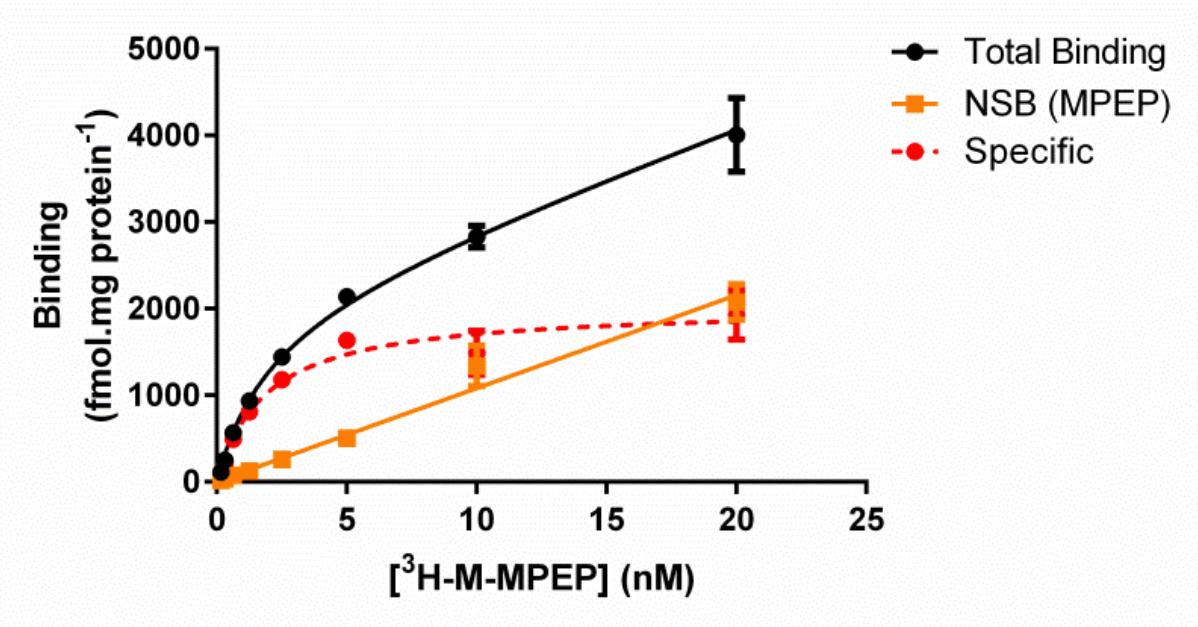

Figure 3.2.1.2 Saturation binding of [^{3}H]M-MPEP in membranes prepared from HEK293 cells transiently expressing hmGlu5. The properties of [^{3}H]M-MPEP binding to mGlu5 receptors were assayed by incubating a range of concentrations (0.1-20 nM) with a set amount of membrane in the absence and presence of 1μM MPEP. The graph shows the combined data from 3 independent experiments performed in duplicate.

Saturation binding analysis revealed [^{3}H]-M-MPEP binds to hmGlu5 with an affinity (K_D) of 1.99 ± 0.59 nM, which is similar to previously reported figures (Gasparini et al., 2002). Receptor expression in this system (B_{MAX}) was 2096 ± 191 fmol.mg^{-1}. This represents a sufficient signal window for the pharmacological characterisation of ligands acting at this mGlu5 binding site.

3.2.2 LSN-2814617 and VU0430644 inhibit radioligand binding at the MPEP site of hmGlu5

The MPEP binding site is perhaps the most well characterised on the mGlu5 receptor, with several different classes of allosteric modulator binding at this location (Malherbe et al., 2003). Radioligand inhibition binding studies were performed, using [^{3}H]-M-MPEP as a probe, in order to discover the site of action of LSN-2814617 and VU0430644. Firstly, the ability of three reference compounds, MPEP, CDPPB, and (S)-3,5-DHPG, to competitively inhibit the binding of [^{3}H]-M-MPEP at hmGlu5, under equilibrium conditions, was assessed in order to validate the assay (Figure 3.2.2.1). A set concentration of [^{3}H]-M-MPEP, approximately equal to the K_D concentration calculated in section 3.2.1, was incubated with a range of concentrations of ligand for 90 minutes at room temperature, prior to rapid vacuum filtration through glass fibre filters. The mGlu5 NAM MPEP and the mGlu5 PAM CDPPB inhibited the binding of radioligand in a concentration-dependent manner with pK_i values of 8.2 ± 0.08 and 5.74 ± 0.22, respectively. These affinity values are similar to those reported previously (Gasparini et al., 2002; Kinney et al., 2005). The Group I orthosteric agonist (S)-3,5-DHPG did not have any effect on the binding of [^{3}H]-M-MPEP, indicating that there is no cooperativity of binding between the orthosteric agonist and the allosteric radioligand.

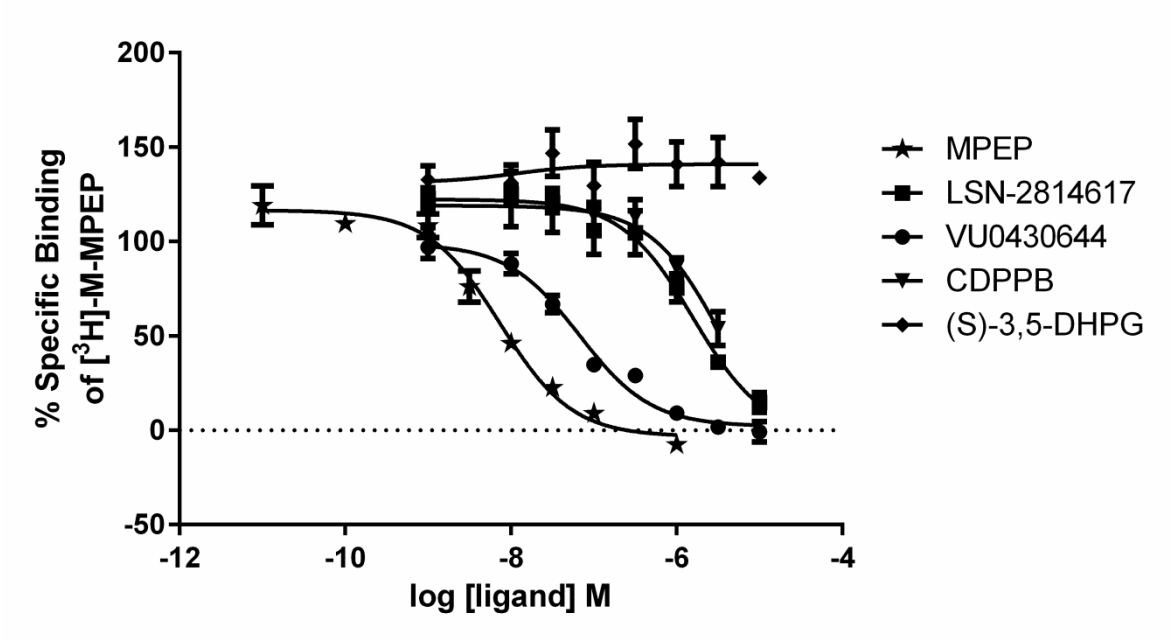

Figure 3.2.2.1 Inhibition of the binding of [^{3}H]-M-MPEP by various ligands. A range of concentrations of ligand were incubated with a set concentration, approximately equivalent to K_D, of [^{3}H]-M-MPEP. The graph shows the combined data from 3 independent experiments performed in duplicate. Quantitative analysis of the data is summarised in Table 3.2.2.1.

Table 3.2.2.1 A summary of the quantitative analysis of ligands binding at hmGlu5 in HEK293 cell membranes.

Compound	pK_i	n
MPEP	8.24 ± 0.08	3
LSN-2814617	5.91 ± 0.14	3
VU0430644	7.29 ± 0.09	3
CDPPB	5.74 ± 0.22	3
(S)-3,5-DHPG	-	3

The previously reported mGlu5 PAM LSN-2814617, and the previously unpublished PAM VU0430644, were also assessed for their ability to inhibit the binding of the radioligand. Both LSN-2814617 and VU0430644 fully inhibited the binding of radioligand in a concentration-dependent manner with pK_i of values of 5.91 ± 0.14 and 7.29 ± 0.09, respectively. This data suggests that both LSN-2814617 and VU0430644 bind at the MPEP site. The quantitative analysis of these compounds is summarised in Table 3.2.2.1.

3.2.3 PAMs of mGlu5 display differing cooperativities with the orthosteric site

PAMs of mGlu5 acting at the MPEP binding site have been previously demonstrated to increase the affinity of orthosteric agonists in membranes from the rat cortex and cultured rat cortical astrocytes (Bradley et al., 2011). In order to assess whether this effect occurs with (S)-3,5-DHPG at the human receptor radioligand binding assays were performed using HEK293 cell membranes transiently transfected with hmGlu5. The ability of LSN-2814617 and VU0430644 to potentiate the affinity of (S)-3,5-DHPG at the human mGlu5 receptor was assessed, and compared to the reference compounds CDPPB and ADX-47273. The ability of these ligands to inhibit a K_D concentration of [^{3}H]-M-MPEP was assessed as in section 3.2.2 or in the presence of a concentration of (S)-3,5-DHPG sufficient to occupy the orthosteric site (Figure 3.2.3.1). As before all compounds decreased the binding of the radioligand in a concentration dependent manner in the absence of (S)-3,5-DHPG. In the presence of 10 μM (S)-3,5-DHPG, the affinity of LSN-2814617 and VU0430644 was slightly increased (Figure 3.2.3.1A and B), inferring a weak positive cooperativity between the PAMs and the orthosteric agonist, however, this increase was not statistically significant when the curves were compared ($p > 0.05$, unpaired Student's t-test). CDPPB and ADX-47273 displayed a larger, statistically significant increase in affinity (Figure 3.2.3.1C and D, $p < 0.05$, unpaired Student's t-test), which suggests that these PAMs display a higher cooperativity with

(S)-3,5-DHPG than LSN-2814617 and VU0430644. The cooperativity values of the reference compounds with (S)-3,5-DHPG are comparable to those previously reported between these PAMs and the orthosteric agonist L-quisqualic acid (Bradley et al., 2011), suggesting that they do not display probe dependency. The pharmacological properties of these compounds, calculated using the allosteric ternary complex model, are summarised in Table 3.2.3.1.

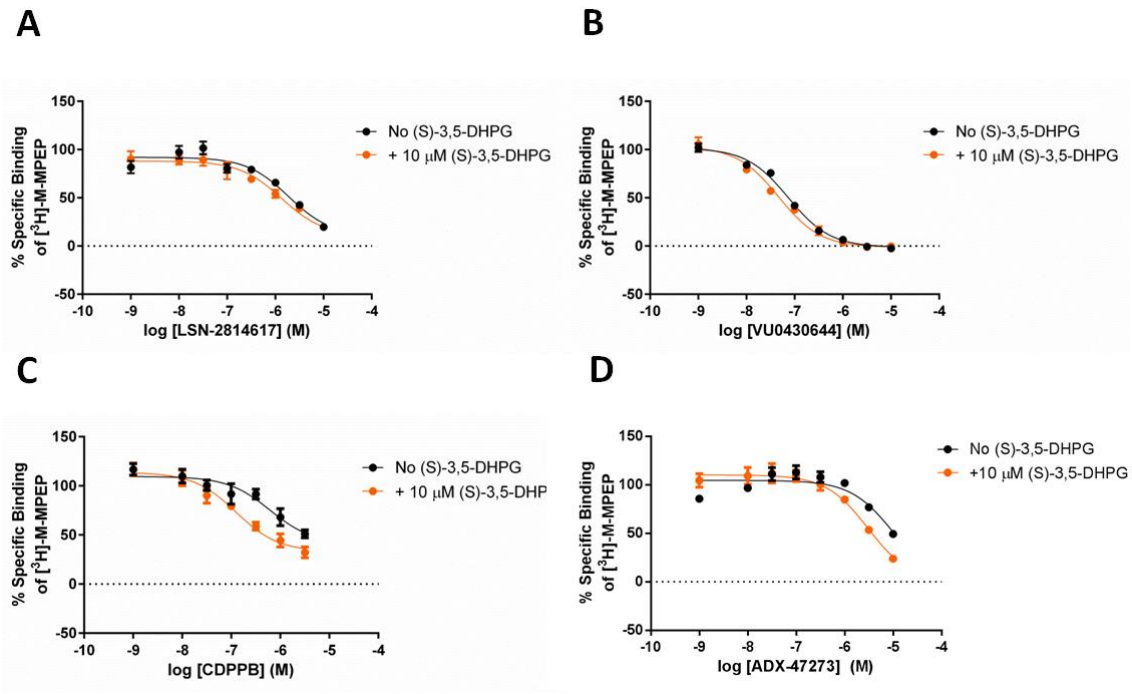

Figure 3.2.3.1 The ability of the radioligand to bind specifically to an allosteric site on the receptor was assessed in the presence of a range of concentrations of (A) LSN-2814617, (B) VU0430644, (C) CDPPB, or (D) ADX-47273. The effect of an orthosteric compound, (S)-3,5-DHPG, on the affinity of these compounds was also determined. These graphs represent the combined data of 3-4 independent experiments performed in duplicate. A summary of the analysis of this data can be found in Table 3.2.3.1.

Table 3.2.3.1 A summary of the quantitative analysis of ligands binding at hmGlu5 in HEK293 cell membranes in the absence and presence of (S)-3,5-DHPG. Statistical significance between the pKi in the absence and presence of (S)-3,5-DHPG was determined with an unpaired Student's t-test.

Compound	pK_i				α	n
	No (S)-3,5-DHPG	+ 10 μM (S)-3,5-DHPG		ΔpK_i (log α)		
LSN-2814617	5.87 ± 0.12	6.02 ± 0.13	N.S	N.D.	≈1.00	3
VU0430644	7.27 ± 0.06	7.48 ± 0.06	N.S	N.D.	≈1.00	3
CDPPB	6.24 ± 0.19	6.79 ± 0.15	*	0.55	3.55	4
ADX-47273	5.07 ± 0.13	5.67 ± 0.15	**	0.60	3.98	4

* $p < 0.05$
** $p < 0.01$

3.2.4 AV12 cells stably co-expressing hmGlu5 with EAAT1 are suitable for functional studies

Studying the function of mGlu5 in recombinant cell lines is complicated by the fact the orthosteric agonist, L-glutamate, is an endogenously produced amino acid in all cell types. An AV12 cell line expressing EAAT1 reduces the extracellular level of L-glutamate and allows study of the receptor in the absence of activation by endogenous L-glutamate. Initial transfection, selection and validation of the stable cell line expressing hmGlu5 was kindly performed by Lilly (Surrey, UK). The expression of hmGlu5 in the AV12 stable cell line was also confirmed using immunochemical techniques herein (Figure 3.2.4.1). Western blotting using an mGlu5 specific antibody showed the presence of a protein band with a molecular weight of approximately 150 kDa in whole cell lysates of the hmGlu5-AV12-EAAT1 cell line, with no band present in the untransfected cells (Figure 3.2.4.1A). Equal protein loading was confirmed by immunoassaying the levels of beta-tubulin, a cytoskeletal protein expressed in many tissue types. Immunocytochemical analysis of untransfected cells (Figure 3.2.4.1B) and the hmGlu5-AV12-EAAT1 cells (Figure 3.2.4.1C) was performed by immunostaining with an mGlu5 specific antibody and DAPI In untransfected and hmGlu5 transfected cells, nuclear staining with DAPI was clear, however, mGlu5 staining was only visible in hmGlu5 transfected cells.

The mGlu5 receptor couples mainly to the Gq/11 pathway, activating phospholipase C resulting in the production of inositol phosphates and diacyl-glycerol, which ultimately leads to the release of intracellular calcium and the activation of PKC (Schoepp et al., 1990). With this in mind, the functional response of the hmGlu5-AV12-EAAT1 cell line was assessed by measuring agonist-stimulated intracellular calcium release using the fluorescent, calcium-sensitive probe Fluo4-AM, detected using a fluorescent imaging plate reader (FLIPR). (S)-3,5-DHPG induced a concentration-dependent increase in intracellular calcium release (Figure 3.2.4.1D), with an pEC_{50} value of 5.85 ± 0.06, comparable to previously reported values

(O'Brien et al., 2003). The (S)-3,5-DHPG stimulated release could be fully inhibited by 1 μM MPEP, indicating that the calcium release induced by agonist in this cell line is hmGlu5-dependent. This data shows this cell line expresses hmGlu5 at a level suitable for use in functional studies.

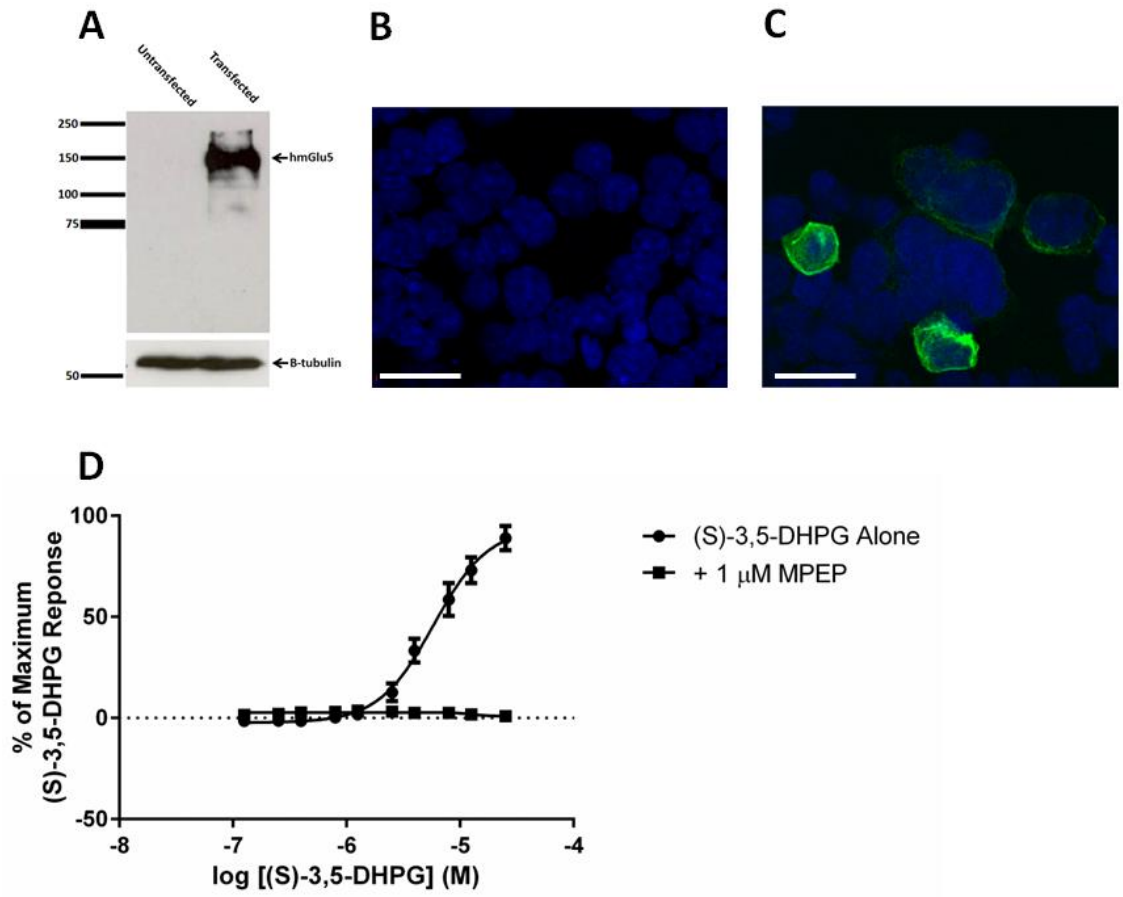

Figure 3.2.4.1 The expression of hmGlu5 in a stably transfected AV12 cell line was assessed using immunochemical and fluorimetric methods. An immunoblot analysis of membranes from either untransfected or AV12 cells stably transfected with hmGlu5 was performed with an anti-mGlu5 primary antibody, and an anti-ß-tubulin antibody to assess protein loading (A). Immunocytochemical analysis was performed on paraformaldehyde-fixed AV12 cells which were either untransfected (B), or stably transfected with hmGlu5 (C). Imaging was performed at 40x magnification with the scale bar representing 20 μm. The activation of the Gq/11 pathway in response to a range of concentrations (100 nM to 30 uM) to the Group I selective metabotropic glutamate receptor agonist (S)-3,5-DHPG was assessed by imaging transient calcium release using Fluo-4 AM as a probe (D). The ability of the mGlu5 specific negative allosteric modulator MPEP to inhibit this response was also assayed. Panel (A), (B), and (C) show representative examples from three independent experiments performed in singlicate. Panel (D) shows the combined data of three independent experiments performed in triplicate, where each data point represents the mean ± S.E.M.

3.2.5 LSN-2814617 and VU0430644 are positive modulators of hmGlu5 function

Section 3.2.3 demonstrated the ability of four PAMs of mGlu5 to increase the affinity of orthosteric agonist. PAMs can also potentiate receptor action by increasing the ability of an orthosteric agonist to activate a receptor, a property known as functional cooperativity (ß). Furthermore, they can activate the receptor in the absence of agonist, so-called allosteric agonism (May et al., 2007). The ability of one unpublished and three previously reported PAMs of mGlu5 to potentiate the release of intracellular calcium in the hmGlu5-AV12-EAAT1 cell line upon agonist stimulation was assessed using FLIPR (Figure 3.2.5.1). LSN-2814617 and VU0430644 acted as PAMs, causing a concentration-dependent increase in the potency of (S)-3,5-DHPG with a maximal response of 188.8 ± 4.4 % and 200.9 ± 6.3 %, respectively, of the response evoked by (S)-3,5-DHPG stimulation alone (Figure 3.2.5.1A and B).. The data was analysed using an operational model of allosterism, and revealed LSN-2814617 displays almost double the cooperativity with (S)-3,5-DHPG compared to VU0430644. Using the α values generated in section 3.3.3, the contribution of cooperativity of binding and functional cooperativity can be derived. This analysis suggests that LSN-2814617 and VU0430644 potentiate (S)-3,5-DHPG responses by increasing the ability of the agonist to activate hmGlu5.

The previously reported PAM CDPPB caused a concentration-dependent increase in the potency of (S)-3,5-DHPG with a maximal response of 193.8 ± 8.9 % of the response evoked by (S)-3,5-DHPG stimulation alone (Figure 3.2.5.1C). Furthermore, CDPPB potentiated the response induced by (S)-3,5-DHPG to a greater extent than either LSN-2814617 or VU0430644. The cooperativity value displayed herein is concurrent with previously reported values (Gilmour et al., 2013). Deriving the contribution of affinity and efficacy driven cooperativity, as before, showed that CDPPB primarily potentiates hmGlu5 activation by increasing the affinity of the agonist, rather than enhancing the ability of (S)-3,5-DHPG to activate the receptor.

This allosteric mode of action has been reported previously and is different to that of LSN-2814617 and VU0430644 (Bradley et al., 2011).

Finally, the previously reported PAM ADX-47273 caused a concentration-dependent increase in the potency of (S)-3,5-DHPG with a maximal response of 369.0 ± 7.2 % of the response evoked by (S)-3,5-DHPG stimulation alone (Figure 3.2.5.1D). ADX-47273 has a larger potentiating action than the other PAMs tested herein, displaying a cooperativity nearly quadruple that of CDPPB. Combining the functional data with the cooperativity of binding value generated previously shows that ADX-47273 potentiates (S)-3,5-DHPG responses mainly by increasing the ability of the agonist to transduce a signal, rather than increasing the affinity at the orthosteric site, a mechanistically different mode of potentiation to CDPPB.. The cooperativity values for LSN-2814617, CDPPB, and ADX-47273 are comparable to previously reported values (Gilmour et al., 2013). Quantitative analysis of the effect of these allosteric modulators using the operational model of allosterism is summarised in Table 3.2.5.1.

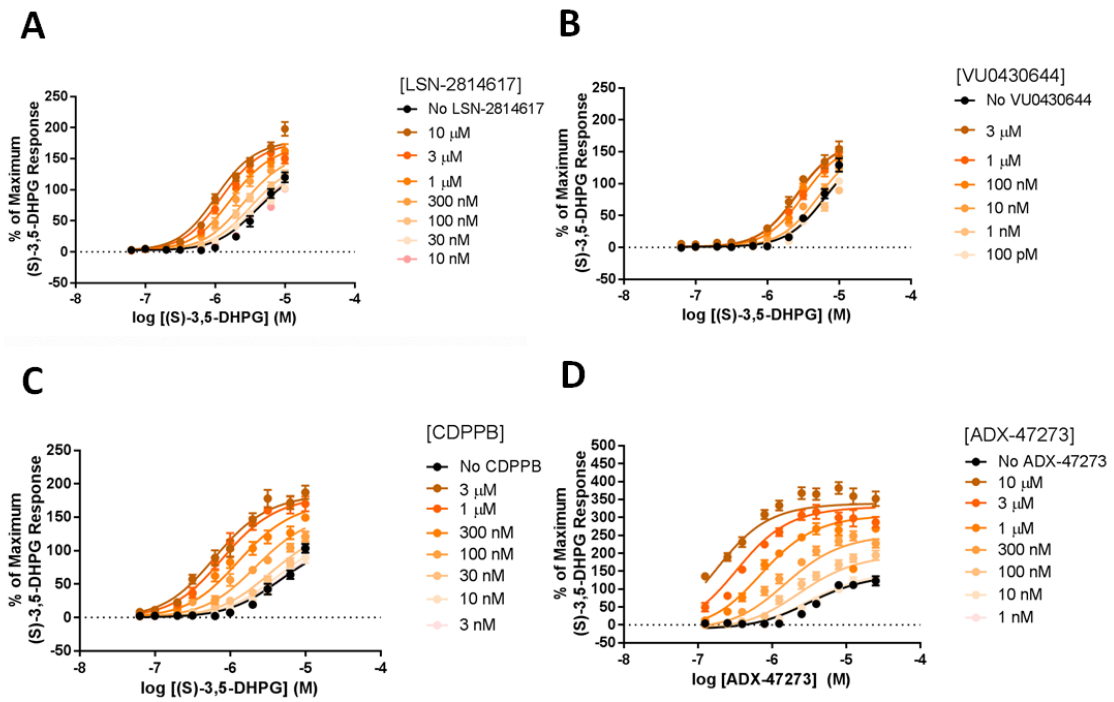

Figure 3.2.5.1 The ability of the allosteric ligands LSN-2814617 (A), VU0430644 (B), CDPPB (C), and ADX-47273 (D) to potentiate the activation of the hmGlu5 receptor by the orthosteric agonist (S)-3,5-DHPG in a concentration dependent manner was assessed in stably transfected AV12 cells. Cells were pre-incubated (5 mins) with a range of concentrations of potentiator before the addition of a range of concentrations of (S)-3,5-DHPG. The data shown represents the mean ± S.E.M from three independent experiments performed in triplicate. Analysis using the operational model of allosterism is summarised in **Table 3.2.5.1**.

Table 3.2.5.1 A summary of the quantitative analysis of ligands acting at hmGlu5 in our stably transfected hmGlu5-AV12-EAAT1 cell line using the operational model of allosterism.

Compound	Potency (pEC50)	Combined Cooperativity (αβ)	Cooperativity of Function (β)	n
(S)-3,5-DHPG	5.85 ± 0.06	-	-	4
LSN-2814617	-	≈4.16	4.16	3
VU0430644	-	≈2.49	2.49	3
CDPPB	-	11.01	3.10	3
ADX-47273	-	41.04	10.40	3

3.2.6 Expression of mGlu5 in membranes prepared from adult Wistar rat cortex

Given that animal models are often used in order to study the function of mGlu5 *in vivo,* it is important to characterise the action of compounds in the rat homologue of the receptor in case species differences are present. The expression of rmGlu5 in membranes prepared from adult Wistar rat cortex samples was assayed using immunoblot and radioligand binding techniques (Figure 3.2.6.1). Western blotting using an mGlu5 specific antibody showed the presence of a protein band with a molecular weight of approximately 150 kDa in membranes prepared from rat cortex samples, with no band present in membranes prepared from mGlu5 knock-out mouse cortex samples (Figure 3.2.6.1A). Equal protein loading was confirmed by immunoassaying the levels of GAPDH. The level of mGlu5 was assessed in membranes prepared from adult Wistar rat cortex samples. A membrane titration was performed, and based on that 100 μg.well^{-1} was chosen for radioligand binding experiments due to a high signal window and a depletion value less than 10 % (*data not shown*). To further investigate the expression of mGlu5 in our membrane preparations, a [^{3}H]-M-MPEP saturation analysis was performed (Figure 3.2.6.1B). Saturation binding analysis revealed [^{3}H]-M-MPEP binds to hmGlu5 with an affinity (K_D) of 1.68 ± 0.43 nM. Receptor expression in this system (B_{MAX}) was 1082 ± 161 fmol.mg^{-1}. The K_D and B_{MAX} of [^{3}H]-M-MPEP binding to mGlu5 in rat brain membrane from our experiments are in agreement with previously reported data (Hintermann et al., 2007). This data suggests that membrane preparations from rat cortex are suitable for the study of ligands acting at the mGlu5 receptor.

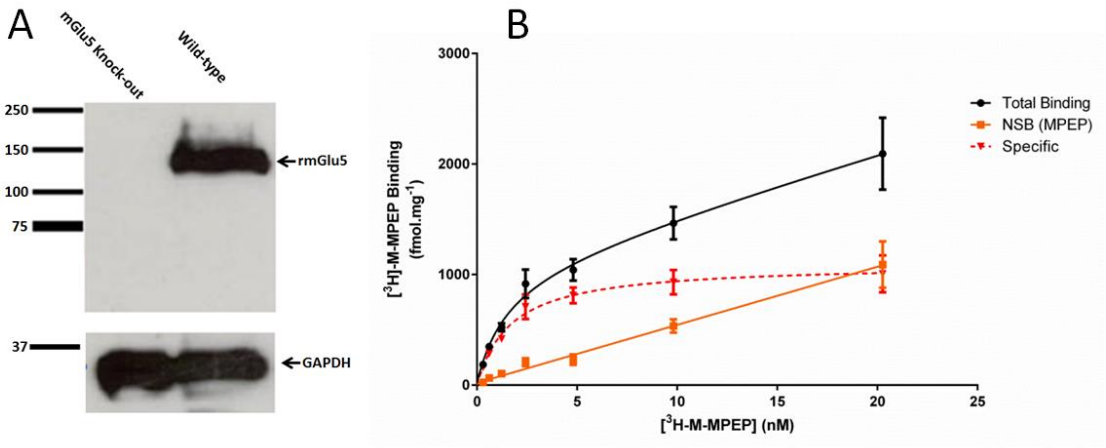

Figure 3.2.6.1 The expression of mGlu5 in membranes prepared from adult wistar rat cortex samples was assessed using immunoblot and radioligand binding methods. An immunoblot analysis of membranes from either wild-type rat cortex samples or membranes prepared from mouse mGlu5 knock-out brains was performed with an anti-mGlu5 primary antibody, and an anti-GAPDH antibody to assess protein loading (A). Saturation binding of [^{3}H]M-MPEP in membranes prepared from adult rat cerebral cortex (B). The properties of [^{3}H]M-MPEP binding to mGlu5 receptors were assayed by incubating a range of concentrations (0.1-20 nM) with a set amount of rat cortex membrane in the absence and presence of 1 uM MPEP. The graph shows the combined data from 3 independent experiments performed in duplicate.

3.2.7 *LSN-2814617 and VU-0430644 display no significant co-operativity of binding at the rat receptor*

Differences in the affinity cooperativity of mGlu5 PAMs and orthosteric agonists have been reported between rat astrocyte and rat cortex membranes (Bradley et al., 2011). In order to assess the affinity cooperativity between the orthosteric binding site and three PAMs acting at MPEP binding site of mGlu5 in the rat cortex, inhibition binding experiments were performed in the absence and presence of 10 μM (S)-3,5-DHPG as before (Figure 3.2.7.1). LSN-2814617 and VU0430644 all inhibited the binding of [^{3}H]-M-MPEP in a concentration dependent manner, with pK_i values comparable to those generated at the human mGlu5 receptor. Furthermore, the affinity cooperativity between the PAMs and (S)-3,5-DHPG was similar to that in the human receptor, suggesting that there is no difference in the action of these compounds at the rat and the human receptor.

In order to assess whether LSN-2814617 or VU0430644 display any probe dependency at mGlu5, the effect of orthosteric binding site occupancy by L-quisqualic acid on the affinity of these compounds was assayed in membranes prepared from rat cortex samples (Figure 3.2.7.2). The cooperativity of LSN-2814617 or VU0430644 were not significantly different from those generated in the presence of (S)-3,5-DHPG ($p > 0.05$, unpaired, two-tailed Student's t-test), suggesting no probe dependence. The quantitative analysis of these experiments using the allosteric ternary complex model is summarised in Table 3.2.7.2.

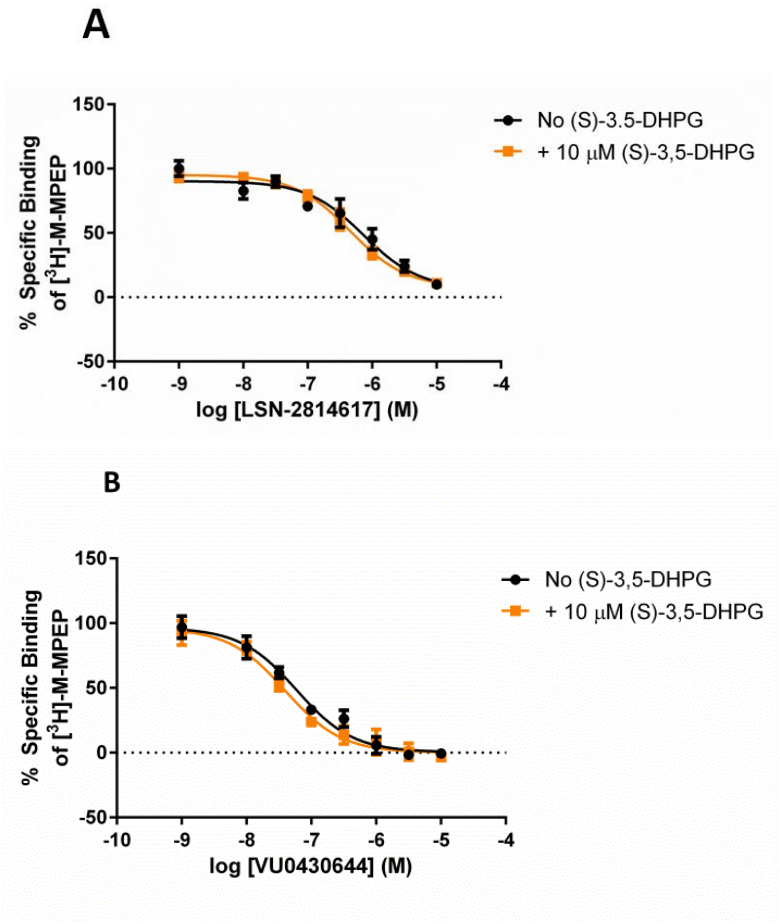

Figure 3.2.7.1 The ability of a set concentration, approximately equivalent to the K_D, of [^{3}H]M-MPEP to bind in membranes prepared from rat cortex. The ability of the radioligand to bind specifically to an allosteric site on the receptor was assessed in the presence of a range of concentrations of (A) LSN-2814617, or (B) VU0430644. The effect of an orthosteric compound, (S)-3,5-DHPG, on the pharmacological properties of these compounds was also determined. These graphs represent the combined data of 3 independent experiments performed in duplicate. A summary of the analysis of this data can be found in Table 3.2.7.1.

Table 3.2.7.1 A summary of the quantitative analysis of ligands binding at mGlu5 in rat cortex membranes in the absence and presence of (S)-3,5-DHPG.

Compound	pK_i				α	n
	No (S)-3,5-DHPG	+ 10 μM (S)-3,5-DHPG		ΔpK_i (log α)		
LSN-2814617	6.34 ± 0.16	6.54 ± 0.09	N.S.	N.D.	1.00	3
VU0430644	7.57 ± 0.06	7.74 ± 0.06	N.S.	N.D.	1.00	3

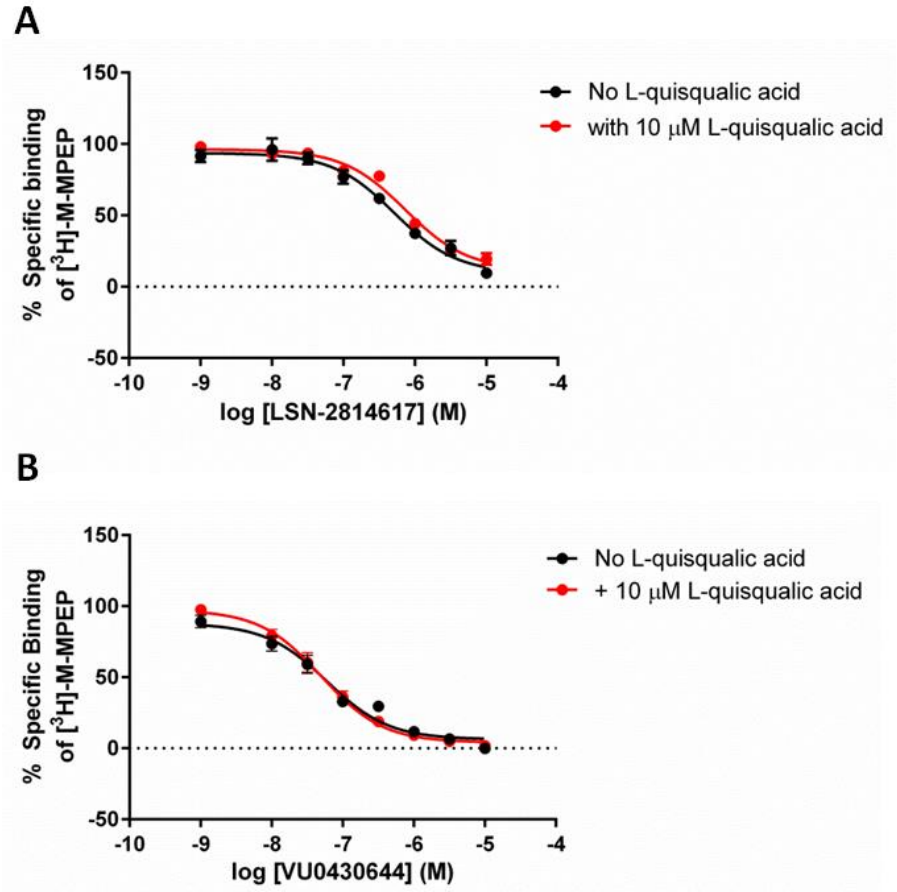

Figure 3.2.7.2 The ability of a set concentration, approximately equivalent to the K_D, of [^{3}H]M-MPEP to bind in membranes prepared from rat cortex. The ability of the radioligand to bind specifically to an allosteric site on the receptor was assessed in the presence of a range of concentrations of (A) LSN-2814617 or (B) VU0430644. The effect of an orthosteric compound, L-quisqualic acid, on the pharmacological properties of these compounds was also determined. These graphs represent the combined data of 3-4 independent experiments performed in duplicate. A summary of the analysis of this data can be found in Table 3.2.7.2.

Table 3.2.7.2 A summary of the quantitative analysis of ligands binding at mGlu5 in rat cortex membranes in the absence and presence of (S)-3,5-DHPG.

Compound	pK_i				α	n
	No L-quisqualic acid	+ 10 μM L-quisqualic acid		ΔpK_i (log α)		
LSN-2814617	6.56 ± 0.11	6.47 ± 0.08	N.S.	N.D.	≈1.00	3
VU0430644	7.49 ± 0.07	7.59 ± 0.09	N.S.	N.D.	≈1.00	4

3.2.8 LSN-2814617 and VU0430644 potentiate the mGlu5 receptor in cultured rat cortical neurons

In order to investigate the functional effect of the mGlu5 PAMs on (S)-3,5-DHPG induced calcium release at the rat receptor primary cortical neurons from the rat were grown for 7 DIV and mGlu5 response was assessed by measuring agonist-stimulated intracellular calcium release using Fluo4-AM, detected using a fluorescent imaging plate reader (FLIPR). (S)-3,5-DHPG induced a concentration-dependent increase in intracellular calcium release (Figure 3.2.8.1), with an pEC_{50} value of 5.95 ± 0.01, comparable to previously reported values (Gilmour et al., 2013). The (S)-3,5-DHPG stimulated release could be robustly inhibited by 1 μM MPEP, though a (S)-3,5-DHPG response equal to 7.25 ± 0.35 % of the maximum (S)-3,5-DHPG response could be obtained. In the presence of 1 μM MPEP, (S)-3,5-DHPG caused intracellular calcium release with a pEC_{50} value of 5.39 ± 0.04. This indicated that the calcium release induced by agonist in this cell line is mostly mGlu5-dependent, with a small proportion of that response transduced through another receptor, likely mGlu1.

The ability of LSN-2814617 and VU0430644 to potentiate the release of intracellular calcium in cultured primary cortical neurons upon agonist stimulation was also assessed (Figure 3.2.8.2). Both PAMs potentiated the (S)-3,5-DHPG induced intracellular calcium release, with values comparable to those generated previously at the human receptor. The allosteric mode of action of each PAM in terms of cooperativity was preserved across species. The quantitative analysis of this data is summarised in Table 3.2.5.1.

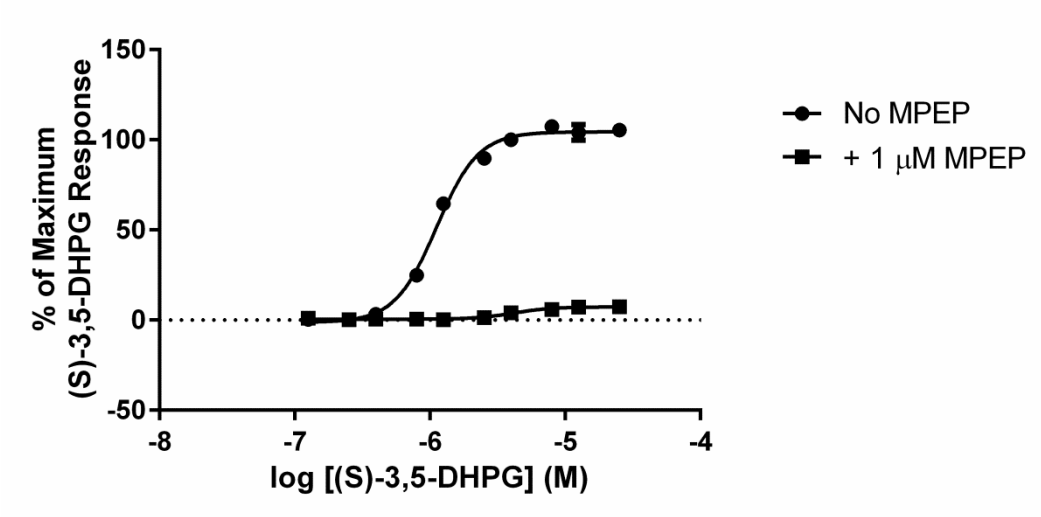

Figure 3.2.8.1 The activation of the Gq/11 pathway in cultured rat primary cortical neurons (DIV7) in response to a range of concentrations (100 nM to 30 μM) to the group I selective metabotropic glutamate receptor agonist (S)-3,5-DHPG was assessed by imaging transient calcium release using Fluo-4 AM as a probe. The ability of the $mGlu_5$ specific negative allosteric modulator MPEP to inhibit this response was also assayed. The graph shows the combined data of two independent experiments performed in triplicate, where each data point represents the mean ± S.E.M.

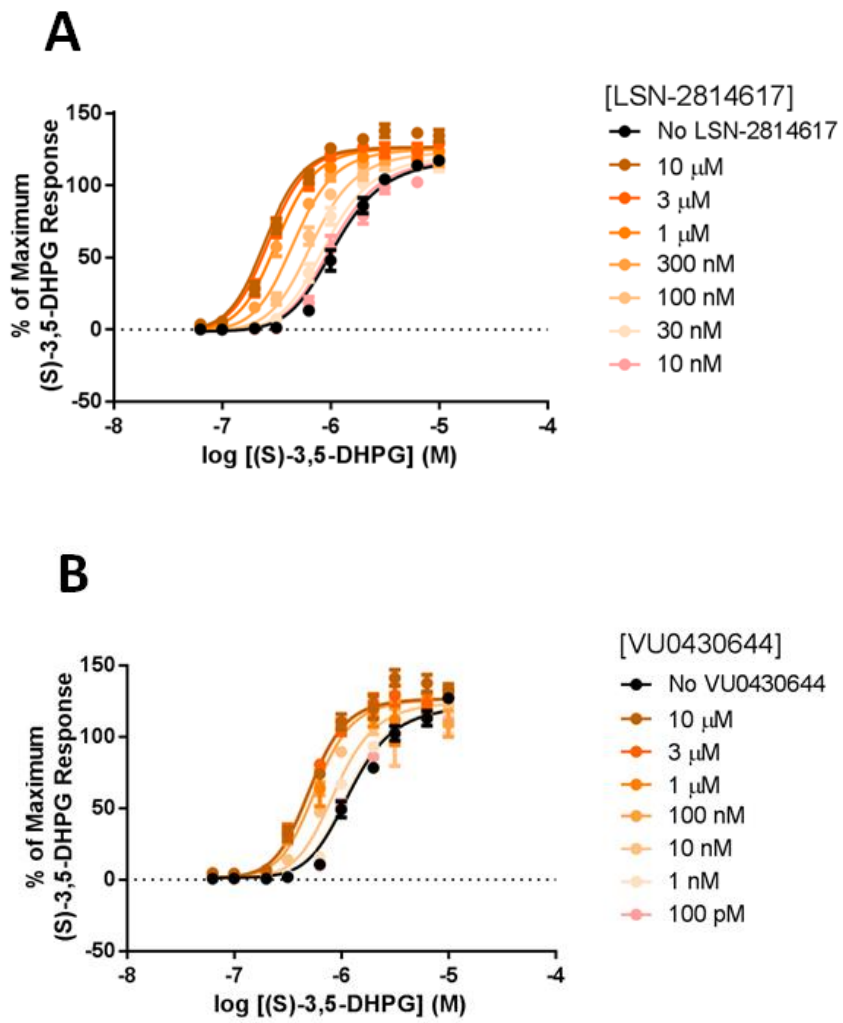

Figure 3.2.8.2 The ability of the allosteric ligands LSN-2814617 (A) and VU0430644 (B) to potentiate the activation of the mGlu5 receptor by the orthosteric agonist (S)-3,5-DHPG in a concentration dependent manner was assessed in rat cortical neurons grown for 7 days *in vitro*. Cells were pre-incubated (3 mins) with a range of concentrations of potentiator before the addition of a range of concentrations of DHPG. The data shown represents the mean ± S.E.M from two independent experiments performed in triplicate. Analysis using the operational ternary complex model are summarised in Table 3.2.8.2.

Table 3.2.8.2 A summary of the quantitative analysis of ligands acting at mGlu5 in cultured rat primary cortical neurons using the operational model of allosterism.

Compound	Potency (pEC50)	Combined Cooperativity (αβ)	Cooperativity of Function (β)	n
(S)-3,5-DHPG	5.95 ± 0.01	-	-	2
LSN-2814617	-	≈3.35	3.35	2
VU0430644	-	≈1.92	1.92	2

3.3 Discussion

Orthosteric compounds acting at mGlu5 have failed to progress to the clinic to date due to lack of blood-brain barrier permeability and poor subtype selectivity. Allosteric modulators hold great promise in overcoming these issues by allowing the development of small molecule ligands that exploit the more heterologous TMDs of these receptors (Conn et al., 2009). NAMs and PAMs of mGlu5 have been extensively studied for several characteristics. The *in vivo* effects of allosteric modulators in mouse models of multiple disease types have given a great insight into their potential therapeutic use. For example, negative allosteric modulators have shown promise in mouse models of fragile X syndrome, Alzheimer's disease, anxiety, depression, and addiction (Michalon et al. 2012; Kumar et al. 2015; Tatarczyńska et al. 2001; Lea & Faden 2006). Positive allosteric modulators may also be beneficial therapeutically, for instance CDPPB has been shown to be effective in mouse models of schizophrenia and Huntington's disease (Doria et al., 2015; Gastambide et al., 2012).

Understanding the *in vivo* effects of these compounds is useful for predicting their potential therapeutic use, as well as allowing insight into their bioavailability and pharmacokinetic properties. It is equally important that the *in vitro* pharmacological characteristics are not ignored, as understanding the properties of the compound acting at a molecular level is key to driving discovery of further compounds. Allosteric modulators of all types, NAMs, SAMs, and PAMs, have been reported for mGlu5 and delineation of their pharmacological properties often focuses on the measure of affinity (K_i) and potency (EC_{50}). Recently, efforts have been made to understand the underlying mechanisms by which PAMs of mGlu5 modulate the action of the orthosteric ligands: by a combination of cooperativity of binding (α) and cooperativity of function (ß) (Bradley et al., 2011; Langmead and Christopoulos, 2006). Bradley et al. (2011) found that CDPPB displayed a combined cooperativity (αß) value of 25 in astrocytes, using [^{3}H]IP_x accumulation as the probe for Gq/11 activity, and that the α value for

CDPPB was different for mGlu5 expressed in membranes prepared from rat astrocytes and rat cortex. The experimental data generated herein for the human mGlu5 receptor in recombinant AV12 cells shows that CDPPB has a combined co-operativity (αß) of 11.01 in this system, with a co-operativity of binding (α) of 3.55, and an efficacy co-operativity (ß) of 3.10. Care should be taken when comparing this data with that of the aforementioned study for several reasons: Firstly, the data herein was generated using a different functional assay, with a different timepoint for measurement of the response. The operational model of agonism assumes the ligands and receptor are at equilibrium (Black and Leff, 1983), and that cannot be assumed to be true with FLIPR as the measurement point is after only 3 minutes of pre-incubation with allosteric modulator, and the immediate response of the agonist. Secondly, the data for CDPPB has been generated in homologues from different species of the mGlu5 receptor, rat and human, and there may be species specific differences between these receptors. Finally, where (S)-3,5-DHPG was used as an agonist herein, the aforementioned study used L-quisqualic acid. Therefore, the difference could be an example of probe dependency. As a further study it would be interesting to address these points by repeating the functional data herein using the IP_x assay with rat receptors expressed in these recombinant cells to see whether this is an example of species specific effects. In order to elucidate whether this is an example of probe dependence, the effect of these PAMs on L-quisqualic acid response could be assayed using FLIPR, so that the orthosteric ligands can be compared in the same system.

It is worth noting that the maximum response of the system herein increases with increasing concentration of allosteric modulator at the human mGlu5 receptor. One possible explanation is that the kinetics of the response are altered by the allosteric modulators, and given that FLIPR measures the average fluorescence of a plurality of cells, this could manifest as an increased peak response. Comparing the time to peak of the calcium response to (S)-3,5-DHPG in the absence and presence of these PAMs would elucidate whether this explanation is true. It is also interesting to note that

this effect was not observed for the rat mGlu5 receptor data herein, indicating that perhaps there is a species specific effect on kinetics if that is the explanation for the increased response in this system. This increase in the maximum response has been noted for mGluRs in other assay types (Fell et al., 2011; Mathiesen et al., 2003). In one of these studies, the mGlu2 PAM, THICC showed a concentration dependent increase in maximum response of mGlu2 to L-glutamate stimulation as measured by GTPγS binding (Fell et al., 2011). With hindsight the data to answer this question with respect to my own functional data would have been readily available, but regrettably it could not be included at the time of writing.

The cooperativity values generated in this study using primary tissues were in concurrence with those generated in recombinant systems. This perhaps showed that the recombinant system provides a good analogue for delineating the cooperativity of compounds at the receptor level between species and native and recombinant systems. With this in mind we generated cooperativity values for another previously reported PAM: ADX-47273. In our study this compound displayed different properties to those shown in the previous report, and the same caveats apply. Interestingly, our data showed that ADX-47273 potentiates the actions of (S)-3,5-DHPG to almost quadruple that which CDPPB does, and these allosteric modulators appear to act in a mechanistically different way: Though both compounds display cooperativity of binding and function, ADX-47273 has a greater effect on enhancing the ability of the orthosteric ligand to induce a response, whereas CDPPB increases the ability of the orthosteric ligand to bind to hmGlu5. These allosteric modes of action are in agreement with studies previously reporting these findings (Bradley et al., 2011).

The recently reported PAM LSN-2814617 induced a fold-shift in (S)-3,5-DHPG potency in rat cortical neurons and in recombinant AV12 cells in good agreement with our own data in the same systems (Gilmour et al., 2013). Interestingly, LSN-2814617 potentiation appears to be efficacy driven, with insignificant co-operativity of binding. The unpublished PAM

VU0430644 appeared to act in much the same way as LSN-2814617 though with a smaller degree of modulation. Interestingly, VU0430644 was the ligand with the highest affinity at mGlu5, followed by CDPPB, LSN-2814617, and ADX-47273 in descending order. In contrast, combined cooperativity values were highest in ADX-47273, followed by CDPPB, LSN-2814617, and VU0430644 in descending order. The decoupling of these aspects of ligand action show the importance of fully delineating the action of allosteric modulation in terms of cooperativity. Furthermore, by studying the diverse chemical structures of these compounds perhaps structure activity relationships can begin to be rationalised. For example, studies have already demonstrated which chemical moieties on the CDPPB molecule are responsible for affinity and efficacy of the compound (Zou et al., 2011). This study showed that understanding how a compound works on a molecular level allows us to develop compounds with different properties, and indeed it demonstrated that substitution of specific chemical groups yielded compounds with a lower efficacy. This may be desirable therapeutically if a smaller degree of mGlu5 modulation is required to correct a receptor in a disease state.

Given our inhibition binding data, it is clear that [^{3}H]-M-MPEP is binding at the MPEP binding site, as MPEP fully inhibited the binding of the radioligand. In addition VU0430644, LSN-2814617, CDPPB, and ADX-47273 all appear to bind at the MPEP binding site. Perhaps utilising mutagenesis techniques would help us to understand which moieties of each compound interact with which residue and could unlock a structure-activity relationship to allow similar divergent molecules to be discovered. It is known that PAMs acting at other sites on mGlu5, have displayed stimulus bias, whereby certain downstream signalling events are preferentially activated in the presence of agonist. For example, CPPHA does not activate MAPK pathways, but can robustly potentiate intracellular calcium release (Zhang et al., 2005). Whether these differences are due to differing binding sites on the mGlu5 receptor, mechanistic differences in their allosteric action, or both remains to be delineated and investigating the signalling

bias of the allosteric modulators outlined in this chapter would potentially offer insight. It is interesting to speculate whether PAMs which increase the affinity of orthosteric agonists lead to signalling profiles typical of those agonists, whereas perhaps PAMs which alter the coupling of the orthosteric agonist to a functional response could potentially alter their signalling profile by differently enhancing the ability of the agonist to couple to G protein or ß-arrestin mediated responses. Indeed LY2033298, a PAM acting at the muscarinic M4 receptor, has been demonstrated to have differing cooperativity of function depending on which downstream signalling pathway is probed (Leach et al., 2009). Understanding these allosteric properties may be critical in the development of compounds that retain therapeutic efficacy without potentiating potentially harmful signalling cascades.

Chapter 4. Exploring the use of a constitutive dimer construct for investigating the pharmacological consequences of heterodimerisation of mGlu1 and mGlu5

4.1 Introduction

The dimerisation of Family C GPCRs is accepted to be crucial for their function (Pin et al., 2003). The homodimerisation of mGlu5 was the first to be reported, based on experimental evidence that higher order oligomers of mGlu5 were observed from immunoblotting experiments where proteins were separated by SDS-PAGE. Romano et al. (1996) reported that an HA-tagged mGlu5 construct could co-immunoprecipitate with a wild-type version of the receptor, providing the first evidence that mGlu5 forms homodimers. This study provides evidence that homodimers are covalently linked by disulphide bonds, as the dimeric version of the receptor was not found under reducing conditions, where the disulphide bonds would be broken. Furthermore, a truncated form of the receptor lacking the LBD could not immunoprecipitate with the wild-type, showing that a major mediator of dimerisation was within 17 kDa of the N-terminus of the receptor. Further studies showed that the LBD of many mGluRs can form stable dimers in their own right, and though dimerisation involves disulphide bridges between LBDs, such as between Cys140 residues in mGlu1, they can also form through hydrophobic interactions between the upper lobes of the LBD (Han and Hampson, 1999; Kunishima et al., 2000; Okamoto et al., 1998; Ray and Hauschild, 2000). Since these early investigations, many structural aspects of mGluR dimerisation have been delineated.

The recently published crystal structure of mGlu1 noted that dimerisation may also be mediated by the TMDs, with a hydrophobic pocket located at the 1st and 2nd TMD associating with cholesterol molecules between the

protomers (Wu et al., 2014). Furthermore, the C-terminal tail is also thought to be involved in the formation of the mGluR homodimers. For instance, the mGlu1 splice-variants differentially form homodimers, with mGlu1a failing to dimerise with mGlu1b (Robbins et al., 1999). The only structural difference between these splice variants is the C-terminal tail, and moieties contained therein may play a role in dimerisation.

The effect of dimerisation on activation of the mGluRs has been extensively studied. The crystal structure of the LBD of mGlu1 bound with agonist or antagonist showed that the two lobes of each protomer are open when the receptor is inactive, with the lower lobe of each LBD relatively far apart, and upon agonist binding the two lobes of each protomer close, and the lower lobes move closer together (Kunishima et al., 2000; Tsuchiya et al., 2002). Indeed, closure of the LBD moves the lower lobes at least 28 Å closer together. Further study showed that this change in LBD orientation induces movement in the 1st and 2nd ICLs of mGlu1, with the 2nd ICL of each protomer moving closer together, and the 1st ICL moving apart (Tateyama et al., 2004). Given the importance of the 2nd ICL in G protein coupling of mGlu1, it is clear that the movement of this domain upon activation of the dimer may be involved in its signal transduction (Gomeza et al., 1996).

The effect of dimerisation on the activation characteristics of the mGluRs has been the focus of recent study. In one such study the dimerisation properties of the $GABA_{B1}$ and $GABA_{B2}$ C-terminal tails to produce a constitutive mGlu1 heterodimer in which one of the protomers could be inhibited by the mGlu5 specific NAM MPEP (Hlavackova et al., 2005). This study showed that antagonism of one protomer did not prevent the full activation of the other. Furthermore, when one protomer is blocked using MPEP the single, uninhibited protomer is equal to the response of the whole dimer, indicating that only one protomer is activating the G protein heterotrimer. This was further confirmed using a mutant form of mGlu5 which responds to Ro 01-6128, an mGlu1 specific PAM (Goudet et al., 2005). In this study they used the $GABA_{B1}$ and $GABA_{B2}$ C-terminal tails to create

constitutive heterodimers of the mutant form of mGlu5 and the wild-type mGlu5 receptor. The heterodimer could be fully potentiated in the presence of Ro 01-6128, indicating again that a single protomer was required for the full response. Furthermore, mGlu1 and mGlu5 heterodimers responded in the same way to DFB and to Ro 01-6128, and the presence of both PAMs did not increase the response further. This indicated that perhaps at any dimer, only a single G protein heterotrimer is associated, and this theory is supported by evidence from family A dimers (Banères and Parello, 2003). Interestingly, it has been reported that the monomeric form of mGlu2 cannot signal through G proteins in the presence of agonist, despite retaining the ability to bind agonist and couple to G proteins (El Moustaine et al., 2012). This is likely because the movement of the LBDs in the family C dimers discussed previously are vital in shifting the receptor to the active confirmation, and it is reasonable to expect that this will translate to all mGluRs.

It is interesting to speculate whether, given their high homology, the mGluRs can form heterodimers. Early evidence suggested that mGlu1 and mGlu5 do not form heterodimers with each other, as mGlu1a and mGlu5 do not co-immunoprecipitate (Romano et al., 1996b). Interestingly, despite the lack of evidence for inter-mGluR heterodimerisation, there is evidence that mGlu2 forms an oligomer with the family A $5HT_{2A}$ receptor (Moreno et al., 2011). Binding of the mGlu2 ligand LY379268 to the receptor was markedly reduced in 5HT2A knock-out mouse cortex membranes and *vice versa*. Furthermore, mGlu5 has been shown to form heterodimers with several family A GPCRs, for example μ-opioid receptors, and compounds have been engineered which interact with these heterodimers producing robust antinociceptive effects (Akgün et al., 2013). The heterodimerisation of mGlu5 with the adenosine A2a receptor and the dopamine D2 receptor has also been reported in the literature (Cabello et al., 2009). It is clear that unearthing mGlu1 and mGlu5 heterodimers has the potential to allow even greater manipulation of these receptors, if not for therapeutic benefit, than

at least to allow us to increase our understanding of the nature of these receptors.

The use of pharmacological techniques, such as those described herein, is perhaps superior to immunochemical techniques as they give an insight into the actual structural interaction between protomers. In the case of binding, it is fair to assume that any changes induced by dimerisation are due to direct, structural interactions between the protomers. In functional assays, it is difficult to rule out crosstalk or associated protein complexes for the differential behaviour of the dimer.

In this chapter I use mutant forms of the human mGlu1 and mGlu5 receptors (See Table 4.1.1) where the C-terminal tail has been replaced with the C-tail of either $GABA_{B1a}$ or $GABA_{B2}$ to promote heterodimerisation at the cell surface as previously described (Brock et al., 2007; Goudet et al., 2005; Hlavackova et al., 2005). $GABA_{B1}$ receptors are retained in the endoplasmic reticulum due to an RSRR moiety in the C-terminal tail. This is occluded by coiled-coil association with the C-terminal tail of $GABA_{B2}$, allowing dimerised receptors to traffic to the cell surface (Pagano et al., 2001). The use of a KKXX retention motif with the $GABA_{B2}$ tail has been shown robustly in the literature to allow distinct control over the composition of mGluR receptor dimers at the cell surface for use in functional studies (Brock et al., 2007). In these constructs only the association of C1 and C2-KKTN coiled-coiled domains occludes the RSRR and KKXX retention motifs, meaning only the heterodimers are expressed at the cell surface. This system has been used within this chapter to allow the study of the pharmacology of ligands acting at the mGlu1-mGlu5 heterodimer. The system was kindly validated by Lilly (Surrey, UK) by assaying the function and expression of the constructs using FLIPR and immunofluorescent techniques (*data not shown*). The constructs have been further characterised herein using immunofluorescent and whole-cell ELISA techniques on transiently transfected HEK293 cells. Importantly, the study on which these constructs are based on showed that these

chimaeric, forced dimers do not form tetramers (Brock et al., 2007), and the resulting pharmacological effects can be reasonably assumed to be the result of dimerisation, and not the formation of higher order oligomers, such as a 'dimer of dimers'. I investigate the functional significance of this dimerisation with respect to receptor activation, prior to investigating the effect of dimerisation on ligand binding in the dimer. Finally, interactions observed in this heterodimerisation model are used to investigate, using radioligand binding techniques, whether there is pharmacological evidence of heterodimerisation between mGlu1 and mGlu5 in the mouse brain. Existence of such a heterodimer *in vivo* could potentially lead to therapeutics able to target this subpopulation in a highly specific manner.

Table 4.1.1 Constructs used within this chapter

Construct	Description	Diagram
HA-mGlu5b	N-terminally HA-tagged full length human mGlu5 receptor	
mGlu1-C2-KKTN	Human mGluR1a (Met1-Ser33) with an HA tag (YPYDVPDYA) and human mGluR1 (Ser34-Met858) and human $GABA_{B2}$ (Gln761-E821) and a C-terminal KKTN motif	
mGlu5-C2-KKTN	Human mGluR5b (Met1-Ser22) with an HA tag (YPYDVPDYA) and human mGluR5b (Ser23-Met845) and human $GABA_{B2}$ (Gln761-E821) and a C-terminal KKTN motif	
mGlu5-C1	Human mGluR5b (Met1-Ser22) with a FLAG tag (DYKDDDDK) and human mGluR5 (Ser23-Met845) And the human $GABA_{B1a}$ C-terminal tail (Lys875-Stop962)	
mGlu5.5/mGlu1.5	mGlu5-C2-KKTN or mGlu1-C2-KKTN co-transfected with mGlu5-C1	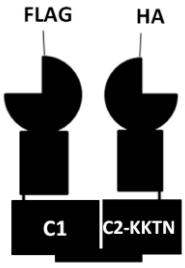

4.2 Results

4.2.1 mGluR receptor chimeras with $GABA_B$ C-terminal tails are functional in vitro

AV12 cell lines co-expressing EAAT1 and either the human mGlu1, mGlu5, the constitutively homodimerised mGlu5 constructs (referred to hereafter as mGlu5.5) or the constitutively heterodimerised mGlu1 and mGlu5 constructs (referred to hereafter as mGlu1.5) were cloned and validated by Lilly (Surrey, UK, data not shown). The functional response of these constructs were assessed by measuring agonist-stimulated intracellular calcium release using the fluorescent probe Fluo4-AM, detected using a fluorescent imaging plate reader (FLIPR). In all cell lines (S)-3,5-DHPG induced a concentration-dependent increase in intracellular calcium release (Figure 4.2.1.1). The potency of (S)-3,5-DHPG was lowest in mGlu1 expressing AV12 cells, with a pEC_{50} value of 5.41 ± 0.04. (S)-3,5-DHPG had comparable potencies at mGlu5, mGlu5.5, and mGlu1.5. Though (S)-3-5-DHPG has increased potency at mGlu1.5 dimers, the effect is not statistically significant ($p > 0.05$, one-way ANOVA). This data shows that mGlu5.5 and mGlu1.5 constructs in these stable cell lines produce a functional response when stimulated with agonist. Quantitative and statistical analyses of (S)-3,5-DHPG action in these cell lines are summarised in Table 4.2.1.1.

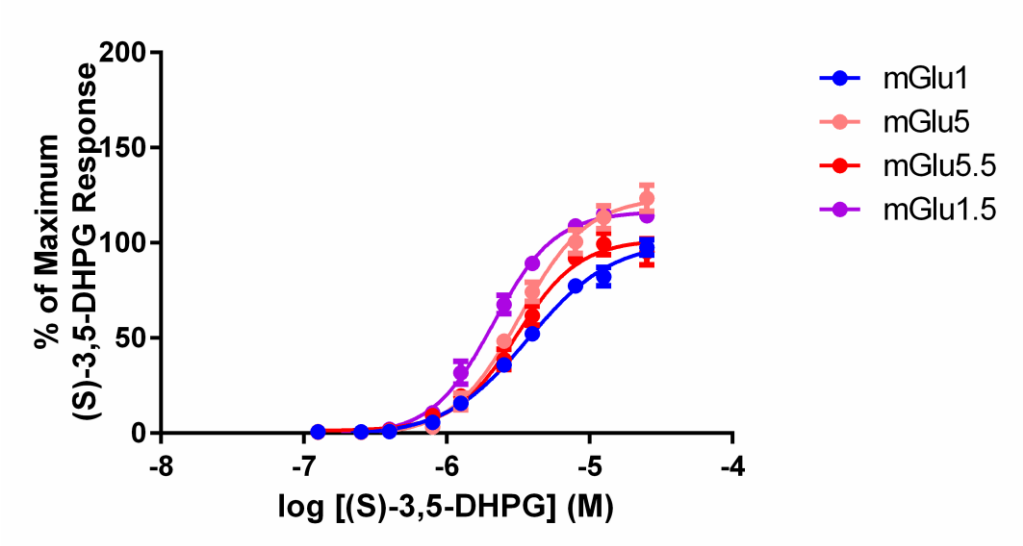

Figure 4.2.1.1 The activation of the Gq/11 pathway in AV12 cells stably expressing either mGlu1, mGlu5, the constitutive mGlu5 homodimer (mGlu5.5), or the constitutive mGlu1 and mGlu5 heterodimer (mGlu1.5) in response to a range of concentrations (100 nM to 30 uM) to the group I selective metabotropic glutamate receptor agonist (S)-3,5-DHPG was assessed by imaging transient calcium release using Fluo-4 AM as a probe. The graph shows the combined data of three independent experiments performed in triplicate, where each data point represents the mean ± S.E.M. Analysis using the operational model of agonism and statistical analysis are summarised in Table 4.2.1.1.

Table 4.2.1.1 A summary of the quantitative analysis, using the operational model of agonism, of (S)-3,5-DHPG acting at the mGlu1, mGlu5, mGlu5.5, or mGlu1.5 constructs stably transfected into AV12 cell lines co-expressing EAAT1. Data shown represents 3 independent experiments performed in triplicate expressed as mean ± S.E.M. Statistical analyses represent the results of a Tukey's HSD post-hoc test following a one-way ANOVA.

Compound	Receptor	pEC50		n
(S)-3,5-DHPG	mGlu1	5.41 ± 0.04	N.S.	3
	mGlu5	5.47 ± 0.03	N.S.	3
	mGlu5.5	5.51 ± 0.03	N.S.	3
	mGlu1.5	5.68 ± 0.02	N.S.	3

N.S. $p > 0.05$

4.2.2 The Action of mGlu5 PAMs acting at the MPEP site is inhibited at the mGlu1 and mGlu5 heterodimer

In order to assess the effect of heterodimerisation on PAMs acting at the mGlu5 protomer, LSN-2814617, CDPPB, and ADX-47273 were assessed for their ability to potentiate the release of intracellular calcium in the mGlu1, mGlu5, mGlu5.5, and mGlu1.5 expressing AV12 cells upon agonist stimulation was assessed, using a FLIPR with Fluo4-AM as a probe (Figures 4.2.2.1-3). Neither LSN-2814617, CDPPB, or ADX47273 displayed any concentration-dependent potentiation at the mGlu1 receptor, though maximal concentrations of CDPPB and ADX-47273 did display intrinsic efficacy at this receptor (Panel A in Figures 4.2.2.1-3).

All three PAMs displayed concentration-dependent effect on the (S)-3,5-DHPG response at the mGlu5 and mGlu5.5 receptors with approximately equal potentiation (Panels B and C in Figures 4.2.2.1-3). The maximal intracellular calcium release induced by (S)-3,5-DHPG in the presence of LSN-2814617 was 138.6 ± 4.3% and 172.7 ± 6.4% of the maximum induced by (S)-3,5-DHPG alone at mGlu5 and mGlu5.5, respectively. For CDPPB, the maximal response was 152.4 ± 3.2% and 203.9 ± 4.7% for mGlu5 and mGlu5.5, respectively. Finally, the maximal response for ADX-47273 was 366.7 ± 5.0% and 332.6 ± 4.5% for mGlu5 and mGlu5.5, respectively. The EC_{50} shifts of (S)-3,5-DHPG in the absence or presence of a high concentration of these PAMs were not significantly different between mGlu5 and mGlu5.5 ($p > 0.05$, one-way ANOVA with Tukey's HSD post hoc test).

In contrast, all three PAMs displayed a significantly reduced ability to potentiate (S)-3,5-DHPG response at the mGlu1.5 receptor (Panel D in Figures 4.2.3.1-3, $p < 0.05$, Tukey's HSD post hoc test). The maximal response of (S)-3,5-DHPG was 113.5 ± 2.9%, 133.7 ± 3.8%, and 366.6 ± 10.9% for LSN-2814617, CDPPB, and ADX-47273, respectively. The quantitative analyses of the compounds using a four parameter logistic equation (*See Methods*), as well as the statistical analyses of LSN-2814617, CDPPB, and ADX-47273 are summarised in Table 4.2.2.1, 4.2.2.2, and 4.2.2.3,

respectively. These data show that the heterodimerisation of mGlu5 with mGlu1 significantly inhibits the action of PAMs acting at the MPEP site on the mGlu5 protomer. Note that for figure 4.2.2.3, the potency of (S)-3,5-DHPG appears somewhat lower at mGlu1 than in other experiments. This data was gathered at a different time to the other data, and the lowered potency likely reflects a change in the receptor expression of the stable cell line over this time period.

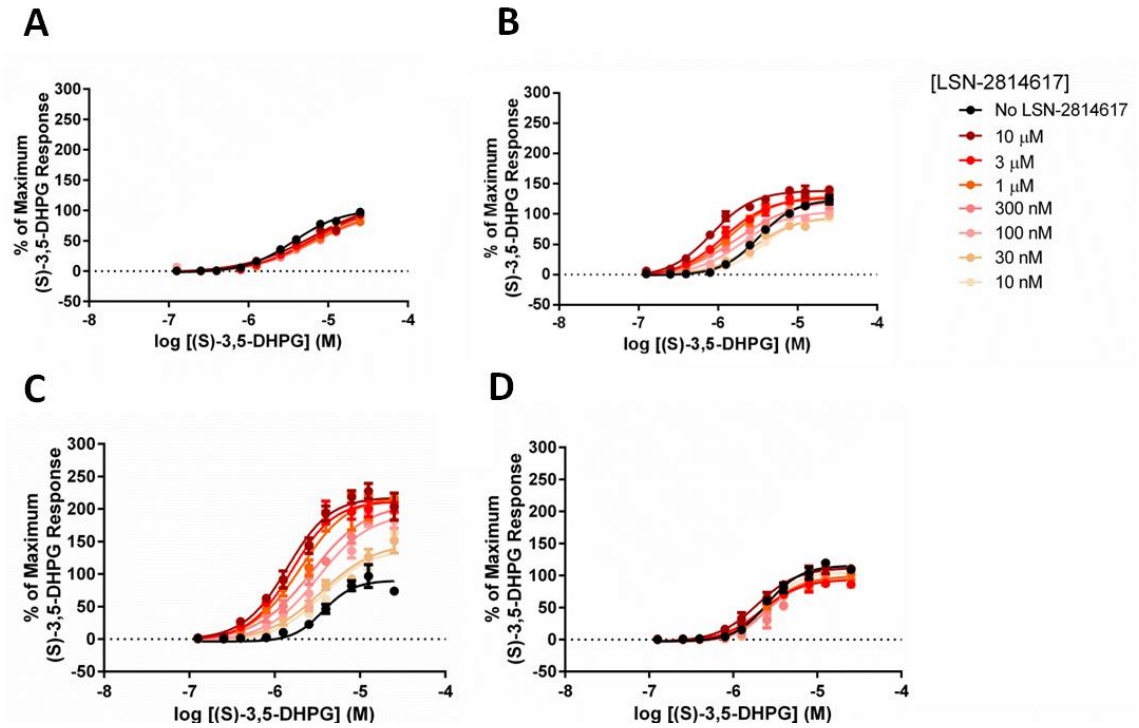

Figure 4.2.2.1 The ability of the allosteric ligand LSN-2814617 to potentiate the activation of the mGlu1 (A), mGlu5 (B), the constitutive mGlu5 homodimer (C), or the constitutive mGlu1-mGlu5 heterodimer (D) by the orthosteric agonist (S)-3,5-DHPG in a concentration dependent manner was assessed in stably transfected AV12 cells. Cells were pre-incubated (3 mins) with a range of concentrations of potentiator before the addition of a range of concentrations of (S)-3,5-DHPG. The data shown represents the mean ± S.E.M. from three independent experiments performed in triplicate. Analysis using a four parameter logistic equation and statistical analyses are summarised in Table 4.2.2.1.

Table 4.2.2.1 A summary of the quantitative analysis, using a four parameter logistic equation, of LSN-2814617 acting at the mGlu1, mGlu5, mGlu5.5, or mGlu1.5 constructs stably transfected into AV12 cell lines co-expressing EAAT1. Data shown represents 3 independent experiments performed in triplicate expressed as mean ± S.E.M. Statistical analyses represent the results of a Tukey's HSD post-hoc test following a one-way ANOVA.

Receptor	pEC_{50} of (S)-3,5-DHPG		ΔpEC_{50}	n
	No LSN-2814617	+ 10 μM LSN-2814617		
mGlu1	-	-	-	3
mGlu5	5.49 ± 0.03	6.08 ± 0.05	0.59	3
mGlu5.5	5.51 ± 0.03	6.06 ± 0.06	0.55	3
mGlu1.5	5.67 ± 0.02	5.84 ± 0.03	0.17**††	3

* $p < 0.05$ vs. mGlu5
** $p < 0.01$ vs. mGlu5
† $p < 0.05$ vs. mGlu5.5
†† $p < 0.01$ vs. mGlu5.5

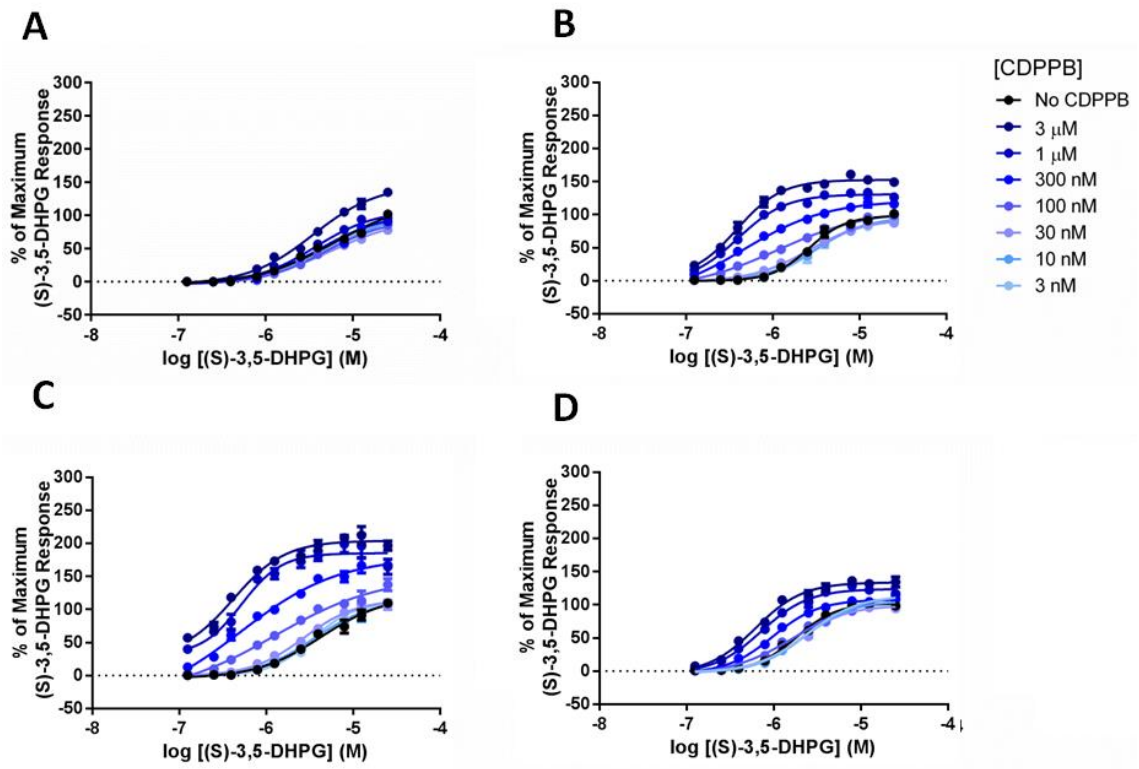

Figure 4.2.2.2 The ability of the allosteric ligand CDPPB to potentiate the activation of the mGlu1 (A), mGlu5 (B), the constitutive mGlu5 homodimer (C), or the constitutive mGlu1-mGlu5 heterodimer (D) by the orthosteric agonist (S)-3,5-DHPG in a concentration dependent manner was assessed in stably transfected AV12 cells. Cells were pre-incubated (3 mins) with a range of concentrations of potentiator before the addition of a range of concentrations of (S)-3,5-DHPG. The data shown represents the mean ± S.E.M. from three independent experiments performed in triplicate. Analysis using a four parameter logistic equation and statistical analyses are summarised in Table 4.2.2.2.

Table 4.2.2.2 A summary of the quantitative analysis, using a four-parameter logistic equation, of CDPPB acting at the mGlu1, mGlu5, mGlu5.5, or mGlu1.5 constructs stably transfected into AV12 cell lines co-expressing EAAT1. Data shown represents 3 independent experiments performed in triplicate expressed as mean ± S.E.M. Statistical analyses represent the results of a Tukey's HSD post-hoc test following a one-way ANOVA.

Receptor	pEC_{50} of (S)-3,5-DHPG		ΔpEC_{50}	n
	No CDPPB	+ 3 μM CDPPB		
mGlu1	-	-	-	3
mGlu5	5.58 ± 0.04	6.41 ± 0.07	0.83	3
mGlu5.5	5.37 ± 0.09	6.38 ± 0.10	1.01	3
mGlu1.5	5.74 ± 0.03	6.20 ± 0.06	0.46*†	3

* $p < 0.05$ vs. mGlu5
** $p < 0.01$ vs. mGlu5
† $p < 0.05$ vs. mGlu5.5
†† $p < 0.01$ vs. mGlu5.5

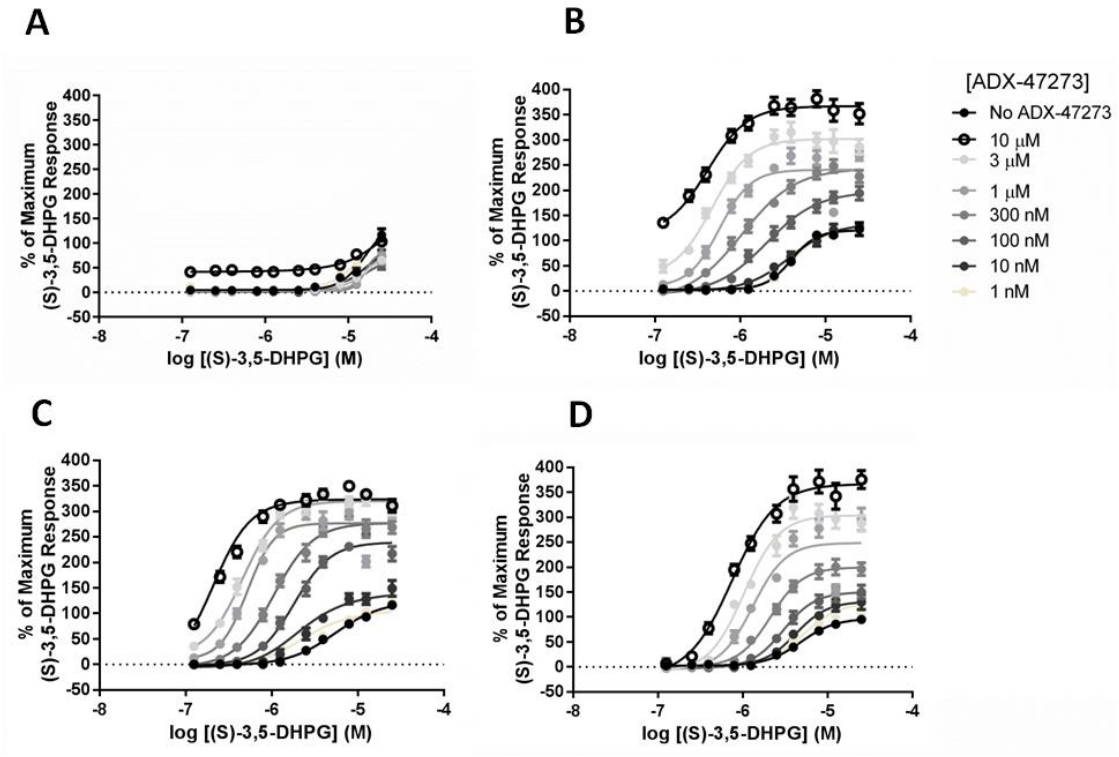

Figure 4.2.2.3 The ability of the allosteric ligand ADX-47273 to potentiate the activation of the mGlu1 (A), mGlu5 (B), the constitutive mGlu5 homodimer (C), or the constitutive mGlu1-mGlu5 heterodimer (D) by the orthosteric agonist (S)-3,5-DHPG in a concentration dependent manner was assessed in stably transfected AV12 cells. Cells were pre-incubated (3 mins) with a range of concentrations of potentiator before the addition of a range of concentrations of (S)-3,5-DHPG. The data shown represents the mean ± S.E.M. from three independent experiments performed in triplicate. Analysis using a four parameter logistic equationand statistical analyses are summarised in Table 4.2.2.3.

Table 4.2.2.3 A summary of the quantitative analysis, using a four parameter logistic equation, of ADX-47273 acting at the mGlu1, mGlu5, mGlu5.5, or mGlu1.5 constructs stably transfected into AV12 cell lines co-expressing EAAT1. Data shown represents 3 independent experiments performed in triplicate expressed as mean ± S.E.M. Statistical analyses represent the results of a Tukey's HSD post-hoc test following a one-way ANOVA. Functional data of ADX-47273 acting at mGlu5 is taken from Chapter 3.

Receptor	pEC_{50} of (S)-3,5-DHPG		ΔpEC_{50}	n
	No ADX-47273	+ 10 μM ADX-47273		
mGlu1	-	-	-	3
mGlu5	5.40 ± 0.03	6.38 ± 0.09	0.98	3
mGlu5.5	5.26 ± 0.04	6.60 ± 0.11	1.34	3
mGlu1.5	5.31 ± 0.04	6.12 ± 0.05	0.81*††	3

* $p < 0.05$ vs. mGlu5
** $p < 0.01$ vs. mGlu5
† $p < 0.05$ vs. mGlu5.5
†† $p < 0.01$ vs. mGlu5.5

4.2.3 The action of the dual mGlu1 and mGlu5 PAM CPPHA is unaffected by heterodimerisation between these receptors

CPPHA is a PAM of both mGlu1 and mGlu5, however, unlike the PAMs previously used it does not bind to the MPEP site (Bradley et al., 2011; Zhao et al., 2007). To assess whether the heterodimerisation of mGlu1 and mGlu5 is a binding site-dependent effect, the ability of CPPHA to potentiate (S)-3,5-DHPG stimulated intracellular calcium release was assessed in all four cell lines (Figure 4.2.3.1). CPPHA potentiated the action of (S)-3,5-DHPG in a concentration-dependent manner, inducing a maximal response of 179.4 ± 4.4%, 160.1 ± 4.8%, 186.1 ± 4.1%, and 169.3 ± 3.1% at mGlu1, mGlu5, mGlu5.5, and mGlu1.5, respectively. There was no significant difference in the EC_{50} shift induced by CPPHA of at any of the constructs ($p > 0.05$, one-way ANOVA), showing that heterodimerisation of mGlu1 and mGlu5 does not cause a significant inhibition of CPPHA action at the mGlu5 protomer. The quantitative analysis of CPPHA action using a four parameter logistic equation, as well as the statistical analysis of the action of CPPHA are summarised in Table 4.2.3.1.

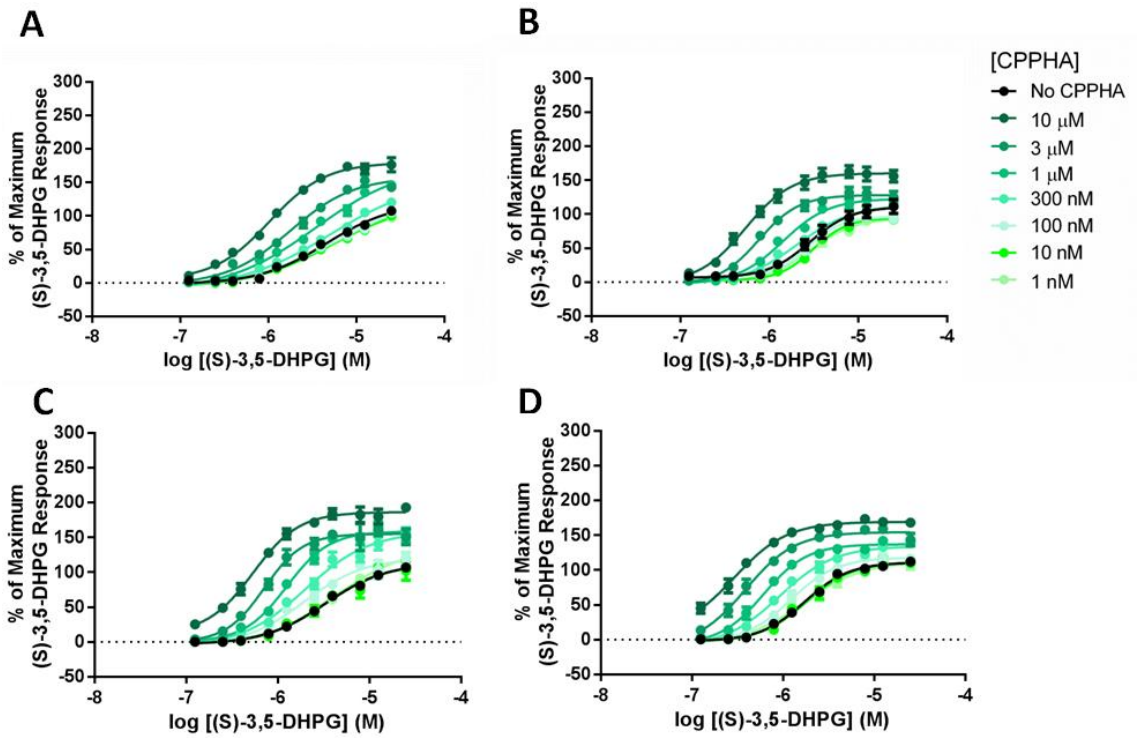

Figure 4.2.3.1 The ability of the allosteric ligand CPPHA to potentiate the activation of the mGlu1 (A), mGlu5 (B), the constitutive mGlu5 homodimer (C), or the constitutive mGlu1-mGlu5 heterodimer (D) by the orthosteric agonist (S)-3,5-DHPG in a concentration dependent manner was assessed in stably transfected AV12 cells. Cells were pre-incubated (3 mins) with a range of concentrations of potentiator before the addition of a range of concentrations of (S)-3,5-DHPG. The data shown represents the mean ± S.E.M. from three independent experiments performed in triplicate. Analysis using a four parameter logistic equation and statistical analyses are summarised in Table 4.2.3.1.

Table 4.2.3.1 A summary of the quantitative analysis, using a four parameter logistic equation, of CPPHA acting at the mGlu1, mGlu5, mGlu5.5, or mGlu1.5 constructs stably transfected into AV12 cell lines co-expressing EAAT1. Data shown represents 3 independent experiments performed in triplicate expressed as mean ± S.E.M. Statistical analyses represent the results of a one-way ANOVA.

Receptor	pEC_{50} of (S)-3,5-DHPG		ΔpEC_{50}		n
	No CPPHA	+ 10 μM CPPHA			
mGlu1	5.34 ± 0.07	5.98 ± 0.04	0.64	N.S.	3
mGlu5	5.54 ± 0.06	6.27 ± 0.07	0.73	N.S.	3
mGlu5.5	5.48 ± 0.04	6.27 ± 0.06	0.79	N.S.	3
mGlu1.5	5.76 ± 0.03	6.53 ± 0.13	0.77	N.S.	3

N.S. $p > 0.05$

4.2.4 The action of an mGlu1 PAM is not inhibited by heterodimerisation of mGlu1 with mGlu5

PAMs of mGlu1, such as Ro 67-4853, have been shown to bind to mGlu1 at a topographically homologous site to the MPEP binding site of mGlu5 (Pagano et al., 2000). To assess whether the inhibitory action of mGlu1 on mGlu5 PAMs in the heterodimer is reciprocal, the ability of the hmGlu1 specific PAM Ro 67-4853 to potentiate (S)-3,5-DHPG stimulated intracellular calcium release was assessed in all four cell lines (Figure 4.2.4.1). Ro 67-4853 acted as a PAM at both mGlu1 (4.2.4.1A) and mGlu1.5 (4.2.4.1D), causing a concentration-dependent increase in the potency of (S)-3,5-DHPG with a maximal response of 162.0 ± 5.5% and 202.0 ± 4.5%, respectively. The potentiation induced by Ro 67-4853 was not significantly different between the mGlu1 and mGlu1.5 heterodimer, indicating that the occupation of the orthosteric site of mGlu5 by (S)-3,5-DHPG does not inhibit the action of Ro 67-4853 ($p > 0.05$, unpaired, one-tailed Student's t-test). Ro 67-4853 did not potentiate the (S)-3,5-DHPG response at mGlu5 (4.2.4.1B) or mGlu5.5 (4.2.4.1C) receptor constructs. The quantitative analysis of the data using a four parameter logistic equation, as well as the statistical analyses of the data, is summarised in Table 4.2.4.1.

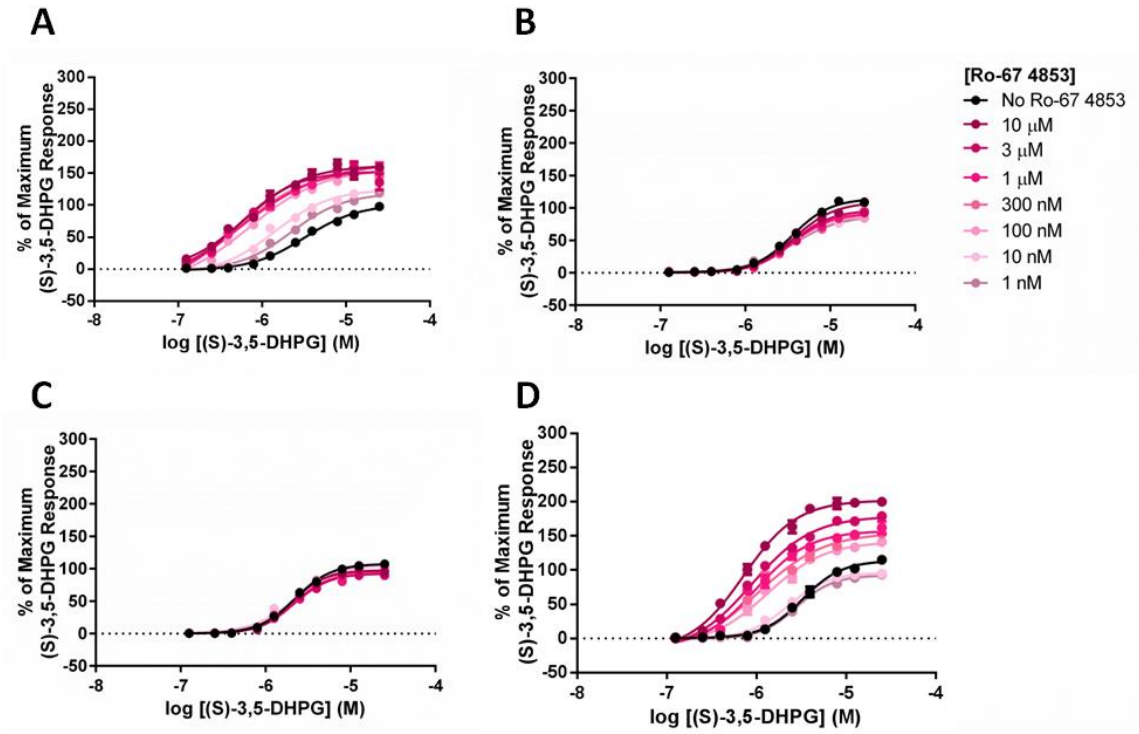

Figure 4.2.4.1 The ability of the allosteric ligand Ro-67 5853 to potentiate the activation of the mGlu1 (A), mGlu5 (B), the constitutive mGlu5 homodimer (C), or the constitutive mGlu1-mGlu5 heterodimer (D) by the orthosteric agonist (S)-3,5-DHPG in a concentration dependent manner was assessed in stably transfected AV12 cells. Cells were pre-incubated (3 mins) with a range of concentrations of potentiator before the addition of a range of concentrations of (S)-3,5-DHPG. The data shown represents the mean ± S.E.M. from three independent experiments performed in triplicate. Analysis using a four parameter logistic equation and statistical analyses are summarised in Table 4.2.4.1.

Table 4.2.4.1 A summary of the quantitative analysis, using a four parameter logistic equation, of Ro-67 4853 acting at the mGlu1, mGlu5, mGlu5.5, or mGlu1.5 constructs stably transfected into AV12 cell lines co-expressing EAAT1. Data shown represents 3 independent experiments performed in triplicate expressed as mean ± S.E.M. Statistical analyses represent two-tailed, unpaired Student's t-tests with a significance value set at 5%.

Receptor	pEC_{50} of (S)-3,5-DHPG		ΔpEC_{50}		n
	No Ro-67 4853	+ 10 μM Ro-67 4853			
mGlu1	5.49 ± 0.05	6.19 ± 0.09	0.70	-	3
mGlu5	-	-	-	-	3
mGlu5.5	-	-	-	-	3
mGlu1.5	5.49 ± 0.03	6.14 ± 0.04	0.66	N.S.	3

N.S. ($p > 0.05$) vs. mGlu1

4.2.5 Heterodimerisation of mGlu1 and mGlu5 has differential effects on the inhibitory action of an mGlu5 NAM and an mGlu1-selective NAM

Given the inhibitory effect of heterodimerisation on the action of PAMs acting at the mGlu5 protomer, it is possible that mGlu1 occupancy by (S)-3,5-DHPG could also affect the mGlu5 NAM MPEP, which binds at the same site as LSN-2814617, CDPPB, and ADX-47273. With that in mind, the ability of the mGlu5 NAM MPEP to inhibit the (S)-3,5-DHPG response was assessed in all four receptor constructs (Figure 4.2.5.1). MPEP fully inhibited the response of (S)-3,5-DHPG at both the mGlu5 and mGlu5.5 receptors, with comparable pIC50 values of 8.89 ± 0.06 and 8.59 ± 0.02, respectively. The IC_{50} value for mGlu5 is comparable to previously reported values (Gasparini et al., 1999). MPEP did not inhibit the action of (S)-3,5-DHPG at mGlu1, however, at the mGlu1.5 heterodimer the response was inhibited to 44.0 ± 8.2% of the maximum induced by (S)-3,5-DHPG alone. Furthermore, the pIC50 value of MPEP acting at the mGlu1.5 heterodimer was 7.82 ± 0.09, significantly different to that of mGlu5 alone ($p < 0.01$, one-way ANOVA with Tukey's HSD post-hoc analysis). This suggests that the occupancy of the mGlu1 protomer by (S)-3,5-DHPG inhibits the potency of MPEP and switches the inhibition of MPEP from a full non-competitive antagonist to a partial antagonist.

To assess whether mGlu5 can inhibit NAM action at the mGlu1 protomer, similar experiments were performed on all four cell lines with the mGlu1 selective inhibitor JNJ16259685 (Figure 4.2.5.2). JNJ16259685 acted as a full inhibitor at the mGlu1 and mGlu1.5 receptors, though with significantly differing pIC50 values of 8.54 ± 0.01 and 7.72 ± 0.03, respectively ($p < 0.01$, one-way ANOVA with Tukey's HSD post-hoc analysis). Full inhibition of the (S)-3,5-DHPG response at mGlu5 and mGlu5.5 was not observed, though analysis suggests the inhibition would be complete in concordance with previous reports (Lavreysen et al., 2004). Quantative analysis revealed JNJ16259685 acted at mGlu5 and mGlu5.5 with pIC_{50} values of 6.14 ± 0.03 and 6.29 ± 0.06, respectively. The quantitative and statistical analyses of

MPEP and JNJ16259685 acting at these receptors is summarised in Tables 4.2.5.1 and 4.2.5.2, respectively. Taken together, this data suggests that heterodimerisation of mGlu1 and mGlu5 reduces the potency of NAMs acting at both protomers. Interestingly the negative cooperativity of MPEP was reduced at the heterodimer, but this effect was not observed for JNJ16259685 which was fully able to inhibit the dimer response at concentrations where one would expect mGlu5 to be relatively uninhibited by this PAM. These results combined suggest that mGlu1 and mGlu5 are functionally interdependent in this system.

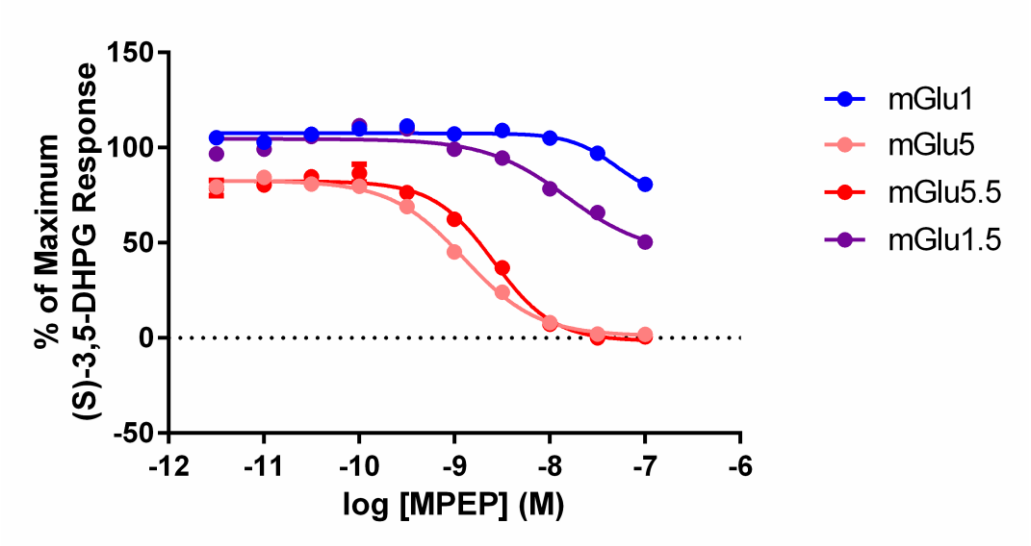

Figure 4.2.5.1 The ability of the allosteric ligand MPEP to inhibit the activation of the mGlu1 (A), mGlu5 (B), the constitutive mGlu5 homodimer (C), or the constitutive mGlu1-mGlu5 heterodimer (D) by the orthosteric agonist (S)-3,5-DHPG in a concentration dependent manner was assessed in stably transfected AV12 cells. Cells were pre-incubated (3 mins) with a range of concentrations of NAM before the addition of a set concentration (10 μM) of (S)-3,5-DHPG. The data shown represents the mean ± S.E.M. from three independent experiments performed in sextuplicate. Pharmacological and statistical analyses are summarised in Table 4.2.5.1.

Table 4.2.5.1 A summary of the quantitative analysis of MPEP acting at the mGlu1, mGlu5, mGlu5.5, or mGlu1.5 constructs stably transfected into AV12 cell lines co-expressing EAAT1. Data shown represents 3 independent experiments performed in sextuplicate expressed as mean ± S.E.M. Statistical analyses represent the results of a Tukey's HSD post-hoc test following a one-way ANOVA.

Receptor	pIC_{50} of MPEP	n
mGlu1	-	3
mGlu5	8.89 ± 0.06	3
mGlu5.5	8.59 ± 0.02	3
mGlu1.5	7.82 ± 0.09**††	3

* $p < 0.05$ vs. mGlu5
** $p < 0.01$ vs. mGlu5
† $p < 0.05$ vs. mGlu5.5
†† $p < 0.01$ vs. mGlu5.5

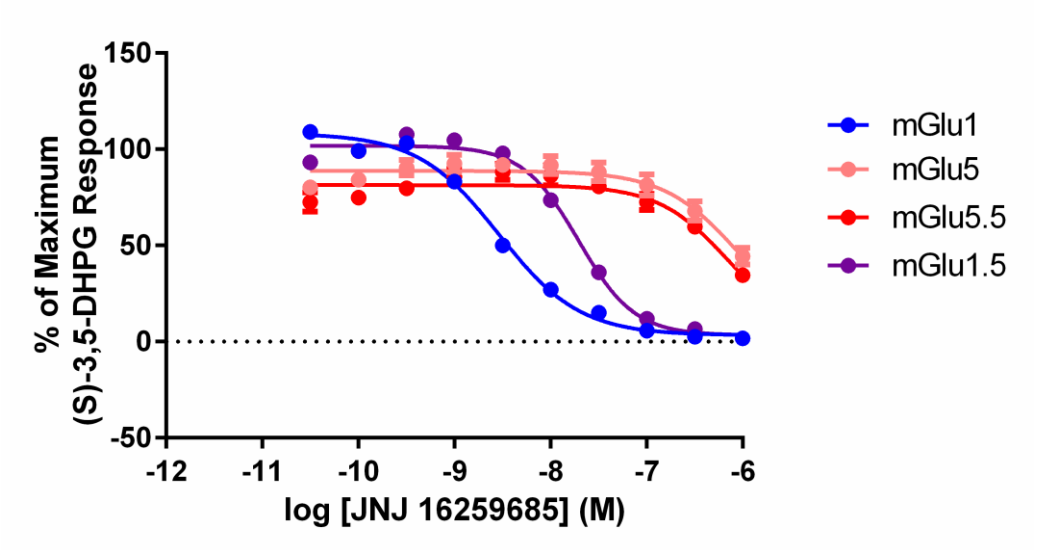

Figure 4.2.5.2 The ability of the allosteric ligand JNJ16259685 to inhibit the activation of the mGlu1 (A), mGlu5 (B), the constitutive mGlu5 homodimer (C), or the constitutive mGlu1-mGlu5 heterodimer (D) by the orthosteric agonist (S)-3,5-DHPG in a concentration dependent manner was assessed in stably transfected AV12 cells. Cells were pre-incubated (3 mins) with a range of concentrations of NAM before the addition of a set concentration (10 μM) of (S)-3,5-DHPG. The data shown represents the mean ± S.E.M. from three independent experiments performed in sextuplicate. Pharmacological and statistical analyses are summarised in Table 4.2.5.2.

Table 4.2.5.2 A summary of the quantitative analysis of MPEP acting at the mGlu1, mGlu5, mGlu5.5, or mGlu1.5 constructs stably transfected into AV12 cell lines co-expressing EAAT1. Data shown represents 3 independent experiments performed in sextuplicate expressed as mean ± S.E.M. Statistical analyses represent the results of a Tukey's HSD post-hoc test following a one-way ANOVA.

Receptor	pIC_{50} of JNJ16259685	n
mGlu1	$8.54 \pm 0.01^{**††}$	3
mGlu5	$6.44 \pm 0.03^{‡‡}$	3
mGlu5.5	$6.29 \pm 0.06^{‡‡}$	3
mGlu1.5	$7.72 \pm 0.03^{**††‡‡}$	3

* $p < 0.05$ vs. mGlu5
** $p < 0.01$ vs. mGlu5
† $p < 0.05$ vs. mGlu5.5
†† $p < 0.01$ vs. mGlu5.5
‡ $p < 0.05$ vs. mGlu1
‡‡ $p < 0.01$ vs. mGlu1

4.2.6 Co-expression of mGlu1-C1 or mGlu5-C1 constructs with the mGlu5-C2 construct allows receptor dimer trafficking to the cell membrane

In order to assess the effect of replacing the mGlu1 and mGlu5 C-terminal tail with those of the $GABA_{B2}$-KKTN (N-terminally HA-tagged mGlu1 or mGlu5 with the $GABAB_2$ C-terminal tail and KKXX retention motif, referred to hereafter as HA-mGlu1-C2-KKTN or HA-mGlu5-C2-KKTN, respectively) or $GABA_{B1}$ (N-terminally FLAG-tagged mGlu5 with the $GABAB_1$ C-terminal tail, referred to hereafter as FLAG-mGlu5-C1) receptors, the expression of these constructs was assessed when transiently transfected alone, or transiently co-transfected using immunocytochemical techniques (Figures 4.2.6.1 and 4.2.6.2).

Immunocytochemical analysis of untransfected cells, or cells expressing either N-terminally HA-tagged full length mGlu5, HA-mGlu1-C2-KKTN, HA-mGlu5-C2-KKTN, or FLAG-mGlu5-C1 was performed by immunostaining either permeabilised or non-permeabilised samples with primary antibodies recognising the HA-epitope (*N*-YPYDVPDYA-*C*) and the FLAG-epitope (*N*-DYKDDDDK-*C*) and DAPI (Figure 4.2.6.1). Except for the N-terminally HA-tagged full length mGlu5 receptor, immunostaining was not observed in chimeric constructs in non-permeabilised cells, however, immunostaining was present for all of the constructs when cells were permeabilised. This suggests that the receptor constructs with these $GABA_B$ tails are retained intracellularly when expressed alone. In contrast, when constructs expressing the $GABA_{B2}$-KKTN tail were co-expressed with the mGlu5 receptor bearing the $GABA_{B1}$ tail, immunostaining was evident in both the permeablised and non-permeabilised cells (Figure 4.2.6.2). This suggests that association of the $GABA_{B1}$ and $GABA_{B2}$-KKTN tails allows trafficking of the receptor dimer to the cell surface.

In order to assess the level of cell surface expression of the receptor constructs alone and co-expressed, a whole cell ELISA was performed on both non-permeabilised and permeabilised cells (Figure 4.2.6.3). The expression of the full length N-terminally HA-tagged mGlu5 receptor alone,

or the HA-mGlu1-C2-KKTN or HA-mGlu5-C2-KKTN co-expressed with the FLAG-mGlu5-C1 was generally higher at the cell surface than when these constructs were expressed alone. The expression of these constructs at the cell surface was concurrent with the immunocytochemical data and with previously reported data (Brock et al., 2007; Goudet et al., 2005).

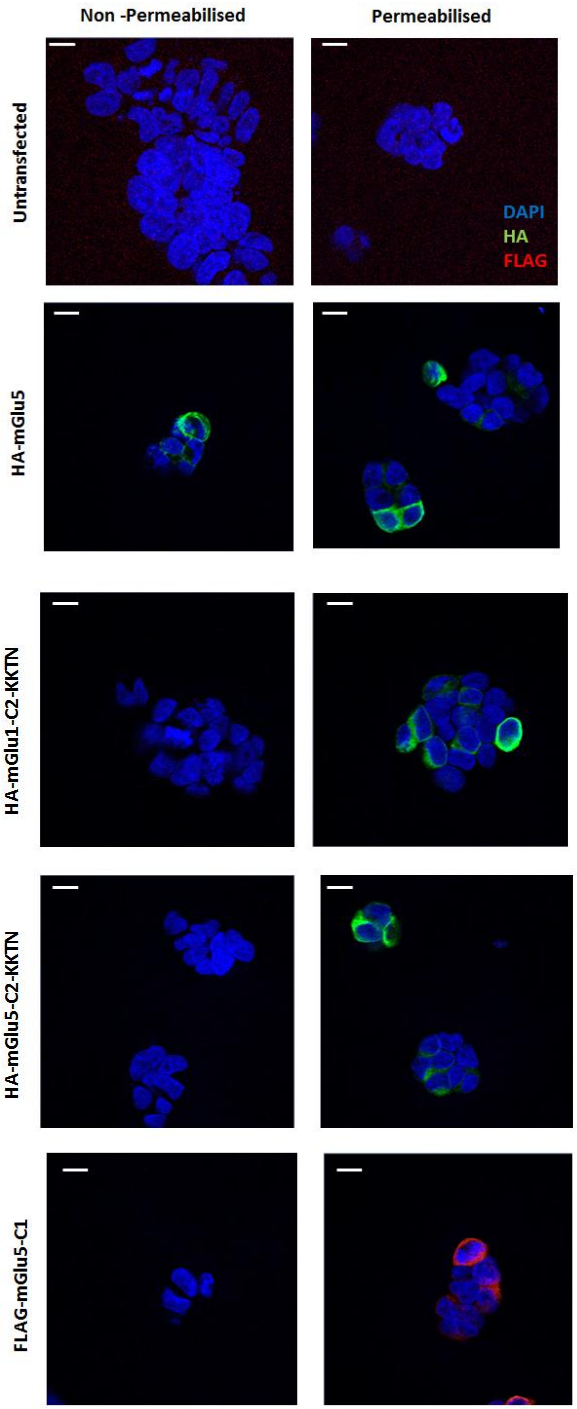

Figure 4.2.6.1 Immunocytochemical analysis was performed on paraformaldehyde-fixed HEK cells which were either untransfected or transiently transfected with an N-terminally HA-tagged mGlu5 receptor, an N-terminally HA-tagged mGlu1 receptor with a $GABA_{B2}$-KKTN tail (HA-mGlu1-C2-KKTN), an N-terminally HA-tagged mGlu5 receptor with a $GABA_{B2}$-KKTN tail (HA-mGlu5-C2-KKTN), or an N-terminally FLAG-tagged mGlu5 receptor with the corresponding $GABA_{B1}$ tail (FLAG-mGlu5-C1). The panels on the left show unpermeabilised cells and the panels on the right show permeabilised cell. The images represent 40x magnification with the scale bar representing 20 µm. Images shown are single representative experiments from three independent experiments.

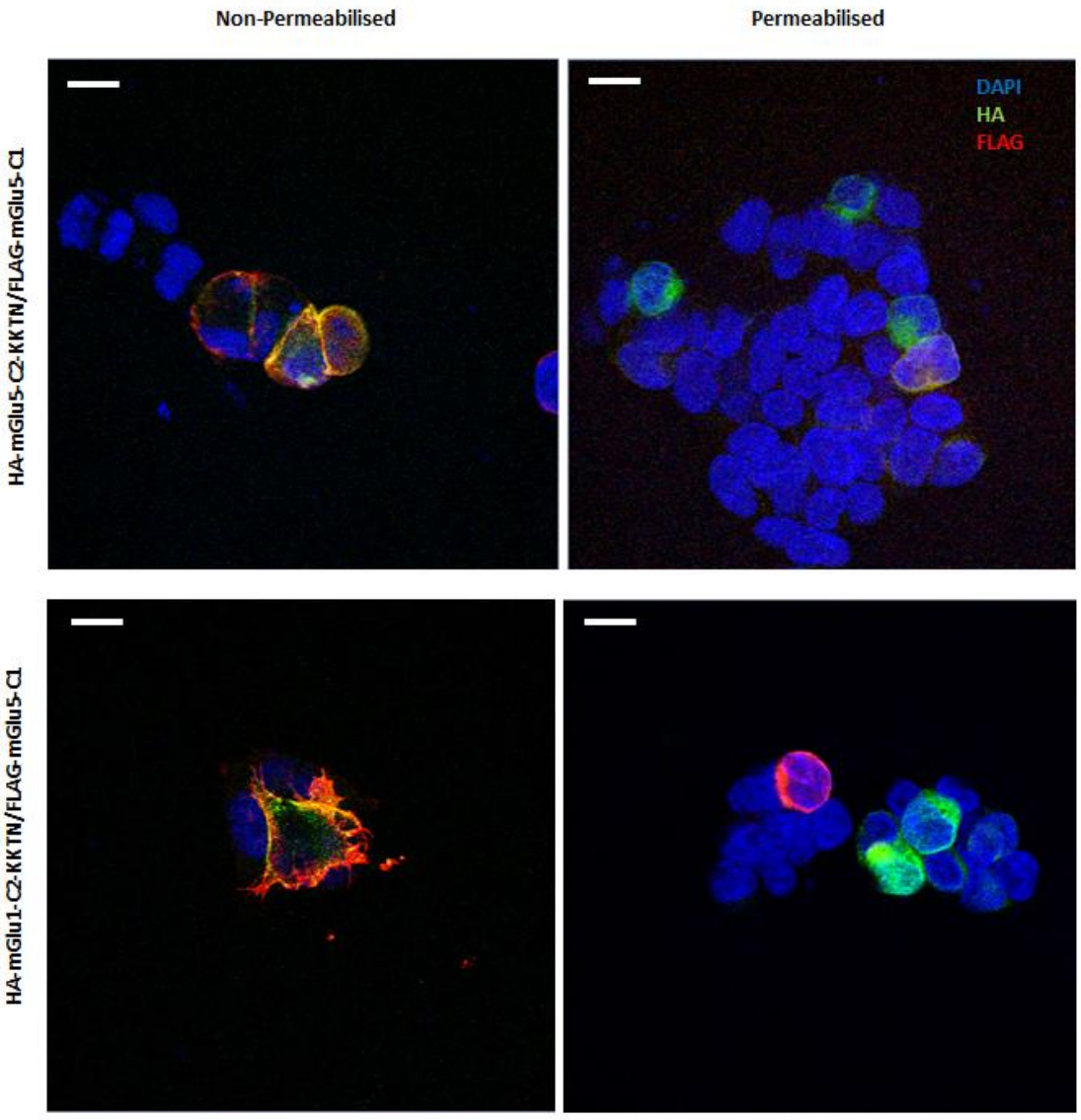

Figure 4.2.6.2 Immunocytochemical analysis was performed on paraformaldehyde-fixed HEK cells which were either untransfected or transiently co-transfected with an N-terminally HA-tagged mGlu5 receptor with a $GABA_{B2}$-KKTN tail (mGlu5-C2-KKTN) or an N-terminally HA-tagged mGlu1 receptor with a $GABA_{B2}$-KKTN tail (mGlu1-C2-KKTN), and an N-terminally FLAG-tagged mGlu5 receptor with the corresponding $GABA_{B1}$ tail (FLAG-mGlu5-C1). The panels on the left show unpermeabilised cells and the panels on the right show cells permeabilised with 0.25% Triton X-100. The images represent 40x magnification with the scale bar representing 20 µm. Images shown are single representative experiments.

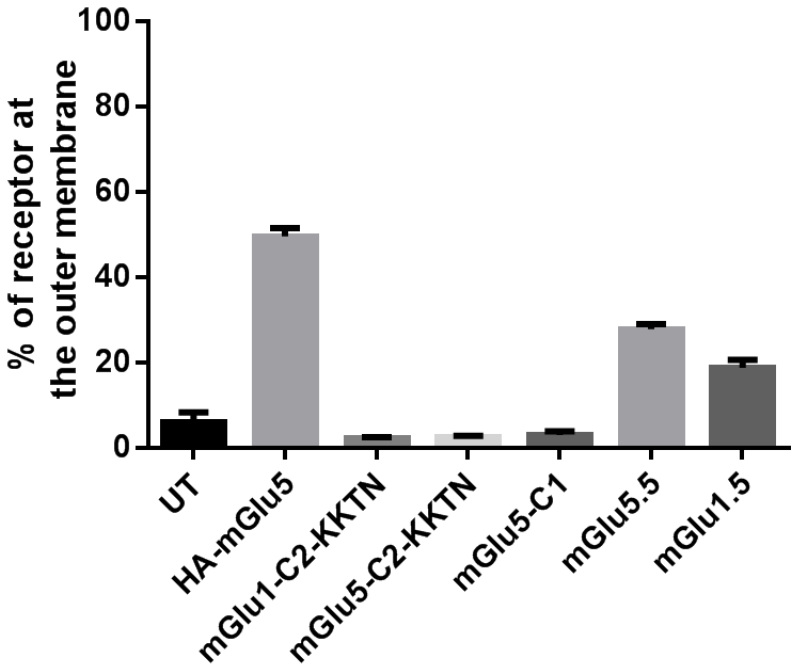

Figure 4.2.6.3 The percentage of HA-tagged receptors present at the membrane was determined by whole cell ELISA on both non-permeabilised (cell surface expression) and permeabilised (total expression) HEK293 cells transiently transfected with full length HA-tagged mGlu5 (HA-mGlu5), HA tagged mGlu1 or mGlu5 with the $GABAB_{2\text{-}KKTN}$ tail (mGlu1-C2-KKTN and mGlu5-C2-KKTN, respectively FLAG-tagged mGlu5 with the GABAB1 tail (mGlu5-C1) , 5C2-KKTN and 5C1 co-transfected (mGlu5.5) or 1C2-KKTN and 5C1 co-transfected (mGlu1.5) constructs. The data shown represents the ratio of the number of receptors detected in non-permeabilised cells over the number detected in permeabilised cells. The graph shown represents the mean ± S.D. of a single representative experiment performed in triplicate.

4.2.7 Heterodimerisation of mGlu1 and mGlu5 does not affect [^{3}H]-M-MPEP binding

In order to assess whether the mGlu1 protomer has any effect on NAMs acting at the MPEP binding site the affinity of [^{3}H]-M-MPEP binding at either mGlu5, mGlu5.5, or mGlu1.5 in membranes prepared from HEK293 cells was delineated. Firstly, a membrane titration was performed and based on that 30 μg.well^{-1} was chosen for radioligand binding experiments due to a high signal window and a depletion value less than 10 % (*data not shown*). In order to assess the affinity of the radioligand a [^{3}H]-M-MPEP saturation analysis was performed (Figure 4.2.7.1). No significant difference was observed in the affinity (K_D) of [^{3}H]-M-MPEP binding at mGlu5, mGlu5.5, or mGlu1.5 expressing membranes or the receptor expression (B_{MAX}) in these samples (one-way ANOVA, Tukey's HSD post-hoc test $p > 0.05$).

4.2.8 Allosteric modulators of mGlu1 have no effect on the binding of LSN-2814617

Our functional data suggests that the mGlu1 protomer has an inhibitory effect on PAMs acting at the MPEP site of the mGlu5 protomer in the heterodimer. In order to assess the effect of mGlu1 allosteric site occupancy at the dimer constructs, the ability of the LSN-2814617 to inhibit the binding of [^{3}H]-M-MPEP, in the absence and presence of either the mGlu1 selective NAM JNJ16259685 or the mGlu1 specific PAM Ro-67 4853, was assessed in membranes prepared from HEK293 cells transiently expressing mGlu5 or mGlu1.5 (Figures 4.2.8.1 and 4.2.8.2).

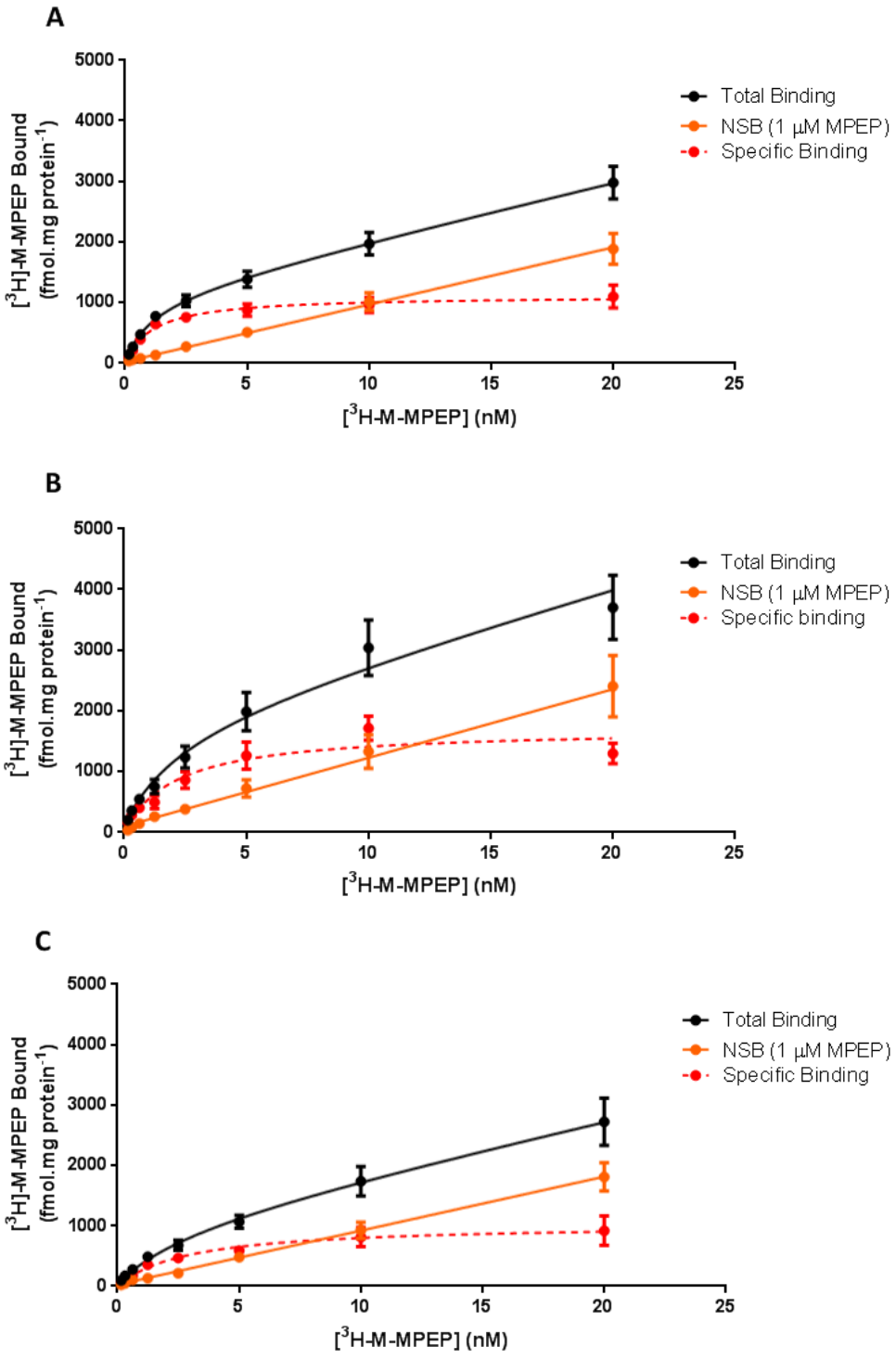

Figure 4.2.7.1 Saturation binding of [^{3}H]M-MPEP in membranes prepared from HEK293 cells transiently expressing either mGlu5 (A), the constitutive mGlu5 homodimer (B), or the constitutive mGlu1-mGlu5 heterodimer (C). The properties of [^{3}H]M-MPEP binding to mGlu5 receptors were assayed by incubating a range of concentrations (0.1-20 nM) with a set amount of membrane in the absence and presence of 1uM MPEP to define non-specific binding (NSB). The graph shows the combined data from 3 independent experiments performed in duplicate. The graphs show the combined data from 3 independent experiments performed in duplicate. Quantitative analysis of the data is summarised in Table 4.2.7.1.

Table 4.2.7.1 A summary of the saturation analysis of [^{3}H]-M-MPEP binding at mGlu5 in HEK293 cell membranes prepared from cells transiently transfected with either mGlu5, mGlu5.5 or mGlu1.5 constructs. Mean ± S.E.M. from three independent experiments performed in duplicate are shown. Statistical analysis represents the results of a one-way ANOVA with a Tukey's HSD post-hoc analysis.

Receptor	**Affinity (nM)**	**B_{MAX} (fmol.mg^{-1})**		**n**
mGlu5	1.25 ± 0.20	1119 ± 124	N.S.	3
mGlu5.5	2.35 ± 0.27	1824 ± 378	N.S.	3
mGlu1.5	3.09 ± 0.73	1038 ± 239	N.S.	3

N.S. $p > 0.05$

The mGlu1 selective NAM, JNJ16259685, had no effect on the binding of [^{3}H]-M-MPEP at either mGlu5 or the mGlu1.5 construct, showing that occupation of the mGlu1 protomer with a NAM does not inhibit the binding of a NAM at the mGlu5 protomer (Figure 4.2.8.1A). As before, LSN-2814617 inhibited the binding of [^{3}H]-M-MPEP in a concentration-dependent manner at mGlu5 (Figure 4.2.8.1B) and mGlu1.5 (Figure 4.2.8.1C), however, no significant difference between the pKi of LSN-2814617 at either construct was observed whether JNJ16259685 was present or not ($p > 0.05$, unpaired, one-tailed Student's t-test). This suggests that the occupancy of the mGlu1 allosteric site by this NAM has no effect on the affinity of LSN-2814617 at the mGlu5 protomer. The pharmacological and statistical analyses of this data is summarised in Table 4.2.8.1.

Given that the inhibition of mGlu5 PAMs was only observed in the active form of the dimer, perhaps occupation of the mGlu1 protomer with a PAM induces a conformation closer to the active state of the receptor. With this in mind, the ability of the mGlu1 specific PAM Ro 67-4853 to inhibit the binding of either [^{3}H]-M-MPEP or LSN-2814617 was assessed in the mGlu1.5 membranes, and compared to the wild-type mGlu5 membranes. Ro 67-4853 had no effect on the binding of [^{3}H]-M-MPEP at either mGlu5 or the mGlu1.5 construct (Figure 4.2.5.2A), indicating that the occupancy of the mGlu1 protomer with a PAM does not inhibit binding of the NAM at the MPEP binding site of the mGlu5 protomer. Furthermore, there was no significant difference between the pKi of LSN-2814617 at either construct whether Ro 67-4853 was present or not ($p > 0.05$, unpaired, one-tailed Student's t-test). This implies that the occupancy of the mGlu1 allosteric site with a PAM has no inhibitory effect on ligand binding at the MPEP site. The pharmacological and statistical analyses of this data is summarised in Table 4.2.5.1.

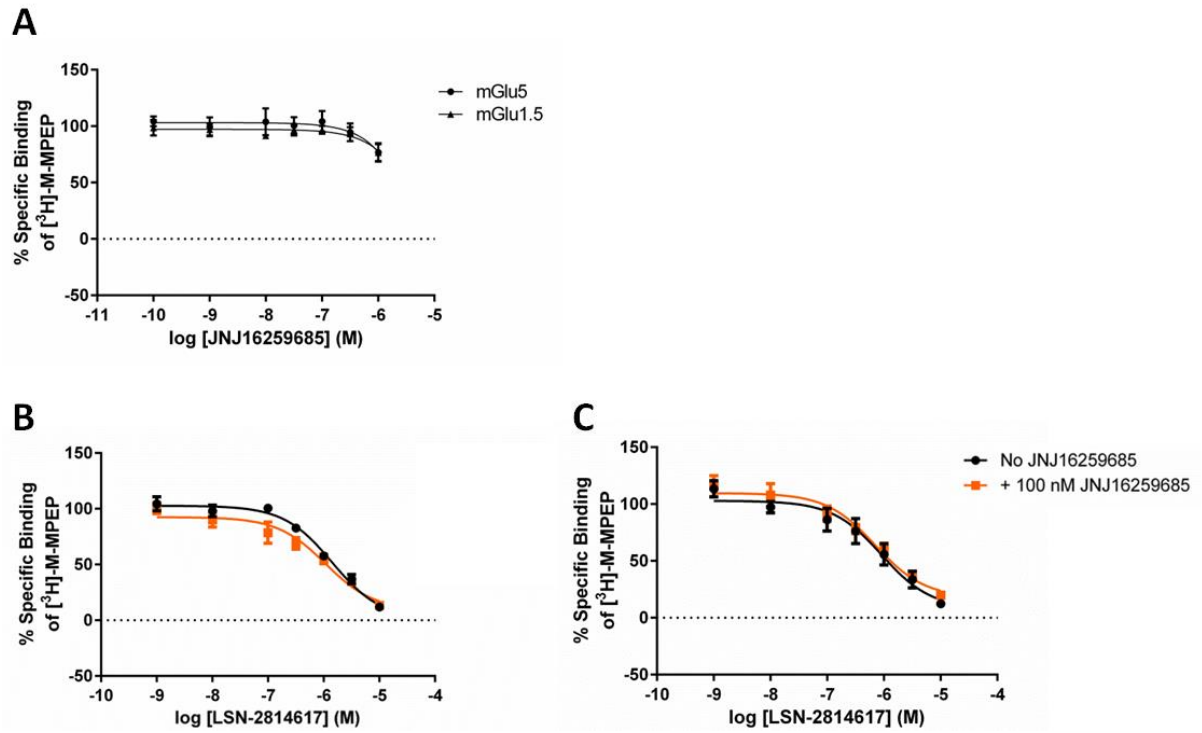

Figure 4.2.8.1 The ability of the hmGlu1 selective allosteric modulator JNJ16259685 to alter [^{3}H]-M-MPEP binding at the hmGlu5 receptor was assessed. A set concentration of [^{3}H]-M-MPEP, approximately equal to its K_D, was incubated in the presence of a range of concentrations (1 fM to 1 μM) of JNJ16259685 and a set amount of HEK293 membranes transiently expressing either the mGlu5 receptor or the constitutive mGlu1-mGlu5 heterodimer (A). The ability of the radioligand to bind specifically to an allosteric site on the mGlu5 receptor in membranes prepared from HEK293 membranes transiently expressing either the mGlu5 receptor (B) or the constitutive mGlu1-mGlu5 heterodimer (C) was assessed in the presence of a range of concentrations of LSN-2814617 (1 nM to 1 μM). The effect of the hmGlu1 specific allosteric modulator JNJ16259685 on the pharmacological properties of LSN-2814617 was also determined. These graphs represent the combined data of 3 independent experiments performed in duplicate. A summary of the analysis of this data can be found in Table 4.2.8.1.

Table 4.2.8.1 A summary of the pharmacological and statistical analysis of LSN-2814617 binding in the absence and presence of JNJ16259685 at mGlu5 in HEK293 cell membranes prepared from cells transiently transfected with either mGlu5 or mGlu1.5 constructs. The p-value represents the result of an unpaired, two-tailed Student's t-test with a significance value set at 5%.

	pK_i of LSN-2814617				
Receptor	**Control**	**p-value vs. mGlu5**	**+ 100 nM JNJ16259685**	**p-value vs. mGlu5**	**n**
mGlu5	6.06 ± 0.04	N/A	6.25 ± 0.14	N/A	3
mGlu1.5	6.17 ± 0.20	>0.05	6.24 ± 0.07	>0.05	3

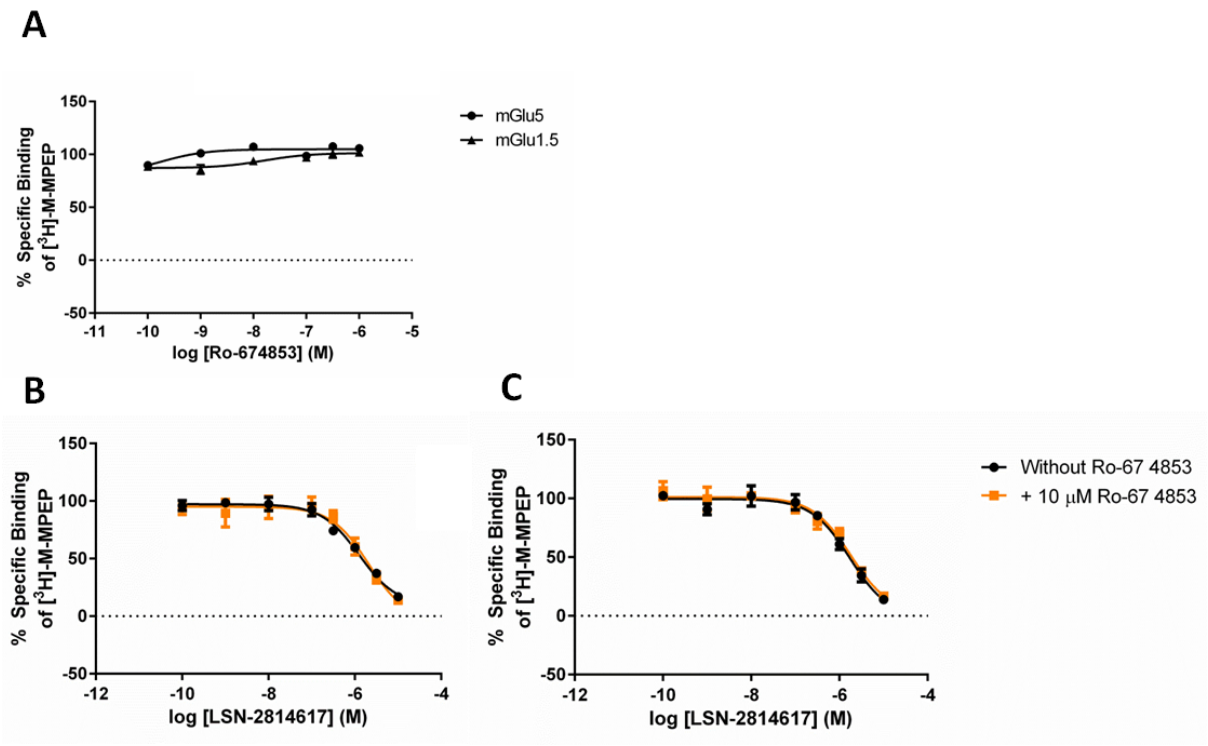

Figure 4.2.8.2 The ability of the hmGlu1 selective allosteric modulator JNJ16259685 to alter [^{3}H]-M-MPEP binding at the hmGlu5 receptor was assessed. A set concentration of [^{3}H]-M-MPEP, approximately equal to its K_D, was incubated in the presence of a range of concentrations (1 fM to 1 μM) of Ro 67-4853 and a set amount of HEK293 membranes transiently expressing either the mGlu5 receptor or the constitutive mGlu1-mGlu5 heterodimer (A). The ability of the radioligand to bind specifically to an allosteric site on the mGlu5 receptor in membranes prepared from HEK293 membranes transiently expressing either the mGlu5 receptor (B) or the constitutive mGlu1-mGlu5 heterodimer (C) was assessed in the presence of a range of concentrations of LSN-2814617 (1 nM to 1 μM). The effect of the hmGlu1 specific allosteric modulator Ro 67-4853 on the pharmacological properties of LSN-2814617 was also determined. These graphs represent the combined data of 3 independent experiments performed in duplicate. A summary of the analysis of this data can be found in Table 4.2.8.2.

Table 4.2.8.2 A summary of the pharmacological and statistical analysis of LSN-2814617 binding in the absence and presence of Ro 67-4853 at mGlu5 in HEK293 cell membranes prepared from cells transiently transfected with either mGlu5 or mGlu1.5 constructs. The p-value represents the result of an unpaired, two-tailed Student's t-test with a significance value set at 5%.

	pK_i of LSN-2814617				
Receptor	**Control**	**p-value vs. mGlu5**	**+ 10 μM Ro 67-4853**	**p-value vs. mGlu5**	**n**
mGlu5	6.02 ± 0.09	N/A	5.98 ± 0.08	N/A	3
mGlu1.5	6.06 ± 0.12	>0.05	6.04 ± 0.14	>0.05	3

4.2.9 Orthosteric occupancy of mGlu1 has no effect on LSN-2814617 acting at the mGlu5 protomer of the heterodimer

Given that Ro 67-4853 has no intrinsic efficacy, it is likely that the fully active conformation of the mGlu1 TMDs is not induced by the binding of this ligand. In order to assess whether the fully active conformation of the mGlu1 protomer causes inhibition of mGlu5 PAM binding at the MPEP site, the binding of LSN-2814617 was assessed in the presence of the orthosteric group I mGluR selective agonist (S)-3,5-DHPG in membranes prepared from HEK293 cells expressing either the mGlu5.5 or mGlu1.5 constructs (Figures 4.2.9.1). The quantitative and statistical analysis of the action of LSN-2814617under these conditions are summarised in Table 4.2.9.1-3, respectively.

At the mGlu5 receptor, the affinity of LSN-2814617 in both the presence and absence of (S)-3,5-DHPG was comparable to my previous results (Chapter 3, Figure 3.2.3.1A). The affinity of LSN-2814617 was unaffected by the presence and absence of (S)-3,5-DHPG at either the mGlu5.5 or mGlu1.5 receptors (Figure 4.2.9.1), with no significant difference between the mGlu1.5 and mGlu5.5 affinity values under either condition ($p > 0.05$, one-way ANOVA, Tukey's HSD post-hoc analysis). This indicated that the orthosteric occupancy of the mGlu1 receptor had no effect on the binding of this PAM at the MPEP site of the mGlu5 protomer.

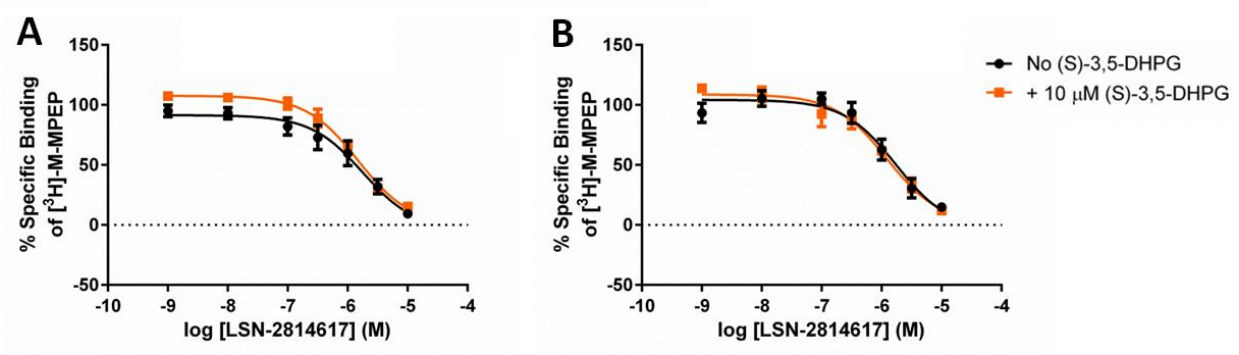

Figure 4.2.9.1 The ability of the [^{3}H]-M-MPEP to bind specifically to an allosteric site on the mGlu5 receptor in membranes prepared from HEK293 membranes transiently expressing either the constitutive mGlu5 homodimer (A), or the constitutive mGlu1-mGlu5 heterodimer (B) was assessed in the presence of a range of concentrations of LSN-2814617 (1 nM to 3 μM). The effect of the group I orthosteric agonist (S)-3,5-DHPG on the pharmacological properties of LSN-2814617 was also determined. These graphs represent the combined data of 3 independent experiments performed in duplicate. A summary of the pharmacological and statistical analysis of this data can be found in Table 4.2.9.2.

Table 4.2.9.1 A summary of the pharmacological and statistical analysis of LSN-2814617 binding in the absence and presence of (S)-3,5-DHPG at mGlu5 in HEK293 cell membranes prepared from cells transiently transfected with either mGlu5, mGlu5.5 or mGlu1.5 constructs. The p-value represents the result of a one-way ANOVA with a Tukey's HSD post-hoc analysis. *Data for the binding of LSN-2814617 at mGlu5 is taken from Chapter 3.

	pK_i of LSN-2814617				
Receptor	**Control**		**+ 10 μM (S)-3,5-DHPG**		**n**
mGlu5*	5.87 ± 0.12	N.S.	6.02 ± 0.13	N.S.	3
mGlu5.5	5.87 ± 0.11	N.S.	5.89 ± 0.15	N.S.	3
mGlu1.5	5.83 ± 0.17	N.S.	6.11 ± 0.11	N.S.	3

N.S. $p > 0.05$

4.2.10 The affinity of mGlu5 allosteric modulators are unaffected in mGlu1 KO mice, regardless of the orthosteric occupancy state

In order to assess whether the pharmacological interaction between mGlu1 and mGlu5 between CDPPB and (S)-3,5-DHPG in the mGlu1.5 construct from the previous section translates into native tissue, the pharmacological profile of these compounds was evaluated in membranes prepared from mouse cortex samples from wild-type and mGlu1 knockout mice (Figure 4.2.10.1). The expression of mGlu1 in both the wild-type and knockout cortex samples was verified using immunoblotting after separation of proteins by SDS-PAGE (Figure 4.2.10.1A). Western blotting using an mGlu1 specific antibody showed the presence of a protein band with a molecular weight of approximately 150 kDa in the membranes derived from wild-type mouse cortex samples, with no band present in the mGlu1 knock-out mouse cortex membrane samples, confirming ablation of mGlu1 expression in these animals. With an mGlu5 specific antibody, a band of approximately 150 kDa was observed in both samples, which indicated equal protein loading as well as unaffected mGlu5 expression in wild-type and mGlu1 knock-out animals.

The pharmacological properties of [^{3}H]-M-MPEP binding at mGlu5 in membranes prepared from both samples were characterised by homologous binding (Figure 4.2.10.1B). In membranes prepared from wild-type mouse cortex samples [^{3}H]-M-MPEP bound with a K_D of 8.71 ± 0.02, with a B_{MAX} of 552.9 ± 107.3 fmol.mg^{-1}. In membranes prepared from mGlu1 knock-out mouse cortex samples [^{3}H]-M-MPEP bound with a K_D of 8.71 ± 0.06, with a B_{MAX} of 729.6 ± 131.1 fmol.mg^{-1}. There was no significant difference between K_D and B_{MAX} of the radioligand in the membranes prepared from wild-type or mGlu1 knock-out cortex samples ($p > 0.05$, unpaired, two-tailed Student's t-test). This mirrors what was observed in our model system using chimeric heterodimer constructs. In order to assess whether orthosteric occupancy with (S)-3,5-DHPG inhibits the binding of CDPPB as in our chimeric model, the pharmacological characteristics of CDPPB binding at mGlu5 in the absence and presence of (S)-3,5-DHPG were determined in membranes

prepared from both wild-type and mGlu1 knock-out mice (Figure 4.2.10.1C). In contrast to the data generated using the chimeric heterodimer, there was no significant difference between the pKi values of CDPPB binding at mGlu5 in either wild-type or mGlu1 knock-out membrane samples whether or not (S)-3,5-DHPG was present ($p > 0.05$, unpaired, two-tailed Student's t-test). This data taken together suggests that mGlu1 expression in the mouse brain does not have a significant effect on ligands binding at the mGlu5 receptor. Pharmacological and statistical analyses of this data is summarised in Table 4.2.10.1.

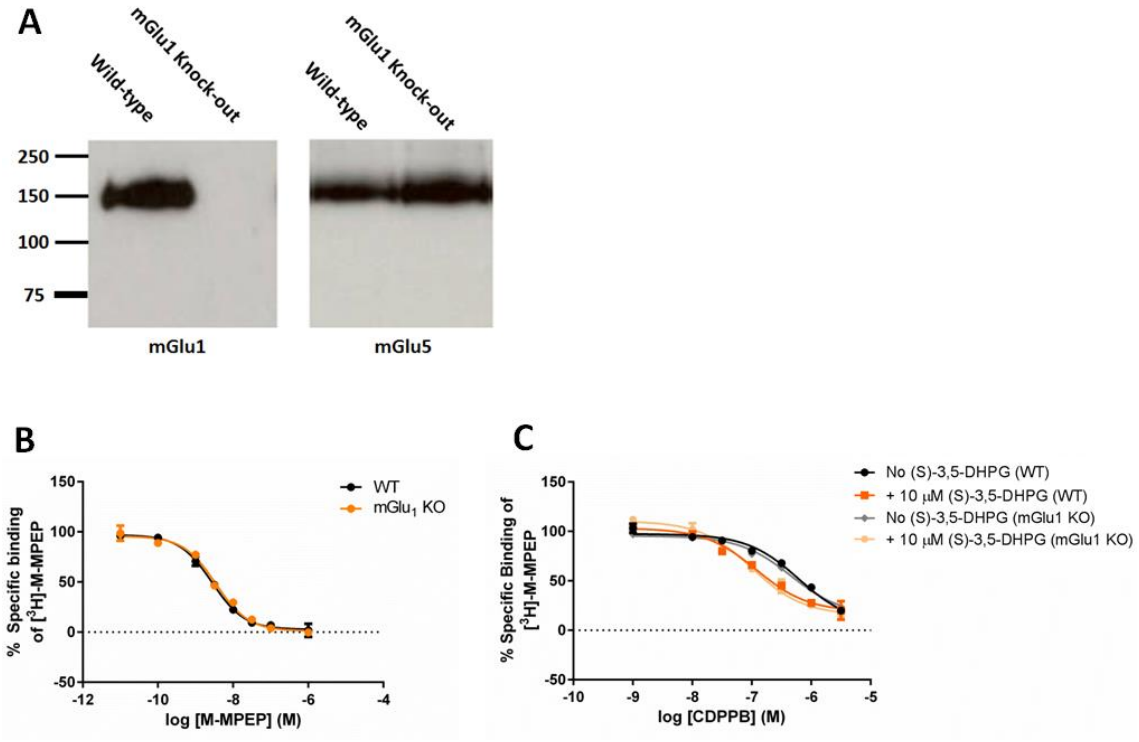

Figure 4.2.10.1 The pharmacological properties of the mGlu5 receptor expressed in membranes from mGlu1 knock-out (KO) mice were investigated and compared to membranes from a wild-type mouse brain. The expression of mGlu1 and mGlu5 were investigated by immunoblot (A). The data shown represents a single representative example from three independent experiments. The pharmacological properties of [^{3}H]-M-MPEP binding to the mGlu5 receptor in membranes created from both mGlu1 knock-out and wild-type mouse cortex samples were assessed using a range of concentrations of M-MPEP (10 fM to 1 μM) (B). The ability of [^{3}H]-M-MPEP to bind specifically to an allosteric site on the mGlu5 receptor in membranes prepared from both mGlu1 knock-out and wild type mouse brains were assessed in the presence of a range of concentrations of CDPPB (1 nM to 3 μM). The effect of the group I orthosteric agonist (S)-3,5-DHPG on the pharmacological properties of CDPPB was also determined. These graphs represent the combined data from three independent experiments performed in duplicate. A summary of the analysis of the pharmacological data is shown in Table 4.2.10.1.

Table 4.2.10.1 A summary of the pharmacological and statistical analysis of ligands binding in the absence and presence of (S)-3,5-DHPG at mGlu5 in membranes prepared from wild-type and mGlu1 knock-out cortex samples. The p-value represents the result of an unpaired, two-tailed Student's t-test with a significance value set at 5%.

Compound	**WT pK_i** **Mean ± S.E.M.**	**mGlu1 KO pK_i** **Mean ± S.E.M.**		**n**
M-MPEP	8.71 ± 0.06	8.71 ± 0.02	N.S.	3
CDPPB	6.53 ± 0.02	6.67 ± 0.03	N.S.	3
CDPPB + 10 μM (S)-3,5-DHPG	7.25 ± 0.09	7.52 ± 0.12	N.S.	3

N.S. $p > 0.05$

4.3 Discussion

Heterodimerisation of mGlu5 has been reported with μ-opioid, adenosine A2a, and dopaminergic D2 receptors, and these interactions have physiological and pharmacological implications for the action of the receptor (Akgün et al., 2013; Cabello et al., 2009). The molecular determinants of these interactions have not been elucidated, but given that mGlu1 and mGlu5 both constitutively homodimerise, and given the high sequence identity between these two receptors, it is surprising that heterodimerisation of these receptors has not been conclusively demonstrated *in vivo*. In the present chapter mutant mGlu1 and mGlu5 receptor constructs, in which the C-terminal tails are replaced with those of the $GABA_{B1}$ and $GABA_{B2}$ with a KKXX (in this case, KKTN) retention motif, were used to induce heterodimerisation at the cell surface and study the pharmacological interaction between the group I receptors. This approach has previously been used in to investigate the functional nature of mGluR dimers (Brock et al., 2007; Goudet et al., 2005; Hlavackova et al., 2005).

Data herein showed that the group I selective agonist (S)-3,5-DHPG did not have significantly higher potency at the mGlu1.5 construct, compared to either the mGlu1, mGlu5, or mGlu5.5 constructs. Replacing the mGluR C-terminal tails with those of the $GABA_B$ protomers does not have a potentiating effect on G protein-coupling as demonstrated by data herein showing the mGlu5.5 dimer construct did not display an increased potency compared to the wild-type mGlu5 receptor.

The effect of each receptor protomer on the overall activation of the dimer was investigated using the mGlu5 selective PAMs LSN-2814617, CDPPB, and ADX-47273. The potentiation of all three of these compounds was reduced by approximately half in the mGlu1.5 heterodimer compared to the wild-type or mutant homodimer, suggesting that the heterodimerisation of mGlu5 with mGlu1 had an inhibitory effect on the potentiation of mGlu5. This could perhaps be explained by the fact that approximately half of the receptors are signalling through the mGlu1 protomers, which are not

potentiated by these ligands, and so the overall potentiation of the dimer would be reduced compared to dimers where both can be activated by the ligand. Indeed, the dual mGlu1-mGlu5 PAM CPPHA showed no significant difference in potentiation between mGlu1, mGlu5, mGlu5.5 and mGlu1.5 constructs, in agreement with this explanation. However, this explanation is not sufficient given that the potentiation induced by Ro 67-4853, which is mGlu1 specific at the human receptor, was not significantly reduced in the mGlu1.5 heterodimer compared to the wild-type mGlu1 receptor. The data herein suggests that perhaps mGlu1 is having an inhibitory effect on the function of mGlu5, but this effect is not equally reciprocal. Remarkably, a similar asymmetric effect has been observed in cell lines expressing mGlu2 heterodimerised with mGlu4 (Kammermeier, 2012; Yin et al., 2014). In this recent study PHCCC, a PAM of mGlu4, displayed markedly reduced cooperativity when mGlu4 was heterodimerised with mGlu2. Furthermore VU0155041, an mGlu4 PAM acting at a different site to PHCCC, had increased cooperativity when the receptor was heterodimerised with mGlu2. In contrast, mGlu2 specific PAMs were not affected to the same extent by heterodimerisation. The similarity between these findings and the findings of this thesis is striking, and perhaps there are common structural changes at the heterodimer which can explain these effects in both heterodimers.

One possible explanation for this asymmetric functional interdependence is that the activation of the mGlu1 protomer with (S)-3,5-DHPG somehow inhibits the action of the PAM at mGlu5. Given studies showing that the 5th TMD is likely the dimer interface of the mGluR TMDs (Yanagawa et al., 2011), perhaps activation of the mGlu1 receptor causes a change in the position of the 5th TMD of the mGlu5 protomer. This helix is known to form part of the MPEP binding site, with many PAMs interacting with residues within this α-helix (Gregory et al., 2014). Indeed, mutation of the Y658 residue on the 5th TMD converted of an mGlu5 PAM, VU0405396, into a NAM (Gregory et al., 2013). Perhaps movement of the mGlu5 TMDs induced by mGlu1 activation could lead to a reduced affinity or cooperativity of PAMs acting at this site. This would also explain why the potentiation

induced by CPPHA is unaffected by the heterodimerisation: CPPHA is known to be reliant on the F585 residue in the 1st TMD of mGlu5, and F599 in the 1st TMD of mGlu1 (Chen et al., 2008) and so movement of the 5th TMD of either receptor may not inhibit the action of CPPHA action by virtue of the topographical distinction of the binding site of this ligand. It is therefore possible that the difference in the amount of inhibition is site-dependent, with the MPEP binding site PAMs of mGlu5 more susceptible to 5th TMD movement than PAMs acting at the CPPHA site. Furthermore, perhaps the lack of inhibition of mGlu1 can be explained by evidence suggesting that the 1st and 2nd TMDs of this receptor are responsible for the dimer interface (Wu et al., 2014). Agonist bound crystal structures of the TMDs of mGlu1 and mGlu5 receptors would be useful in establishing how the tertiary structure of the TMDs changes upon receptor activation. With this information, the effect of heterodimerisation on PAM action at each protomer could be rationalised.

If the mGlu1 receptor was having an inhibitory effect on the MPEP binding pocket of the mGlu5 protomer in its own right then one would expect MPEP to have a reduced antagonistic effect and indeed the data showed that MPEP inhibited the response of the mGlu1.5 construct to only half that of the wild-type mGlu5. Perhaps a direct steric hindrance at the MPEP binding site by mGlu1 is responsible, as the potency of MPEP was reduced at the mGlu1.5 construct compared to the wild-type mGlu5 and mGlu5.5 homodimer constructs, which is explained by the involvement of the 5th TMD in the MPEP binding pocket discussed previously. A similar effect of heterodimerisation has been noted previously for neuropeptide Y (NPY) receptors 1 and 5, where the heterodimerisation switched the mode of antagonism from a surmountable effect to insurmountable (Kilpatrick et al., 2015). Interestingly, the potency of JNJ16259685, an mGlu1 selective NAM, was also significantly reduced at the mGlu1.5 heterodimer compared to mGlu1, however, at concentrations where it had no effect on the mGlu5 or mGlu5.5 constructs it was still able to fully inhibit the mGlu1.5 response. This evidence supports the conclusion that the inhibition of the MPEP site

by the mGlu1 protomer is not reciprocal. Given that JNJ16259685 has been previously shown to bind in the same binding pocket as Ro 67-4853 (Lavreysen et al., 2004), perhaps again the reduction in potency could be explained by the movement of the 5th TMDs induced by activation of the mGluR protomer.

An alternative interpretation could be due to the relative occupancy of the compounds at the mGlu1 and mGlu5 orthosteric binding sites. Given that the occupancy of both protomers of the dimer with an agonist has been shown to increase responses over single protomer activation (Kniazeff et al., 2004), it could be that the contribution of mGlu1 to the overall response is greater than that of mGlu5 due to the increased affinity (S)-3,5-DHPG displays at mGlu1 compared to mGlu5 (Mutel et al., 2000). This would manifest as asymmetry of the contribution of mGlu5 and mGlu1 ligands, and may be the reason for this observed change. A further study to elucidate whether there is any heterodimer-dependent pharmacology between mGlu1 and mGlu5 could be to mutate the residues, Cys694 and Thr695, responsible for G protein coupling at the mGlu1 protomer in the constitutive heterodimer constructs herein (Francesconi and Duvoisin, 1998). This would mean that 100% of the functional response comes from mGlu5, and any inhibition of PAM activation would be caused by inhibition of mGlu5 activation due to heterodimerisation of mGlu1 and mGlu5.

In order to elucidate whether steric hindrance exists between the mGlu1 and mGlu5 receptor binding sites, we used the constitutive dimer constructs to generate membranes which express the mGlu1.5 and mGlu5.5 heterodimers, and compared the pharmacological profile of compounds acting at these receptors to the wild-type mGlu5 receptor. The ability of these constructs to limit cell surface expression of these receptors to their dimerised form has been demonstrated previously by Lilly (data not shown) and other studies (Brock et al., 2007; Goudet et al., 2005; Hlavackova et al., 2005). Immunocytochemical data in this study showed that transiently transfected HEK293 cells only express mGlu5.5 and mGlu1.5 dimers at the

cell surface, though the level of expression of these receptors is heterologous. Furthermore, the whole cell ELISA data generated in this study showed that the expression of the constructs with the modified C-terminal tails is highly dependent on transfection efficiency of each protomer construct, with half the probability of dimer expression at the cell surface compared to the mGlu5 receptor. Though only the dimer constructs are expressed at the cell surface it is likely that monomeric constructs, as well as other combinations of dimer, are expressed and retained in the endoplasmic reticulum. Despite this, differences in the pharmacology of membranes prepared from cells expressing mGlu1.5 can still be compared to wild-type mGlu5 receptors as any difference due to the replacement of mGlu1 and mGlu5 C-terminal tails with those of the $GABA_B$ receptors can be accounted for using the mGlu5.5 construct.

No significant difference in the pharmacology of mGlu5 was observed between the mGlu5, mGlu5.5 and mGlu1.5 dimers in this assay, suggesting that there is no obvious steric hindrance at the MPEP binding site induced by heterodimerisation with mGlu1. Interpretation of this data is complex because though the membrane preparation likely harvests the extracellular membrane, where mGlu1.5 heterodimers are the dominant population, it also likely includes intracellular membranes such as the Golgi apparatus and endoplasmic reticulum, which may contain monomers, mGlu5-C1 homodimers, and other combinations of the constructs used. A better, but certainly not perfect experiment would be to perform these binding experiments in whole cells, however, this would not guarantee that the radioligand would not penetrate the cell membrane and interact with the other possible dimers induced by this system.

The use of radioligand binding to delineate the presence and pharmacological consequences of heterodimerisation *in vivo* has been previously demonstrated using 5-HT_{2A} and mGlu2 receptor ligands (Moreno et al., 2011). The radioligand binding data in this thesis showed that the affinity of the radioligand was unaffected in the mGlu1 knock-out

membranes compared to the wild-type, indicating that there was no steric hindrance in the binding of this compound due to mGlu1. Similarly, the affinity of CDPPB was unaffected in the presence or absence of (S)-3,5-DHPG, suggesting that the binding and allosteric properties of this compound are unaffected by the mGlu1 receptor. There are several possible explanations for the lack of binding interaction between mGlu1 and mGlu5 in *ex vivo* samples. Firstly, perhaps mGlu1 and mGlu5 do not form heterodimers *in vivo* though this would be surprising given that mGlu1 and mGlu5 have been shown to dimerise when co-transfected into recombinant cells (Doumazane et al., 2011). Secondly, perhaps mGlu1 and mGlu5 do not interact pharmacologically, despite the evidence from the constitutive mGlu1.5 heterodimer constructs. Finally, perhaps *in vivo* mGlu1 and mGlu5 heterodimers represent a small minority of the total receptor population, so any pharmacological interaction is obscured by the dominant homodimer populations. A recently reported study using functional readouts of group I mGluR action in native cells to study heterodimerisation perhaps provides a method to investigate the existence and functional consequence of group I mGluR heterodimerisation *in vivo* (Sevastyanova and Kammermeier, 2014). Using cultured medium spiny neurons, or other native tissues where mGlu1 and mGlu5 are highly expressed, to investigate whether PAMs of mGlu5 have a reduced ability to potentiate agonist response could provide conclusive evidence that these dimers exist and are functionally interdependent in native systems.

The modification of GPCRs in order to induce dimerisation at the cell surface has been used to evaluate signalling properties of these receptors with some success. For example, a system using a bimolecular fluorescence complementation (BiFC) system in NPY receptors and the ß2-adrenoceptor has provided evidence that dimerisation has pharmacological and regulatory consequences across GPCR families (Kilpatrick et al., 2015). In the case of the mGluRs, using the natural 'quality control' properties of the $GABA_B$ receptor has given great insight into the effect of dimerisation at these receptors. Studies using these receptors have led to many insights into the

function of the mGluR homodimer. It is important to understand the limits of these systems, and in the present study, we have shown that the action of allosteric modulators at these complexes displays asymmetry and probe dependency. Though previous studies using these constructs have provided evidence that the full activity of the dimer can be achieved by potentiation of either protomer of the dimer (Goudet et al., 2005), the data suggests that this phenomenon is highly dependent on both the ligand and target. This is highlighted by the data presented herein showing that PAMs of mGlu5 are unable to potentiate the response of the heterodimer to the same degree as the homodimer, but the mGlu1 PAM does. The use of mGluRs modified with $GABA_{B1}$ and $GABA_{B2}$-KKTN tails to drive dimerisation at the cell membrane, based on previous studies (Brock et al., 2007), was validated furthermore by the immunocytochemical and whole-cell ELISA performed on transiently transfected HEK293 cells herein. It showed that mGlu1 or mGlu5 receptor chimaeras where the C-terminal tail has been replaced with that of $GABA_{B2}$-KKTN will only reach the cell surface in the presence of the corresponding $GABA_{B1}$ tail. This makes this model incredibly useful for studying the interaction between mGluR heterodimers, and these constructs make good candidates for the study of other inter-mGluR heterodimers.

Understanding pharmacological interactions between mGlu1 and mGlu5, such as those demonstrated in this chapter, is key to understanding potential pharmacological consequences of the dimerisation *in vivo*. Indeed, functional consequences of heterodimerisation of mGlu5 and the μ-opioid receptors has already been demonstrated (Akgün et al., 2013). Such pharmacological interactions have also been shown to be important for inter-mGluR heterodimers, with PAMs of mGlu4 failing to potentiate the action of their target receptor in mGlu2/4 heterodimers expressed in corticostriatal neurons (Yin et al., 2014). Furthermore, the findings herein extend the pharmacological toolbox available for the study of heterodimerisation of mGlu1 and mGlu5 *in vivo*. Such heterodimerisation has not been conclusively demonstrated, however, given that the full length receptors do dimerise in recombinant systems, it is only a matter of time

until they are demonstrated in native systems (Doumazane et al., 2011). The findings of this chapter could be readily translated to native systems where mGlu1 and mGlu5 are expressed in order to provide conclusive evidence of heterodimerisation *in vivo*.

Chapter 5 – Investigating Neuronal Cell Death Induced by Positive Allosteric Modulators Acting at the mGlu5 Receptor

5.1 Introduction

The ionotropic glutamate receptors have long been known to induce excitotoxic cell death of neurones in the CNS (Sattler and Tymianski, 2001). In brief, an abundance of glutamate in the synapse causes prolonged, abnormal influx of Ca^{2+} into the neuronal cells through NMDA receptors and Ca^{2+} permeable AMPA or kainate receptors. This influx of Ca^{2+}, along with intracellular Ca^{2+} release, overwhelms the signalling and regulatory mechanisms of the cell leading to free-radical formation and metabolic dysfunction ultimately resulting in cell death. This process of excitotoxic cell death is thought to be involved in the pathology of many diseases of the CNS, such as cerebral ischemia and neurodegenerative diseases (Choi, 1992; Mattson, 2000). Indeed memantine, an NMDA receptor antagonist clinically validated for the treatment of Alzheimer's disease, has been shown to be neuroprotective in both *in vivo* and *in vitro* models (Parsons et al., 1999). Given that glutamate is the neurotransmitter responsible for excitotoxic cell death, it is reasonable to assume that the mGluRs may also play a role in neuronal cell death.

A lack of potent subtype specific agonists of group I mGluRs limited the ability to study the effects of mGlu5 activation on cell death. *In vitro* studies using the mGlu5 selective agonist CHPG showed that mGlu5 activation attenuates cell death in cortical neurons co-cultured with microglia (Byrnes et al., 2009). Furthermore, CHPG induced activation of mGlu5 inhibits neuronal cell death in primary cortical cultures treated with amyloid-beta (Movsesyan et al., 2004). The discovery of mGlu5 specific PAMs have allowed the study of this receptor in isolation. Studies performed *in vitro* paint a complex picture; for instance, CDPPB has been shown to be protective against neuronal injury, inhibiting lactate-dehydrogenase (LDH)

release in a concentration-dependent manner in a cultured neuronal model of traumatic brain injury (Chen et al., 2012). In addition to these *in vitro* observations, *in vivo* studies have shown that mGlu5 PAMs can have neuroprotective action. For example, in a mouse model of Huntington's disease, CDPPB decreased striatal cell death via an AKT-related mechanism (Doria et al., 2015). Similarly VU0360172 administration significantly reduced the size of lesions induced by traumatic brain injury in the mouse cortex and hippocampus (Loane et al., 2014).

In contrast, reports have recently been published which show that some mGlu5 PAMs are intrinsically neurotoxic. Chronic administration of a high-dose of the mGlu5 PAMs 5PAM523, 5PAM000, 5PAM413, and 5PAM916 caused seizures and neuronal cell loss in the hippocampus and auditory cortex of treated mice (Parmentier-Batteur et al., 2014). The lack of neurotoxicity in mGlu5 knock-out mice suggests that this effect is dependent on the action of mGlu5. Further studies have shown that this is not a unique effect of this chemical series: VU0424465 also induces neurotoxicity, providing further evidence that toxicity is caused by an mGlu5-dependent mechanism, and not caused by a metabolite or related compound acting elsewhere (Conde-Ceide et al., 2015).

In this chapter, I investigate the effect of chronic, high-dose LSN-2814617 administration in the mouse brain using immunohistochemical methods. Furthermore, I attempt to model this neurotoxicity using primary cortical cultures in order to provide an *in vitro* model for further investigation of the toxic signalling mechanism and to aid screening of future mGlu5 PAMs.

5.2 Results

5.2.1 Evaluating the action of LSN-2814617 in the Hippocampus

Based on previous reports, mGlu5 PAMs are neurotoxic, with neurones present in the hippocampus displaying nuclear condensation with an eosinophilic cytoplasm, 'typical morphological characteristics of necrotic neurons stained with H&E' (Parmentier-Batteur et al., 2014). In order to assess the action of LSN-2814617 in the mouse hippocampus, histochemical and immunohistochemical methods were applied to brain samples obtained from mice treated with either vehicle or 100 $mg.kg^{-1}$ of LSN-2814617 for 7 days. Haemotoxylin and eosin (H & E) staining was used to visualise cells in coronal sections of the hippocampus from formalin-fixed mouse brains. In the vehicle treated brains, neuronal staining was evident, and there were no necrotic neurones (as defined above) present in the dentate gyrus, CA3 or CA1 regions (Figure 5.2.1.1). Similarly, in the LSN-2814617 treated brains there was no evidence of necrotic neurones in the dentate gyrus, CA3, or CA1 regions (Figure 5.2.1.2). In order to assess the identity of cell-types present, coronal sections of the dentate gyrus in the hippocampus from both animal groups were stained with an antibody specific for glial fibrillary acidic protein (GFAP), a marker for astrocytes, and NeuN, a neurone specific marker, and visualised with appropriate fluorescent secondary antibodies (Figure 5.2.1.3). The fluorescent secondary antibodies did not display non-specific staining (Figure 5.2.1.3A). In both the vehicle and LSN-2814617 treated brains, the dentate gyrus was heavily stained by NeuN, indicating a population of neuronal cells. GFAP staining was also evident in the surrounding area, however, there was no obvious difference in the level of GFAP staining, indicating that astrocytes were present, but not elevated in drug-treated animals. In order to assess the level of mGlu5 expression, coronal sections of the hippocampus from vehicle and drug-treated animals were stained with an anti-mGlu5 antibody, and visualised as before (Figure 5.2.1.4). The mGlu5 receptor was expressed in both vehicle and LSN-2814617 treated animals, with staining visible in the dentate gyrus and the

surrounding area, indicating expression in both neurones and glial cell types. There was no obvious difference in the expression of mGlu5 between vehicle and drug treated animals. In order to assess whether LSN-2814617 activates mGlu5 expressed in these cell types, Gq/11 activity was investigated using an antibody specific for c-fos, a transcription factor intrinsically linked to Gq/11 activation (Edling et al., 2007). Staining of c-fos was clearly elevated in the dentate gyrus of LSN-2814617 treated mice compared to vehicle treated mice, indicating that LSN-2814617 is present at sufficient concentrations to activate mGlu5 in the these samples (Figure 5.2.1.5).

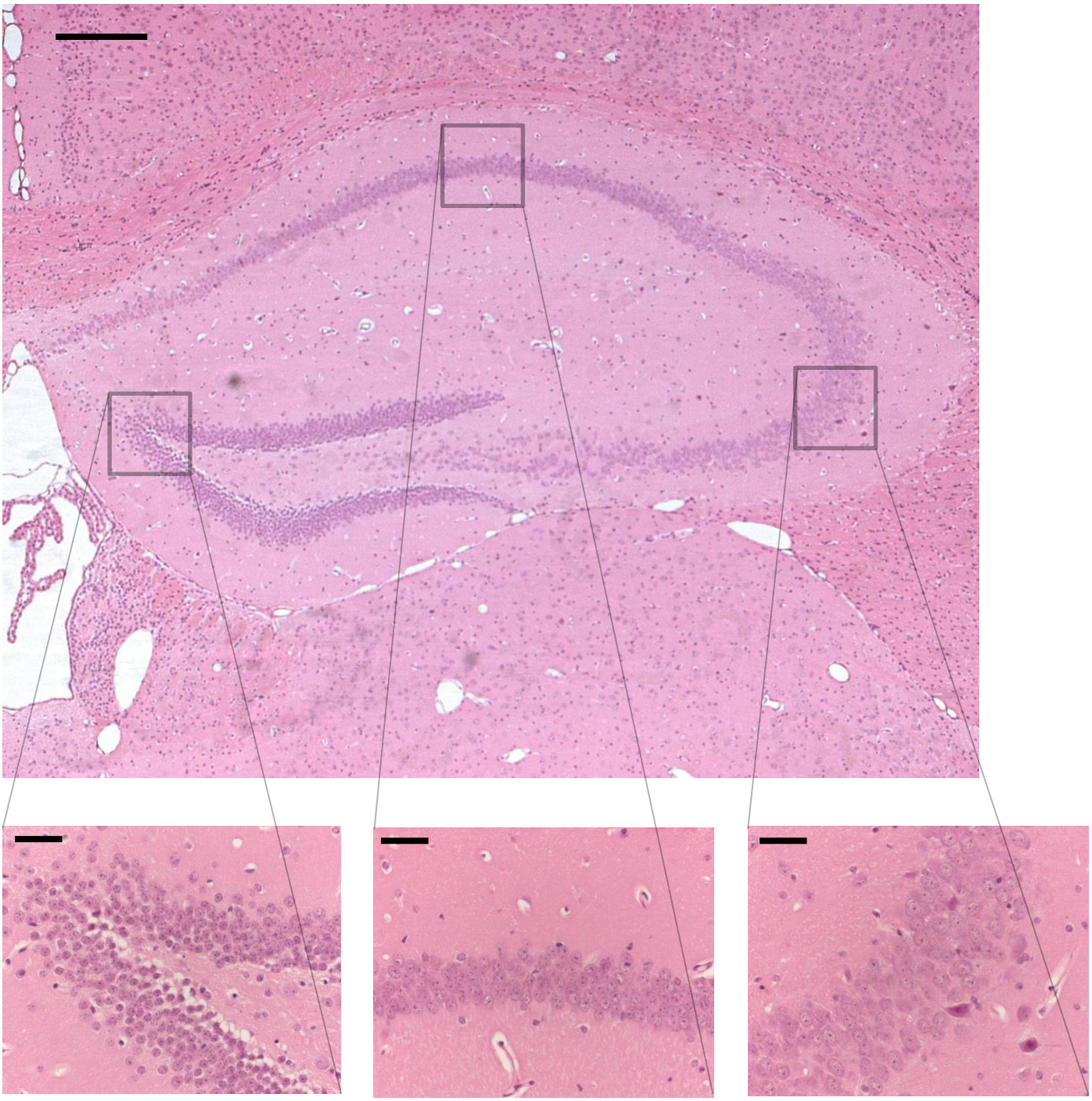

Figure 5.2.1.1 Images from an H&E stained coronal section of the hippocampus of a perfusion fixed brain from a mouse treated with vehicle once a day for 7 days. The image shows the hippocampus at 5x magnification with the scale bar representing 500 µm (top). Close up images are shown of the dentate gyrus (left), CA3 (middle), and CA1 (right) of the hippocampus at 40x magnification with the scale bar representing 50 µm. The images are of a brain from a single animal, chosen as a representative sample of eight animals.

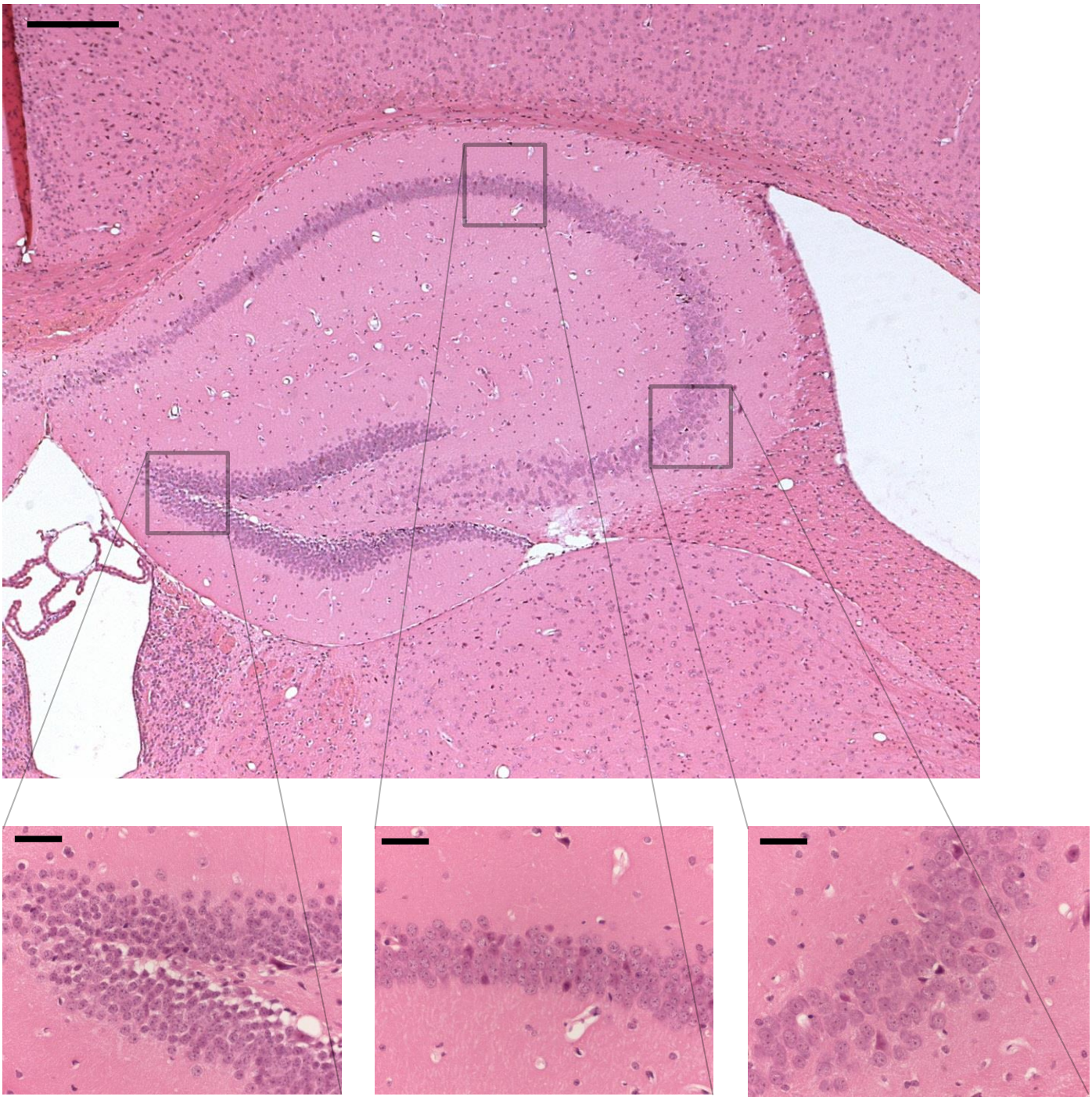

Figure 5.2.1.2 Images from an H&E stained coronal section of the hippocampus of a perfusion fixed brain from a mouse treated with 100 mg.kg^{-1} LSN-2814617 once a day for 7 days. The image shows the hippocampus at 5x magnification with the scale bar representing 500 µm (top). Close up images are shown of the dentate gyrus (left), CA3 (middle), and CA1 (right) of the hippocampus at 40x magnification with the scale bar representing 50 µm. The images are of a brain from a single animal, chosen as a representative sample of eight animals.

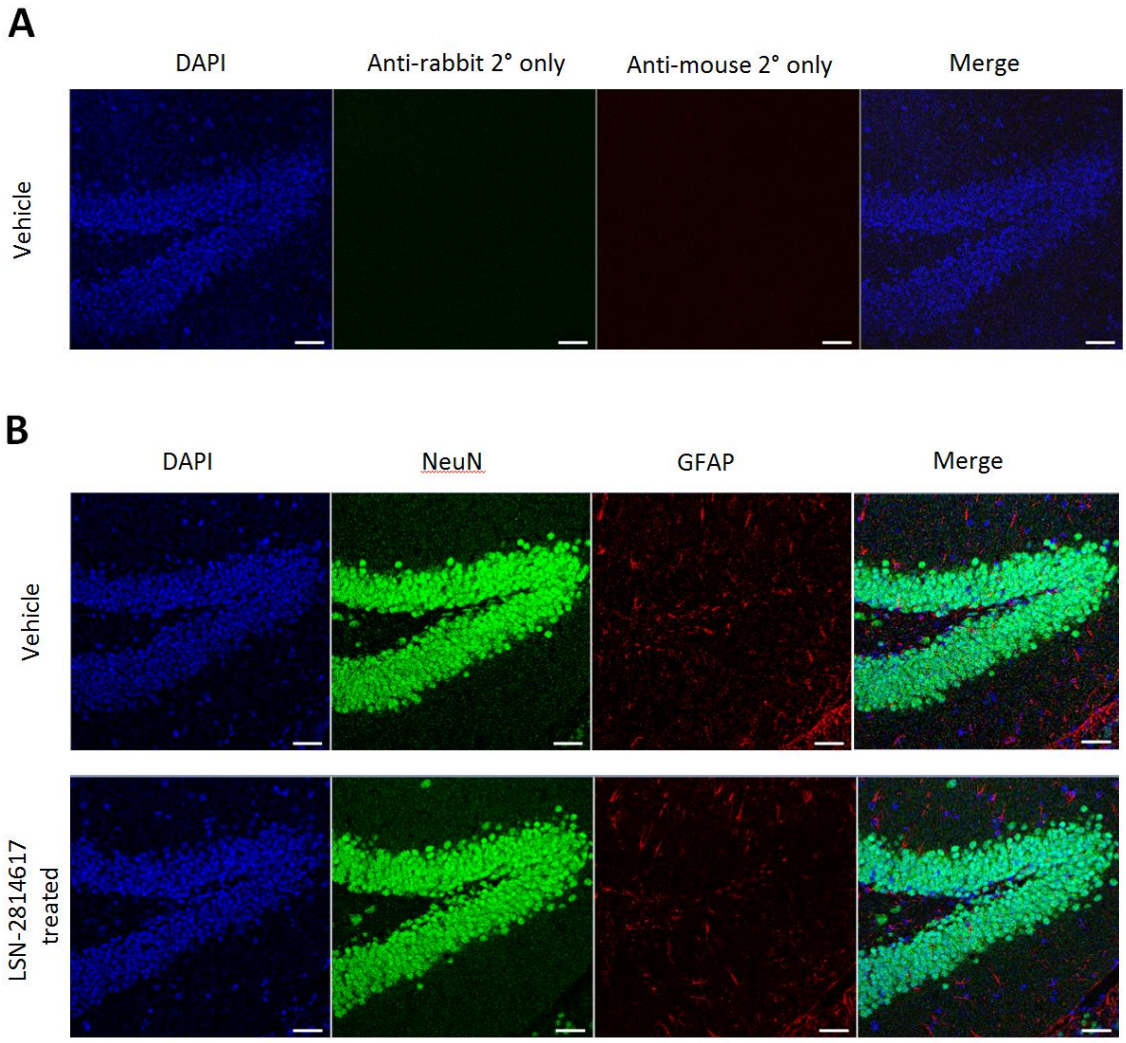

Figure 5.2.1.3 Images from an immunohistochemical analysis of the hippocampus of a perfusion fixed brain from a mouse treated with vehicle or 100 mg.kg^{-1} LSN-2814617 once a day for 7 days. The top panel (A) shows the dentate gyrus stained with DAPI, a flourescent secondary anti-rabbit antibody, and a fluorescent secondary anti-mouse antibody. Panel (B) shows the dentate gyrus stained with NeuN and GFAP primary antibodies and their corresponding fluorescent secondary antibodies. All images were taken at 40x magnification using confocal microscopy with the scale bar representing 50 µm.

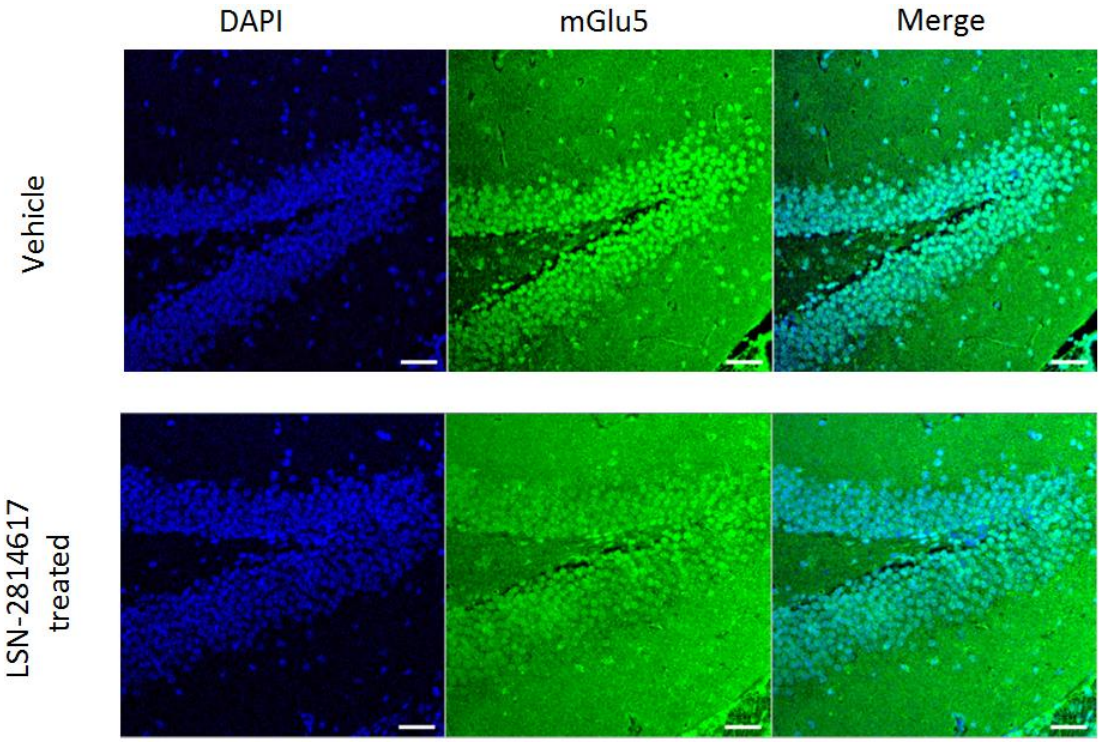

Figure 5.2.1.4 Images from an immunohistochemical analysis of the hippocampus of a perfusion fixed brain from a mouse treated with vehicle or 100 mg.kg^{-1} LSN-2814617 once a day for 7 days. The images show the dentate gyrus stained with an anti- mGlu5 primary antibody with the corresponding fluorescent secondary antibodies. All images were taken at 40x magnification using confocal microscopy with the scale bar representing 50 µm.

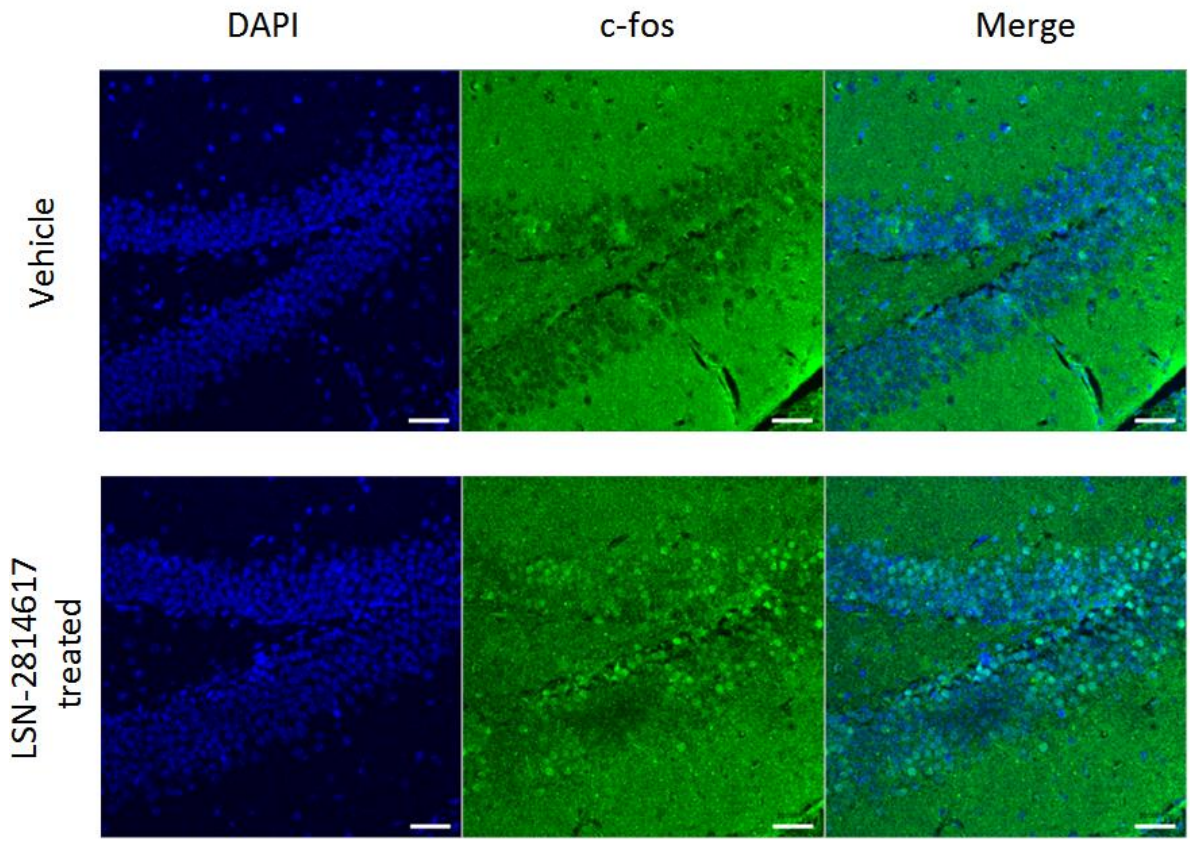

Figure 5.2.1.5 Images from an immunohistochemical analysis of the hippocampus of a perfusion fixed brain from a mouse treated with vehicle or 100 $mg.kg^{-1}$ LSN-2814617 once a day for 7 days. The images show the dentate gyrus stained with an anti- c-fos primary antibody with the corresponding fluorescent secondary antibodies. All images were taken at 40x magnification using confocal microscopy with the scale bar representing 50 μm.

5.2.2 Evaluating the action of LSN-2814617 in the anterior cortex of the mouse brain

Previous reports suggest that chronic treatment with mGlu5 PAMs produces neurotoxicity, with necrotic neurones present in the anterior cortex, specifically the auditory cortex (Parmentier-Batteur et al., 2014). The effect of chronic, high-dose treatment with LSN-2814617 in the mouse anterior cortex was investigated with histochemical and immunohistochemical methods in slices from formalin-fixed brains of mice treated with vehicle or 100 $mg.kg^{-1}$ of LSN-2814617 for 7 days. H & E staining showed the presence of pkynotic neurones in the midsection, dorso-ventrally, of the anterior cortex of treated animals (illustrated in Figure 5.2.2.1A and C), which were absent in vehicle treated animals (Figure 5.2.2.1B). Necrotic neurones are characterised by a fragmented nucleus surrounded by diffuse magenta staining (illustrated in Figure 5.2.2.2). These necrotic neurones were specifically localised to this section, with the surrounding areas absent of any neuronal cell death in treated animals, however, the number of necrotic neurones was highly variable. The total number of neurones in the cortical portion of each section from untreated and treated animals was estimated, and found to be the same (Figure 4.2.2.3A). The total number of necrotic neurones in both vehicle and drug-treated brain samples was counted manually, and revealed that the degree of cell death was highly variable in the drug treated animals (Figure 4.2.2.3B).

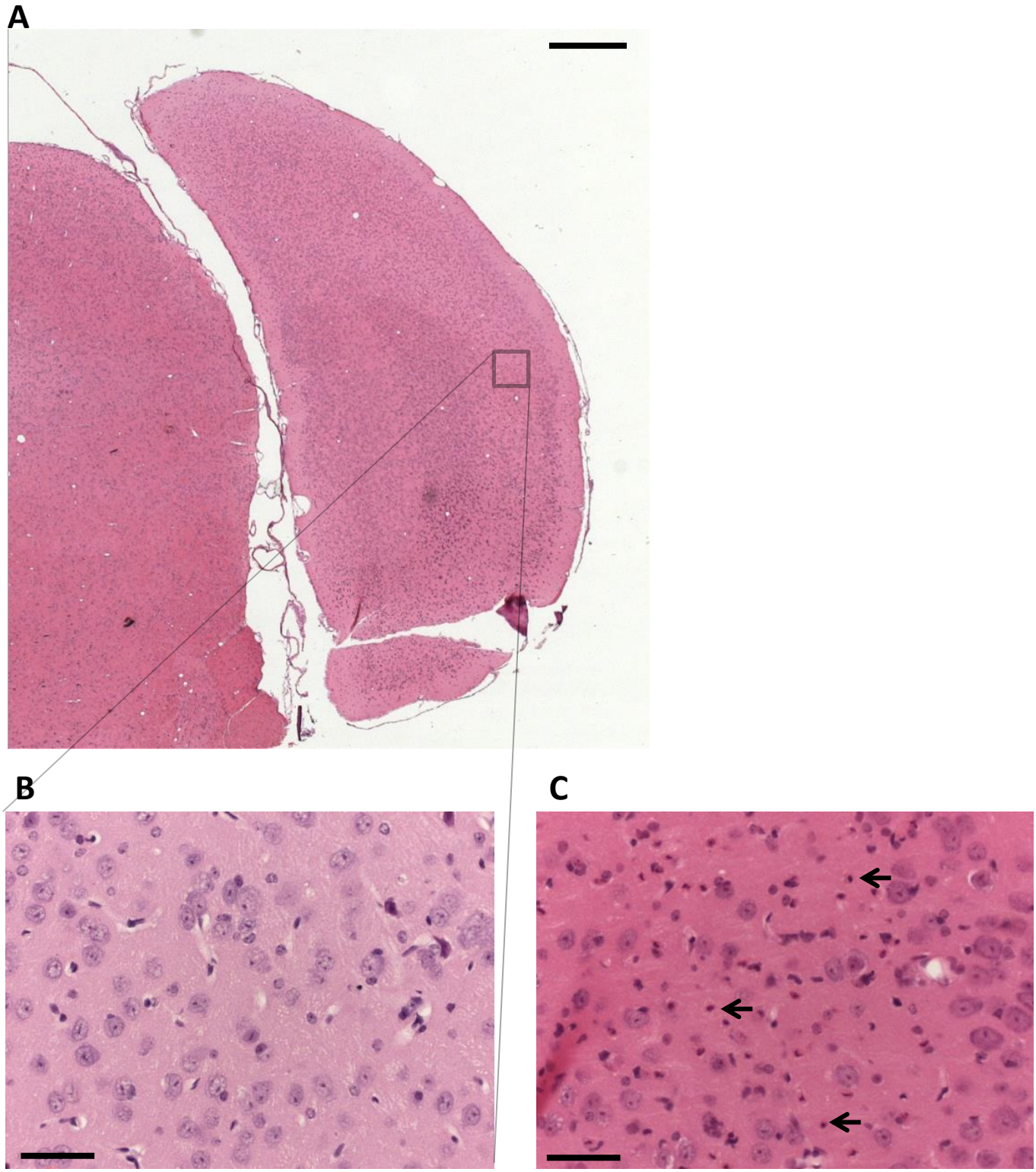

Figure 5.2.2.1 Images from an H&E stained coronal section of the anterior cortex of a perfusion fixed brain from a mouse. The image shows the left hemisphere of the cortex at 2.5x magnification with the scale bar representing 1000 µm (A). Close up images are shown of the middle section (dorso-ventrally) of the cortex from the brain of a mouse treated with vehicle (B) or 100mg.kg^{-1} LSN-2814617 (C) once a day for 7 days. Necrotic neurons are indicated by a leftward arrow and three examples are given, though more may be present. These images were taken at 40x magnification with the scale bar representing 50 µm. The images are of a brain from a single animal, chosen as a representative sample of eight animals.

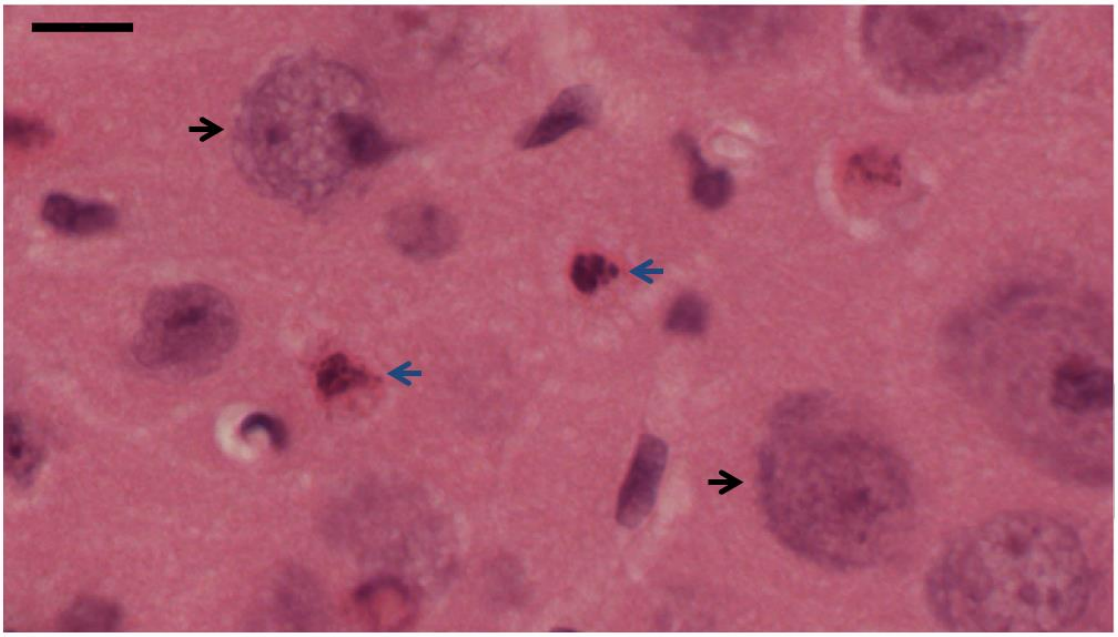

Figure 5.2.2.2 Images from an H&E stained coronal section of the anterior cortex of a perfusion fixed brain from a mouse. Typical example neurons are indicated with a black arrow, example necrotic neurons are indicated by a blue arrow and two examples of each are given. These images were taken at 40x magnification with the scale bar representing 10 μm. The image is a single coronal section chosen as a representative example from 8 treated animals.

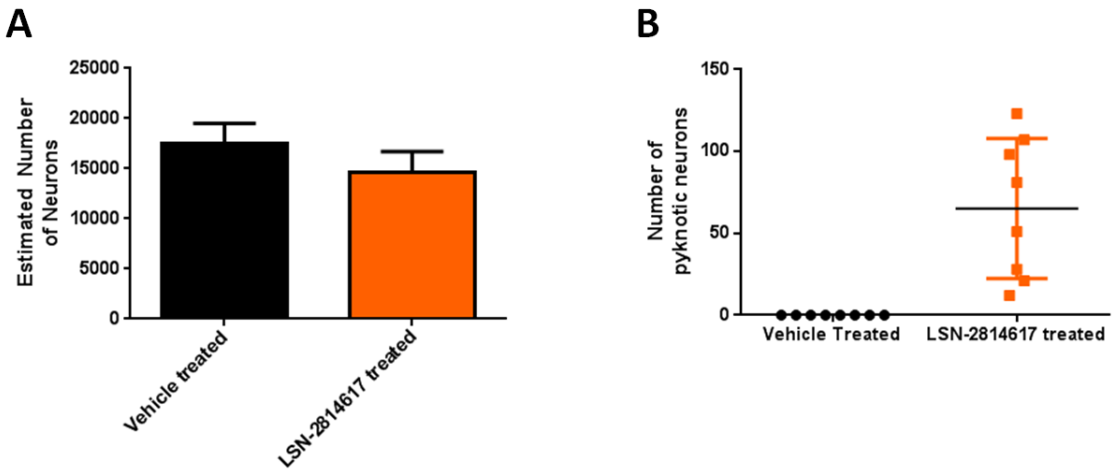

Figure 5.2.2.3 The number of total neurons in one hemisphere of the coronal sections of the anterior cortex from a mouse brain were estimated (*See Methods*). The total estimated number of neurons are shown as the mean ± S.D. from three mouse brains from mice treated with vehicle or 100 $mg.kg^{-1}$ LSN-2814617 for 7 days (A). The total number of necrotic neurons present in a coronal section were manually counted from each mouse (B). The graph is a scatter plot showing each individual section from 8 separate animals in each group with the mean and standard deviation.

Immunohistochemical techniques were used in order to assess the effects of LSN-2814617 in the midsection of the anterior cortex. The coronal sections from mice treated with 100 $mg.kg^{-1}$ of LSN-2814617 had an increased expression of c-fos in the midsection of the anterior cortex and an apparent increase or activation of astrocytes across the cortex, indicated by GFAP immunostaining, compared to the vehicle treated animals (Figure 5.2.2.4 and Figure 5.2.2.5). The effect of chronic LSN-2814617 administration on mGlu5 expression in the anterior cortex was also assessed (Figure 5.2.2.6). In the dorso-lateral midsection of the cortex, mGlu5 expression was reduced in the drug-treated animals compared to the wild-type (Figure 5.2.2.6A). The antibody used did not display any non-specific staining (Figure 5.2.2.6B). Taken together, these data show that LSN-2814617 activates mGluR5 in this area of the cortex, and furthermore, astrocytic invasion of this area is occurring as a direct consequence of LSN-2814617 action.

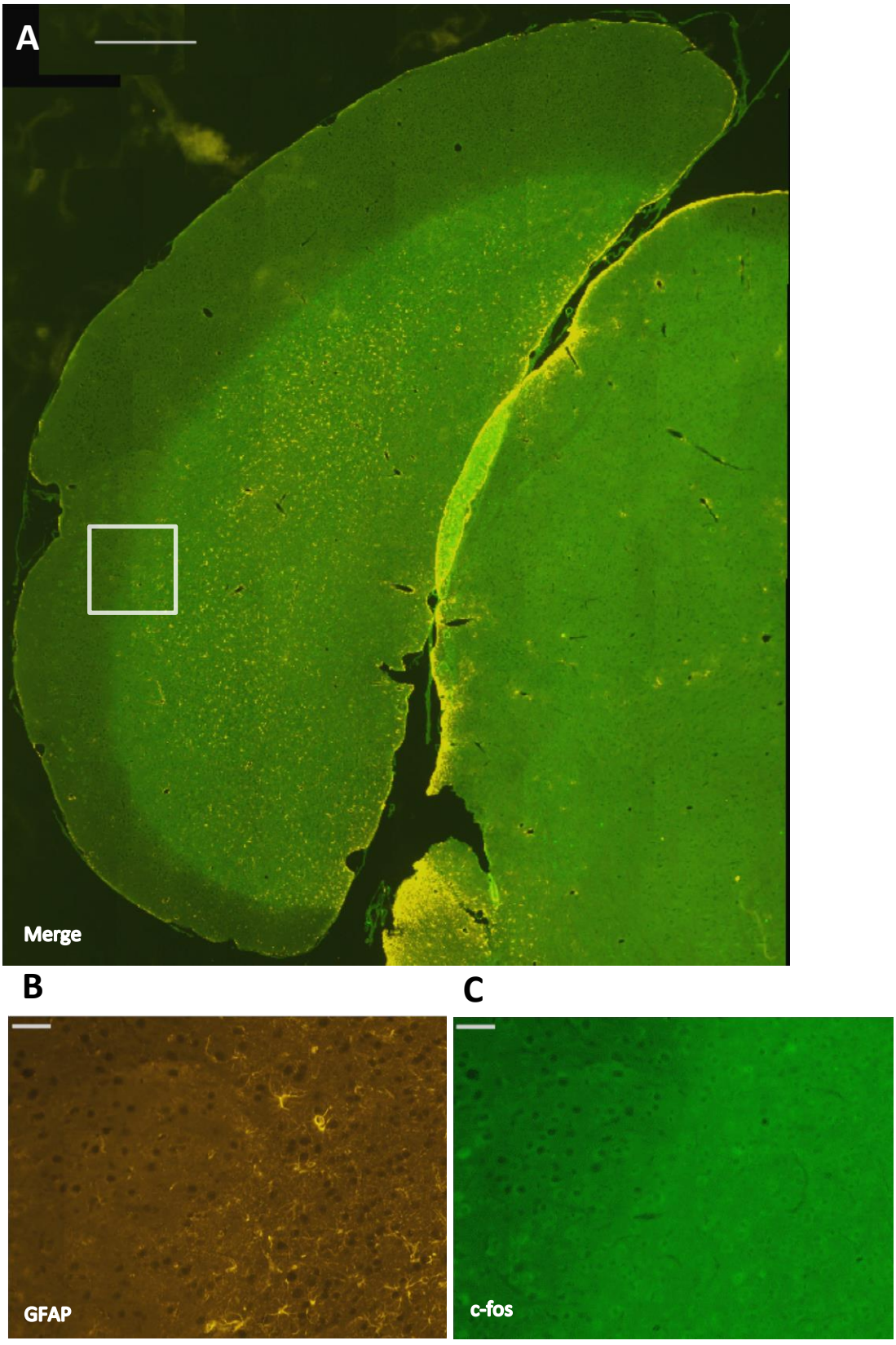

Figure 5.2.2.4 Images from a coronal section of the anterior cortex of a perfusion fixed brain from a mouse treated with vehicle for 7 days immunostained using anti-GFAP (orange) and anti-c-fos (green) primary antibodies. (A) The image shows a tilescan of images taken at 40x magnification with the scale bar representing 1000 µm. Close up images of the midsection of the cortex (highlighted in A with a white square) show GFAP (B) or c-fos (C) immunostaining. These images were taken at 40x magnification using fluorescent photography with the scale bar representing 50 µm. The images are of a brain from a single animal, chosen as a representative sample of three animals.

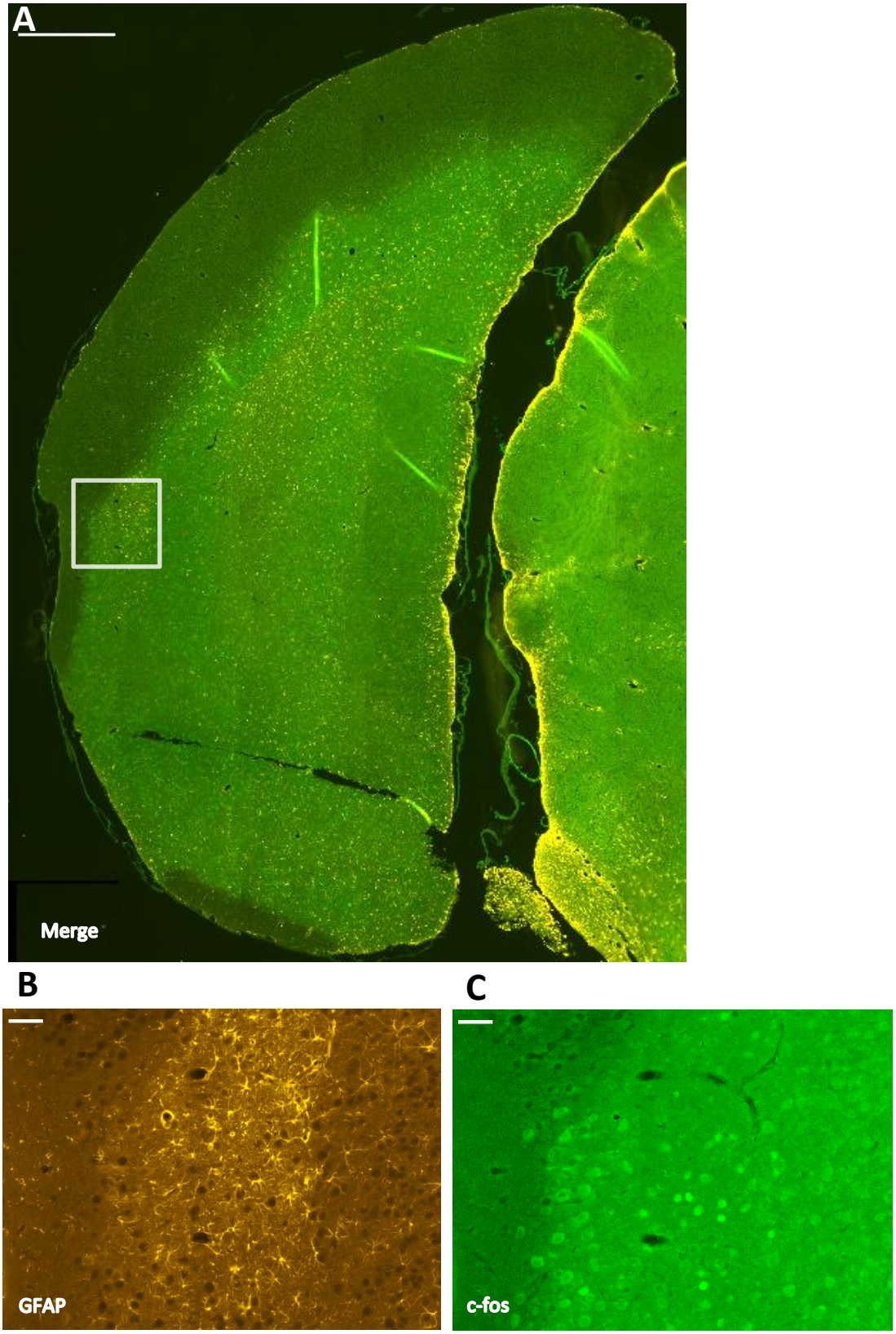

Figure 5.2.2.5 Images from a coronal section of the anterior cortex of a perfusion fixed brain from a mouse treated with 100 mg.kg^{-1} LSN-2814617 for 7 days immunostained using anti-GFAP (orange) and anti-c-fos (green) primary antibodies. (A) The image shows a tilescan of images taken at 40x magnification with the scale bar representing 1000 µm. Close up images of the midsection of the cortex (highlighted in A with a white square) show GFAP (B) or c-fos (C) immunostaining. These images were taken at 40x magnification using fluorescent microscopy with the scale bar representing 50 µm. The images are of a brain from a single animal, chosen as a representative sample of three animals.

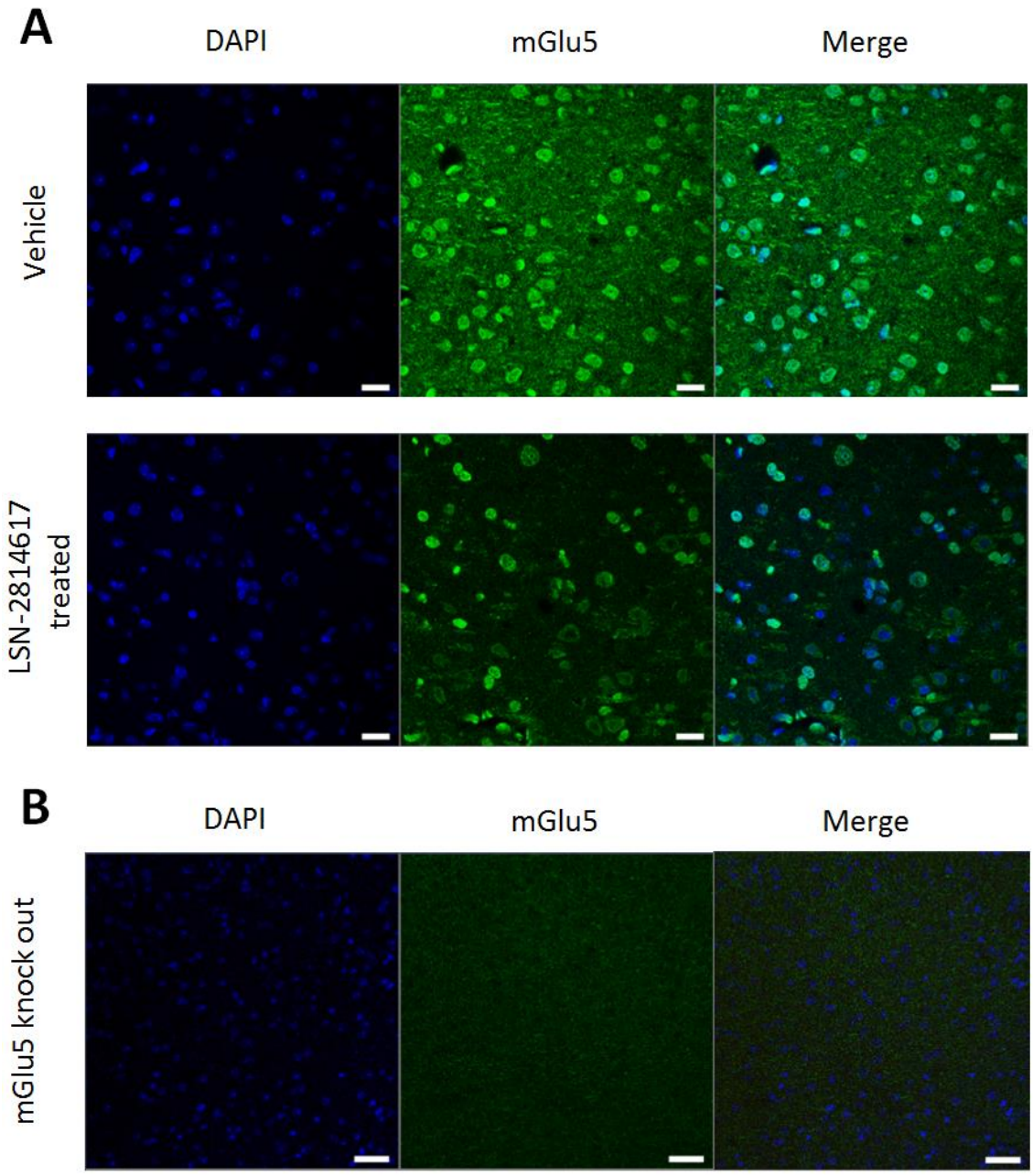

Figure 5.2.2.6 Images from an immunohistochemical analysis of the anterior cortex of a perfusion fixed brain from a mouse treated with vehicle or 100 mg.kg^{-1} LSN-2814617 once a day for 7 days. The images in panel (A) show sections from the mid-cortex (dorsolaterally) of the left hemisphere of the anterior cortex stained with an anti- mGlu5 primary antibody with the corresponding fluorescent secondary antibody. The images shown represent a section from a single animal at 40x magnification using confocal microscopy with the scale bar representing 50 μM, chosen as representative of three independent experiments. The images in panel B show mGlu5 knock-out mouse (B) stained with an anti- mGlu5 primary antibody with the corresponding fluorescent secondary antibody. All images were taken at 20x magnification with the scale bar representing 100 μM and represent a single representative image from three independent experiments.

5.2.3 Modelling the Neurotoxicity of mGlu5 using Primary Cortical Neurones from the Rat

Given that the neuronal damage induced by mGlu5 PAMs in the mouse brain is highly localised, an *in vitro* model using primary cortical neurones is potentially a superior angle from which to approach study of the signalling cascades involved. With this in mind, the ability of mGlu5 allosteric modulators to affect glutamate-induced neurotoxicity was assessed in primary rat cortical neurone cultures. The ability of a set concentration of LSN-2814617 and MPEP to affect neuronal cell death induced by a range of concentrations of glutamate was assessed in neurones, grown for 7 days *in vitro* (DIV), using LDH activity as a measure of cell death (Figure 5.2.3.1). L-glutamate induced a concentration-dependent increase in LDH activity indicating neuronal death was occurring (Figure 5.2.3.1A). LSN-2814617 did not potentiate the neurotoxicity of L-glutamate, however, the negative allosteric modulator MPEP reduced LDH activity to 65.1 ± 0.3 % of the maximum induced by L-glutamate alone. Further experiments showed that the neuroprotective effect of MPEP was not concentration-dependent, indicating that this is an off-target effect (Figure 5.2.3.1B). The pharmacological and statistical analyses of these data are summarised in Table 5.2.3.1.

It is possible that LSN-2814617 does not alter total cell death, but rather increases the rate at which L-glutamate induces excitotoxic cell death. With this in mind, LDH activity was assessed at various time-points over 24 hours in primary cortical neurones grown for 7 DIV in the presence of an LD_{80} concentration of L-glutamate alone, or with a set concentration of LSN-2814617 or MPEP (Figure 5.2.3.2). L-glutamate induced 50% cell death after 306 ± 21 minutes. The addition of LSN-2814617 did not affect the rate of cell death, however, MPEP reduced the maximum cell death to 21.3 ± 2.9% of the maximum induced by L-glutamate alone, with 50% of the maximal cell death under these conditions occurring after 479 ± 75 minutes.

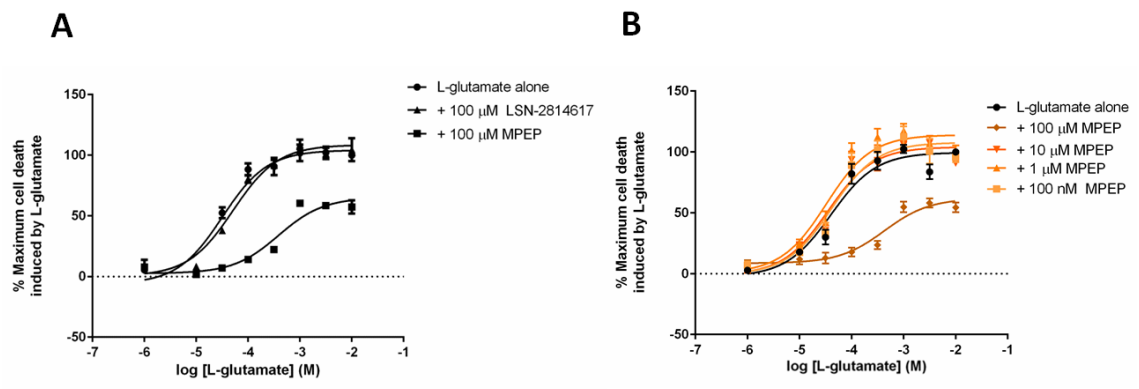

Figure 5.2.3.1 The ability of allosteric modulators to affect the excitotoxic cell death of rat cortical neurons grown *in vitro* for 7 days was assessed using an enzymatic lactate dehydrogenase colourometric assay. A range of concentrations of the neurotransmitter L-glutamate (1 μM to 10 mM) was incubated in the absence or presence of a set concentration of LSN-2814617 or MPEP for 24 hours before a media sample was taken and analysed for lactate dehydrogenase activity (A). A range of concentrations of L-glutamate (1 μM to 10 mM) was incubated with a range of concentrations of MPEP (100 nM to 100 μM) for 24 hours before a sample of media was taken and assayed for lactate dehydrogenase activity (B). The graphs show the combined data shown as mean ± S.E.M. of three independent experiments performed in duplicate. Pharmacological and statistical analyses of the data is summarised in Table 5.2.3.1.

Table 5.2.3.1 A summary of the quantitative analysis of ligands inducing excitotoxic cell death in mixed primary cortical neurones grown for 7 DIV. pLD50 and the total % of cell death induced under each condition are expressed as mean ± S.E.M. Statistical analyses were performed with an unpaired, two-tailed Student's t-test.

Compounds	pLD_{50}	p-value	% of maximum cell death induced by L-glutamate	p-value	n
L-glutamate alone	4.49 ± 0.09	-	104.2 ± 2.9	-	3
+ 100 µM LSN-2814617	4.29 ± 0.08	>0.05	108.5 ± 2.9	>0.05	3
+ 100 µM MPEP	3.41 ± 0.10	<0.01	65.1 ±3.1	<0.01	3

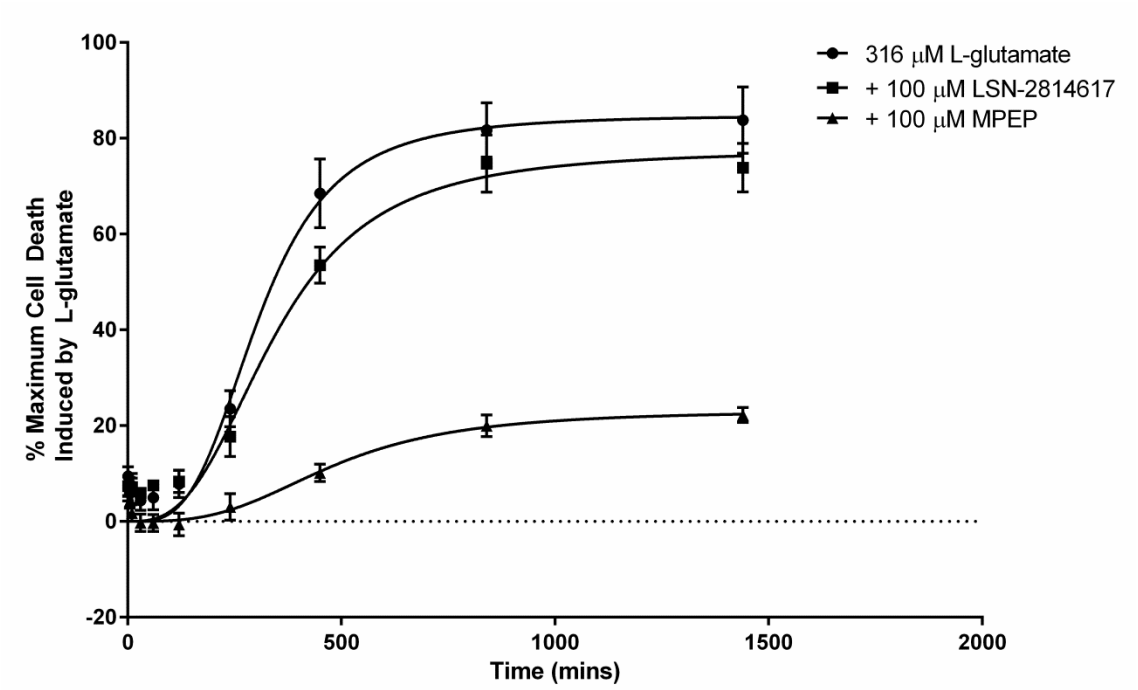

Figure 5.2.3.2 The ability of allosteric modulators to affect the rate of excitotoxic cell death of rat cortical neurons grown *in vitro* for 7 days was assessed using an enzymatic lactate dehydrogenase colourometric assay. A set of concentration of the neurotransmitter L-glutamate was incubated in the absence or presence of a set concentration of LSN-2814617 or MPEP for a range of incubation times (0 to 24h) before a media sample was taken and analysed for lactate dehydrogenase activity. The graphs show the combined data shown as mean ± S.E.M. of three independent experiments performed in duplicate.

5.2.4 Modelling the Neurotoxicity of mGlu5 using Primary Mixed Cortical Cultures of Neurones and Astrocytes

Given that astrocytes were increasingly localised nearby the site of neuronal damage in the mouse cortex, determining whether they play a key role in the cell death induced by LSN-2814617 deserved investigation. With this in mind, the level of expression of mGlu5 and the astrocytic marker GFAP was immunoassayed in primary cultures, in the absence or presence of the glial inhibitor arabinose C, over 21 DIV (Figure 5.2.4.1). In mixed primary cultures, expression of both mGlu5 and GFAP increased over 21 days, plateauing after 14 DIV (Figure 5.2.4.1A-C). In primary cultures grown in the presence of arabinose C, mGlu5 expression was lower than in mixed cultures overall, though it plateaued after 14 DIV as before. GFAP expression was absent, indicating the absence of astrocytes in these primary cultures (Figure 5.2.4.1D-E).

The suitability of mixed neuronal cultures grown for 14 DIV as a model of LSN-2814617 toxicity was assessed using LDH activity as a measure of cell death as before (Figure 5.2.4.2). L-glutamate induced a concentration dependent increase in LDH activity indicating excitotoxic cell death. The maximum LDH activity induced by L-glutamate represented approximately 22% of the maximum upon lysis of the cells, indicating that neuronal cells account for approximately a fifth of the total cells in the mixed culture. LSN-2814617 did not significantly change either the ability of L-glutamate to induce cell death, or the total amount of cell death ($p > 0.05$, unpaired, two-tailed Student's t-test). This data suggests that this model does not accurate reflect the neurotoxic action of LSN-2814617 demonstrated *in vivo*. Pharmacological and statistical analyses of this data is summarised in Table 5.2.4.1.

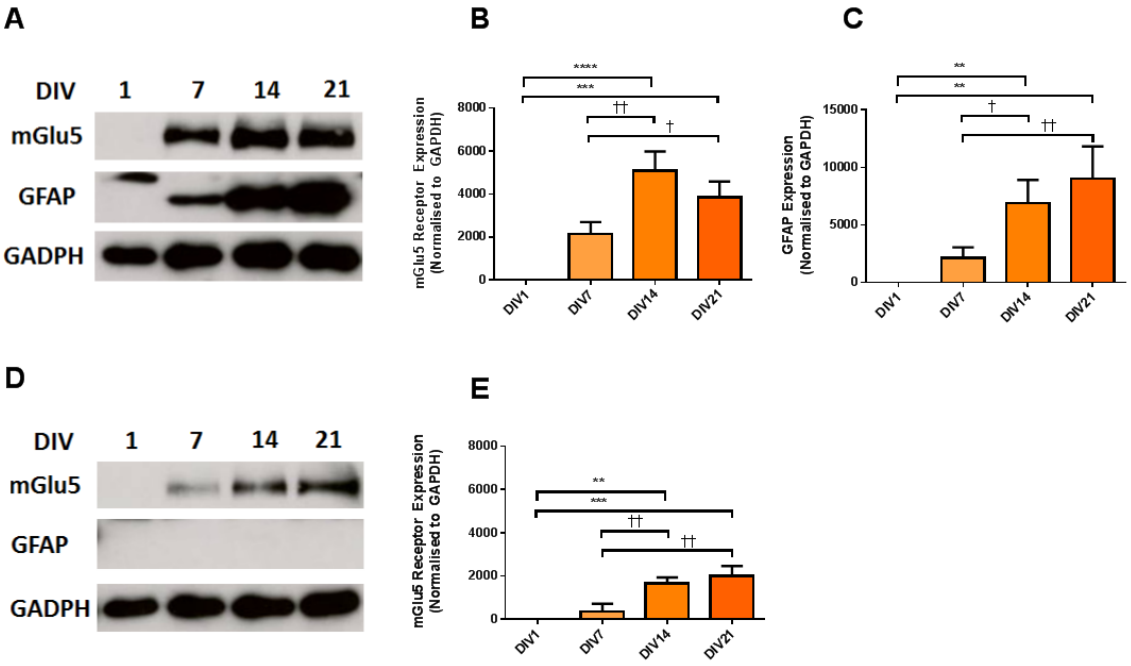

Figure 5.2.4.1 The expression of mGlu5 and the glial marker GFAP in rat cortical neurons grown over the course of 21 days *in vitro* was assessed by an immunoblot assay. An immunoblot analysis of solubilised protein samples from rat cortical neurons grown in the absence (A, mixed cultures) or presence (D, pure neuronal cultures) of Ara-C were seperated by SDS-PAGE before being assayed with an anti- mGlu5, anti- GFAP, or anti-GAPDH primary antibody. These images show a representative example of three independent experiments. The graphs show the densitometric analysis of mGlu5 expression in mixed cultures (B) and neuronal cultures (E), and GFAP expression in mixed cultures (C). The graphs show the combined data expressed as the mean ± S.D. from three independent experiments. Comparisons between the groups was performed with a One-way ANOVA with Tukey's HSD post-hoc analysis. Versus DIV1, $p < 0.05$ is denoted by *, $p < 0.01$ is denoted by **, $p < 0.005$ is denoted by ***, and $p < 0.001$ is denoted by ****. Versus DIV7, $p < 0.05$ is denoted by † and $p < 0.01$ is denoted by ††.

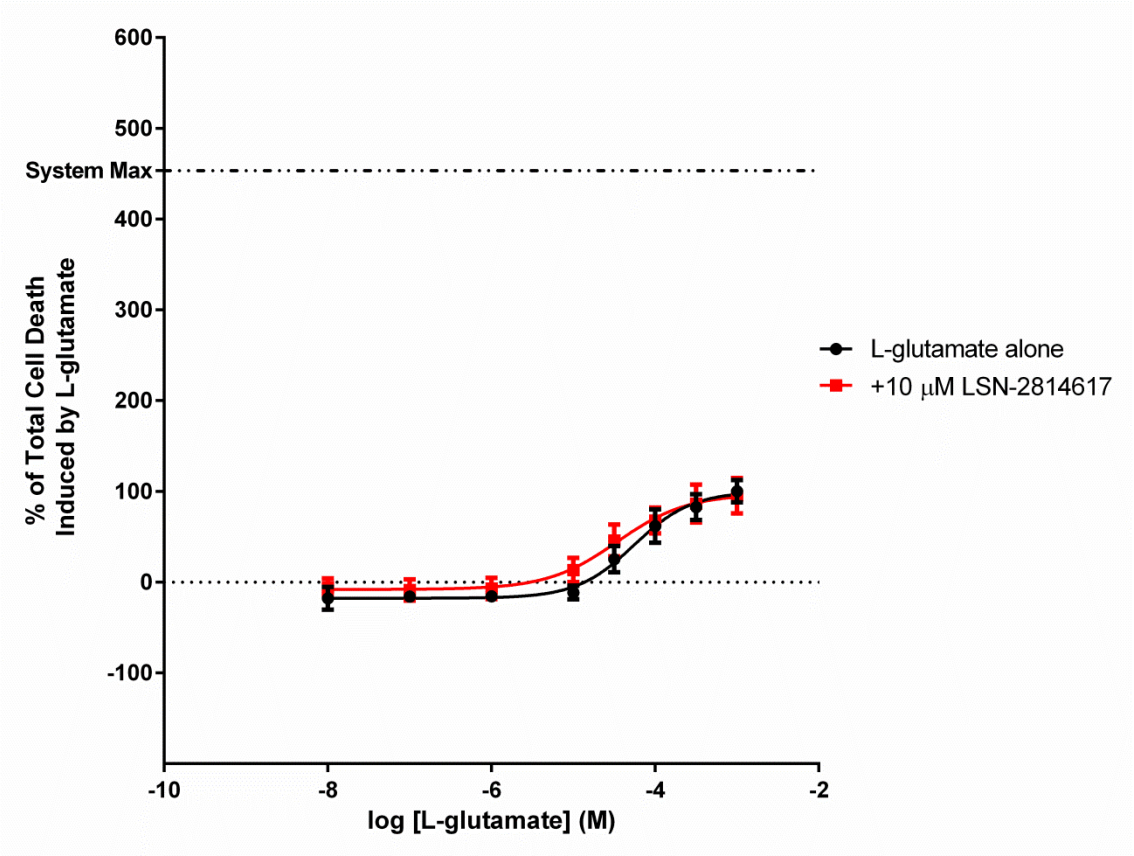

Figure 5.2.4.2 The ability of the mGlu5 allosteric modulator LSN-2814617 to affect the excitotoxic cell death of mixed cultures of rat cortical neurons and glial cells grown *in vitro* for 14 days was assessed using an enzymatic lactate dehydrogenase colourometric assay. A range of concentrations of the neurotransmitter L-glutamate (10 nM to 10 mM) was incubated in the absence or presence of a set concentration of LSN-2814617 or 24 hours before a media sample was taken and analysed for lactate dehydrogenase activity The graphs show the combined data shown as mean ± S.E.M. of three independent experiments performed in duplicate. Pharmacological and statistical analyses of the data is summarised in Table 4.2.5.1.

Table 5.2.4.1 A summary of the quantitative analysis of ligands inducing excitotoxic cell death in mixed primary cortical cultures grown for 14 DIV. pLD50 and the total % of cell death induced under each condition are expressed as mean ± S.E.M. Statistical analyses were performed with an unpaired, two-tailed Student's t-test.

Compounds	pLD_{50}	p-value	% of maximum cell death induced by L-glutamate	p-value	n
L-glutamate alone	4.20 ± 0.34	-	102.1 ± 6.2	-	3
+ 10 µM LSN-2814617	4.46 ± 0.17	>0.05	97.1 ± 7.8	>0.05	3

5.3 Discussion

Several PAMs of mGlu5, from diverse chemical series, have been previously reported to induce neuronal cell death in the mouse brain (Conde-Ceide et al., 2015; Parmentier-Batteur et al., 2014). In this chapter I explored the action of LSN-2814617 in the mouse brain, and attempted to develop an *in vitro* model for the neurotoxicity of mGlu5 PAMs. The histochemical data data from formalin-fixed, coronal sections from mice treated for 7 days with a high dose of LSN-2814617 provided some insight into the *in vivo* consequences of mGlu5 potentiation. Though mGlu5 receptors are expressed in the hippocampus and LSN-2814617 increases their activation above normal levels, as evidenced by the increased presence of c-fos shown herein, we found no evidence of cell death in this part of the mouse brain. This is contrary to in-house data (not shown) and studies performed with other mGlu5 PAMs (Parmentier-Batteur et al., 2014). There are many possibilities as to why this is the case, for instance, coronal sectioning of the brain only gives insight into a specific plane on the rostro-caudal axis. Without sectioning and investigating the whole hippocampus across several animals one cannot rule out the possibility, however slim, that evidence of neuronal cell death has been missed. The immunohistochemical staining for the presence of GFAP and NeuN showed no obvious difference in the number of astrocytes or neurons between vehicle treated animals or those treated with LSN-2814617. Reactive astrocytes are known to localise to damage in the CNS, and perhaps increased GFAP immunostaining in the drug-treated animal brains would have shown whether neuronal cell death was occurring (Ridet et al., 1997).

In contrast to the histochemical data generated in the hippocampus, neuronal cell death was evident and obvious in the anterior cortex of all treated animals, in agreement with previous studies (Parmentier-Batteur et al., 2014). The extent of cell death was highly variable across the sample set, however, the same caveats about the coronal sectioning of the brain discussed previously apply. Though the neuronal cell death occurs in the

same section of the cortex as the neuronal cell death previously reported (Parmentier-Batteur et al., 2014), fluorojade C staining herein would have confirmed beyond doubt that the cell death observed is neuronal and not glial. Immunohistochemical data revealed an increase in c-fos activation in this rostro-caudal section of the cortex, and GFAP staining was also increased. Firstly, the increase in c-fos staining suggests that the mGlu5 PAM LSN-2814617 is active in this section of the brain and, secondly, increased GFAP staining indicates astrocytes are localised in close proximity to the site of damage. The increased astrocytic staining is no surprise given that astrogliosis, the activation of astrocytes in damaged neuronal tissue, is a well-documented phenomenon (Castillo-Ruiz et al., 2007). The expression of mGlu5 in this area was shown to be reduced in the drug treated animals compared to the vehicle treated. Whether this is due to receptor downregulation or neuronal loss is unclear.

In order to critically evaluate the specificity of the mGlu5 antibody, mGlu5 knockout mice were stained as a matter of course (Figure 5.2.2.6). No staining was evident in samples derived from mGlu5 knockout mice (Figure 5.2.2.6B). Furthermore, the anti-mGlu5 antibody did not bind to the mGlu1 knockout mousebrain samples assayed by Western blot in Chapter 4 (Figure 4.2.10.1A). Given the assumption that if the antibody was not mGlu5 specific, one could expect it to bind to its closest homologue, mGlu1, the specificity of the anti-body seems apparent. For the anti-c fos antibody, given that the staining appears more pronounced in samples where presumably mGlu5 is activated, and furthermore the cell bodies and specific extracellular regions are stained, not the entire local region, the antibody is appears to be reasonably specific (Figures 5.2.1.2, 5.2.2.4, and 5.2.2.5). Staining of a tissue sample in which c-fos is not expressed would have made a good control to elucidate the specificity of this antibody.

Though the immunohistochemical data presented in this study provides us with a snapshot of the effects of LSN-2814617 administration in the brain, interpretation of the images is qualitative in nature and beset by caveats.

Given the precise localisation of cell death, immunoassay of the whole brain by western blot or other techniques seems a bleak prospect, and indeed my own immunoblot investigations failed to yield any data of note (*data not shown*).

The data herein is displayed qualitatively, as this appears to be the most robust display. To quantify the whole section would diminish the presence of the highly localised effect of LSN-2814617, and choosing a single region from each cortex would be questionable. To illustrate, one could choose an area with barely any staining, or take an image slightly further away and find an area with increased staining. Since there is no objective rationale for choosing any one area for quantification, a qualitative display is how I have chosen to display data of this type, as has been done in the relevant published literature (Parmentier-Batteur et al., 2014).

In order to provide a high-throughput, quantitative measure of the ability of LSN-2814617 to induce cell death in neurons, the use of cultured primary cortical neurons was evaluated as a model of mGlu5 potentiation in the brain. Such models have been extensively used to provide insight into the role and downstream signalling of ionotropic glutamate receptors and other synaptic signal transducers in neuronal cell death (Erdö et al., 1991; Luo et al., 2003; Zhou et al., 2013). Based on previous studies into the neuroprotective abilities of mGlu5 against NMDA receptor-induced excitotoxicity, primary neuronal cultures grown for 7 days *in vitro* were evaluated as a model (Lea et al., 2005). My data showed that glutamate could induce excitotoxic cell death in a concentration-dependent manner and, in agreement with previous studies, a high concentration of MPEP could inhibit glutamate induced cell death. The effect of MPEP was not concentration-dependent and likely represents an off target effect, perhaps at NMDA receptors, as previously described (Lea et al., 2005; O'Leary et al., 2000). LSN-2814617 had no effect on the ability of glutamate to induce cell death in these neuronal cultures. Similarly, LSN-2814617 had no effect on the rate of cell death induced by glutamate in primary cortical neurons. In

conclusion, the evidence presented herein provides evidence that primary cortical neuron cultures are not a suitable model for neurotoxicity induced by LSN-2814617, despite the fact that mGlu5 present in neurons cultured this way can be potentiated by the PAM as shown in chapter 3. These findings do show that the direct potentiation of NMDA currents by mGlu5 in cortical neurons is not the cause of the neurotoxic profile of LSN-2814617. The mGlu5 receptor is known to potentiate NMDA receptor currents by a PKC-dependent phosphorylation of the NR1 subunit, a critical subunit in the NMDA tetramer (Chen et al., 2011; Choe et al., 2006). It would be of interest to assess whether this phosphorylation is occurring in our primary cortical neuron model in order to rule out this potentiation as the cause of LSN-2814617 induced neurotoxicity.

In this chapter, I further characterised the expression of mGlu5 in both pure neuronal and mixed cortical cultures over 21 DIV. Immunoblot data showed that in both neuronal and mixed cultures mGlu5 expression increased, plateauing at approximately 14 DIV. Mixed cultures had markedly increased mGlu5 expression compared to pure neuronal culture, and the presence of astrocytes is clearly indicated with a rising expression of GFAP over 21 DIV, plateauing at 14 DIV. Neuronal cell death induced by amyloid-beta has previously been shown to be mediated by astrocytes in culture and so it is possible, given the high expression of mGlu5 in astrocytes, that these glia are also responsible for the neurotoxic effect of mGlu5 PAMs (Garwood et al., 2011). Though glutamate induced concentration-dependent cell death in mixed cultures grown for 14 DIV, this excitotoxic cell death was not potentiated by LSN-2814617 in experiments described herein. This shows that excitotoxic cell death induced by glutamate in either pure neuronal cultures or mixed cultures of neurons and astrocytes are not valid models of the cytotoxic action of mGlu5 PAMs. The experimental modelling with cortical cultures herein would have benefitted from further experiments where the ability of mGlu5 was considered more acutely. By using (S)-3,5-DHPG as the agonist, with increasing concentrations of LSN-2814617, we could have elucidated whether LSN-2814617 could induce cell death

through its action on mGlu5 alone. Similarly the use of stronger potentiators of mGlu5 action, such as ADX-47273, would have provided perhaps a more pronounced effect on cell death.

Recent studies have suggested that glutamate is not the only endogenous ligand capable of activating mGlu5 receptors, with amyloid-beta increasingly implicated in mGlu5 signalling in the brain (Um et al., 2013). Amyloid-beta oligomers have also been shown to induce cell-death in primary cortical cultures (Alberdi et al., 2010), and it would be interesting to see whether this cell-death can be potentiated by mGlu5 PAMs. Studies in cultured primary hippocampal neurons has shown the activation of mGlu5 to be protective against amyloid-beta induced cell death, however, and so whether this model is more suitable for the study of the neurotoxicity of LSN-2814617 is debatable (Liu et al., 2005). In the absence of a suitable model, the exact mechanism of mGlu5 induced cell death remains unclear. Another possible explanation of the toxic action of LSN-2814617 could be explained by signalling bias. The neuroprotective action of CDPPB has been shown to be AKT-dependent (Doria et al., 2015). Perhaps LSN-2814617 does not potentiate this pathway, instead increasing other pathways which contribute to neurotoxicity. Studies where several downstream pathways of LSN-2814617 are considered would be of use in establishing the neurotoxic action of this, and other neurotoxic PAMs. Given the high expression of mGlu5 across various regions of the CNS, the reason why only specific neuronal populations appear to be affected remains unclear (Romano et al., 1996a; Shigemoto et al., 1993). It is likely that some localised 'flavour' of mGlu5 is responsible. Whether a specific protein interaction, differential synaptic environment, or a unique signalling profile of the neurons is involved remains to be delineated.

Chapter 6. Final discussion

The mGlu5 receptor is a highly attractive drug target, validated in several animal models. For example, inhibition of mGlu5 has shown efficacy in animal models of anxiety (Porter et al., 2005; Swanson et al., 2005; Tatarczyńska et al., 2001), Fragile X syndrome (Bear et al., 2004; Hamilton et al., 2014; Michalon et al., 2012; Yan et al., 2005), pain (Dogrul et al., 2000; Olive et al., 2005; Spooren et al., 2001), and neurodegenerative disorders (Hamilton et al., 2014; Schiefer et al., 2004; Vernon et al., 2005). Activation of mGlu5 is thought to be a potential avenue for the treatment of schizophrenia (Kinney et al., 2005; Liu et al., 2008), Huntington's disease (Doria et al., 2015), as well as having pro-cognitive effects (Ayala et al., 2009; Balschun et al., 2006; Fowler et al., 2013). The development of allosteric modulators overcame early hurdles encountered in drug development, like a lack of subtype-selectivity and poor blood-brain barrier penetration (Gasparini and Spooren, 2007; Schoepp et al., 1999), however, some mGlu5 PAMs have recently been shown to be neurotoxic (Parmentier-Batteur et al., 2014). Though the toxicity was demonstrated to be mGlu5-dependent, as evidence by the lack of toxicity in mGlu5 knock-out mice, the mechanism of neurotoxicity remains poorly understood. Understanding the mechanism of action of these compounds, as well as the functional diversity of mGlu5, will be crucial in overcoming these issues. This thesis extends previous studies into the allosteric mode of action of mGlu5 PAMs by delineating the allosteric action of the previously reported PAM LSN-2814617 and the previously unpublished PAM VU0430644 (Bradley et al., 2011; Gilmour et al., 2013). Furthermore the asymmetric functional interdependence of mGlu1 dimerised with mGlu5, which may have consequences for the function of the receptor *in vivo,* is demonstrated herein. Finally, the signalling and neurotoxic action of LSN-2814617 in the hippocampus and cortex is demonstrated, and attempts are made to model these interactions with native tissues.

6.1 Differing modes of action of the mGlu5 positive allosteric modulators

The data presented in chapter 3 expanded on the previous characterisation of the allosteric mode of action of two positive allosteric modulators of mGlu5, CDPPB and ADX-47273 (Bradley et al., 2011), providing further evidence that CDPPB and ADX-47273 have differing modes of action at the mGlu5 receptor. In concurrence with the previous report, CDPPB acted to increase the affinity of the orthosteric compound (S)-3,5-DHPG to a greater extent than it increases the coupling of the orthosteric site to a functional response. In contrast, ADX-47273 potentiated the response of the mGlu5 receptor primarily by increasing the ability of the orthosteric ligand to induce a functional response, increasing affinity at the orthosteric site to a lesser degree. The analyses of allosteric cooperativity were extended to two further compounds, LSN-2814617 and VU0430644, which potentiate (S)-3,5-DHPG agonism of the mGlu5 receptor to a lesser degree than the two reference compounds in this study. Both LSN-2814617 and VU0430644 acted in a mechanistically similar way, with efficacy driven allosteric potentiation. This represents the first published delineation of the mode of action for these two PAMs. DFB, another mGlu5 PAM, has previously been shown equally potentiate both the affinity and efficacy of orthosteric agonist (Bradley et al., 2011) It has been suggested that in recombinant cell lines such as HEK293 cells allosteric potentiation induced by PAMs of mGlu5 is solely due to cooperativity of function (Gregory et al., 2012). The data herein directly refutes that claim, as CDPPB clearly displayed a mechanism of action dependent on cooperativity of affinity in recombinant cell membranes, in agreement with previous studies in native tissue (Bradley et al., 2011). Furthermore, the data generated for LSN-2814617 and VU0430644 in rat cortex and rat cortical neurones was in good agreement with the recombinant human mGlu5 data, showing that these compounds do not display species-dependent differences. Therefore, any differences in the allosteric mode of action are examples of probe dependence, rather than a result of the species under study using these probes.

The discovery and characterisation of the allosteric action of novel ligands is important if we are to understand what structure activity relationships exist between the allosteric modulator and the receptor. For example, subtle changes in the distal phenyl ring of MPEP can convert this NAM into a full PAM (Sharma et al., 2008) and altering the size of chemical groups in this position could yield stronger or weaker potentiation, allowing nuanced design of positive allosteric modulators. The ability to design compounds with limited potentiation has been suggested to be a theoretical advantage in applications where only a slight modulation is required, as the compound can be administered at high dose without the risk of overdosing typical for orthosteric agonists (May et al., 2007). In the case of mGlu5, limiting the maximum potentiation induced by an allosteric ligand may allow receptor potentiation at a level that is sufficient for therapeutic benefit, whilst avoiding side-effects associated with overstimulation. For example, weak potentiators have been proposed as a solution to the neurotoxicity seen in animals undergoing chronic, high-dose administration of mGlu5 PAMs (Conn et al., 2009; Parmentier-Batteur et al., 2014). The concentration of these toxic PAMs at which efficacy was maintained without the neurotoxic profile was estimated to be equivalent to a 2-fold shift in the potency of glutamate, and it was suggested that limiting the maximum cooperativity of a positive allosteric modulator to a two-fold potency shift would allow high dosing of compound without risk of toxicity. This suggestion lead to the development of recently reported positive allosteric modulators which have a saturable potentiation limited to that safety margin, though the toxicological profile of these ligands have not yet been disclosed (Ellard et al., 2015; Huang et al., 2016).

The value of delineating the allosteric mode of action to develop structure-activity relationships is clear, however, the importance of affinity versus efficacy driven cooperativity in a therapeutic context is debatable. Afterall, combined cooperativity (αß) gives us the measure of the strength of allosteric action, and presumably there is little difference between a PAM that acts through modulation of affinity or efficacy. To highlight this point, the

cannabinoid CB_1 receptor negative allosteric modulator Org27569 is a positive modulator with respect to binding, inducing a 14 fold increase in the affinity of the orthosteric agonist CP55940. This positive cooperativity is overshadowed by the allosteric effects on efficacy, where Org27569 reduces the efficacy of CP55940 by 144-fold (Price et al., 2005), and so it acts as a NAM overall.

Perhaps a more therapeutically relevant question is to what extent an allosteric modulator can potentiate different functional readouts; so-called 'signalling bias'. To use the above example, the allosteric modulator Org27569 acted as a negative allosteric modulator of cannabinoid receptor 1 (CB1) receptor $G\alpha_i$ signalling, but acted as a PAM of ß-arrestin mediated internalisation of this receptor (Ahn et al., 2012). It is now understood that the conformational state of a receptor is not as simple as moving between active and inactive isomers, but that every ligand has the potential to induce a unique conformation of the receptor which can lead to a unique functional response (Khoury et al., 2014). This is highlighted by the signalling profile of LY2033298, a PAM of muscarinic M_4 receptors which potentiated intracellular calcium mobilization to half the level of receptor internalization (Leach et al., 2009). Given the differing modes of action for the mGlu5 PAMs described, it is interesting to speculate whether each archetype represents a different conformation of the receptor. Furthermore, it would be interesting to examine the signalling profiles of each ligand to see whether the differing modes of action lead to a biased response. Indeed, VU0409511, an mGlu5 PAM acting at the MPEP binding site, has recently been reported to enhance Gq/11 signalling of mGlu5 without potentiating NMDA receptor currents (Rook et al., 2015; Zhou et al., 2015). The mGlu5-dependent neurotoxicity induced by PAMs is reportedly absent in this compound, but it maintains dose-dependent antipsychotic activity in mouse models. Biased ligands such as these may provide the key to maintaining therapeutic aspects of mGlu5 signalling whilst avoiding adverse events. This has been demonstrated for the opioid receptors where orthosteric agonists such as morphine can induce lethal side effects such as respiratory

depression (McNicol et al., 2003). By understanding structure activity relationships between allosteric modulators and their target receptor, an allosteric modulator was designed which favours analgesia, a G protein-dependent signalling outcome, over respiratory depression, a ß-arrestin mediated outcome (Manglik et al., 2016). This shows the promise of developing structure activity relationships, which will aid drug development across the GPCR superfamily.

6.2 Heterodimerisation of mGlu1 and mGlu5 has pharmacological consequences for the action of allosteric modulators of mGlu5

As well as understanding the action of ligands at the receptor, understanding the pharmacological consequences of heterodimerisation of the receptor is also important. Heterodimerisation has already been demonstrated to have pharmacological effect across the GPCR superfamily. For example, allosteric modulators acting at the μ-opioid receptor, such as DAMGO, were able to increase the binding of [^{3}H]-deltorphin at the δ-opioid receptor in μ/δ-opioid heterodimers (Fujita et al., 2014). Given that deltorphin is a naturally produced opioid peptide, coupled with the fact that overstimulation of opioid receptors can cause lethal side effects, this finding has obvious implications for the development of ligands acting at these receptors (Kieffer, 1995). Heterodimerisation also has pharmacological effects in the mGluR family. For instance, the inhibition of mGlu5 with MPEP impairs the phosphorylation, internalisation, and desensitization of μ-opioid receptors when these receptors heterodimerise (Schröder et al., 2009). Inter-mGluR heterodimerisation was also recently reported and interestingly the group I mGluRs were shown to exclusively heterodimerise with each other (Doumazane et al., 2011). Functional interdependence between mGlu2 and mGlu4 serves as an example of the pharmacological consequences of inter-mGluR heterodimerisation, with PAMs of either mGlu2 or mGlu4 unable to potentiate glutamate response when the receptors are expressed as a dimer (Kammermeier, 2012; Yin et al., 2014). Given that mGlu1 and mGlu5 heterodimerise *in vitro* (Doumazane et al.,

2011), but it has not been conclusively demonstrated *in vivo* (Sevastyanova and Kammermeier, 2014), studying these heterodimers for unique pharmacological profiles could provide a framework for identifying their existence in native tissues.

In order to study the pharmacological interaction between mGlu1 and mGlu5, modified mGlu1 and mGlu5 receptors with $GABA_B$ C-terminal tails were used to ensure that heterodimers were the dominant population of receptors at the cell surface, using models where one protomer has the C-terminal tail of $GABAB_1$ with the RSRR retention motif, and the other protomer has the $GABA_{B2}$ tail with an added KKXX-type retention motif (Brock et al., 2007). This approach has been extensively used in order to explore the functional and regulatory consequences of dimerisation in Family C GPCRs (Brock et al., 2007; Goudet et al., 2005; Hlavackova et al., 2005). In chapter 4, pharmacological techniques were employed to investigate the consequences of the heterodimerisation of mGlu5 with mGlu1 using these recombinant constructs.

By characterising and comparing the functional effects of orthosteric agonists and allosteric modulators between the wild-type receptors and chimeric dimers, this study provides evidence that the mGlu1 receptor appears to inhibit the action of allosteric ligands acting at the mGlu5 receptor to a greater degree than the mGlu5 receptor affects the mGlu1 receptor. This was demonstrated by the repeated finding that PAMs acting at the MPEP site of the mGlu5 protomer were consistently reduced to half the potentiation they display at wild-type mGlu5 receptor. In contrast, the mGlu1 PAM Ro 67-4853 was not inhibited to the same extent, implying a reduced ability of mGlu5 to inhibit the action of mGlu1 PAMs. This conflicts data from previous studies which proposed that the binding of PAMs to a single protomer is sufficient for the full activation of the dimer (Goudet et al., 2005; Hlavackova et al., 2005). One possible explanation is that this effect is site-dependent: The mGlu5 PAMs used herein bind at the MPEP site (Feng et al., 2015), whereas DFB binds at an overlapping, but distinct

site (Mühlemann et al., 2006). It is therefore possible that DFB is uninhibited by the mGlu1 protomer, whereas CDPPB, LSN-2814617, and ADX-47273 display significant inhibition.

This idea of site-dependent inhibition is supported by data herein showing that CPPHA, a PAM of mGlu1 and mGlu5, is completely unaffected by the heterodimerisation. Furthermore, this asymmetric inhibition has been observed for heterodimers of mGlu2 and mGlu4 receptors (Yin et al., 2014), and so it is possible that there are common structural changes upon activation which mediate this effect in inter-mGluR heterodimers. Given that the 5th TMD is thought to be the dimeric interface, perhaps movement of the TMDs of mGlu5 is altered somehow by the presence or activation of mGlu1 (Yanagawa et al., 2011). There is evidence, for instance, that CDPPB interacts with asparagine 747 in the 5th TMD of mGlu5 through a hydrogen bond (Feng et al., 2015), though DFB also interacts with this residue and so this residue cannot be the sole determinant of this functional interdependence.

The reason why the mGlu1 PAM Ro 67-4853 is not affected is unclear. One possible explanation is that the 1st TMD, which is on the opposite side of the helical bundle to the Ro 67-4853 binding site (Harpsøe et al., 2015; Knoflach et al., 2001), is thought to be the dimer interface for mGlu1 (Wu et al., 2014). This would mean that activation of mGlu1 could sterically inhibit the 5th TMD of mGlu5 where the MPEP binding site is located, without inhibition of PAMs at the binding site on the mGlu1 protomer. Interestingly, antagonists of both mGlu1 and mGlu5 were inhibited by heterodimerisation: MPEP had a reduced potency, and its mode of action switched from full to partial antagonism but JNJ16259685 was able to fully inhibit both receptors with reduced potency, at a concentration where only mGlu1 is significantly inhibited. The result does not contradict the result where Ro 67-4853 was unaffected, as this PAM binds at a different site to JNJ16259685 (Hemstapat et al., 2006). Further studies which delineate the binding site of Ro 67-4853 fully would allow us to rationalise why this

compound is unaffected by mGlu1-mGlu5 heterodimerisation. Though previous studies demonstrated that a heterodimer comprised of a mutant mGlu1 receptor which can interact with MPEP and the wild-type mGlu1 are not inhibited by MPEP, our data suggests that mGlu1 and mGlu5 do not dimerise in the same way as this mutant, and this MPEP can antagonise mGlu1-mGlu5 heterodimers.

Previous studies have successfully used radioligand binding techniques to demonstrate the existence and pharmacological consequences of heterodimerisation in native tissue samples (Moreno et al., 2011). In this study, we used the chimeric mGlu1 and mGlu5 constructs to produce membranes expressing mGlu1 and mGlu5 heterodimers, and characterised the action of [^{3}H]-M-MPEP acting at mGlu5 in these membranes. Furthermore, the allosteric action of mGlu1 and mGlu5 allosteric ligands were fully characterised to provide a pharmacological interaction that could clarify the existence of these heterodimers *in vivo*. These binding studies performed herein showed no change in pharmacology at mGlu5 in mGlu1 and mGlu5 heterodimers. Interpretation of this data is difficult because, as previously discussed, these membranes likely include intracellular membrane bound compartments, with immature forms of the receptor dimer, as well as combinations of dimer which would be present in these intracellular membranes. No pharmacological difference was found in membranes prepared from native tissues where mGlu1 has been knocked-out, suggesting that the heterodimer does not exist as a significant population *in vivo*. Indeed, early evidence suggested that mGlu1 and mGlu5 do not heterodimerise *in vivo* (Romano et al., 1996b), however, recent evidence has emerged suggesting that mGlu1 and mGlu5 receptors can form heterodimers, and that it may have consequences for the development of ligands acting at these dimers. For example, a unique pharmacological profile was observed when primary neurons from the superior cervical ganglion were co-transfected with full length mGlu1 and mGlu5 receptors. In this model, specific antagonists of mGlu1 and mGlu5 inhibited the action of glutamate to an extent that cannot be explained by inhibition of their

respective targets alone, showing that perhaps these receptors interact pharmacologically in native systems (Sevastyanova and Kammermeier, 2014). Furthermore, they demonstrated that medium spiny neurons from the striatum, which express both mGlu1 and mGlu5 (Kerner et al., 1997; Tallaksen-Greene et al., 1998), display greater inhibition by mGlu1 and mGlu5 antagonists than can be explained by functionally independent receptors. Perhaps translating the data generated with mGlu5 PAMs from this thesis into the medium spiny neuronal cultures described by (Sevastyanova and Kammermeier, 2014), could provide further insight into whether mGlu1 and mGlu5 heterodimers exist and how they interact *in vivo*.

6.3 LSN-2814617 is toxic to neurons in specific CNS locations

As discussed in brief previously, chronic high-dose administration of mGlu5 PAMs has been shown to be neurotoxic *in vivo*, by a mechanism which is mGlu5-dependent (Parmentier-Batteur et al., 2014). This has not been reported for all PAMs of mGlu5, for example, studies with CDPPB suggest that it has neuroprotective action in several models of neuronal degeneration including traumatic brain injury and Huntington's disease (Chen et al., 2012; Doria et al., 2015). In chapter 5, the consequences of chronic, high-dose LSN-2814617 administration in the mouse brain was investigated, and the use of primary cortical neuronal and mixed cultures were evaluated to provide a high-throughput model of mGlu5 PAM toxicity. Histological data displayed herein showed that LSN-2814617 is brain-penetrant, and active in both the hippocampus and anterior cortex of the mouse brain, as evidenced by the increased immunostaining of c-fos, a transcription factor activated by ERK phosphorylation induced by mGlu5 (Mao et al., 2005b). Interestingly, despite mGlu5 activation in the hippocampus and anterior cortex, the neurotoxicity of LSN-2814617 was only observed in a relatively small locus of the anterior cortex. The mGlu5 receptor is known to play a role in LTP in the neocortex (Sourdet et al., 2003), and persistent reinforcement of synaptic signalling by LTP is thought

to lead to excitotoxic cell death (McEachern and Shaw, 1999). This would perhaps begin to explain why persistent activation of mGlu5 with LSN-2814617 induces cell death in neurones, but is insufficient to explain why the cell death is localised acutely, given that mGlu5 is expressed throughout the CNS (Romano et al., 1996a). One can speculate that perhaps the neurones susceptible to LSN-2814617 induced neurodegeneration are more susceptible to mGlu5-mediated dysfunction. For example, audiogenic seizures are shown to be reduced in fragile X mouse models, where mGlu5 expression is reduced by half, which implies that neurones in these areas are more susceptible to dysfunction induced by mGlu5 activation (Michalon et al., 2012). Further studies, perhaps with functional MRI (fMRI) techniques, would reveal the extent to which different brain areas are affected by LSN-2814617 administration. Indeed, fMRI study of the mGlu5 specific antagonist MTEP has shown that mGlu5 inhibition is heterogenous across different areas of the cortex (Simon et al., 2011), and logic dicates that this heterogeneity is likely true for activators of mGlu5 such as LSN-2814617.

Increased astrocyte staining was observed in LSN-2814617-treated animals, demonstrated herein by GFAP immunostaining, and previous studies have shown that mGlu5 expression in astrocytes is increased in this cell-type after epileptic events and in response to neuronal damage (Aronica et al., 2000; Ferraguti et al., 2001; Gwak and Hulsebosch, 2005; Ulas et al., 2000). It is my opinion that the upregulation of astrocytes upon LSN-2814617 treatment is a response to the neuronal damage induced by chronic mGlu5 activation, a phenomenon known as astrogliosis (Drouin-Ouellet et al., 2011). During astrogliosis, astrocytes invade the damaged area and attenuate further excitotoxic damage by releasing vasoconstrictors and increasing glutamate uptake (Iadecola and Nedergaard, 2007; Vermeiren et al., 2005). The effects of LSN-2814617 administration on mGlu5 in astrocytes is unknown, however, our primary culture models demonstrated that LSN-2814617 had no effect on neuronal cell loss induced by glutamate whether or not astrocytes are present. Further study into the effects of LSN-

2814617 acting at mGlu5 in astrocytes would perhaps help to elucidate what effect PAM administration has on astrocytic cell signalling. Two PAMs of mGlu5, DFB and CPPHA, have already shown signalling bias in astrocytes (Zhang et al., 2005), and understanding the pathways activated by LSN-2814617 will be an important step in understanding what role astrocytes are playing in the neurotoxicity of this PAM *in vivo*.

The role of mGlu5 ligands as neurotoxic or neuroprotective agents is highly controversial in the literature, with both *in vivo* and *in vitro* studies providing contradictory evidence (discussed in Flor et al., 2002). Early studies were hampered by the lack of availability of compounds able to specifically target each member of the group I mGluRs (Nicoletti et al., 1999). Studies performed *in vitro* with the mGlu5-selective agonist CHPG showed that mGlu5 activation could attenuate amyloid-beta induced cell death in cultured cortical neurons (Movsesyan et al., 2004). Furthermore, the neuroprotective action of CHPG was shown to occur *in vivo*, reducing neuronal cell loss in the cortex induced by traumatic brain injury via activation of the AKT (Chen et al., 2012). AKT can inactivate several cell death promoting effectors, such as caspase-9 and Bad (Cardone, 1998; Datta et al., 2016), and so activation of mGlu5 may be neuroprotective by increasing the activity of AKT and subsequently decreasing the activity of cell-death effectors. The discovery of allosteric modulators has provided a more nuanced tool to delineate the role of the mGlu5 receptor in neuronal cell death, however, the evidence remains just as contradictory. For instance CDPPB, a PAM of mGlu5, is robustly neuroprotective both *in vitro* and *in vivo*. The administration of CDPPB in cultured striatal neurons, even at low concentrations, was found to be neuroprotective against glutamate-induced excitotoxic cell death (Doria et al., 2015). In the same study, long term administration of CDPPB in a mouse-model of Huntington's disease was found to prevent cell death robustly, with the number of neurons in the striatum significantly higher than in the untreated mice. In contrast, administration of other mGlu5 PAMs such as LSN-2814617 in this study, or the structurally distinct PAMS 5PAM23, 5PAM000, and 5PAM413 have

been shown to cause significant neuronal loss in the mouse brain, especially in the anterior cortex (Parmentier-Batteur et al., 2014). One possible explanation for the divergence of mGlu5 PAM neurotoxicity is that these compounds display heterogenous signalling bias. For example, given that the neuroprotective effect of CDPPB is AKT –dependent, and several PAMs of mGlu5 can activate AKT signalling in the absence of orthosteric agonist (Doria et al., 2015), perhaps the neurotoxic PAMs do not activate these pathways, or even inhibit their activation. Examining LSN-2814617 or any of the toxic mGlu5 PAMs described herein for their ability to activate AKT, would be the first step in delineating what aspects of their mGlu5 signalling is responsible for the neurotoxic action of this receptor.

6.4 Concluding remarks

In this thesis, previous studies into the allosteric mode of action of PAMs of mGlu5 have been corroborated and extended with additional data about two ligands previously uncharacterised in this way (Bradley et al., 2011): LSN2814617 and VU0430644. The characterisation of ligands in this way will inform future studies into the structure-activity relationships that exist between PAMs and the mGlu5 receptor. By understanding which ligand-receptor interactions dictate cooperative effects, it's possible that PAMs could be designed which have bespoke pharmacological profiles and indeed studies have already begun delineating structure activity relationships between allosteric modulators and mGlu5 (Gregory et al., 2014, 2013, 2012; Turlington et al., 2013). These studies have demonstrated the importance of the 3rd, 5th, 6th and 7th TMDs for mediating cooperativity with the orthosteric site but could be further extended by determining what residues are important for the divergent allosteric mode of action of mGlu5 PAMs, such as that displayed between CDPPB, ADX-47273, and LSN-2814617.

As discussed previously, this thesis also demonstrates the inhibition of mGlu5 PAMs acting at the MPEP site induced by heterodimerisation of mGlu5 with mGlu1. This is the first report, to my knowledge, showing that mGlu1 and mGlu5 display asymmetric functional interdependence which is

binding-site specific. This type of interaction has been previously noted between heterodimers of mGlu2 and mGlu4, which shows that there may be common aspects of these interactions across the mGluR family (Yin et al., 2014). Obviously the functional inter-dependence between mGlu1 and mGlu5 was only demonstrated herein using mutant forms of the receptor, and so whether these interactions persist in full length, wild-type receptors is worth future exploration. If shown to exist *in vivo*, these PAMs will possess a pharmacological profile with which group I mGluR heterodimers can be potentiated to a smaller degree to other mGlu5 heterodimers, though their pharmacological profile at other mGlu5 heterodimers such as mGlu5/D_2 and mGlu5/μ-opioid will need to be characterised (Akgün et al., 2013; Cabello et al., 2009).

Finally this thesis demonstrated that LSN-2814617 is neurotoxic in specific loci of the rat brain when chronically administered at high dose in agreement with reports of other neurotoxic PAMs (Parmentier-Batteur et al., 2014). The exact mechanism of neurotoxicity remains unknown, but perhaps the lowest-hanging fruit would be to explore signalling bias of these neurotoxic compounds, given the previous reports showing that CDPPB was neuroprotective in an AKT-dependent fashion previously discussed (Doria et al., 2015). In fact delineating the signalling bias of LSN-2814617 could inform all three aspects of this thesis: By understanding whether LSN-2814617 displays signalling bias at the wild-type mGlu5 receptor, structure activity relationships could be used to guide development of PAMs towards downstream signalling pathways which avoid adverse events and promote therapeutic effects. This approach has been recently demonstrated for opioid receptors (Manglik et al., 2016), where a compound was designed which would activate therapeutically indicated G protein-dependent signalling pathways, without potentiating G protein-independent pathways (Bohn, 1999; Bohn et al., 2000). Furthermore, heterodimerisation has been shown to engender signalling bias in heterodimers of two family A GPCRs: the dopamine D_1 and D_2 receptors (Rashid et al., 2007). Expressed alone, these receptors signal through Gs and Gi/o to alter cAMP signalling, however,

when heterodimerised the dimer complex signals through Gq to activate PLC and induce intracellular calcium release. It would be of significant interest to assess whether mGlu1 and mGlu5 heterodimers display a unique signalling profile. Though this thesis has demonstrated that Gq is still activated by (S)-3,5-DHPG in the heterodimer, it is possible that G protein independent pathways are affected by heterodimerisation, and this was not tested herein. Furthermore, whether the full length mGlu1 and mGlu5 heterodimerise and display differing signalling profiles remains unknown. Understanding these increasingly complex facets of the mGlu5 receptor may help to develop a compound with properties that allow progression to the clinic: an objective which, to date, has not been achieved (Lindsley et al., 2016).

Appendix

5'-
ATGGTCCTTCTGTTGATCCTGTCAGTCTTACTTTTGAAAGAAGATGTCCGTGGGAGTGCACAGTCCAGTGAGAGGAGGGTGGTGGCTCACATGCCGG
GTGACATCATTATTGGAGCTCTCTTTTCTGTTCATCACCAGCCTACTGTGGACAAAGTTCATGAGAGGAAGTGTGGGGCGGTCCGTGAACAGTATGGC
ATTCAGAGAGTGGAGGCCATGCTGCATACCCTGGAAAGGATCAATTCAGACCCCACACTCTTGCCCAACATCACACTGGGCTGTGAGATAAGGGACT
CCTGCTGGCATTCGGCTGTGGCCCTAGAGCAGAGCATTGAGTTCATAAGAGATTCCCTCATTTCTTCAGAAGAGGAAGAAGGCTTGGTACGCTGTGT
GGATGGCTCCTCCTCTTCCTTCCGCTCCAAGAAGCCCATAGTAGGGGTCATTGGGCCTGGCTCCAGTTCTGTAGCCATTCAGGTCCAGAATTTGCTCC
AGCTTTTCAACATACCTCAGATTGCTTACTCAGCAACCAGCATGGATCTGAGTGACAAGACTCTGTTCAAATATTTCATGAGGGTTGTGCCTTCAGAT
GCTCAGCAGGCAAGGGCCATGGTGGACATAGTGAAGAGGTACAACTGGACCTATGTATCAGCCGTGCACACAGAAGGCAACTATGGAGAAAGTGGG
ATGGAAGCCTTCAAAGATATGTCAGCGAAGGAAGGGATTTGCATCGCCCACTCTTACAAAATCTACAGTAATGCAGGGGAGCAGAGCTTTGATAAGC
TGCTGAAGAAGCTCACAAGTCACTTGCCCAAGGCCCGGGTGGTGGCCTGCTTCTGTGAGGGCATGACGGTGAGAGGTCTGCTGATGGCCATGAGGC
GCCTGGGTCTAGCGGGAGAATTTCTGCTTCTGGGCAGTGATGGCTGGGCTGACAGGTATGATGTGACAGATGGATATCAGCGAGAAGCTGTTGGTGG
CATCACAATCAAGCTCCAATCTCCCGATGTCAAGTGGTTTGATGATTATTATCTGAAGCTCCGGCCAGAAACAAACCACCGAAACCCTTGGTTTCAAG
AATTTTGGCAGCATCGTTTTCAGTGCCGACTGGAAGGGTTTCCACAGGAGAACAGCAAATACAACAAGACTTGCAATAGTTCTCTGACTCTGAAAACA
CATCATGTTCAGGATTCCAAAATGGGATTTGTGATCAACGCCATCTATTCGATGGCCTATGGGCTCCACAACATGCAGATGTCCCTCTGCCCAGGCTA
TGCAGGACTCTGTGATGCCATGAAGCCAATTGATGGACGGAAACTTTTGGAGTCCCTGATGAAAACCAATTTTACTGGGGTTTCTGGAGATACGATCC
TATTCGATGAGAATGGAGACTCTCCAGGAAGGTATGAAATAATGAATTTCAAGGAAATGGGAAAAGATTACTTTGATTATATCAACGTTGGAAGTTGG
GACAATGGAGAATTAAAAATGGATGATGATGAAGTATGGTCCAAGAAAAGCAACATCATCAGATCTGTGTGCAGTGAACCATGTGAGAAAGGCCAGA
TCAAGGTGATCCGAAAGGGAGAAGTCAGCTGTTGTTGGACCTGTACACCTTGTAAGGAGAATGAGTATGTCTTTGATGAGTACACATGCAAGGCATG
CCAACTGGGGTCTTGGCCCACTGATGATCTCACAGGTTGTGACTTGATCCCAGTACAGTATCTTCGATGGGGTGACCCTGAACCCATTGCAGCTGTGG
TGTTTGCCTGCCTTGGCCTCCTGGCCACCCTGTTTGTTACTGTAGTCTTCATCATTTACCGTGATACACCAGTAGTCAAGTCCTCAAGCAGGGAACTCT
GCTACATTATCCTTGCTGGCATCTGCCTGGGCTACTTATGTACCTTCTGCCTCATTGCGAAGCCCAAACAGATTTACTGCTACCTTCAGAGAATTGGC
ATTGGTCTCTCCCCAGCCATGAGCTACTCAGCCCTTGTAACAAAGACCAACCGTATTGCAAGGATCCTGGCTGGCAGCAAGAAGAAGATCTGTACCAA
AAAGCCCAGATTCATGAGTGCCTGTGCCCAGCTAGTGATTGCTTTCATTCTCATATGCATCCAGTTGGGCATCATCGTTGCCCTCTTTATAATGGAGC
CTCCTGACATAATGCATGACTACCCAAGCATTCGAGAAGTCTACCTGATCTGTAACACCACCAACCTAGGAGTTGTCACTCCACTTGGATACAATGGA
TTGTTGATTTTGAGCTGCACCTTCTATGCGTTCAAGACCAGAAATGTTCCAGCTAACTTCAACGAGGCCAAGTATATCGCCTTCACAATGTACACGAC
CTGCATTATATGGCTAGCTTTTGTGCCAATCTACTTTGGCAGCAACTACAAAATCATCACCATGTGTTTCTCGGTCAGCCTCAGTGCCACAGTGGCCC
TAGGCTGCATGTTTGTGCCGAAGGTGTACATCATCCTGGCCAAACCAGAGAGAAACGTGCGCAGCGCCTTCACCACATCTACCGTGGTGCGCATGCA
TGTAGGGGATGGCAAGTCATCCTCCGCAGCCAGCAGATCCAGCAGCCTAGTCAACCTGTGGAAGAGAAGGGGCTCCTCTGGGGAAACCTTAAGTTCC
AATGGAAAATCCGTCACGTGGGCCCAGAATGAGAAGAGCAGCCGGGGGCAGCACCTGTGGCAGCGCCTGTCCATCCACATCAACAAGAAAGAAAAC
CCCAACCAAACGGCCGTCATCAAGCCCTTCCCCAAGAGCACGGAGAGCCGTGGCCTGGGCGCTGGCGCTGGCGCAGGCGGGAGCGCTGGGGGCGTG
GGGGCCACGGGCGGTGCGGGCTGCGCAGGCGCCGGCCCAGGCGGGCCCGAGTCCCCAGACGCCGGCCCCAAGGCGCTGTATGATGTGGCCGAGGC
TGAGGAGCACTTCCCGGCGCCCGCGCGGCCGCGCTCACCGTCGCCCATCAGCACGCTGAGCCACCGCGCGGGCTCGGCCAGCCGCACGGACGACGA
TGTGCCGTCGCTGCACTCGGAGCCTGTGGCGCGCAGCAGCTCCTCGCAGGGCTCCCTCATGGAGCAGATCAGCAGTGTGGTCACCCGCTTCACGGCC
AACATCAGCGAGCTCAACTCCATGATGCTGTCCACCGCGGCCCCCAGCCCCGGCGTCGGCGCCCCGCTCTGCTCGTCCTACCTGATCCCCAAAGAGA
TCCAGTTGCCCACGACCATGACGACCTTTGCCGAAATCCAGCCTCTGCCGGCCATCGAAGTCACGGGCGGCGCGCAGCCCGCGGCAGGGGCGCAGG
CGGCTGGGGACGCGGCCCGGGAGAGCCCCGCGGCCGGTCCCGAGGCTGCGGCCGCCAAGCCAGACCTGGAGGAGCTGGTGGCTCTCACCCCGCCG
TCCCCCTTCAGAGACTCGGTGGACTCGGGGAGCACAACCCCCAACTCGCCAGTGTCCGAGTCGGCCCTCTGTATCCCGTCGTCTCCCAAATATGACA
CTCTTATCATAAGAGATTACACTCAGAGCTCCTCGTCGTTGTGA-3'

MVLLLILSVLLLKEDVRGSAQSSERRVVAHMPGDIIIGALFSVHHQPTVDKVHERKCGAVREQYGIQRVEAMLH
TLERINSDPTLLPNITLGCEIRDSCWHSAVALEQSIEFIRDSLISSEEEEGLVRCVDGSSSSFRSKKPIVGVIGPGSS
SVAIQVQNLLQLFNIPQIAYSATSMDLSDKTLFKYFMRVVPSDAQQARAMVDIVKRYNWTYVSAVHTEGNYGES
GMEAFKDMSAKEGICIAHSYKIYSNAGEQSFDKLLKKLTSHLPKARVVACFCEGMTVRGLLMAMRRLGLAGEF
LLLGSDGWADRYDVTDGYQREAVGGITIKLQSPDVKWFDDYYLKLRPETNHRNPWFQEFWQHRFQCRLEGFP
QENSKYNKTCNSSLTLKTHHVQDSKMGFVINAIYSMAYGLHNMQMSLCPGYAGLCDAMKPIDGRKLLESLMK
TNFTGVSGDTILFDENGDSPGRYEIMNFKEMGKDYFDYINVGSWDNGELKMDDDEVWSKKSNIIRSVCSEPCE
KGQIKVIRKGEVSCCWTCTPCKENEYVFDEYTCKACQLGSWPTDDLTGCDLIPVQYLRWGDPEPIAAVVFACLG
LLATLFVTVVFIIYRDTPVVKSSSRELCYIILAGICLGYLCTFCLIAKPKQIYCYLQRIGIGLSPAMSYSALVTKTNRI
ARILAGSKKKICTKKPRFMSACAQLVIAFILICIQLGIIVALFIMEPPDIMHDYPSIREVYLICNTTNLGVVTPLGYN
GLLILSCTFYAFKTRNVPANFNEAKYIAFTMYTTCIIWLAFVPIYFGSNYKIITMCFSVSLSATVALGCMFVPKVYI
ILAKPERNVRSAFTTSTVVRMHVGDGKSSSAASRSSSLVNLWKRRGSSGETLSSNGKSVTWAQNEKSSRGQHL
WQRLSIHINKKENPNQTAVIKPFPKSTESRGLGAGAGAGGSAGGVGATGGAGCAGAGPGGPESPDAGPKALYD
VAEAEEHFPAPARPRSPSPISTLSHRAGSASRTDDDVPSLHSEPVARSSSSQGSLMEQISSVVTRFTANISELNSM
MLSTAAPSPGVGAPLCSSYLIPKEIQLPTTMTTFAEIQPLPAIEVTGGAQPAAGAQAAGDAARESPAAGPEAAAA
KPDLEELVALTPPSPFRDSVDSGSTTPNSPVSESALCIPSSPKYDTLIIRDYTQSSSSLstop

Figure A1 Sequence data showing the full nucleotide sequence of the hmGlu5b receptor used in this thesis, followed by the amino acid sequence.

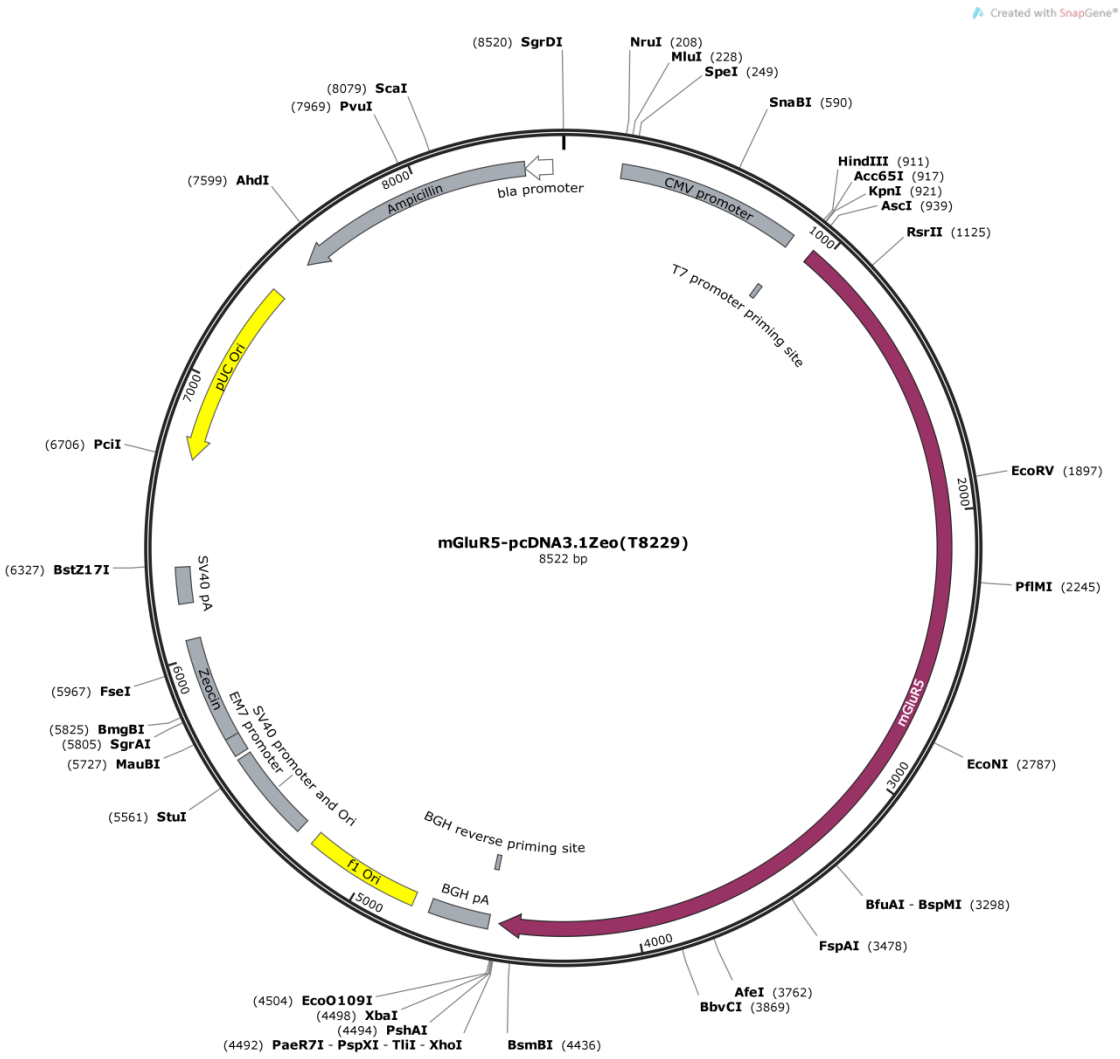

Figure A2 Diagram showing the vector for the hmGlu5b construct used in this thesis.

5’-
atggtcgggctccttttgtttttttttcccagcgatcttttttggaggtgtcccttctccccagaagccccggcaggaaagtgttgctggcaggagcgtcgTACCCATAC
GATGTTCCAGATTACGCTtctcagcgctcggtggccagaatggacggagatgtcatcattggagccctcttctcagtccatcaccagcctccggccgagaa
agtgcccgagaggaagtgtggggagatcagggagcagtatggcatccagagggtggaggccatgttccacacgttggataagatcaacgcggacccggtcctcctgc
ccaacatcaccctgggcagtgagatccgggactcctgctggcactcttccgtggctctggaacagagcattgagttcattagggactctctgatttccattcgagatgaga
aggatgggatcaaccggtgtctgcctgacggccagtccctccccccaggcaggactaagaagcccattgcgggagtgatcggtcccggctccagctctgtagccattca
agtgcagaacctgctccagctcttcgacatccccagatcgcttattcagccacaagcatcgacctgagtgacaaaacttgtacaaatacttcctgagggttgtcccttct
gacactttgcaggcaagggccatgcttgacatagtcaaacgttacaattggacctatgtctctgcagtccacacggaagggaattatggggagagcggaatggacgct
ttcaaagagctggctgcccaggaaggcctctgtatcgcccattctgacaaaatctacagcaacgctggggagaagagctttgaccgactcttgcgcaaactccgagag
aggcttcccaaggctagagtggtggtctgcttctgtgaaggcatgacagtgcgaggactcctgagcgccatgcggcgccttggcgtcgtgggcgagttctcactcattgg
aagtgatggatgggcagacagagatgaagtcattgaaggttatgaggtggaagccaacgggggaatcacgataaagctgcagtctccagaggtcaggtcatttgat
gattatttcctgaaactgaggctggacactaacacgaggaatccctggttccctgagttctggcaacatcggttccagtgccgccttccaggacaccttctggaaaatccc
aactttaaacgaatctgcacaggcaatgaaagcttagaagaaaactatgtccaggacagtaagatggggtttgtcatcaatgccatctatgccatggcacatgggctg
cagaacatgcaccatgccctctgccctggccacgtgggcctctgcgatgccatgaagcccatcgacggcagcaagctgctggacttcctcatcaagtcctcattcattgga
gtatctggagaggaggtgtggtttgatgagaaaggagacgctcctggaaggtatgatatcatgaatctgcagtacactgaagctaatcgctatgactatgtgcacgtt
ggaacctggcatgaaggagtgctgaacattgatgattacaaaatccagatgaacaagagtggagtggtgcggtctgtgtgcagtgagccttgcttaaagggccagat
taaggttatacggaaaggagaagtgagctgctgctggatttgcacggcctgcaaagagaatgaatatgtgcaagatgagttcacctgcaaagcttgtgacttgggat
ggtggcccaatgcagatctaacaggctgtgagcccattcctgtgcgctatcttgagtggagcaacatcgaatccattatagccatcgccttttcatgcctgggaatccttg
ttaccttgtttgtcaccctaatctttgtactgtaccgggacacaccagtggtcaaatcctccagtcgggagctctgctacatcatcctagctggcatcttccttggttatgtgt
gcccattcactctcattgccaaacctactaccacctcctgctacctccagcgcctcttggttggcctctcctctgcgatgtgctactctgctttagtgactaaaaccaatcgta
ttgcacgcatcctggctggcagcaagaagaagatctgcacccggaagcccaggttcatgagtgcctgggctcaggtgatcattgcctcaattctgattagtgtgcaacta
accctggtggtaaccctgatcatcatggaacccctatgcccattctgtcctacccaagtatcaaggaagtctaccttatctgcaataccagcaacctgggtgtggtggcc
cctttgggctacaatggactcctcatcatgagctgtacctactatgccttcaagacccgcaacgtgcccgccaacttcaacgaggccaaatatatcgcgttcaccatgtac
accacctgtatcatctggctagctttgtgcccatttactttgggagcaactacaagatcatcacaacttgctttgcagtgagtctcagtgtaacagtggctctggggtgca
tgttcactcccaagatgtacatcattattgccaagcctgagaggaatgtccgcagtgccttcaccacctctgatgttgtccgcatgcagttcactcagaatcagaagaaa
gaagattctaaaacgtccacctcggtcaccagtgtgaaccaagccagcacatcccgcctggagggcctacagtcagaaaaccatcgcctgcgaatgaagatcacaga
gctggataaagacttggaagaggtcaccatgcagctgcaggacacaccagaaAAGAAAACGAACTAA -3’

MVGLLLFFFPAIFLEVSLLPRSPGRKVLLAGASYPYDVPDYASQRSVARMDGDVIIGALFSVHHQPPAEKVPERK
CGEIREQYGIQRVEAMFHTLDKINADPVLLPNITLGSEIRDSCWSSVALEQSIEFIRDSLISIRDEKDGINRCLPDG
QSLPPGRTKKPIAGVIGPGSSSVAIQVQNLLQLFDIPQIAYSATSIDLSDKTLYKYFLRVVPSDTLQARAMLDIVKR
YNWTYVSAVHTEGNYGESGMDAFKELAAQEGLCIAHSDKIYSNAGEKSFDRLLRKLRERLPKARVVVCFCEGM
TVRGLLSAMRRLGVVGEFSLIGSDGWADRDEVIEGYEVEANGGITIKLQSPEVRSFDYFLKLRLDTNTRNPWFP
EFWQHRFQCRLPGHLLENPNFKRICTGNESLEENYVQDSKMGFVINAIYAMAHGLQNMHHALCPGHVGLCDA
MKPIDGSKLLDFLIKSSFIGVSGEEVWFDEKGDAPGRYDIMNLQYTEANRYDYVHVGTWHEGVLNIDDYKIQM
NKSGVVRSVCSEPCLKGQIKVIRKGEVSCCWICTACKENEYVQDEFTCKACDLGWWPNADLTGCEPIPVRYLE
WSNIESIIAIAFSCLGILVTLFVTLIFVLYRDTPVVKSSSRELCYIILAGIFLGYVCPFTLIAKPTTTSCYLQRLLVGLS
SAMCYSALVTKTNRIARILAGSKKKICTRKPRFMSAWAQVIIASILISVQLTLVVTLIIMEPPMPILSYPSIKEVYLI
CNTSNLGVVAPLGYNGLLIMSCTYYAFKTRNVPANFNEAKYIAFTMYTTCIIWLAFVPIYFGSNYKIITTCFAVSL
SVTVALGCMFTPKMYIIIAKPERNVRSAFTTSDVVRMQFTQNQKKEDSKTSTSVTSVNQASTSRLEGLQS
ENHRLRMKITELDKDLEEVTMQLQDTPEKKTNstop

Figure A3 Sequence data showing the full nucleotide sequence of the HA-hmGlu1-C2-KKTN chimaeric receptor used in this thesis, followed by the amino acid sequence. The mGlu1 sequence, HA tag, GABAB2a tail, and KKXX retention motif are highlighted in yellow, cyan, green, and grey, respectively.

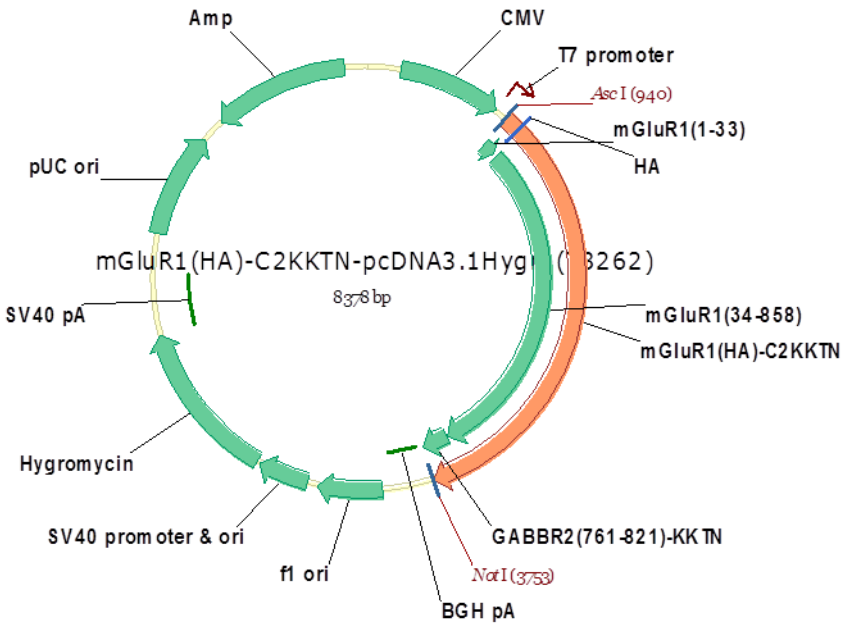

Figure A4 Diagram showing the vector for the HA-mGlu1-C2-KKTN construct used in this thesis.

5’-
atggtccttctgttgatcctgtcagtcttacttttgaaagaagatgtccgtgggagtgcacagtccTACCCATACGATGTTCCAGATTACGCTagtga
gaggagggtggtggctcacatgccgggtgacatcattattggagctctcttttctgttcatcaccagcctactgtggacaaagttcatgagaggaagtgtggggcggtcc
gtgaacagtatggcattcagagagtggaggccatgctgcataccctggaaaggatcaattcagaccccacactcttgcccaacatcacactgggctgtgagataaggg
actcctgctggcattcggctgtggccctagagcagagcattgagttcataagagattccctcatttcttcagaagaggaagaaggcttggtacgctgtgtggatggctcc
tcctcttccttccgctccaagaagcccatagtaggggtcattgggcctggctccagttctgtagccattcaggtccagaatttgctccagcttttcaacatacctcagattgc
ttactcagcaaccagcatggatctgagtgacaagactctgttcaaatatttcatgagggttgtgccttcagatgctcagcaggcaagggccatggtggacatagtgaag
aggtacaactggacctatgtatcagccgtgcacacagaaggcaactatggagaaagtgggatggaagccttcaaagatatgtcagcgaaggaagggatttgcatcg
cccactcttacaaaatctacagtaatgcaggggagcagagctttgataagctgctgaagaagctcacaagtcacttgcccaaggcccgggtggtggcctgcttctgtga
gggcatgacggtgagaggtctgctgatggccatgaggcgcctgggtctagcgggagaatttctgcttctgggcagtgatggctgggctgacaggtatgatgtgacaga
tggatatcagcgagaagctgttggtggcatcacaatcaagctccaatctcccgatgtcaagtggtttgatgattattatctgaagctccggccagaaacaaaccaccga
aaccttggtttcaagaattttggcagcatcgttttcagtgccgactggaagggtttccacaggagaacagcaaatacaacaagacttgcaatagttctctgactctga
aaacacatcatgttcaggattccaaaatgggatttgtgatcaacgccatctattcgatggcctatgggctccacaacatgcagatgtccctctgcccaggctatgcagga
ctctgtgatgccatgaagccaattgatggacggaaacttttggagtccctgatgaaaaccaattttactggggtttctggagatacgatcctattcgatgagaatggag
actctccaggaaggtatgaaataatgaatttcaaggaaatgggaaaagattactttgattatatcaacgttggaagttgggacaatggagaattaaaaatggatga
tgatgaagtatggtccaagaaaagcaacatcatcagatctgtgtgcagtgaaccatgtgagaaaggccagatcaaggtgatccgaaagggagaagtcagctgttgt
tggacctgtacaccttgtaaggagaatgagtatgtctttgatgagtacacatgcaaggcatgccaactggggtcttggcccactgatgatctcacaggttgtgacttgat
cccagtacagtatcttcgatggggtgaccctgaacccattgcagctgtggtgtttgcctgccttggcctcctggccaccctgtttgttactgtagtcttcatcatttaccgtga
tacaccagtagtcaagtcctcaagcagggaactctgctacattatccttgctggcatctgcctgggctacttatgtaccttctgcctcattgcgaagcccaaacagatttac
tgctaccttcagagaattggcattggtctctccccagccatgagctactcagcccttgtaacaaagaccaaccgtattgcaaggatcctggctggcagcaagaagaaga
tctgtaccaaaaagcccagattcatgagtgcctgtgcccagctagtgattgctttcattctcatatgcatccagttgggcatcatcgttgccctctttataatggagcctcct
gacataatgcatgactacccaagcattcgagaagtctacctgatctgtaacaccaccaacctaggagttgtcactccacttggatacaatggattgttgattttgagctg
caccttctatgcgttcaagaccagaaatgttccagctaacttcaacgaggccaagtatatcgccttcacaatgtacacgacctgcattatatggctagcttttgtgccaat
ctactttggcagcaactacaaaatcatcaccatgtgtttctcggtcagcctcagtgccacagtggccctaggctgcatgtttgtgccgaaggtgtacatcatcctggccaa
accagagagaaacgtgcgcagcgccttcaccacatctaccgtggtgcgcatgcagttcactcagaatcagaagaaagaagattctaaaacgtccacctcggtcaccag
tgtgaaccaagccagcacatcccgcctggagggcctacagtcagaaaaccatcgcctgcgaatgaagatcacagagctggataaagacttggaagaggtcaccatgc
agctgcaggacacaccagaaAAG AAA ACG AAC TAA-3’

MVLLLILSVLLLKEDVRGSAQSYPYDVPDYASERRVVAHMPGDIIIGALFSVHHQPTVDKVHERKCGAVREQYGI
QRVEAMLHTLERINSDPTLLPNITLGCEIRDSCWHSAVALEQSIEFIRDSLISSEEEEGLVRCVDGSSSSFRSKKPI
VGVIGPGSSSVAIQVQNLLQLFNIPQIAYSATSMDLSDKTLFKYFMRVVPSDAQQARAMVDIVKRYNWTYVSAV
HTEGNYGESGMEAFKDMSAKEGICIAHSYKIYSNAGEQSFDKLLKKLTSHLPKARVVACFCEGMTVRGLLMAM
RRLGLAGEFLLLGSDGWADRYDVTDGYQREAVGGITIKLQSPDVKWFDDYYLKLRPETNHRNPWFQEFWQHR
FQCRLEGFPQENSKYNKTCNSSLTLKTHHVQDSKMGFVINAIYSMAYGLHNMQMSLCPGYAGLCDAMKPIDG
RKLLESLMKTNFTGVSGDTILFDENGDSPGRYEIMNFKEMGKDYFDYINVGSWDNGELKMDDDEVWSKKSNII
RSVCSEPCEKGQIKVIRKGEVSCCWTCTPCKENEYVFDEYTCKACQLGSWPTDDLTGCDLIPVQYLRWGDPEPI
AAVVFACLGLLATLFVTVVFIIYRDTPVVKSSSRELCYIILAGICLGYLCTFCLIAKPKQIYCYLQRIGIGLSPAMSY
SALVTKTNRIARILAGSKKKICTKKPRFMSACAQLVIAFILICIQLGIIVALFIMEPPDIMHDYPSIREVYLICNTTN
LGVVTPLGYNGLLILSCTFYAFKTRNVPANFNEAKYIAFTMYTTCIIWLAFVPIYFGSNYKIITMCFSVSLSATVAL
GCMFVPKVYIILAKPERNVRSAFTTSTVVRMQFTQNQKKEDSKTSTSVTSVNQASTSRLEGLQSENHRLRMKIT
ELDKDLEEVTMQLQDTPEKKTNstop

Figure A5 Sequence data showing the full nucleotide sequence of the HA-hmGlu5-C2-KKTN chimaeric receptor used in this thesis, followed by the amino acid sequence. The mGlu1 sequence, HA tag, GABAB2a tail, and KKXX retention motif are highlighted in yellow, cyan, green, and grey, respectively.

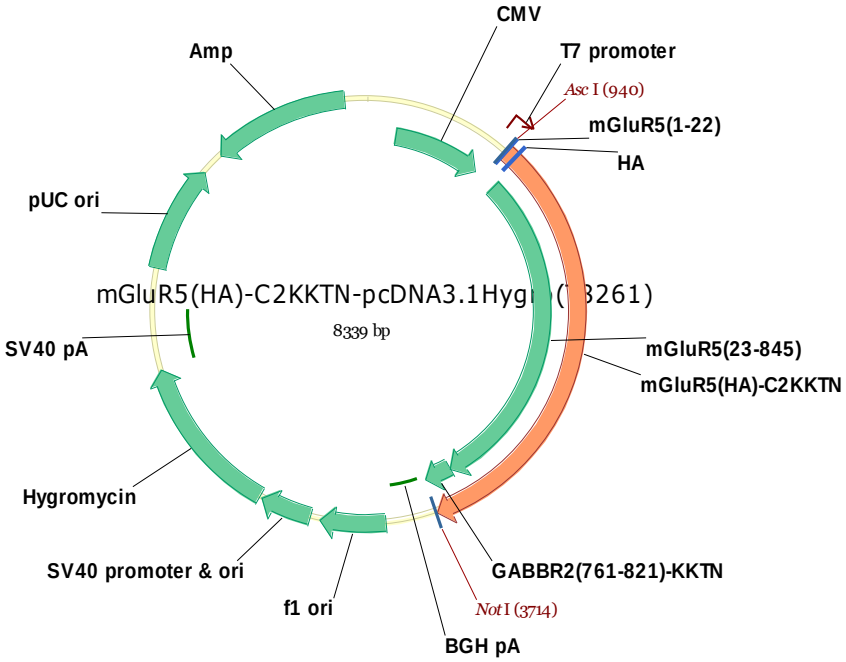

Figure A6 Diagram showing the vector for the HA-mGlu5-C2-KKTN construct used in this thesis.

5’-
atggtccttctgttgatcctgtcagtcttacttttgaaagaagatgtccgtgggagtgcacagtccGACTACAAGGACGACGATGACAAGagtgagag
gagggtggtggctcacatgccgggtgacatcattattggagctctcttttctgttcatcaccagcctactgtggacaaagttcatgagaggaagtgtggggcggtccgtg
aacagtatggcattcagagagtggaggccatgctgcataccctggaaaggatcaattcagaccccacactcttgcccaacatcacactgggctgtgagataagggact
cctgctggcattcggctgtggccctagagcagagcattgagttcataagagattccctcatttcttcagaagaggaagaaggcttggtacgctgtgtggatggctcctcc
tcttccttccgctccaagaagcccatagtaggggtcattgggcctggctccagttctgtagccattcaggtccagaatttgctccagcttttcaacatacctcagattgctta
ctcagcaaccagcatggatctgagtgacaagactctgttcaaatatttcatgagggttgtgccttcagatgctcagcaggcaagggccatggtggacatagtgaagag
gtacaactggacctatgtatcagccgtgcacacagaaggcaactatggagaaagtgggatggaagccttcaaagatatgtcagcgaaggaagggatttgcatcgccc
actcttacaaaatctacagtaatgcaggggagcagagctttgataagctgctgaagaagctcacaagtcacttgcccaaggcccgggtggtggcctgcttctgtgagg
gcatgacggtgagaggtctgctgatggccatgaggcgcctgggtctagcgggagaatttctgcttctgggcagtgatggctgggctgacaggtatgatgtgacagatg
gatatcagcgagaagctgttggtggcatcacaatcaagctccaatctcccgatgtcaagtggtttgatgattattatctgaagctccggccagaaacaaaccaccgaaa
cccttggtttcaagaattttggcagcatcgttttcagtgccgactggaagggtttccacaggagaacagcaaatacaacaagacttgcaatagttctctgactctgaaa
acacatcatgttcaggattccaaaatgggatttgtgatcaacgccatctattcgatggcctatgggctccacaacatgcagatgtccctctgcccaggctatgcaggactc
tgtgatgccatgaagccaattgatggacggaaacttttggagtccctgatgaaaaccaattttactggggtttctggagatacgatcctattcgatgagaatggagact
ctccaggaaggtatgaaataatgaatttcaaggaaatgggaaaagattactttgattatatcaacgttggaagttgggacaatggagaattaaaaatggatgatga
tgaagtatggtccaagaaaagcaacatcatcagatctgtgtgcagtgaaccatgtgagaaaggccagatcaaggtgatccgaaagggagaagtcagctgttgttgg
acctgtacaccttgtaaggagaatgagtatgtctttgatgagtacacatgcaaggcatgccaactggggtcttggcccactgatgatctcacaggttgtgacttgatccc
agtacagtatcttcgatggggtgaccctgaacccattgcagctgtggtgtttgcctgccttggcctcctggccaccctgtttgttactgtagtcttcatcatttaccgtgatac
accagtagtcaagtcctcaagcagggaactctgctacattatccttgctggcatctgcctgggctacttatgtaccttctgcctcattgcgaagcccaaacagatttactgc
taccttcagagaattggcattggtctctccccagccatgagctactcagcccttgtaacaaagaccaaccgtattgcaaggatcctggctggcagcaagaagaagatct
gtaccaaaaagcccagattcatgagtgcctgtgcccagctagtgattgctttcattctcatatgcatccagttgggcatcatcgttgccctctttataatggagcctcctga
cataatgcatgactacccaagcattcgagaagtctacctgatctgtaacaccaccaacctaggagttgtcactccacttggatacaatggattgttgattttgagctgca
ccttctatgcgttcaagaccagaaatgttccagctaacttcaacgaggccaagtatatcgccttcacaatgtacacgacctgcattatatggctagcttttgtgccaatct
actttggcagcaactacaaaatcatcaccatgtgtttctcggtcagcctcagtgccacagtggccctaggctgcatgtttgtgccgaaggtgtacatcatcctggccaaac
cagagagaaacgtgcgcagcgccttcaccacatctaccgtggtgcgcatgaagacagggtcatcgaccaacaacaacgaggaggagaagtcccggctgttggagaa
ggagaaccgtgaactggaaaagatcattgctgagaaagaggagcgtgtctctgaactgcgccatcaactccagtctcggcagcagctccgctcccggcgccacccacc
gacacccccagaaccctctgggggcctgcccaggggacccctgagccccccgaccggcttagctgtgatgggagtcgagtgcatttgctttataagtga-3’

MVLLLILSVLLLKEDVRGSAQSDYKDDDDKSERRVVAHMPGDIIIGALFSVHHQPTVDKVHERKCG
AVREQYGIQRVEAMLHTLERINSDPTLLPNITLGCEIRDSCWHSAVALEQSIEFIRDSLISSEEEEGL
VRCVDGSSSSFRSKKPIVGVIGPGSSSVAIQVQNLLQLFNIPQIAYSATSMDLSDKTLFKYFMRVVPS
DAQQARAMVDIVKRYNWTYVSAVHTEGNYGESGMEAFKDMSAKEGICIAHSYKIYSNAGEQSFDK
LLKKLTSHLPKARVVACFCEGMTVRGLLMAMRRLGLAGEFLLLGSDGWADRYDVTDGYQREAVG
GITIKLQSPDVKWFDDYYLKLRPETNHRNPWFQEFWQHRFQCRLEGFPQENSKYNKTCNSSLTLK
THHVQDSKMGFVINAIYSMAYGLHNMQMSLCPGYAGLCDAMKPIDGRKLLESLMKTNFTGVSGD
TILFDENGDSPGRYEIMNFKEMGKDYFDYINVGSWDNGELKMDDDEVWSKKSNIIRSVCSEPCEK
GQIKVIRKGEVSCCWTCTPCKENEYVFDEYTCKACQLGSWPTDDLTGCDLIPVQYLRWGDPEPIAA
VVFACLGLLATLFVTVVFIIYRDTPVVKSSSRELCYIILAGICLGYLCTFCLIAKPKQIYCYLQRIGIGL
SPAMSYSALVTKTNRIARILAGSKKKICTKKPRFMSACAQLVIAFILICIQLGIIVALFIMEPPDIMHD
YPSIREVYLICNTTNLGVVTPLGYNGLLILSCTFYAFKTRNVPANFNEAKYIAFTMYTTCIIWLAFVP
IYFGSNYKIITMCFSVSLSATVALGCMFVPKVYIILAKPERNVRSAFTTSTVVRMKTGSSTNNNEEE
KSRLLEKENRELEKIIAEKEERVSELRHQLQSRQQLRSRRHPPTPPEPSGGLPRGPPEPPDRLSCD
GSRVHLLYKstop

Figure A7 Sequence data showing the full nucleotide sequence of the FLAG-hmGlu5-C1 chimaeric receptor used in this thesis, followed by the amino acid sequence. The mGlu1a sequence, FLAG tag, and $GABA_{B1}$ tail are highlighted in yellow, cyan, and green, respectively.

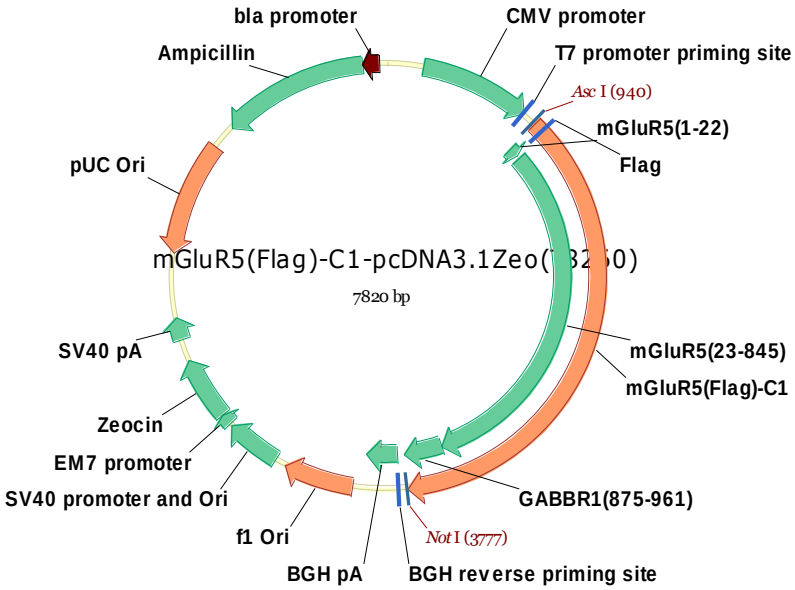

Figure A8 Diagram showing the vector for the FLAG-mGlu5-C1 construct used in this thesis.

Bibliography

Abe, T., Sugihara, H., Nawa, H., Shigemoto, R., Mizuno, N., Nakanishi, S., 1992. Molecular characterization of a novel metabotropic glutamate receptor mGluR5 coupled to inositol phosphate/Ca2+ signal transduction. J. Biol. Chem. 267, 13361–13368.

Acher, F.C., Bertrand, H.O., 2005. Amino acid recognition by venus flytrap domains is encoded in an 8-residue motif. Biopolym. - Pept. Sci. Sect. 80, 357–366. doi:10.1002/bip.20229

Ahn, K.H., Mahmoud, M.M., Kendall, D.A., 2012. Allosteric modulator ORG27569 induces CB1 cannabinoid receptor high affinity agonist binding state, receptor internalization, and Gi protein-independent ERK1/2 kinase activation. J. Biol. Chem. 287, 12070–12082. doi:10.1074/jbc.M111.316463

Ahn, S., Shenoy, S.K., Wei, H., Lefkowitz, R.J., 2004. Differential kinetic and spatial patterns of beta-arrestin and G protein-mediated ERK activation by the angiotensin II receptor. J. Biol. Chem. 279, 35518–35525. doi:10.1074/jbc.M405878200

Ahn, S.M., Choe, E.S., 2009. Activation of group I metabotropic glutamate receptors increases serine phosphorylation of GluR1 alpha-amino-3-hydroxy-5-methylisoxazole-4-propionic acid receptors in the rat dorsal striatum. J Pharmacol Exp Ther 329, 1117–1126. doi:jpet.108.149542 [pii]\r10.1124/jpet.108.149542

Aiba, A., Chen, C., Herrup, K., Rosenmund, C., Stevens, C.F., Tonegawa, S., 1994a. Reduced hippocampal long-term potentiation and context-specific deficit in associative learning in mGluR1 mutant mice. Cell 79, 365–375. doi:10.1016/0092-8674(94)90204-6

Aiba, A., Kano, M., Chen, C., Stanton, M.E., Fox, G.D., Herrup, K., Zwingman, T.A., Tonegawa, S., 1994b. Deficient cerebellar long-term depression and impaired motor learning in mGluR1 mutant mice. Cell

79, 377–388. doi:10.1016/0092-8674(94)90205-4

Akgün, E., Javed, M.I., Lunzer, M.M., Smeester, B.A., Beitz, A.J., Portoghese, P.S., 2013. Ligands that interact with putative MOR-mGluR5 heteromer in mice with inflammatory pain produce potent antinociception. Proc. Natl. Acad. Sci. U. S. A. 110, 11595–9. doi:10.1073/pnas.1305461110

Akkus, F., Ametamey, S.M., Treyer, V., Burger, C., Johayem, A., Umbricht, D., Gomez Mancilla, B., Sovago, J., Buck, A., Hasler, G., 2013. Marked global reduction in mGluR5 receptor binding in smokers and ex-smokers determined by [11C]ABP688 positron emission tomography. Proc. Natl. Acad. Sci. 110 , 737–742. doi:10.1073/pnas.1210984110

Alagarsamy, S., Rouse, S.T., Junge, C., Hubert, G.W., Gutman, D., Smith, Y., Conn, P.J., 2002. NMDA-induced phosphorylation and regulation of mGluR5. Pharmacol. Biochem. Behav. 73, 299–306. doi:10.1016/S0091-3057(02)00826-2

Alagarsamy, S., Saugstad, J., Warren, L., Mansuy, I.M., Gereau IV, R.W., Conn, P.J., 2005. NMDA-induced potentiation of mGluR5 is mediated by activation of protein phosphatase 2B/calcineurin. Neuropharmacology 49, 135–145. doi:10.1016/j.neuropharm.2005.05.005

Alberdi, E., Sánchez-Gómez, M.V., Cavaliere, F., Pérez-Samartín, A., Zugaza, J.L., Trullas, R., Domercq, M., Matute, C., 2010. Amyloid ß oligomers induce Ca2+ dysregulation and neuronal death through activation of ionotropic glutamate receptors. Cell Calcium 47, 264–272. doi:http://dx.doi.org/10.1016/j.ceca.2009.12.010

Alewijnse, A.E., Timmerman, H., Jacobs, E.H., Smit, M.J., Roovers, E., Cotecchia, S., Leurs, R., 2000. The Effect of Mutations in the DRY Motif on the Constitutive Activity and Structural Instability of the Histamine H2Receptor. Mol. Pharmacol. 57 , 890–898.

Allen, J. a, Roth, B.L., 2011. Strategies to discover unexpected targets for drugs active at G protein-coupled receptors. Annu. Rev. Pharmacol. Toxicol. 51, 117–144. doi:10.1146/annurev-pharmtox-010510-100553

Allen, J.W., Eldadah, B.A., Faden, A.I., 1999. ß-Amyloid-induced apoptosis of cerebellar granule cells and cortical neurons: Exacerbation by selective inhibition of group I metabotropic glutamate receptors. Neuropharmacology 38, 1243–1252. doi:10.1016/S0028-3908(99)00044-1

Ango, F., Albani-Torregrossa, S., Joly, C., Robbe, D., Michel, J.-M., Pin, J.-P., Bockaert, J., Fagni, L., 1999. A simple method to transfer plasmid DNA into neuronal primary cultures: functional expression of the mGlu5 receptor in cerebellar granule cells. Neuropharmacology 38, 793–803. doi:http://dx.doi.org/10.1016/S0028-3908(99)00005-2

Annoura, H., Fukunaga, A., Uesugi, M., Tatsuoka, T., Horikawa, Y., 1996. A novel class of antagonists for metabotropic glutamate receptors, 7-(hydroxyimino)cyclopropa[b]chromen-1a-carboxylates. Bioorganic Med. Chem. Lett. 6, 763–766. doi:10.1016/0960-894X(96)00104-7

Anwyl, R., 1999. Metabotropic glutamate receptors: Electrophysiological properties and role in plasticity. Brain Res. Rev. doi:10.1016/S0165-0173(98)00050-2

Aramori, I., Nakanishi, S., 1992. Signal transduction and pharmacological characteristics of a metabotropic glutamate receptor, mGluR1, in transfected CHO cells. Neuron 8, 757–65. doi:10.1016/0896-6273(92)90096-V

Aronica, E., Gorter, J.A., Ijlst-Keizers, H., Rozemuller, A.J., Yankaya, B., Leenstra, S., Troost, D., 2003. Expression and functional role of mGluR3 and mGluR5 in human astrocytes and glioma cells: opposite regulation of glutamate transporter proteins. Eur. J. Neurosci. 17, 2106–2118. doi:10.1046/j.1460-9568.2003.02657.x

Aronica, E., van Vliet, E.A., Mayboroda, O.A., Troost, D., da Silva, F.H.,

Gorter, J.A., 2000. Upregulation of metabotropic glutamate receptor subtype mGluR3 and mGluR5 in reactive astrocytes in a rat model of mesial temporal lobe epilepsy. Eur J Neurosci 12, 2333–2344.

Attwood, T.K., Findlay, J.B.C., 1994. Fingerprinting g-protein-coupled receptors. Protein Eng. Des. Sel. 7, 195–203. doi:10.1093/protein/7.2.195

Awad, H., Hubert, G.W., Smith, Y., Levey, A.I., Conn, P.J., 2000. Activation of metabotropic glutamate receptor 5 has direct excitatory effects and potentiates NMDA receptor currents in neurons of the subthalamic nucleus. J. Neurosci. 20, 7871–7879. doi:20/21/7871 [pii]

Ayala, J.E., Chen, Y., Banko, J.L., Sheffler, D.J., Williams, R., Telk, A.N., Watson, N.L., Xiang, Z., Zhang, Y., Jones, P.J., Lindsley, C.W., Olive, M.F., Conn, P.J., 2009. mGluR5 positive allosteric modulators facilitate both hippocampal LTP and LTD and enhance spatial learning. Neuropsychopharmacology 34, 2057–2071. doi:10.1038/npp.2009.30

Bai, M., Trivedi, S., Brown, E.M., 1998. Dimerization of the extracellular calcium-sensing receptor (CaR) on the cell surface of CaR-transfected HEK293 cells. J. Biol. Chem. 273, 23605–23610. doi:10.1074/jbc.273.36.23605

Ballesteros, J., Kitanovic, S., Guarnieri, F., Davies, P., Fromme, B.J., Konvicka, K., Chi, L., Millar, R.P., Davidson, J.S., Weinstein, H., Sealfon, S.C., 1998. Functional microdomains in G-protein-coupled receptors: The conserved arginine-cage motif in the gonadotropin-releasing hormone receptor. J. Biol. Chem. 273, 10445–10453. doi:10.1074/jbc.273.17.10445

Ballesteros, J.A., Jensen, A.D., Liapakis, G., Rasmussen, S.G.F., Shi, L., Gether, U., Javitch, J.A., 2001. Activation of the ß2-Adrenergic Receptor Involves Disruption of an Ionic Lock between the Cytoplasmic Ends of Transmembrane Segments 3 and 6. J. Biol. Chem. 276, 29171–29177. doi:10.1074/jbc.M103747200

Balschun, D., Zuschratter, W., Wetzel, W., 2006. Allosteric enhancement of metabotropic glutamate receptor 5 function promotes spatial memory. Neuroscience 142, 691–702. doi:10.1016/j.neuroscience.2006.06.043

Banères, J.-L., Parello, J., 2003. Structure-based Analysis of GPCR Function: Evidence for a Novel Pentameric Assembly between the Dimeric Leukotriene B4 Receptor BLT1 and the G-protein. J. Mol. Biol. 329, 815–829. doi:http://dx.doi.org/10.1016/S0022-2836(03)00439-X

Barber, R.D., Harmer, D.W., Coleman, R. a, Clark, B.J., 2005. GAPDH as a housekeeping gene: analysis of GAPDH mRNA expression in a panel of 72 human tissues. Physiol. Genomics 21, 389–395. doi:10.1152/physiolgenomics.00025.2005

Barnes, M.R., Duckworth, D.M., Beeley, L.J., 2016. Frizzled proteins constitute a novel family of G protein-coupled receptors, most closely related to the secretin family. Trends Pharmacol. Sci. 19, 399–400. doi:10.1016/S0165-6147(98)01246-2

Bear, M.F., Huber, K.M., Warren, S.T., 2004. The mGluR theory of fragile X mental retardation. Trends Neurosci. doi:10.1016/j.tins.2004.04.009

Bergwitz, C., Gardella, T.J., Flannery, M.R., Potts, J.T., Kronenberg, H.M., Goldring, S.R., Jüppner, H., 1996. Full activation of chimeric receptors by hybrids between parathyroid hormone and calcitonin. Evidence for a common pattern of ligand-receptor interaction. J. Biol. Chem. 271, 26469–26472. doi:10.1074/jbc.271.43.26469

Bessis, A.-S., Rondard, P., Gaven, F., Brabet, I., Triballeau, N., Prezeau, L., Acher, F., Pin, J.-P., 2002. Closure of the Venus flytrap module of mGlu8 receptor and the activation process: Insights from mutations converting antagonists into agonists. Proc. Natl. Acad. Sci. U. S. A. 99, 11097–11102. doi:10.1073/pnas.162138699

Bhouri, M., Farrow, P. a, Motee, A., Yan, X., Battaglia, G., Di Menna, L., Riozzi, B., Nicoletti, F., Fitzjohn, S.M., Bashir, Z.I., 2014. mGlu1

receptor-induced LTD of NMDA receptor transmission selectively at Schaffer collateral-CA1 synapses mediates metaplasticity. J. Neurosci. 34, 12223–9. doi:10.1523/JNEUROSCI.0753-14.2014

Blaabjerg, M., Fang, L., Zimmer, J., Baskys, A., 2003. Neuroprotection against NMDA excitotoxicity by group I metabotropic glutamate receptors is associated with reduction of NMDA stimulated currents. Exp. Neurol. 183, 573–580. doi:10.1016/S0014-4886(03)00204-8

Black, J.W., Leff, P., 1983. Operational Models of Pharmacological Agonism. Proc. R. Soc. B Biol. Sci. 220, 141–162. doi:10.1098/rspb.1983.0093

Bohn, L.M., 1999. Enhanced Morphine Analgesia in Mice Lacking Beta-Arrestin 2. Science (80-.). 286, 2495–2498. doi:10.1126/science.286.5449.2495

Bohn, L.M., Gainetdinov, R.R., Lin, F.T., Lefkowitz, R.J., Caron, M.G., 2000. Mu-opioid receptor desensitization by beta-arrestin-2 determines morphine tolerance but not dependence. Nature 408, 720–723. doi:10.1038/35047086

Bowery, N.G., Bettler, B., Froestl, W., Gallagher, J.P., Marshall, F., Raiteri, M., Bonner, T.I., Enna, S.J., 2002. International Union of Pharmacology. XXXIII. Mammalian γ-Aminobutyric AcidB Receptors: Structure and Function. Pharmacol. Rev. 54 , 247–264.

Brabet, I., Mary, S., Bockaert, J., Pin, J.P., 1995. Phenylglycine derivatives discriminate between mGluR1- and mGluR5-mediated responses. Neuropharmacology 34, 895–903. doi:10.1016/0028-3908(95)00079-L

Bradford, M.M., 1976. A rapid and sensitive method for the quantitation of microgram quantities of protein using the principle of protein dye binding. Anal. Biochem. 72, 248–254. doi:10.1016/0003-2697(76)90527-3

Bradley, S.J., Challiss, R.A.J., 2011. Defining protein kinase/phosphatase isoenzymic regulation of mGlu5 receptor-stimulated phospholipase C

and Ca2+ responses in astrocytes. Br. J. Pharmacol. 164, 755–771. doi:10.1111/j.1476-5381.2011.01421.x

Bradley, S.J., Langmead, C.J., Watson, J.M., Challiss, R.A.J., 2011. Quantitative analysis reveals multiple mechanisms of allosteric modulation of the mGlu5 receptor in rat astroglia. Mol. Pharmacol. 79, 874–885. doi:10.1124/mol.110.068882

Brakeman, P.R., Lanahan, a a, O'Brien, R., Roche, K., Barnes, C. a, Huganir, R.L., Worley, P.F., 1997. Homer: a protein that selectively binds metabotropic glutamate receptors. Nature. doi:10.1038/386284a0

Bräuner-Osborne, H., Wellendorph, P., Jensen, A.A., 2007. Structure, pharmacology and therapeutic prospects of family C G-protein coupled receptors. Curr. Drug Targets 8, 169–84. doi:10.2174/138945007779315614

Brock, C., Oueslati, N., Soler, S., Boudier, L., Rondard, P., Pin, J.-P., 2007. Activation of a Dimeric Metabotropic Glutamate Receptor by Intersubunit Rearrangement. J. Biol. Chem. 282, 33000–33008. doi:10.1074/jbc.M702542200

Brody, S. a, Dulawa, S.C., Conquet, F., Geyer, M. a, 2004. Assessment of a prepulse inhibition deficit in a mutant mouse lacking mGlu5 receptors. Mol. Psychiatry 9, 35–41. doi:10.1038/sj.mp.4001404

Brody, S.A., Conquet, F., Geyer, M.A., 2003. Disruption of prepulse inhibition in mice lacking mGluR1. Eur. J. Neurosci. 18, 3361–3366. doi:10.1111/j.1460-9568.2003.03073.x

Brown, E.M., Pollak, M., Chou, Y.H., Seidman, C.E., Seidman, J.G., Hebert, S.C., 1995. Cloning and functional characterization of extracellular Ca2+-sensing receptors from parathyroid and kidney. Bone 17. doi:10.1016/8756-3282(95)00199-N

Bruno, V., Copani, A., Knöpfel, T., Kuhn, R., Casabona, G., Dell' Albani, P.,

Condorelli, D.F., Nicoletti, F., 1995. Activation of metabotropic glutamate receptors coupled to inositol phospholipid hydrolysis amplifies NMDA-induced neuronal degeneration in cultured cortical cells. Neuropharmacology 34, 1089–1098. doi:10.1016/0028-3908(95)00077-J

Bruno, V., Ksiazek, I., Battaglia, G., Lukic, S., Leonhardt, T., Sauer, D., Gasparini, F., Kuhn, R., Nicoletti, F., Flor, P.J., 2000. Selective blockade of metabotropic glutamate receptor subtype 5 is neuroprotective. Neuropharmacology 39, 2223–2230. doi:10.1016/S0028-3908(00)00079-4

Burnette, W.N., 1981. "Western Blotting": Electrophoretic transfer of proteins from sodium dodecyl sulfate-polyacrylamide gels to unmodified nitrocellulose and radiographic detection with antibody and radioiodinated protein A. Anal. Biochem. 112, 195–203. doi:http://dx.doi.org/10.1016/0003-2697(81)90281-5

Byrnes, K.R., Stoica, B., Loane, D.J., Riccio, A., Davis, M.I., Faden, A.I., 2009. Metabotropic glutamate receptor 5 activation inhibits microglial associated inflammation and neurotoxicity. Glia 57, 550–560. doi:10.1002/glia.20783

Cabello, N., Gandía, J., Bertarelli, D.C.G., Watanabe, M., Lluís, C., Franco, R., Ferré, S., Luján, R., Ciruela, F., 2009. Metabotropic glutamate type 5, dopamine D2 and adenosine A 2a receptors form higher-order oligomers in living cells. J. Neurochem. 109, 1497–1507. doi:10.1111/j.1471-4159.2009.06078.x

Cai, Z., Schools, G.P., Kimelberg, H.K., 2000. Metabotropic glutamate receptors in acutely isolated hippocampal astrocytes: Developmental changes of mGluR5 mRNA and functional expression. Glia 29, 70–80. doi:10.1002/(SICI)1098-1136(20000101)29:1<70::AID-GLIA7>3.0.CO;2-V

Camón, L., Vives, P., de Vera, N., Martínez, E., 1998. Seizures and neuronal damage induced in the rat by activation of group I metabotropic glutamate receptors with their selective agonist 3,5-dihydroxyphenylglycine. J. Neurosci. Res. 51, 339–348.

Cardone, M.H., 1998. Regulation of Cell Death Protease Caspase-9 by Phosphorylation. Science (80-.). 282, 1318–1321. doi:10.1126/science.282.5392.1318

Carron, C., Pascal, A., Djiane, A., Boucaut, J.-C., Shi, D.-L., Umbhauer, M., 2003. Frizzled receptor dimerization is sufficient to activate the Wnt/ß-catenin pathway. J. Cell Sci. 116, 2541–2550.

Cartmell, J., Schoepp, D.D., 2000. Regulation of neurotransmitter release by metabotropic glutamate receptors. J. Neurochem. 75, 889–907.

Castillo-Ruiz, M.M., Campuzano, O., Acarin, L., Castellano, B., Gonzalez, B., 2007. Delayed neurodegeneration and early astrogliosis after excitotoxicity to the aged brain. Exp. Gerontol. 42, 343–354. doi:10.1016/j.exger.2006.10.008

Cellulaire, N., It, S., 1995. Facilitatory Coupling between a Glutamate Metabotropic Receptor and Dihydropyridine-Sensitive Calcium Channels in Cultured Cerebellar Granule Cells. Culture 15, 135–143.

Challiss, R. a, Mistry, R., Gray, D.W., Nahorski, S.R., 1994. Modulatory effects of NMDA on phosphoinositide responses evoked by the metabotropic glutamate receptor agonist 1S,3R-ACPD in neonatal rat cerebral cortex. Br. J. Pharmacol. 112, 231–239.

Chavis, P., Fagni, L., Bockaert, J., Lansman, J.B., 1995. Modulation of calcium channels by metabotropic glutamate receptors in cerebellar granule cells. Neuropharmacology 34, 929–937. doi:10.1016/0028-3908(95)00082-H

Chen, B.-S., Roche, K.W., 2007. Regulation of NMDA receptors by

phosphorylation. Neuropharmacology 53, 362–368. doi:10.1016/j.neuropharm.2007.05.018

Chen, C.-M., Strapps, W., Tomlinson, A., Struhl, G., 2004. Evidence that the cysteine-rich domain of Drosophila Frizzled family receptors is dispensable for transducing Wingless. Proc. Natl. Acad. Sci. U. S. A. 101, 15961–6. doi:10.1073/pnas.0407103101

Chen, H.-H., Liao, P.-F., Chan, M.-H., 2011. mGluR5 positive modulators both potentiate activation and restore inhibition in NMDA receptors by PKC dependent pathway. J. Biomed. Sci. 18, 19. doi:10.1186/1423-0127-18-19

Chen, T., Cao, L., Dong, W., Luo, P., Liu, W., Qu, Y., Fei, Z., 2012. Protective effects of mGluR5 positive modulators against traumatic neuronal injury through PKC-dependent activation of MEK/ERK pathway. Neurochem. Res. 37, 983–990. doi:10.1007/s11064-011-0691-z

CHEN, T.A.O., ZHANG, L.E.I., QU, Y.A.N., HUO, K.A.I., JIANG, X., FEI, Z., 2012. The selective mGluR5 agonist CHPG protects against traumatic brain injury in vitro and in vivo via ERK and Akt pathway. Int. J. Mol. Med. 29, 630–636. doi:10.3892/ijmm.2011.870

Chen, Y., Goudet, C., Pin, J., Conn, P.J., 2008. N-{4-Chloro-2-[(1,3-dioxo-1,3-dihydro-2H-isoindol-2-yl)methyl]phenyl}-2-hydroxybenzamide (CPPHA) acts through a novel site as a positive allosteric modulator of group 1 metabotropic glutamate receptors. Mol. Pharmacol. 73, 909–918. doi:10.1124/mol.107.040097

Chen, Y., Nong, Y., Goudet, C., Hemstapat, K., de Paulis, T., Pin, J.-P., Conn, P.J., 2007. Interaction of Novel Positive Allosteric Modulators of Metabotropic Glutamate Receptor 5 with the Negative Allosteric Antagonist Site Is Required for Potentiation of Receptor Responses. Mol. Pharmacol. 71 , 1389–1398. doi:10.1124/mol.106.032425

Chiamulera, C., Epping-Jordan, M.P., Zocchi, A., Marcon, C., Cottiny, C.,

Tacconi, S., Corsi, M., Orzi, F., Conquet, F., 2001. Reinforcing and locomotor stimulant effects of cocaine are absent in mGluR5 null mutant mice. Nat. Neurosci. 4, 873–874. doi:10.1038/nn0901-873

Choe, E.S., Shin, E.H., Wang, J.Q., 2006. Regulation of phosphorylation of NMDA receptor NR1 subunits in the rat neostriatum by group I metabotropic glutamate receptors in vivo. Neurosci. Lett. 394, 246–251. doi:10.1016/j.neulet.2005.10.072

Choi, D.W., 1992. Excitotoxic cell death. J. Neurobiol. doi:10.1002/neu.480230915

Choi, S., Lovinger, D.M., 1996. Metabotropic glutamate receptor modulation of voltage-gated Ca2+ channels involves multiple receptor subtypes in cortical neurons. J Neurosci 16, 36–45.

Clapham, D.E., Neer, E.J., 1997. G PROTEIN βγ SUBUNITS. Annu. Rev. Pharmacol. Toxicol. 37, 167–203. doi:10.1146/annurev.pharmtox.37.1.167

Cleva, R.M., Olive, M.F., 2011. Positive allosteric modulators of type 5 metabotropic glutamate receptors (mGluR5) and their therapeutic potential for the treatment of CNS disorders. Molecules 16, 2097–2106. doi:10.3390/molecules16032097

Coleman, D.E., Berghuis, a M., Lee, E., Linder, M.E., Gilman, a G., Sprang, S.R., 1994. Structures of active conformations of Gi alpha 1 and the mechanism of GTP hydrolysis. Science 265, 1405–1412. doi:10.1126/science.8073283

Conde-Ceide, S., Martínez-Viturro, C.M., Alcázar, J., Garcia-Barrantes, P.M., Lavreysen, H., Mackie, C., Vinson, P.N., Rook, J.M., Bridges, T.M., Daniels, J.S., Megens, A., Langlois, X., Drinkenburg, W.H., Ahnaou, A., Niswender, C.M., Jones, C.K., Macdonald, G.J., Steckler, T., Conn, P.J., Stauffer, S.R., Bartolomé-Nebreda, J.M., Lindsley, C.W., 2015. Discovery of VU0409551/JNJ-46778212: An mGlu 5 Positive

Allosteric Modulator Clinical Candidate Targeting Schizophrenia. ACS Med. Chem. Lett. 6, 716–720. doi:10.1021/acsmedchemlett.5b00181

Conn, P.J., Christopoulos, A., Lindsley, C.W., 2009. Allosteric modulators of GPCRs: a novel approach for the treatment of CNS disorders. Nat. Rev. Drug Discov. 8, 41–54. doi:10.1038/nrd2760

Conn, P.J., Pin, J.P., 1997. Pharmacology and functions of metabotropic glutamate receptors. Annu. Rev. Pharmacol. Toxicol. 37, 205–37. doi:10.1146/annurev.pharmtox.37.1.205

Conquet, F., Bashir, Z.I., Davies, C.H., Daniel, H., Ferraguti, F., Bordi, F., Franz-Bacon, K., Reggiani, A., Matarese, V., Condé, F., 1994. Motor deficit and impairment of synaptic plasticity in mice lacking mGluR1. Nature 372, 237–243. doi:10.1038/372237a0

Corti, C., Restituito, S., Rimland, J.M., Brabet, I., Corsi, M., Pin, J.P., Ferraguti, F., 1998. Cloning and characterization of alternative mRNA forms for the rat metabotropic glutamate receptors mGluR7 and mGluR8. Eur. J. Neurosci. 10, 3629–3641. doi:10.1046/j.1460-9568.1998.00371.x

Cozzoli, D.K., Goulding, S.P., Zhang, P.W., Xiao, B., Hu, J.-H., Ary, A.W., Obara, I., Rahn, A., Abou-Ziab, H., Tyrrel, B., Marini, C., Yoneyama, N., Metten, P., Snelling, C., Dehoff, M.H., Crabbe, J.C., Finn, D. a, Klugmann, M., Worley, P.F., Szumlinski, K.K., 2009. Binge drinking upregulates accumbens mGluR5-Homer2-PI3K signaling: functional implications for alcoholism. J. Neurosci. 29, 8655–8668. doi:10.1523/JNEUROSCI.5900-08.2009

Dann, C.E., Hsieh, J.-C., Rattner, A., Sharma, D., Nathans, J., Leahy, D.J., 2001. Insights into Wnt binding and signalling from the structures of two Frizzled cysteine-rich domains. Nature 412, 86–90.

Datta, S.R., Dudek, H., Tao, X., Masters, S., Fu, H., Gotoh, Y., Greenberg, M.E., 2016. Akt Phosphorylation of BAD Couples Survival Signals to

the Cell-Intrinsic Death Machinery. Cell 91, 231–241. doi:10.1016/S0092-8674(00)80405-5

Davenport, A.P., Alexander, S.P.H., Sharman, J.L., Pawson, A.J., Benson, H.E., Monaghan, A.E., Liew, W.C., Mpamhanga, C.P., Bonner, T.I., Neubig, R.R., Pin, J.P., Spedding, M., Harmar, A.J., 2013. International Union of Basic and Clinical Pharmacology. LXXXVIII. G protein-coupled receptor list: recommendations for new pairings with cognate ligands. Pharmacol. Rev. 65, 967–86. doi:10.1124/pr.112.007179

Davies, C.H., Clarke, V.R., Jane, D.E., Collingridge, G.L., 1995. Pharmacology of postsynaptic metabotropic glutamate receptors in rat hippocampal CA1 pyramidal neurones. Br. J. Pharmacol. 116, 1859–1869.

De Mendoza, A., Sebé-Pedrós, A., Ruiz-Trillo, I., 2014. The evolution of the GPCR signaling system in eukaryotes: Modularity, conservation, and the transition to metazoan multicellularity. Genome Biol. Evol. 6, 606–619. doi:10.1093/gbe/evu038

Decker, T., Lohmann-Matthes, M.L., 1988. A quick and simple method for the quantitation of lactate dehydrogenase release in measurements of cellular cytotoxicity and tumor necrosis factor (TNF) activity. J. Immunol. Methods 115, 61–69. doi:10.1016/0022-1759(88)90310-9

Dekundy, A., Pietraszek, M., Schaefer, D., Cenci, M.A., Danysz, W., 2006. Effects of group I metabotropic glutamate receptors blockade in experimental models of Parkinson's disease. Brain Res. Bull. 69, 318–326. doi:http://dx.doi.org/10.1016/j.brainresbull.2005.12.009

DeWire, S.M., Ahn, S., Lefkowitz, R.J., Shenoy, S.K., 2007. Beta-arrestins and cell signaling. Annu. Rev. Physiol. 69, 483–510. doi:10.1146/annurev.ph.69.013107.100021

Dixon, R.A.F., Kobilka, B.K., Strader, D.J., Benovic, J.L., Dohlman, H.G., Frielle, T., Bolanowski, M. a, Bennett, C.D., Rands, E., Diehl, R.E.,

Mumford, R. a, Slater, E.E., Sigal, I.S., Caron, M.G., Lefkowitz, R.J., Strader, C.D., 1986. Cloning of the gene and cDNA for mammalian ß-adrenergic receptor and homology with rhodopsin. Nature 321, 75–79. doi:10.1038/321075a0

Dogrul, A., Ossipov, M.H., Lai, J., Malan, T.P., Porreca, F., 2000. Peripheral and spinal antihyperalgesic activity of SIB-1757, a metabotropic glutamate receptor (mGLUR5) antagonist, in experimental neuropathic pain in rats. Neurosci. Lett. 292, 115–118. doi:10.1016/S0304-3940(00)01458-0

DOHERTY, A.J., PALMER, M.J., HENLEY, J.M., COLLINGRIDGE, G.L., JANE, D.E., 1997. (RS)-2-Chloro-5-Hydroxyphenylglycine (CHPG) Activates mGlu5, but not mGlu1, Receptors Expressed in CHO Cells and Potentiates NMDA Responses in the Hippocampus. Neuropharmacology 36, 265–267. doi:http://dx.doi.org/10.1016/S0028-3908(97)00001-4

Doré, A.S., Okrasa, K., Patel, J.C., Serrano-Vega, M., Bennett, K., Cooke, R.M., Errey, J.C., Jazayeri, A., Khan, S., Tehan, B., Weir, M., Wiggin, G.R., Marshall, F.H., 2014. Structure of class C GPCR metabotropic glutamate receptor 5 transmembrane domain. Nature 511, 557–62. doi:10.1038/nature13396

Doria, J.G., de Souza, J.M., Andrade, J.N., Rodrigues, H.A., Guimaraes, I.M., Carvalho, T.G., Guatimosim, C., Dobransky, T., Ribeiro, F.M., 2015. The mGluR5 positive allosteric modulator, CDPPB, ameliorates pathology and phenotypic signs of a mouse model of Huntington's disease. Neurobiol. Dis. 73, 163–173. doi:10.1016/j.nbd.2014.08.021

Doumazane, E., Scholler, P., Zwier, J.M., Eric, T., Rondard, P., Pin, J.-P., 2011. A new approach to analyze cell surface protein complexes reveals specific heterodimeric metabotropic glutamate receptors. FASEB J. 25, 66–77. doi:10.1096/fj.10-163147

Drouin-Ouellet, J., Brownell, A.-L., Saint-Pierre, M., Fasano, C., Emond, V., Trudeau, L.-E., Lévesque, D., Cicchetti, F., 2011. Neuroinflammation is associated with changes in glial mGluR5 expression and the development of neonatal excitotoxic lesions. Glia 59, 188–199. doi:10.1002/glia.21086

Edling, Y., Ingelman-Sundberg, M., Simi, A., 2007. Glutamate activates c-fos in glial cells via a novel mechanism involving the glutamate receptor subtype mGlu5 and the transcriptional repressor DREAM. Glia 55, 328–340. doi:10.1002/glia.20464

El Moustaine, D., Granier, S., Doumazane, E., Scholler, P., Rahmeh, R., Bron, P., Mouillac, B., Baneres, J.-L., Rondard, P., Pin, J.-P., 2012. Distinct roles of metabotropic glutamate receptor dimerization in agonist activation and G-protein coupling. Proc. Natl. Acad. Sci. 109, 16342–16347. doi:10.1073/pnas.1205838109

Ellard, J.M., Madin, A., Philps, O., Hopkin, M., Henderson, S., Birch, L., O'Connor, D., Arai, T., Takase, K., Morgan, L., Reynolds, D., Talma, S., Howley, E., Powney, B., Payne, A.H., Hall, A., Gartlon, J.E., Dawson, L.A., Castro, L., Atkinson, P.J., 2015. Identification and optimisation of a series of tetrahydrobenzotriazoles as metabotropic glutamate receptor 5-selective positive allosteric modulators that improve performance in a preclinical model of cognition. Bioorg. Med. Chem. Lett. 25, 5792–5796. doi:http://dx.doi.org/10.1016/j.bmcl.2015.10.050

Eng, A., Hedrick, T., Swanson, G., 2015. mGluR1-ß-arrestin 2 Signaling Mediates Induction of Excitatory Synaptic Plasticity. FASEB J. 29 .

Engelhardt, S., Grimmer, Y., Fan, G.H., Lohse, M.J., 2001. Constitutive activity of the human beta(1)-adrenergic receptor in beta(1)-receptor transgenic mice. Mol. Pharmacol. 60, 712–717.

Engers, D.W., Rodriguez, A.L., Williams, R., Hammond, A.S., Venable, D., Oluwatola, O., Sulikowski, G.A., Conn, P.J., Lindsley, C.W., 2009.

Synthesis, SAR and unanticipated pharmacological profiles of analogues of the mGluR5 ago-potentiator ADX-47273. ChemMedChem 4, 505–511. doi:10.1002/cmdc.200800357

Erdö, S.L., Michler, A., Wolff, J.R., 1991. GABA accelerates excitotoxic cell death in cortical cultures: protection by blockers of GABA-gated chloride channels. Brain Res. 542, 254–258. doi:10.1016/0006-8993(91)91575-L

Fan, G.F., Ray, K., Zhao, X.M., Goldsmith, P.K., Spiegel, A.M., 1998. Mutational analysis of the cysteines in the extracellular domain of the human Ca2+ receptor: Effects on cell surface expression, dimerization and signal transduction. FEBS Lett. 436, 353–356. doi:10.1016/S0014-5793(98)01165-X

Felder, C.C., 1995. Muscarinic acetylcholine receptors: signal transduction through multiple effectors. FASEB J. 9, 619–625. doi:10.1016/j.autneu.2006.10.006

Fell, M.J., Witkin, J.M., Falcone, J.F., Katner, J.S., Perry, K.W., Hart, J., Rorick-Kehn, L., Overshiner, C.D., Rasmussen, K., Chaney, S.F., Benvenga, M.J., Li, X., Marlow, D.L., Thompson, L.K., Luecke, S.K., Wafford, K.A., Seidel, W.F., Edgar, D.M., Quets, A.T., Felder, C.C., Wang, X., Heinz, B.A., Nikolayev, A., Kuo, M., Mayhugh, D., Khilevich, A., Zhang, D., Ebert, P.J., Eckstein, J.A., Ackermann, B.L., Swanson, S.P., Catlow, J.T., Dean, R.A., Jackson, K., Tauscher-Wisniewski, S., Marek, G.J., Schkeryantz, J.M., Svensson, K.A., 2011. N-(4-((2-(trifluoromethyl)-3-hydroxy-4-(isobutyryl)phenoxy)methyl)benzyl)-1-methyl-1H-imidazole-4-carboxamide (THIIC), a novel metabotropic glutamate 2 potentiator with potential anxiolytic/antidepressant properties: in vivo profiling suggests a link betw. J. Pharmacol. Exp. Ther. 336, 165–77. doi:10.1124/jpet.110.172957

Feng, W., Song, Z.H., 2003. Effects of D3.49A, R3.50A, and A6.34E mutations on ligand binding and activation of the cannabinoid-2 (CB2)

receptor. Biochem. Pharmacol. 65, 1077–1085. doi:10.1016/S0006-2952(03)00005-4

Feng, Z., Ma, S., Hu, G., Xie, X.-Q., 2015. Allosteric Binding Site and Activation Mechanism of Class C G-Protein Coupled Receptors: Metabotropic Glutamate Receptor Family. AAPS J. 17, 737–753. doi:10.1208/s12248-015-9742-8

Ferguson, S.S., Downey, W.E., Colapietro, A.M., Barak, L.S., Ménard, L., Caron, M.G., 1996. Role of beta-arrestin in mediating agonist-promoted G protein-coupled receptor internalization. Science 271, 363–366. doi:10.1126/science.271.5247.363

Ferraguti, F., Corti, C., Valerio, E., Mion, S., Xuereb, J., 2001. Activated astrocytes in areas of kainate-induced neuronal injury upregulate the expression of the metabotropic glutamate receptors 2/3 and 5. Exp. Brain Res. 137, 1–11. doi:10.1007/s002210000633

Flint, A.C., Dammerman, R.S., Kriegstein, A.R., 1999. Endogenous activation of metabotropic glutamate receptors in neocortical development causes neuronal calcium oscillations. Proc Natl Acad Sci U S A 96, 12144–12149. doi:10.1073/pnas.96.21.12144

Flor, P.J., Battaglia, G., Nicoletti, F., Gasparini, F., Bruno, V., 2002. Neuroprotective activity of metabotropic glutamate receptor ligands. Adv. Exp. Med. Biol. 513, 197–223. doi:10.1007/978-1-4615-0123-7

Fowler, S.W., Walker, J.M., Klakotskaia, D., Will, M.J., Serfozo, P., Simonyi, A., Schachtman, T.R., 2013. Effects of a metabotropic glutamate receptor 5 positive allosteric modulator, CDPPB, on spatial learning task performance in rodents. Neurobiol. Learn. Mem. 99, 25–31. doi:10.1016/j.nlm.2012.10.010

Francesconi, A., Duvoisin, R.M., 1998. Role of the second and third intracellular loops of metabotropic glutamate receptors in mediating dual signal transduction activation. J. Biol. Chem. 273, 5615–5624.

doi:10.1074/jbc.273.10.5615

Fredriksson, R., Lagerström, M.C., Lundin, L.-G., Schiöth, H.B., 2003. The G-protein-coupled receptors in the human genome form five main families. Phylogenetic analysis, paralogon groups, and fingerprints. Mol. Pharmacol. 63, 1256–72. doi:10.1124/mol.63.6.1256

Fujita, W., Gomes, I., Devi, L. a, 2014. Heteromers of μ-δ opioid receptors: new pharmacology and novel therapeutic possibilities. Br. J. Pharmacol. 1–13. doi:10.1111/bph.12663

Galván, E.J., Pérez-Rosello, T., Gómez-Lira, G., Lara, E., Gutiérrez, R., Barrionuevo, G., 2015. Synapse-specific compartmentalization of signaling cascades for LTP induction in CA3 interneurons. Neuroscience 290, 332–345. doi:http://dx.doi.org/10.1016/j.neuroscience.2015.01.024

Garwood, C.J., Pooler, A.M., Atherton, J., Hanger, D.P., Noble, W., 2011. Astrocytes are important mediators of Aß-induced neurotoxicity and tau phosphorylation in primary culture. Cell Death Dis. 2, e167. doi:10.1038/cddis.2011.50

Gasparini, F., Andres, H., Flor, P.J., Heinrich, M., Inderbitzin, W., Lingenhöhl, K., Müller, H., Munk, V.C., Omilusik, K., Stierlin, C., Stoehr, N., Vranesic, I., Kuhn, R., 2002. [3H]-M-MPEP, a potent, subtype-selective radioligand for the metabotropic glutamate receptor subtype 5. Bioorganic Med. Chem. Lett. 12, 407–409. doi:10.1016/S0960-894X(01)00767-3

Gasparini, F., Lingenhöhl, K., Stoehr, N., Flor, P.J., Heinrich, M., Vranesic, I., Biollaz, M., Allgeier, H., Heckendorn, R., Urwyler, S., Varney, M.A., Johnson, E.C., Hess, S.D., Rao, S.P., Sacaan, A.I., Santori, E.M., Veliçelebi, G., Kuhn, R., 1999. 2-Methyl-6-(phenylethynyl)-pyridine (MPEP), a potent, selective and systemically active mGlu5 receptor antagonist. Neuropharmacology 38, 1493–1503.

doi:http://dx.doi.org/10.1016/S0028-3908(99)00082-9

Gasparini, F., Spooren, W., 2007. Allosteric modulators for mGlu receptors. Curr. Neuropharmacol. 5, 187–94. doi:10.2174/157015907781695900

Gastambide, F., Cotel, M.-C., Gilmour, G., O'Neill, M.J., Robbins, T.W., Tricklebank, M.D., 2012. Selective remediation of reversal learning deficits in the neurodevelopmental MAM model of schizophrenia by a novel mGlu5 positive allosteric modulator. Neuropsychopharmacology 37, 1057–66. doi:10.1038/npp.2011.298

Gay, L.N., Long, J.W., 1949. Clinical evaluation of isopropyl-epinephrine in management of bronchial asthma. J. Am. Med. Assoc. 139, 452–457. doi:10.1001/jama.1949.72900240003008

Gesty-Palmer, D., Chen, M., Reiter, E., Ahn, S., Nelson, C.D., Loomis, C.R., Spurney, R.F., Luttrell, L.M., Lefkowitz, R.J., 2006. Distinct ß-arrestin and G protein dependent pathways for parathyroid hormone receptor stimulated ERK1/2 activation. J. Biol. Chem. 281, 10856–10864. doi:10.1074/jbc.M513380200

Gilmour, G., Broad, L.M., Wafford, K.A., Britton, T., Colvin, E.M., Fivush, A., Gastambide, F., Getman, B., Heinz, B.A., McCarthy, A.P., Prieto, L., Shanks, E., Smith, J.W., Taboada, L., Edgar, D.M., Tricklebank, M.D., 2013. In vitro characterisation of the novel positive allosteric modulators of the mGlu5 receptor, LSN2463359 and LSN2814617, and their effects on sleep architecture and operant responding in the rat. Neuropharmacology 64, 224–239. doi:http://dx.doi.org/10.1016/j.neuropharm.2012.07.030

Gil-Sanz, C., Delgado-García, J.M., Fairén, A., Gruart, A., 2008. Involvement of the mGluR1 Receptor in Hippocampal Synaptic Plasticity and Associative Learning in Behaving Mice. Cereb. Cortex 18 , 1653–1663. doi:10.1093/cercor/bhm193

Gladding, C.M., Collett, V.J., Jia, Z., Bashir, Z.I., Collingridge, G.L., Molnár,

E., 2009. Tyrosine dephosphorylation regulates AMPAR internalisation in mGluR-LTD. Mol. Cell. Neurosci. 40, 267–279. doi:10.1016/j.mcn.2008.10.014

Gomeza, J., Joly, C., Kuhn, R., Knöpfel, T., Bockaert, J., Pin, J.P., 1996. The second intracellular loop of metabotropic glutamate receptor 1 cooperates with the other intracellular domains to control coupling to G-proteins. J. Biol. Chem. 271, 2199–2205. doi:10.1074/jbc.271.4.2199

Goudet, C., Gaven, F., Kniazeff, J., Vol, C., Liu, J., Cohen-Gonsaud, M., Acher, F., Prézeau, L., Pin, J.P., 2004. Heptahelical domain of metabotropic glutamate receptor 5 behaves like rhodopsin-like receptors. Proc. Natl. Acad. Sci. U. S. A. 101, 378–83. doi:10.1073/pnas.0304699101

Goudet, C., Kniazeff, J., Hlavackova, V., Malhaire, F., Maurel, D., Acher, F., Blahos, J., Prézeau, L., Pin, J.P., 2005. Asymmetric functioning of dimeric metabotropic glutamate receptors disclosed by positive allosteric modulators. J. Biol. Chem. 280, 24380–24385. doi:10.1074/jbc.M502642200

Greasley, P.J., Fanelli, F., Rossier, O., Abuin, L., Cotecchia, S., 2002. Mutagenesis and modelling of the alpha(1b)-adrenergic receptor highlight the role of the helix 3/helix 6 interface in receptor activation. Mol. Pharmacol. 61, 1025–32. doi:10.1124/mol.61.5.1025

Gregory, K.J., Nguyen, E.D., Malosh, C., Mendenhall, J.L., Zic, J.Z., Bates, B.S., Noetzel, M.J., Squire, E.F., Turner, E.M., Rook, J.M., Emmitte, K.A., Stauffer, S.R., Lindsley, C.W., Meiler, J., Conn, P.J., 2014. Identification of specific ligand-receptor interactions that govern binding and cooperativity of diverse modulators to a common metabotropic glutamate receptor 5 allosteric site. ACS Chem. Neurosci. Specif. ligand-receptor Interact. that Gov. Bind. Coop. Divers. Modul. to a common metabotropic glutamate Recept. 5 allosteric site 5, 282–295. doi:10.1021/cn400225x

Gregory, K.J., Nguyen, E.D., Reiff, S.D., Squire, E.F., Stauffer, S.R., Lindsley, C.W., Meiler, J., Conn, P.J., 2013. Probing the metabotropic glutamate receptor 5 ($mGlu_5$) positive allosteric modulator (PAM) binding pocket: discovery of point mutations that engender a "molecular switch" in PAM pharmacology. Mol. Pharmacol. 83, 991–1006. doi:10.1124/mol.112.083949

Gregory, K.J., Noetzel, M.J., Rook, J.M., Vinson, P.N., Stauffer, S.R., Rodriguez, A.L., Emmitte, K. a, Zhou, Y., Chun, A.C., Felts, A.S., Chauder, B. a, Lindsley, C.W., Niswender, C.M., Conn, P.J., 2012. Investigating metabotropic glutamate receptor 5 allosteric modulator cooperativity, affinity, and agonism: enriching structure-function studies and structure-activity relationships. Mol. Pharmacol. 82, 860–75. doi:10.1124/mol.112.080531

Griffin, M.T., Figueroa, K.W., Liller, S., Ehlert, F.J., 2007. Estimation of agonist activity at G protein-coupled receptors: analysis of M2 muscarinic receptor signaling through Gi/o,Gs, and G15. J. Pharmacol. Exp. Ther. 321, 1193–207. doi:10.1124/jpet.107.120857

Gurevich, V. V, Dion, S.B., Onorato, J.J., Ptasienski, J., Kim, C.M., Sterne-Marr, R., Hosey, M.M., Benovic, J.L., 1995. Arrestin interactions with G protein-coupled receptors. Direct binding studies of wild type and mutant arrestins with rhodopsin, beta 2-adrenergic, and m2 muscarinic cholinergic receptors. J Biol Chem 270, 720–731. doi:10.1074/jbc.270.2.720

Gwak, Y.S., Hulsebosch, C.E., 2005. Upregulation of Group I metabotropic glutamate receptors in neurons and astrocytes in the dorsal horn following spinal cord injury. Exp. Neurol. 195, 236–243. doi:10.1016/j.expneurol.2005.05.012

Hamann, J., Vogel, B., van Schijndel, G.M.W., van Lier, R.A.W., 1996. The Seven-Span Transmembrane Receptor CD97 Has a Cellular Ligand (CD55, DAF). J. Exp. Med. 184, 1185–1189. doi:10.1084/jem.20130573

Hamilton, A., Esseltine, J.L., DeVries, R.A., Cregan, S.P., Ferguson, S.S.G., 2014. Metabotropic glutamate receptor 5 knockout reduces cognitive impairment and pathogenesis in a mouse model of Alzheimer's disease. Mol. Brain 7, 40. doi:10.1186/1756-6606-7-40

Hamm, H.E., Deretic, D., Arendt, a, Hargrave, P. a, Koenig, B., Hofmann, K.P., 1988. Site of G protein binding to rhodopsin mapped with synthetic peptides from the alpha subunit. Science (80-.). 241, 832–835. doi:10.1126/science.3136547

Han, G., Hampson, D.R., 1999. Ligand binding to the amino-terminal domain of the mGluR4 subtype of metabotropic glutamate receptor. J. Biol. Chem. 274, 10008–10013. doi:10.1074/jbc.274.15.10008

Harmar, A.J., 2001. Family-B G-protein-coupled receptors. Genome Biol. 2, REVIEWS3013. doi:10.1186/gb-2001-2-12-reviews3013

Harpsøe, K., Isberg, V., Tehan, B.G., Weiss, D., Arsova, A., Marshall, F.H., Bräuner-Osborne, H., Gloriam, D.E., 2015. Selective Negative Allosteric Modulation Of Metabotropic Glutamate Receptors – A Structural Perspective of Ligands and Mutants. Sci. Rep. 5, 13869.

Heidinger, V., Manzerra, P., Wang, X.Q., Strasser, U., Yu, S.-P., Choi, D.W., Behrens, M.M., 2002. Metabotropic glutamate receptor 1-induced upregulation of NMDA receptor current: mediation through the Pyk2/Src-family kinase pathway in cortical neurons. J. Neurosci. 22, 5452–5461. doi:20026565

Heller, R.S., Kieffer, T.J., Habener, J.F., 1996. Point mutations in the first and third intracellular loops of the glucagon-like peptide-1 receptor alter intracellular signaling. Biochem. Biophys. Res. Commun. 223, 624–32. doi:10.1006/bbrc.1996.0945

Hemstapat, K., de Paulis, T., Chen, Y., Brady, A.E., Grover, V.K., Alagille, D., Tamagnan, G.D., Conn, P.J., 2006. A Novel Class of Positive Allosteric Modulators of Metabotropic Glutamate Receptor Subtype 1

Interact with a Site Distinct from That of Negative Allosteric Modulators. Mol. Pharmacol. 70 , 616–626. doi:10.1124/mol.105.021857

Herlitze, S., Garcia, D.E., Mackie, K., Hille, B., Scheuer, T., Catterall, W.A., 1996. Modulation of Ca2+ channels by G-protein beta gamma subunits. Nature 380, 258–262. doi:10.1038/380258a0

Hermans, E., Challiss, R.A., 2001. Structural, signalling and regulatory properties of the group I metabotropic glutamate receptors: prototypic family C G-protein-coupled receptors. Biochem. J. 359, 465–484.

Heuss, C., Scanziani, M., Gähwiler, B.H., Gerber, U., 1999. G-protein-independent signaling mediated by metabotropic glutamate receptors. Nat. Neurosci. 2, 1070–1077. doi:10.1038/15996

Hiltscher, R., Seuwen, K., Boddeke, H.W.G.M., Sommer, B., Laurie, D.J., 1998. Functional coupling of human metabotropic glutamate receptor hmGlu(1d): Comparison to splice variants hmGlu(1a) and -(1b). Neuropharmacology 37, 827–837. doi:10.1016/S0028-3908(98)00079-3

Hintermann, S., Vranesic, I., Allgeier, H., Brülisauer, A., Hoyer, D., Lemaire, M., Moenius, T., Urwyler, S., Whitebread, S., Gasparini, F., Auberson, Y.P., 2007. ABP688, a novel selective and high affinity ligand for the labeling of mGlu5 receptors: Identification, in vitro pharmacology, pharmacokinetic and biodistribution studies. Bioorg. Med. Chem. 15, 903–914. doi:http://dx.doi.org/10.1016/j.bmc.2006.10.038

Hlavackova, V., Goudet, C., Kniazeff, J., Zikova, A., Maurel, D., Vol, C., Trojanova, J., Prézeau, L., Pin, J., Blahos, J., 2005. Evidence for a single heptahelical domain being turned on upon activation of a dimeric GPCR. EMBO J. 24, 499–509.

Hoare, S.R.J., 2005. Mechanisms of peptide and nonpeptide ligand binding to Class B G-protein-coupled receptors. Drug Discov. Today. doi:10.1016/S1359-6446(05)03370-2

Hollenstein, K., Kean, J., Bortolato, A., Cheng, R.K.Y., Doré, A.S., Jazayeri, A., Cooke, R.M., Weir, M., Marshall, F.H., 2013. Structure of class B GPCR corticotropin-releasing factor receptor 1. Nature 499, 438–43. doi:10.1038/nature12357

Horn, F., Bettler, E., Oliveira, L., Campagne, F., Cohen, F.E., Vriend, G., 2003. GPCRDB information system for G protein-coupled receptors. Nucleic Acids Res. doi:10.1093/nar/gkg103

Hosey, M.M., 1999. What molecular events underlie heterologous desensitization? Focus on "Receptor phosphorylation does not mediate cross talk between muscarinic M3 and bradykinin B2 receptors." Am. J. Physiol. - Cell Physiol. 277, C856–C858.

Houamed, K.M., Kuijper, J.L., Gilbert, T.L., Haldeman, B.A., O'Hara, P.J., Mulvihill, E.R., Almers, W., Hagen, F.S., 1991. Cloning, expression, and gene structure of a G protein-coupled glutamate receptor from rat brain. Science (80-.). 252, 1318–1321.

Hu, J., Hauache, O., Spiegel, A.M., 2000. Human Ca2+ receptor cysteine-rich domain: Analysis of function of mutant and chimeric receptors. J. Biol. Chem. 275, 16382–16389. doi:10.1074/jbc.M000277200

Huang, H., Degnan, A.P., Balakrishnan, A., Easton, A., Gulianello, M., Huang, Y., Matchett, M., Mattson, G., Miller, R., Santone, K.S., Senapati, A., Shields, E.E., Sivarao, D. V, Snyder, L.B., Westphal, R., Whiterock, V.J., Yang, F., Bronson, J.J., Macor, J.E., 2016. Oxazolidinone-based allosteric modulators of mGluR5: Defining molecular switches to create a pharmacological tool box. Bioorg. Med. Chem. Lett. 26, 4165–4169. doi:http://dx.doi.org/10.1016/j.bmcl.2016.07.065

Huang, Y.Q., Lu, W.Y., Ali, D.W., Pelkey, K.A., Pitcher, G.M., Lu, Y.M., Aoto, H., Roder, J.C., Sasaki, T., Salter, M.W., MacDonald, J.F., 2001. CAKβ/Pyk2 kinase is a signaling link for induction of long-term

potentiation in CA1 hippocampus. Neuron 29, 485–496. doi:10.1016/S0896-6273(01)00220-3

Iadecola, C., Nedergaard, M., 2007. Glial regulation of the cerebral microvasculature. Nat. Neurosci. 10, 1369–1376. doi:10.1038/nn2003

Ichise, T., 2000. mGluR1 in Cerebellar Purkinje Cells Essential for Long-Term Depression, Synapse Elimination, and Motor Coordination. Science (80-.). 288, 1832–1835. doi:10.1126/science.288.5472.1832

Janz, J.M., Farrens, D.L., 2004. Rhodopsin activation exposes a key hydrophobic binding site for the transducin α-subunit C terminus. J. Biol. Chem. 279, 29767–29773. doi:10.1074/jbc.M402567200

Jelsema, C.L., Axelrod, J., 1987. Stimulation of phospholipase A2 activity in bovine rod outer segments by the beta gamma subunits of transducin and its inhibition by the alpha subunit. Proc. Natl. Acad. Sci. U. S. A. 84, 3623–7.

Jingami, H., Nakanishi, S., Morikawa, K., 2003. Structure of the metabotropic glutamate receptor. Curr. Opin. Neurobiol. doi:10.1016/S0959-4388(03)00067-9

Joly, C., Gomeza, J., Brabet, I., Curry, K., Bockaert, J., Pin, J.P., 1995. Molecular, functional, and pharmacological characterization of the metabotropic glutamate receptor type 5 splice variants: comparison with mGluR1. J. Neurosci. 15, 3970–3981.

Kammermeier, P.J., 2012. Functional and pharmacological characteristics of metabotropic glutamate receptors 2/4 heterodimers. Mol. Pharmacol. 82, 438–47. doi:10.1124/mol.112.078501

Kammermeier, P.J., 2010. C-terminal deletion of metabotropic glutamate receptor 1 selectively abolishes coupling to Gαq. Eur. J. Pharmacol. 627, 63–68. doi:10.1016/j.ejphar.2009.10.051

Kammermeier, P.J., Yun, J., 2005. Activation of metabotropic glutamate

receptor 1 dimers requires glutamate binding in both subunits. J. Pharmacol. Exp. Ther. 312, 502–508. doi:jpet.104.073155 [pii]\r10.1124/jpet.104.073155

Kang, D.S., Tian, X., Benovic, J.L., 2013. ß-Arrestins and G protein-coupled receptor trafficking. Methods Enzymol. 521, 91–108. doi:10.1016/B978-0-12-391862-8.00005-3

Kaupmann, K., Schuler, V., Mosbacher, J., Bischoff, S., Bittiger, H., Heid, J., Froestl, W., Leonhard, S., Pfaff, T., Karschin, a, Bettler, B., 1998. Human gamma-aminobutyric acid type B receptors are differentially expressed and regulate inwardly rectifying K+ channels. Proc. Natl. Acad. Sci. U. S. A. 95, 14991–6. doi:10.1073/pnas.95.25.14991

Kawabata, S., Kohara, A., Tsutsumi, R., Itahana, H., Hayashibe, S., Yamaguchi, T., Okada, M., 1998. Diversity of calcium signaling by metabotropic glutamate receptors. J Biol Chem 273, 17381–17385.

Kawabata, S., Tsutsumi, R., Kohara, A., Yamaguchi, T., Nakanishi, S., Okada, M., 1996. Control of calcium oscillations by phosphorylation of metabotropic glutamate receptors. Nature 383, 89–92. doi:10.1038/383089a0

Kerner, J. a, Standaert, D.G., Penney, J.B., Young, A.B., Landwehrmeyer, G.B., 1997. Expression of group one metabotropic glutamate receptor subunit mRNAs in neurochemically identified neurons in the rat neostriatum, neocortex, and hippocampus. Mol. Brain Res. 48, 259–269. doi:10.1016/S0169-328X(97)00102-2

Kew, J.N.C., 2004. Positive and negative allosteric modulation of metabotropic glutamate receptors: emerging therapeutic potential. Pharmacol. Ther. 104, 233–44. doi:10.1016/j.pharmthera.2004.08.010

Khoury, E., Clément, S., Laporte, S.A., 2014. Allosteric and biased G protein-coupled receptor signaling regulation: Potentials for new therapeutics. Front. Endocrinol. (Lausanne).

doi:10.3389/fendo.2014.00068

Kieffer, B.L., 1995. Recent advances in molecular recognition and signal transduction of active peptides: Receptors for opioid peptides. Cell. Mol. Neurobiol. doi:10.1007/BF02071128

Kilpatrick, L.E., Humphrys, L.J., Holliday, N.D., 2015. A G Protein Coupled Receptor Dimer Imaging Assay Reveals Selectively Modified Pharmacology of Neuropeptide Y Y1 / Y5 Receptor Heterodimers. Mol. Pharmacol. 718–732. doi:10.1124/mol.114.095356

Kim, C.H., Braud, S., Isaac, J.T.R., Roche, K.W., 2005. Protein kinase C phosphorylation of the metabotropic glutamate receptor mGluR5 on serine 839 regulates Ca2+ oscillations. J. Biol. Chem. 280, 25409–25415. doi:10.1074/jbc.M502644200

Kinney, G.G., O'Brien, J. a, Lemaire, W., Burno, M., Bickel, D.J., Clements, M.K., Chen, T.-B., Wisnoski, D.D., Lindsley, C.W., Tiller, P.R., Smith, S., Jacobson, M. a, Sur, C., Duggan, M.E., Pettibone, D.J., Conn, P.J., Williams, D.L., 2005. A novel selective positive allosteric modulator of metabotropic glutamate receptor subtype 5 has in vivo activity and antipsychotic-like effects in rat behavioral models. J. Pharmacol. Exp. Ther. 313, 199–206. doi:10.1124/jpet.104.079244

Kitano, J., Kimura, K., Yamazaki, Y., Soda, T., Shigemoto, R., Nakajima, Y., Nakanishi, S., 2002. Tamalin, a PDZ domain-containing protein, links a protein complex formation of group 1 metabotropic glutamate receptors and the guanine nucleotide exchange factor cytohesins. J. Neurosci. 22, 1280–1289. doi:22/4/1280 [pii]

Klein, J., Reymann, K.G., Riedel, G., 1997. Activation of phospholipases C and D by the novel metabotropic glutamate receptor agonist tADA. Neuropharmacology 36, 261–263. doi:10.1016/S0028-3908(96)00174-8

Kniazeff, J., Bessis, A.S., Maurel, D., Ansanay, H., Prezeau, L., Pin, J.P., 2004. Closed state of both binding domains of homodimeric mGlu

receptors is required for full activity. Nat Struct Mol Biol 11, 706–713. doi:10.1038/nsmb794

Knoflach, F., Mutel, V., Jolidon, S., Kew, J.N., Malherbe, P., Vieira, E., Wichmann, J., Kemp, J.A., 2001. Positive allosteric modulators of metabotropic glutamate 1 receptor: characterization, mechanism of action, and binding site. Proc. Natl. Acad. Sci. U. S. A. 98, 13402–7. doi:10.1073/pnas.231358298

Kobilka, 2007. G protein coupled receptor structure and activation. Biochim. Biophys. Acta 1768, 794–807. doi:10.1016/j.bbamem.2006.10.021

Kotecha, S.A., Jackson, M.F., Al-Mahrouki, A., Roder, J.C., Orser, B.A., MacDonald, J.F., 2003. Co-stimulation of MgluR5 and N-methyl-D-aspartate receptors is required for potentiation of excitatory synaptic transmission in hippocampal neurons. J. Biol. Chem. 278, 27742–27749. doi:10.1074/jbc.M301946200

Krasnoperov, V., Lu, Y., Buryanovsky, L., Neubert, T. a, Ichtchenko, K., Petrenko, A.G., 2002. Post-translational proteolytic processing of the calcium-independent receptor of alpha-latrotoxin (CIRL), a natural chimera of the cell adhesion protein and the G protein-coupled receptor. J. Biol. Chem. 277, 46518–26. doi:10.1074/jbc.M206415200

Kuang, D., Yao, Y., Wang, M., Pattabiraman, N., Kotra, L.P., Hampson, D.R., 2003. Molecular Similarities in the Ligand Binding Pockets of an Odorant Receptor and the Metabotropic Glutamate Receptors. J. Biol. Chem. 278, 42551–42559. doi:10.1074/jbc.M307120200

Kumar, A., Dhull, D.K., Mishra, P.S., 2015. Therapeutic potential of mGluR5 targeting in Alzheimer's disease. Front. Neurosci. 9, 1–9. doi:10.3389/fnins.2015.00215

Kunishima, N., Shimada, Y., Tsuji, Y., Sato, T., Yamamoto, M., Kumasaka, T., Nakanishi, S., Jingami, H., Morikawa, K., 2000. Structural basis of glutamate recognition by a dimeric metabotropic glutamate receptor.

Nature 407, 971–977. doi:10.1038/35039564

Lagerstrom, M.C., Schioth, H.B., 2008. Structural diversity of G protein-coupled receptors and significance for drug discovery. Nat Rev Drug Discov 7, 339–357.

Lamb, J.P., Engers, D.W., Niswender, C.M., Rodriguez, A.L., Venable, D.F., Conn, J.P., Lindsley, C.W., 2011. Discovery of molecular switches within the ADX-47273 mGlu5 PAM scaffold that modulate modes of pharmacology to afford potent mGlu5 NAMs, PAMs and partial antagonists, in: Bioorganic and Medicinal Chemistry Letters. pp. 2711–2714. doi:10.1016/j.bmcl.2010.11.119

Lambright, D.G., Sondek, J., Bohm, a, Skiba, N.P., Hamm, H.E., Sigler, P.B., 1996. The 2.0 A crystal structure of a heterotrimeric G protein. Nature. doi:10.1038/379311a0

Lander, E.S., Linton, L.M., Birren, B., Nusbaum, C., Zody, M.C., Baldwin, J., Devon, K., Dewar, K., Doyle, M., FitzHugh, W., Funke, R., Gage, D., Harris, K., Heaford, A., Howland, J., Kann, L., Lehoczky, J., LeVine, R., McEwan, P., McKernan, K., Meldrim, J., Mesirov, J.P., Miranda, C., Morris, W., Naylor, J., Raymond, C., Rosetti, M., Santos, R., Sheridan, A., Sougnez, C., Stange-Thomann, N., Stojanovic, N., Subramanian, A., Wyman, D., Rogers, J., Sulston, J., Ainscough, R., Beck, S., Bentley, D., Burton, J., Clee, C., Carter, N., Coulson, A., Deadman, R., Deloukas, P., Dunham, A., Dunham, I., Durbin, R., French, L., Grafham, D., Gregory, S., Hubbard, T., Humphray, S., Hunt, A., Jones, M., Lloyd, C., McMurray, A., Matthews, L., Mercer, S., Milne, S., Mullikin, J.C., Mungall, A., Plumb, R., Ross, M., Shownkeen, R., Sims, S., Waterston, R.H., Wilson, R.K., Hillier, L.W., McPherson, J.D., Marra, M.A., Mardis, E.R., Fulton, L.A., Chinwalla, A.T., Pepin, K.H., Gish, W.R., Chissoe, S.L., Wendl, M.C., Delehaunty, K.D., Miner, T.L., Delehaunty, A., Kramer, J.B., Cook, L.L., Fulton, R.S., Johnson, D.L., Minx, P.J., Clifton, S.W., Hawkins, T., Branscomb, E., Predki, P., Richardson, P.,

Wenning, S., Slezak, T., Doggett, N., Cheng, J.F., Olsen, A., Lucas, S., Elkin, C., Uberbacher, E., Frazier, M., Gibbs, R.A., Muzny, D.M., Scherer, S.E., Bouck, J.B., Sodergren, E.J., Worley, K.C., Rives, C.M., Gorrell, J.H., Metzker, M.L., Naylor, S.L., Kucherlapati, R.S., Nelson, D.L., Weinstock, G.M., Sakaki, Y., Fujiyama, A., Hattori, M., Yada, T., Toyoda, A., Itoh, T., Kawagoe, C., Watanabe, H., Totoki, Y., Taylor, T., Weissenbach, J., Heilig, R., Saurin, W., Artiguenave, F., Brottier, P., Bruls, T., Pelletier, E., Robert, C., Wincker, P., Smith, D.R., Doucette-Stamm, L., Rubenfield, M., Weinstock, K., Lee, H.M., Dubois, J., Rosenthal, A., Platzer, M., Nyakatura, G., Taudien, S., Rump, A., Yang, H., Yu, J., Wang, J., Huang, G., Gu, J., Hood, L., Rowen, L., Madan, A., Qin, S., Davis, R.W., Federspiel, N.A., Abola, A.P., Proctor, M.J., Myers, R.M., Schmutz, J., Dickson, M., Grimwood, J., Cox, D.R., Olson, M. V, Kaul, R., Raymond, C., Shimizu, N., Kawasaki, K., Minoshima, S., Evans, G.A., Athanasiou, M., Schultz, R., Roe, B.A., Chen, F., Pan, H., Ramser, J., Lehrach, H., Reinhardt, R., McCombie, W.R., de la Bastide, M., Dedhia, N., Blocker, H., Hornischer, K., Nordsiek, G., Agarwala, R., Aravind, L., Bailey, J.A., Bateman, A., Batzoglou, S., Birney, E., Bork, P., Brown, D.G., Burge, C.B., Cerutti, L., Chen, H.C., Church, D., Clamp, M., Copley, R.R., Doerks, T., Eddy, S.R., Eichler, E.E., Furey, T.S., Galagan, J., Gilbert, J.G., Harmon, C., Hayashizaki, Y., Haussler, D., Hermjakob, H., Hokamp, K., Jang, W., Johnson, L.S., Jones, T.A., Kasif, S., Kaspryzk, A., Kennedy, S., Kent, W.J., Kitts, P., Koonin, E. V, Korf, I., Kulp, D., Lancet, D., Lowe, T.M., McLysaght, A., Mikkelsen, T., Moran, J. V, Mulder, N., Pollara, V.J., Ponting, C.P., Schuler, G., Schultz, J., Slater, G., Smit, A.F., Stupka, E., Szustakowski, J., Thierry-Mieg, D., Thierry-Mieg, J., Wagner, L., Wallis, J., Wheeler, R., Williams, A., Wolf, Y.I., Wolfe, K.H., Yang, S.P., Yeh, R.F., Collins, F., Guyer, M.S., Peterson, J., Felsenfeld, A., Wetterstrand, K.A., Patrinos, A., Morgan, M.J., de Jong, P., Catanese, J.J., Osoegawa, K., Shizuya, H., Choi, S., Chen, Y.J., International Human Genome Sequencing, C., 2001. Initial sequencing and analysis of the human genome. Nature

409, 860–921. doi:10.1038/35057062

Langmead, C.J., Christopoulos, A., 2006. Allosteric agonists of 7TM receptors: expanding the pharmacological toolbox. Trends Pharmacol. Sci. 27, 475–481. doi:http://dx.doi.org/10.1016/j.tips.2006.07.009

Lanté, F., de Jésus Ferreira, M.-C., Guiramand, J., Récasens, M., Vignes, M., 2006. Low-frequency stimulation induces a new form of LTP, metabotropic glutamate (mGlu5) receptor- and PKA-dependent, in the CA1 area of the rat hippocampus. Hippocampus 16, 345–360. doi:10.1002/hipo.20146

Laporte, S. a, Oakley, R.H., Zhang, J., Holt, J. a, Ferguson, S.S., Caron, M.G., Barak, L.S., 1999. The beta2-adrenergic receptor/betaarrestin complex recruits the clathrin adaptor AP-2 during endocytosis. Proc. Natl. Acad. Sci. U. S. A. 96, 3712–3717. doi:10.1073/pnas.96.7.3712

Lavreysen, H., Janssen, C., Bischoff, F., Langlois, X., Leysen, J.E., Lesage, A.S.J., 2003. [3H]R214127: a novel high-affinity radioligand for the mGlu1 receptor reveals a common binding site shared by multiple allosteric antagonists. Mol. Pharmacol. 63, 1082–93. doi:10.1124/mol.63.5.1082

Lavreysen, H., Wouters, R., Bischoff, F., Nóbrega Pereira, S., Langlois, X., Blokland, S., Somers, M., Dillen, L., Lesage, A.S.J., 2004. JNJ16259685, a highly potent, selective and systemically active mGlu1 receptor antagonist. Neuropharmacology 47, 961–972. doi:10.1016/j.neuropharm.2004.08.007

Lazareno, S., Birdsall, N.J., 1995. Detection, quantitation, and verification of allosteric interactions of agents with labeled and unlabeled ligands at G protein-coupled receptors: interactions of strychnine and acetylcholine at muscarinic receptors. Mol. Pharmacol. 48, 362–378.

Lea IV, P.M., Faden, A.I., 2006. Metabotropic glutamate receptor subtype 5 antagonists MPEP and MTEP. CNS Drug Rev. doi:10.1111/j.1527-

3458.2006.00149.x

Lea, P.M., Movsesyan, V.A., Faden, A.I., 2005. Neuroprotective activity of the mGluR5 antagonists MPEP and MTEP against acute excitotoxicity differs and does not reflect actions at mGluR5 receptors. Br. J. Pharmacol. 145, 527–34. doi:10.1038/sj.bjp.0706219

Leach, K., Loiacono, R.E., Felder, C.C., McKinzie, D.L., Mogg, A., Shaw, D.B., Sexton, P.M., Christopoulos, A., 2009. Molecular Mechanisms of Action and In Vivo Validation of an M4 Muscarinic Acetylcholine Receptor Allosteric Modulator with Potential Antipsychotic Properties. Neuropsychopharmacology 35, 855–869.

Leach, K., Sexton, P.M., Christopoulos, A., 2007. Allosteric GPCR modulators: taking advantage of permissive receptor pharmacology. Trends Pharmacol. Sci. 28, 382–389. doi:10.1016/j.tips.2007.06.004

Lebon, G., Warne, T., Edwards, P.C., Bennett, K., Langmead, C.J., Leslie, A.G.W., Tate, C.G., 2011. Agonist-bound adenosine A2A receptor structures reveal common features of GPCR activation. Nature 474, 521–525. doi:10.1038/nature10136

Lee, C., Murakami, T., Simonds, W.F., 1995. Identification of a discrete region of the G protein gamma subunit conferring selectivity in beta gamma complex formation. J. Biol. Chem. 270, 8779–8784. doi:10.1074/jbc.270.15.8779

Lefkowitz, R.J., 1998. G protein-coupled receptors. III. New roles for receptor kinases and beta-arrestins in receptor signaling and desensitization. J. Biol. Chem. 273, 18677–18680. doi:10.1074/jbc.273.30.18677

Lewis, J.A., Lebois, E.P., Lindsley, C.W., 2008. Allosteric modulation of kinases and GPCRs: design principles and structural diversity. Curr. Opin. Chem. Biol. doi:10.1016/j.cbpa.2008.02.014

Li, J., Huang, P., Chen, C., de Riel, J.K., Weinstein, H., Liu-Chen, L.-Y., 2001. Constitutive Activation of the μ Opioid Receptor by Mutation of D3.49(164), but Not D3.32(147): D3.49(164) Is Critical for Stabilization of the Inactive Form of the Receptor and for Its Expression. Biochemistry 40, 12039–12050. doi:10.1021/bi0100945

Libri, V., Constanti, A., Zibetti, M., Postlethwaite, M., 1997. Metabotropic glutamate receptor subtypes mediating slow inward tail current (IADP) induction and inhibition of synaptic transmission in olfactory cortical neurones. Br J Pharmacol 120, 1083–1095. doi:10.1038/sj.bjp.0701021

Lindsley, C.W., Emmitte, K.A., Hopkins, C.R., Bridges, T.M., Gregory, K.J., Niswender, C.M., Conn, P.J., 2016. Practical Strategies and Concepts in GPCR Allosteric Modulator Discovery: Recent Advances with Metabotropic Glutamate Receptors. Chem. Rev. acs.chemrev.5b00656. doi:10.1021/acs.chemrev.5b00656

Lindsley, C.W., Wisnoski, D.D., Leister, W.H., O'brien, J. a, Lemaire, W., Williams, D.L., Burno, M., Sur, C., Kinney, G.G., Pettibone, D.J., Tiller, P.R., Smith, S., Duggan, M.E., Hartman, G.D., Conn, P.J., Huff, J.R., 2004. Discovery of positive allosteric modulators for the metabotropic glutamate receptor subtype 5 from a series of N-(1,3-diphenyl-1H-pyrazol-5-yl)benzamides that potentiate receptor function in vivo. J. Med. Chem. 47, 5825–5828. doi:10.1021/jm049400d

Litschig, S., Gasparini, F., Rueegg, D., Stoehr, N., Flor, P.J., Vranesic, I., Prézeau, L., Pin, J.P., Thomsen, C., Kuhn, R., 1999. CPCCOEt, a noncompetitive metabotropic glutamate receptor 1 antagonist, inhibits receptor signaling without affecting glutamate binding. Mol. Pharmacol. 55, 453–61. doi:10.1164/ajrccm.159.3.9607099

Little, K.D., Hemler, M.E., Stipp, C.S., 2004. Dynamic Regulation of a GPCR-Tetraspanin-G Protein Complex on Intact Cells: Central Role of CD81 in Facilitating GPR56-Gαq/11 Association. Mol. Biol. Cell 15 , 2375–2387. doi:10.1091/mbc.E03-12-0886

Liu, F., Gong, X., Zhang, G., Marquis, K., Reinhart, P., Andree, T.H., 2005. The inhibition of glycogen synthase kinase 3beta by a metabotropic glutamate receptor 5 mediated pathway confers neuroprotection to Abeta peptides. J. Neurochem. 95, 1363–72. doi:10.1111/j.1471-4159.2005.03474.x

Liu, F., Grauer, S., Kelley, C., Navarra, R., Graf, R., Zhang, G., Atkinson, P.J., Popiolek, M., Wantuch, C., Khawaja, X., Smith, D., Olsen, M., Kouranova, E., Lai, M., Pruthi, F., Pulicicchio, C., Day, M., Gilbert, A., Pausch, M.H., Brandon, N.J., Beyer, C.E., Comery, T. a, Logue, S., Rosenzweig-Lipson, S., Marquis, K.L., 2008. ADX47273 [S-(4-fluoro-phenyl)-{3-[3-(4-fluoro-phenyl)-[1,2,4]-oxadiazol-5-yl]-piperidin-1-yl}-methanone]: a novel metabotropic glutamate receptor 5-selective positive allosteric modulator with preclinical antipsychotic-like and procognitive activities. J. Pharmacol. Exp. Ther. 327, 827–839. doi:jpet.108.136580 [pii]\n10.1124/jpet.108.136580

Liu, M., Parker, R.M., Darby, K., Eyre, H.J., Copeland, N.G., Crawford, J., Gilbert, D.J., Sutherland, G.R., Jenkins, N.A., Herzog, H., 1999. GPR56, a novel secretin-like human G-protein-coupled receptor gene. Genomics 55, 296–305. doi:10.1006/geno.1998.5644

Loane, D.J., Stoica, B.A., Tchantchou, F., Kumar, A., Barrett, J.P., Akintola, T., Xue, F., Conn, P.J., Faden, A.I., 2014. Novel mGluR5 Positive Allosteric Modulator Improves Functional Recovery, Attenuates Neurodegeneration, and Alters Microglial Polarization after Experimental Traumatic Brain Injury. Neurotherapeutics 11, 857–869. doi:10.1007/s13311-014-0298-6

Logothetis, D.E., Kurachi, Y., Galper, J., Neer, E.J., Clapham, D.E., 1987. The beta gamma subunits of GTP-binding proteins activate the muscarinic K+ channel in heart. Nature. doi:10.1038/325321a0

Lohse, M.J., Andexinger, S., Pitcher, J., Trukawinski, S., Codina, J., Faure, J.P., Caron, M.G., Lefkowitz, R.J., 1992. Receptor-specific

desensitization with purified proteins: Kinase dependence and receptor specificity of ??-arrestin and arrestin in the ??2-adrenergic receptor and rhodopsin systems. J. Biol. Chem. 267, 8558–8564.

Loweth, J. a, Scheyer, A.F., Milovanovic, M., LaCrosse, A.L., Flores-Barrera, E., Werner, C.T., Li, X., Ford, K. a, Le, T., Olive, M.F., Szumlinski, K.K., Tseng, K.Y., Wolf, M.E., 2014. Synaptic depression via mGluR1 positive allosteric modulation suppresses cue-induced cocaine craving. Nat. Neurosci. 17, 73–80. doi:10.1038/nn.3590

Lu, Z.L., Curtis, C. a, Jones, P.G., Pavia, J., Hulme, E.C., 1997. The role of the aspartate-arginine-tyrosine triad in the m1 muscarinic receptor: mutations of aspartate 122 and tyrosine 124 decrease receptor expression but do not abolish signaling. Mol. Pharmacol. 51, 234–41.

Lujan, R., Nusser, Z., Roberts, J.D., Shigemoto, R., Somogyi, P., 1996. Perisynaptic location of metabotropic glutamate receptors mGluR1 and mGluR5 on dendrites and dendritic spines in the rat hippocampus. Eur. J. Neurosci. 8, 1488–1500. doi:DOI 10.1111/j.1460-9568.1996.tb01611.x

Luo, H.R., Hattori, H., Hossain, M.A., Hester, L., Huang, Y., Lee-Kwon, W., Donowitz, M., Nagata, E., Snyder, S.H., 2003. Akt as a mediator of cell death. Proc. Natl. Acad. Sci. 100, 11712–7. doi:10.1073/pnas.1634990100

Luscher, C., Slesinger, P.A., Lüscher, C., Slesinger, P.A., 2010. Emerging roles for G protein-gated inwardly rectifying potassium (GIRK) channels in health and disease. Nat. Rev. Neurosci. 11, 301–315. doi:10.1038/nrn2834

Luttrell, L.M., Ferguson, S.S., Daaka, Y., Miller, W.E., Maudsley, S., Della Rocca, G.J., Lin, F., Kawakatsu, H., Owada, K., Luttrell, D.K., Caron, M.G., Lefkowitz, R.J., 1999a. Beta-arrestin-dependent formation of beta2 adrenergic receptor-Src protein kinase complexes. Science (80-.). 283, 655–661. doi:10.1126/science.283.5402.655

Luttrell, L.M., Ferguson, S.S., Daaka, Y., Miller, W.E., Maudsley, S., Della Rocca, G.J., Lin, F., Kawakatsu, H., Owada, K., Luttrell, D.K., Caron, M.G., Lefkowitz, R.J., 1999b. ß-arrestin-dependent formation of ß2 adrenergic receptor-Src protein kinase complexes. Science (80-.). 283, 655–661. doi:10.1126/science.283.5402.655

Macfarlane, S.R., Seatter, M.J., Kanke, T., Hunter, G.D., Plevin, R., 2001. Proteinase-Activated Receptors. Pharmacol. Rev. 53 , 245–282.

Malherbe, P., Kratochwil, N., Zenner, M.-T., Piussi, J., Diener, C., Kratzeisen, C., Fischer, C., Porter, R.H.P., 2003. Mutational analysis and molecular modeling of the binding pocket of the metabotropic glutamate 5 receptor negative modulator 2-methyl-6-(phenylethynyl)-pyridine. Mol. Pharmacol. 64, 823–832. doi:10.1124/mol.64.4.823

Manglik, A., Lin, H., Aryal, D.K., McCorvy, J.D., Dengler, D., Corder, G., Levit, A., Kling, R.C., Bernat, V., Hübner, H., Huang, X.-P., Sassano, M.F., Giguère, P.M., Löber, S., Da Duan, Scherrer, G., Kobilka, B.K., Gmeiner, P., Roth, B.L., Shoichet, B.K., 2016. Structure-based discovery of opioid analgesics with reduced side effects. Nature advance on, 1–6.

Mannaioni, G., Marino, M.J., Valenti, O., Traynelis, S.F., Conn, P.J., 2001. Metabotropic glutamate receptors 1 and 5 differentially regulate CA1 pyramidal cell function. J. Neurosci. 21, 5925–34.

Mao, L., Yang, L., Arora, A., Eun, S.C., Zhang, G., Liu, Z., Fibuch, E.E., Wang, J.Q., 2005a. Role of protein phosphatase 2A in mGluR5-regulated MEK/ERK phosphorylation in neurons. J. Biol. Chem. 280, 12602–12610. doi:10.1074/jbc.M411709200

Mao, L., Yang, L., Tang, Q., Samdani, S., Zhang, G., Wang, J.Q., 2005b. The scaffold protein Homer1b/c links metabotropic glutamate receptor 5 to extracellular signal-regulated protein kinase cascades in neurons. J. Neurosci. 25, 2741–52. doi:10.1523/JNEUROSCI.4360-04.2005

Marinissen, M.J., Gutkind, J.S., 2001. G-protein-coupled receptors and

signaling networks: Emerging paradigms. Trends Pharmacol. Sci. doi:10.1016/S0165-6147(00)01678-3

Marshall, F.H., Jones, K.A., Kaupmann, K., Bettler, B., 2016. $GABA_B$ receptors – the first 7TM heterodimers. Trends Pharmacol. Sci. 20, 396–399. doi:10.1016/S0165-6147(99)01383-8

Mary, S., Gomeza, J., Prézeau, L., Bockaert, J., Pin, J.P., 1998. A cluster of basic residues in the carboxyl-terminal tail of the short metabotropic glutamate receptor 1 variants impairs their coupling to phospholipase C. J. Biol. Chem. 273, 425–432. doi:10.1074/jbc.273.1.425

Masu, M., Tanabe, Y., Tsuchida, K., Shigemoto, R., Nakanishi, S., 1991. Sequence and expression of a metabotropic glutamate receptor. Nature 349, 760–5. doi:10.1038/349760a0

Mathiesen, J.M., Svendsen, N., Bräuner-Osborne, H., Thomsen, C., Ramirez, M.T., 2003. Positive allosteric modulation of the human metabotropic glutamate receptor 4 (hmGluR4) by SIB-1893 and MPEP. Br. J. Pharmacol. 138, 1026–1030. doi:10.1038/sj.bjp.0705159

Mattson, M.P., 2000. Apoptosis in neurodegenerative disorders [Review]. Nat. Rev. Mol. Cell Biol. 1, 120–129. doi:10.1038/35040009

May, L.T., Leach, K., Sexton, P.M., Christopoulos, A., 2007. Allosteric modulation of G protein-coupled receptors. Annu. Rev. Pharmacol. Toxicol. 47, 1–51. doi:10.1146/annurev.pharmtox.47.120505.105159

McEachern, J.C., Shaw, C.A., 1999. The plasticity-pathology continuum: Defining a role for the LTP phenomenon. J. Neurosci. Res. 58, 42–61. doi:10.1002/(SICI)1097-4547(19991001)58:1<42::AID-JNR6>3.0.CO;2-L

McNicol, E., Horowicz-Mehler, N., Fisk, R.A., Bennett, K., Gialeli-Goudas, M., Chew, P.W., Lau, J., Carr, D., 2003. Management of opioid side effects in cancer-related and chronic noncancer pain: A systematic review. J. Pain. doi:10.1016/S1526-5900(03)00556-X

Meacci, E., Tsai, S.C., Adamik, R., Moss, J., Vaughan, M., 1997. Cytohesin-1, a cytosolic guanine nucleotide-exchange protein for ADP-ribosylation factor. Proc Natl Acad Sci U S A 94, 1745–1748.

Meister, M., Dietrich, A., Gierschik, P., 1995. Identification of a three-amino-acid region in G protein gamma 1 as a determinant of selective beta gamma heterodimerization. Eur J Biochem 234, 171–177.

Meldrum, B.S., 2000. Glutamate as a neurotransmitter in the brain: review of physiology and pathology. J. Nutr. 130, 1007S–15S.

Michal, P., El-Fakahany, E.E., Dolezal, V., 2007. Muscarinic M2 receptors directly activate Gq/11 and Gs G-proteins. J. Pharmacol. Exp. Ther. 320, 607–14. doi:10.1124/jpet.106.114314

Michalon, A., Sidorov, M., Ballard, T.M., Ozmen, L., Spooren, W., Wettstein, J.G., Jaeschke, G., Bear, M.F., Lindemann, L., 2012. Chronic Pharmacological mGlu5 Inhibition Corrects Fragile X in Adult Mice. Neuron 74, 49–56. doi:10.1016/j.neuron.2012.03.009

Miller, W.E., Lefkowitz, R.J., 2001. Expanding roles for ß-arrestins as scaffolds and adapters in GPCR signaling and trafficking. Curr. Opin. Cell Biol. 13, 139–145. doi:http://dx.doi.org/10.1016/S0955-0674(00)00190-3

Miller, W.E., Maudsley, S., Ahn, S., Khan, K.D., Luttrell, L.M., Lefkowitz, R.J., 2000. Beta-arrestin1 interacts with the catalytic domain of the tyrosine kinase c-SRC. Role of beta-arrestin1-dependent targeting of c-SRC in receptor endocytosis. J. Biol. Chem. 275, 11312–11319. doi:10.1074/jbc.275.15.11312

Minakami, R., Katsuki, F., Yamamoto, T., Nakamura, K., Sugiyama, H., 1994. Molecular cloning and the functional expression of two isoforms of human metabotropic glutamate receptor subtype 5. Biochem Biophys Res Commun 199, 1136–1143.

Moreno, J.L., Holloway, T., Albizu, L., Sealfon, S.C., Gonzalez-Maeso, J., 2011. Metabotropic glutamate mGlu2 receptor is necessary for the pharmacological and behavioral effects induced by hallucinogenic 5-HT2A receptor agonists. Neurosci. Lett. 493, 76–79. doi:10.1016/j.neulet.2011.01.046

Morin, D., Cotte, N., Balestre, M.N., Mouillac, B., Manning, M., Breton, C., Barberis, C., 1998. The D136A mutation of the V2 vasopressin receptor induces a constitutive activity which permits discrimination between antagonists with partial agonist and inverse agonist activities. FEBS Lett. 441, 470–475. doi:10.1016/S0014-5793(98)01585-3

Moulton, B.C., Fryer, A.D., 2011. Muscarinic receptor antagonists, from folklore to pharmacology; Finding drugs that actually work in asthma and COPD. Br. J. Pharmacol. doi:10.1111/j.1476-5381.2010.01190.x

Movsesyan, V.A., O'Leary, D.M., Fan, L., Bao, W., Mullins, P.G., Knoblach, S.M., Faden, A.I., 2001. mGluR5 antagonists 2-methyl-6-(phenylethynyl)-pyridine and (E)-2-methyl-6-(2-phenylethenyl)-pyridine reduce traumatic neuronal injury in vitro and in vivo by antagonizing N-methyl-D-aspartate receptors. J Pharmacol Exp Ther 296, 41–47.

Movsesyan, V.A., Stoica, B.A., Faden, A.I., 2004. MGLuR5 activation reduces ß-amyloid-induced cell death in primary neuronal cultures and attenuates translocation of cytochrome c and apoptosis-inducing factor. J. Neurochem. 89, 1528–1536. doi:10.1111/j.1471-4159.2004.02451.x

Mühlemann, A., Ward, N.A., Kratochwil, N., Diener, C., Fischer, C., Stucki, A., Jaeschke, G., Malherbe, P., Porter, R.H.P., 2006. Determination of key amino acids implicated in the actions of allosteric modulation by 3,3′-difluorobenzaldazine on rat mGlu5 receptors. Eur. J. Pharmacol. 529, 95–104. doi:10.1016/j.ejphar.2005.11.008

Murone, M., Rosenthal, A., de Sauvage, F.J., 1999. Sonic hedgehog signaling by the patched-smoothened receptor complex. Curr. Biol. 9, 76–84.

doi:10.1016/S0960-9822(99)80018-9

Musante, V., Neri, E., Feligioni, M., Puliti, A., Pedrazzi, M., Conti, V., Usai, C., Diaspro, A., Ravazzolo, R., Henley, J.M., Battaglia, G., Pittaluga, A., 2008. Presynaptic mGlu1 and mGlu5 autoreceptors facilitate glutamate exocytosis from mouse cortical nerve endings. Neuropharmacology 55, 474–482. doi:10.1016/j.neuropharm.2008.06.056

Mutel, V., Ellis, G.J., Adam, G., Chaboz, S., Nilly, A., Messer, J., Bleuel, Z., Metzler, V., Malherbe, P., Schlaeger, E.-J., Roughley, B.S., Faull, R.L.M., Richards, J.G., 2000. Characterization of [3H]Quisqualate Binding to Recombinant Rat Metabotropic Glutamate 1a and 5a Receptors and to Rat and Human Brain Sections. J. Neurochem. 75, 2590–2601. doi:10.1046/j.1471-4159.2000.0752590.x

Muto, T., Tsuchiya, D., Morikawa, K., Jingami, H., 2007. Structures of the extracellular regions of the group II/III metabotropic glutamate receptors. Proc. Natl. Acad. Sci. U. S. A. 104, 3759–64. doi:10.1073/pnas.0611577104

Nakahara, K., Okada, M., Nakanishi, S., 1997. The metabotropic glutamate receptor mGluR5 induces calcium oscillations in cultured astrocytes via protein kinase C phosphorylation. J. Neurochem. 69, 1467–75. doi:10.1046/j.1471-4159.1997.69041467.x

Nathans, J., Hogness, D.S., 1983. Isolation, sequence analysis, and intron-exon arrangement of the gene encoding bovine rhodopsin. Cell 34, 807–814. doi:10.1016/0092-8674(83)90537-8

Navarro, B., Kennedy, M.E., Velimirovíc, B., Bhat, D., Peterson, a S., Clapham, D.E., 1996. Nonselective and G betagamma-insensitive weaver K+ channels. Science 272, 1950–1953.

Neves, S.R., Ram, P.T., Iyengar, R., 2002. G Protein Pathways. Science (80-.). 296, 1636–1639. doi:10.1126/science.1071550

Neyman, S., Manahan-Vaughan, D., 2008. Metabotropic glutamate receptor 1 (mGluR1) and 5 (mGluR5) regulate late phases of LTP and LTD in the hippocampal CA1 region in vitro. Eur. J. Neurosci. 27, 1345–1352. doi:10.1111/j.1460-9568.2008.06109.x

Nicodemo, A. a, Pampillo, M., Ferreira, L.T., Dale, L.B., Cregan, T., Ribeiro, F.M., Ferguson, S.S.G., 2010. Pyk2 uncouples metabotropic glutamate receptor G protein signaling but facilitates ERK1/2 activation. Mol. Brain 3, 4. doi:10.1186/1756-6606-3-4

Nicoletti, F., Bruno, V., Catania, M. V., Battaglia, G., Copani, A., Barbagallo, G., Ceña, V., Sanchez-Prieto, J., Spano, P.F., Pizzi, M., 1999. Group-I metabotropic glutamate receptors: Hypotheses to explain their dual role in neurotoxicity and neuroprotection. Neuropharmacology 38, 1477–1484. doi:10.1016/S0028-3908(99)00102-1

Niswender, C.M., Conn, P.J., 2010. Metabotropic glutamate receptors: physiology, pharmacology, and disease. Annu. Rev. Pharmacol. Toxicol. 50, 295–322. doi:10.1146/annurev.pharmtox.011008.145533

Noel, J.P., Hamm, H.E., Sigler, P.B., 1993. The 2.2 Å crystal structure of transducin-α complexed with GTPγS. Nature. doi:10.1038/366654a0

O'Brien, J. a, Lemaire, W., Chen, T.-B., Chang, R.S.L., Jacobson, M. a, Ha, S.N., Lindsley, C.W., Schaffhauser, H.J., Sur, C., Pettibone, D.J., Conn, P.J., Williams, D.L., 2003. A family of highly selective allosteric modulators of the metabotropic glutamate receptor subtype 5. Mol. Pharmacol. 64, 731–740. doi:10.1124/mol.64.3.731

O'Brien, J. a, Lemaire, W., Wittmann, M., Jacobson, M. a, Ha, S.N., Wisnoski, D.D., Lindsley, C.W., Schaffhauser, H.J., Rowe, B., Sur, C., Duggan, M.E., Pettibone, D.J., Conn, P.J., Williams, D.L., 2004. A novel selective allosteric modulator potentiates the activity of native metabotropic glutamate receptor subtype 5 in rat forebrain. J. Pharmacol. Exp. Ther. 309, 568–577.

doi:10.1124/jpet.103.061747.domain

O'Hara, P.J., Sheppard, P.O., Thógersen, H., Venezia, D., Haldeman, B.A., McGrane, V., Houamed, K.M., Thomsen, C., Gilbert, T.L., Mulvihill, E.R., 1993. The ligand-binding domain in metabotropic glutamate receptors is related to bacterial periplasmic binding proteins. Neuron 11, 41–52. doi:10.1016/0896-6273(93)90269-W

O'Leary, D.M., Movsesyan, V., Vicini, S., Faden, A.I., 2000. Selective mGluR5 antagonists MPEP and SIB-1893 decrease NMDA or glutamate-mediated neuronal toxicity through actions that reflect NMDA receptor antagonism. Br. J. Pharmacol. 131, 1429–1437. doi:10.1038/sj.bjp.0703715

Okamoto, T., Sekiyama, N., Otsu, M., Shimada, Y., Sato, a, Nakanishi, S., Jingami, H., 1998. Expression and purification of the extracellular ligand binding region of metabotropic glutamate receptor subtype 1. J. Biol. Chem. 273, 13089–13096. doi:10.1074/jbc.273.21.13089

Oldham, W.M., Hamm, H.E., 2008. Heterotrimeric G protein activation by G-protein-coupled receptors. Nat. Rev. Mol. Cell Biol. 9, 60–71. doi:10.1038/nrm2299

Olive, M.F., McGeehan, A.J., Kinder, J.R., McMahon, T., Hodge, C.W., Janak, P.H., Messing, R.O., 2005. The mGluR5 antagonist 6-methyl-2-(phenylethynyl)pyridine decreases ethanol consumption via a protein kinase C epsilon-dependent mechanism. Mol. Pharmacol. 67, 349–55. doi:10.1124/mol.104.003319

Oliveira, L., Paiva, A.C.M., Vriend, G., 1993. A common motif in G-protein-coupled seven transmembrane helix receptors. J. Comput. Aided. Mol. Des. 7, 649–658. doi:10.1007/BF00125323

Osborne, M.P.H., Olive, M.F., 2008. A role for mGluR5 receptors in intravenous methamphetamine self-administration, in: Annals of the New York Academy of Sciences. pp. 206–211.

doi:10.1196/annals.1432.034

Pagano, A., Rovelli, G., Mosbacher, J., Lohmann, T., Duthey, B., Stauffer, D., Ristig, D., Schuler, V., Meigel, I., Lampert, C., Stein, T., Prezeau, L., Blahos, J., Pin, J., Froestl, W., Kuhn, R., Heid, J., Kaupmann, K., Bettler, B., 2001. C-terminal interaction is essential for surface trafficking but not for heteromeric assembly of GABA(b) receptors. J. Neurosci. 21, 1189–202. doi:10.1017/CBO9781107415324.004

Pagano, A., Rüegg, D., Litschig, S., Stoehr, N., Stierlin, C., Heinrich, M., Floersheim, P., Prezèau, L., Carroll, F., Pin, J.-P., Cambria, A., Vranesic, I., Flor, P.J., Gasparini, F., Kuhn, R., 2000. The Non-competitive Antagonists 2-Methyl-6-(phenylethynyl)pyridine and 7-Hydroxyiminocyclopropan[b]chromen-1a-carboxylic Acid Ethyl Ester Interact with Overlapping Binding Pockets in the Transmembrane Region of Group I Metabotropic Glutamate Receptors . J. Biol. Chem. 275 , 33750–33758. doi:10.1074/jbc.M006230200

Palczewski, K., 2006. G protein-coupled receptor rhodopsin. Annu. Rev. Biochem. 75, 743–67. doi:10.1146/annurev.biochem.75.103004.142743

Palczewski, K., Kumasaka, T., Hori, T., Behnke, C.A., Motoshima, H., Fox, B.A., Le Trong, I., Teller, D.C., Okada, T., Stenkamp, R.E., Yamamoto, M., Miyano, M., 2000. Crystal Structure of Rhodopsin: A G Protein-Coupled Receptor. Sci. (New York, NY) 289, 739–745. doi:10.1126/science.1150609

Park, D., Jhon, D.Y., Lee, C.W., Lee, K.H., Rhee, S.G., 1993. Activation of phospholipase C isozymes by G protein beta gamma subunits. J Biol Chem 268, 4573–4576.

Park, J.H., Scheerer, P., Hofmann, K.P., Choe, H.-W., Ernst, O.P., 2008. Crystal structure of the ligand-free G-protein-coupled receptor opsin. Nature 454, 183–187. doi:10.1038/nature07063

Parmentier-Batteur, S., Hutson, P.H., Menzel, K., Uslaner, J.M., Mattson,

B.A., O'Brien, J.A., Magliaro, B.C., Forest, T., Stump, C.A., Tynebor, R.M., Anthony, N.J., Tucker, T.J., Zhang, X.F., Gomez, R., Huszar, S.L., Lambeng, N., Fauré, H., Le Poul, E., Poli, S., Rosahl, T.W., Rocher, J.P., Hargreaves, R., Williams, T.M., 2014. Mechanism based neurotoxicity of mGlu5 positive allosteric modulators - Development challenges for a promising novel antipsychotic target. Neuropharmacology 82, 161–173. doi:10.1016/j.neuropharm.2012.12.003

Parsons, C.G., Danysz, W., Quack, G., 1999. Memantine is a clinically well tolerated N-methyl-D-aspartate (NMDA) receptor antagonist - A review of preclinical data. Neuropharmacology. doi:10.1016/S0028-3908(99)00019-2

Peeters, M.C., Van Westen, G.J.P., Li, Q., Ijzerman, A.P., 2011. Importance of the extracellular loops in G protein-coupled receptors for ligand recognition and receptor activation. Trends Pharmacol. Sci. doi:10.1016/j.tips.2010.10.001

Pierce, K.L., Premont, R.T., Lefkowitz, R.J., 2002. Seven-transmembrane receptors. Nat. Rev. Mol. Cell Biol. 3, 639–50. doi:10.1038/nrm908

Pin, J.P., Bockaert, J., 1999. Molecular tinkering of G protein-coupled receptors: an evolutionary success. EMBO J. 18, 1723–9. doi:10.1093/emboj/18.7.1723

Pin, J.P., Galvez, T., Prézeau, L., 2003. Evolution, structure, and activation mechanism of family 3/C G-protein-coupled receptors. Pharmacol. Ther. doi:10.1016/S0163-7258(03)00038-X

Pin, J.P., Waeber, C., Prezeau, L., Bockaert, J., Heinemann, S.F., 1992. Alternative splicing generates metabotropic glutamate receptors inducing different patterns of calcium release in Xenopus oocytes. Proc. Natl. Acad. Sci. U. S. A. 89, 10331–5. doi:10.1073/pnas.89.21.10331

Pisani, A., Calabresi, P., Centonze, D., Bernardi, G., 1997. Enhancement of NMDA responses by group I metabotropic glutamate receptor activation

in striatal neurones. Br. J. Pharmacol. 120, 1007–1014. doi:10.1038/sj.bjp.0700999

Pitcher, J.A., Freedman, N.J., Lefkowitz, R.J., 1998. G protein-coupled receptor kinases. Annu. Rev. Biochem. 67, 653–692. doi:10.1146/annurev.biochem.67.1.653

Porter, R.H.P., Jaeschke, G., Spooren, W., Ballard, T.M., Büttelmann, B., Kolczewski, S., Peters, J.-U., Prinssen, E., Wichmann, J., Vieira, E., Mühlemann, A., Gatti, S., Mutel, V., Malherbe, P., 2005. Fenobam: a clinically validated nonbenzodiazepine anxiolytic is a potent, selective, and noncompetitive mGlu5 receptor antagonist with inverse agonist activity. J. Pharmacol. Exp. Ther. 315, 711–21. doi:10.1124/jpet.105.089839

Price, M.R., Baillie, G.L., Thomas, A., Stevenson, L.A., Easson, M., Goodwin, R., McLean, A., McIntosh, L., Goodwin, G., Walker, G., Westwood, P., Marrs, J., Thomson, F., Cowley, P., Christopoulos, A., Pertwee, R.G., Ross, R.A., 2005. Allosteric Modulation of the Cannabinoid CB1 Receptor. Mol. Pharmacol. 68, 1484–1495. doi:10.1124/mol.105.016162

Probst, W.C., Snyder, L.A., Schuster, D.I., Brosius, J., Sealfon, S.C., 1992. Sequence alignment of the G-protein coupled receptor superfamily. DNA Cell Biol 11, 1–20.

Raiteri, M., 2008. Presynaptic metabotropic glutamate and GABAB receptors. Handb. Exp. Pharmacol. 373–407. doi:10.1007/978-3-540-74805-2_12

Rall, T.W., Sutherland, E.W., Wosilait, W.D., 1956. THE RELATIONSHIP OF EPINEPHRINE AND GLUCAGON TO LIVER PHOSPHORYLASE: III. REACTIVATION OF LIVER PHOSPHORYLASE IN SLICES AND IN EXTRACTS . J. Biol. Chem. 218 , 483–495.

Rashid, A.J., So, C.H., Kong, M.M.C., Furtak, T., El-Ghundi, M., Cheng, R., O'Dowd, B.F., George, S.R., 2007. D1-D2 dopamine receptor

heterooligomers with unique pharmacology are coupled to rapid activation of Gq/11 in the striatum. Proc. Natl. Acad. Sci. U. S. A. 104, 654–9. doi:10.1073/pnas.0604049104

Rasmussen, S.G., Jensen, a D., Liapakis, G., Ghanouni, P., Javitch, J. a, Gether, U., 1999. Mutation of a highly conserved aspartic acid in the beta2 adrenergic receptor: constitutive activation, structural instability, and conformational rearrangement of transmembrane segment 6. Mol. Pharmacol. 56, 175–184.

Rasmussen, S.G.F., Choi, H.-J., Fung, J.J., Pardon, E., Casarosa, P., Chae, P.S., Devree, B.T., Rosenbaum, D.M., Thian, F.S., Kobilka, T.S., Schnapp, A., Konetzki, I., Sunahara, R.K., Gellman, S.H., Pautsch, A., Steyaert, J., Weis, W.I., Kobilka, B.K., 2011a. Structure of a nanobody-stabilized active state of the ß(2) adrenoceptor. Nature 469, 175–80. doi:10.1038/nature09648

Rasmussen, S.G.F., DeVree, B.T., Zou, Y., Kruse, A.C., Chung, K.Y., Kobilka, T.S., Thian, F.S., Chae, P.S., Pardon, E., Calinski, D., Mathiesen, J.M., Shah, S.T.A., Lyons, J.A., Caffrey, M., Gellman, S.H., Steyaert, J., Skiniotis, G., Weis, W.I., Sunahara, R.K., Kobilka, B.K., 2011b. Crystal structure of the ß2 adrenergic receptor-Gs protein complex. Nature 477, 549–55. doi:10.1038/nature10361

Ray, K., Hauschild, B.C., 2000. Cys-140 is critical for metabotropic glutamate receptor-1 dimerization. J. Biol. Chem. 275, 34245–34251. doi:10.1074/jbc.M005581200

Reid, M.E., Toms, N.J., Bedingfield, J.S., Roberts, P.J., 1999. Group I mGlu receptors potentiate synaptosomal [3H]glutamate release independently of exogenously applied arachidonic acid. Neuropharmacology 38, 477–485. doi:10.1016/S0028-3908(98)00217-2

Ridet, J.L., Malhotra, S.K., Privat, A., Gage, F.H., 1997. Reactive astrocytes: Cellular and molecular cues to biological function. Trends Neurosci.

doi:10.1016/S0166-2236(97)01139-9

Robbins, M.J., Ciruela, F., Rhodes, A., McIlhinney, R.A.J., 1999. Characterization of the Dimerization of Metabotropic Glutamate Receptors Using an N-Terminal Truncation of mGluR1α. J. Neurochem. 72, 2539–2547. doi:10.1046/j.1471-4159.1999.0722539.x

Robitaille, J., MacDonald, M.L.E., Kaykas, A., Sheldahl, L.C., Zeisler, J., Dubé, M.-P., Zhang, L.-H., Singaraja, R.R., Guernsey, D.L., Zheng, B., Siebert, L.F., Hoskin-Mott, A., Trese, M.T., Pimstone, S.N., Shastry, B.S., Moon, R.T., Hayden, M.R., Goldberg, Y.P., Samuels, M.E., 2002. Mutant frizzled-4 disrupts retinal angiogenesis in familial exudative vitreoretinopathy. Nat. Genet. 32, 326–330. doi:10.1038/ng957

Rodriguez, A.L., Nong, Y., Sekaran, N.K., Alagille, D., Tamagnan, G.D., Conn, P.J., 2005. A Close Structural Analog of 2-Methyl-6-(phenylethynyl)-pyridine Acts as a Neutral Allosteric Site Ligand on Metabotropic Glutamate Receptor Subtype 5 and Blocks the Effects of Multiple Allosteric Modulators. Mol. Pharmacol. 68 , 1793–1802. doi:10.1124/mol.105.016139

Rodríguez-Moreno, A., Sistiaga, A., Lerma, J., Sánchez-Prieto, J., 2016. Switch from Facilitation to Inhibition of Excitatory Synaptic Transmission by Group I mGluR Desensitization. Neuron 21, 1477–1486. doi:10.1016/S0896-6273(00)80665-0

Romano, C., Miller, J.K., Hyrc, K., Dikranian, S., Mennerick, S., Takeuchi, Y., Goldberg, M.P., O'Malley, K.L., 2001. Covalent and noncovalent interactions mediate metabotropic glutamate receptor mGlu5 dimerization. Mol. Pharmacol. 59, 46–53.

Romano, C., van den Pol, A.N., O'Malley, K.L., 1996a. Enhanced early developmental expression of the metabotropic glutamate receptor mGluR5 in rat brain: protein, mRNA splice variants, and regional distribution. J. Comp. Neurol. 367, 403–12. doi:10.1002/(SICI)1096-

9861(19960408)367:3<403::AID-CNE6>3.0.CO;2-9

Romano, C., Yang, W.L., O'Malley, K.L., 1996b. Metabotropic glutamate receptor 5 is a disulfide-linked dimer. J. Biol. Chem. 271, 28612–28616. doi:10.1074/jbc.271.45.28612

Rondard, P., Liu, J., Huang, S., Malhaire, F., Vol, C., Pinault, A., Labesse, G., Pin, J.P., 2006. Coupling of agonist binding to effector domain activation in metabotropic glutamate-like receptors. J. Biol. Chem. 281, 24653–24661. doi:10.1074/jbc.M602277200

Rook, J.M., Xiang, Z., Lv, X., Ghoshal, A., Dickerson, J.W., Bridges, T.M., Johnson, K.A., Foster, D.J., Gregory, K.J., Vinson, P.N., Thompson, A.D., Byun, N., Collier, R.L., Bubser, M., Nedelcovych, M.T., Gould, R.W., Stauffer, S.R., Daniels, J.S., Niswender, C.M., Lavreysen, H., Mackie, C., Conde-Ceide, S., Alcazar, J., Bartolomé-Nebreda, J.M., Macdonald, G.J., Talpos, J.C., Steckler, T., Jones, C.K., Lindsley, C.W., Conn, P.J., 2015. Biased mGlu5-Positive Allosteric Modulators Provide In Vivo Efficacy without Potentiating mGlu5 Modulation of NMDAR Currents. Neuron 86, 1029–40. doi:10.1016/j.neuron.2015.03.063

Rosenbaum, D.M., Rasmussen, S.G.F., Kobilka, B.K., 2009. The structure and function of G-protein-coupled receptors. Nature 459, 356–63. doi:10.1038/nature08144

Ross, E.M., Berstein, G., 1993. Regulation of the M1 muscarinic receptor-Gg-phospholipase C-?? pathway by nucleotide exchange and GTP hydrolysis. Life Sci. 52, 413–419. doi:10.1016/0024-3205(93)90296-F

Ross, E.M., Gilman, A.G., 1977. Resolution of some components of adenylate cyclase necessary for catalytic activity. J. Biol. Chem. 252, 6966–6969.

Rovati, G.E., Capra, V., Neubig, R.R., 2007. The highly conserved DRY motif of class A G protein-coupled receptors: beyond the ground state. Mol. Pharmacol. 71, 959–964. doi:10.1124/mol.106.029470

Satow, A., Maehara, S., Ise, S., Hikichi, H., Fukushima, M., Suzuki, G., Kimura, T., Tanaka, T., Ito, S., Kawamoto, H., Ohta, H., 2008. Pharmacological Effects of the Metabotropic Glutamate Receptor 1 Antagonist Compared with Those of the Metabotropic Glutamate Receptor 5 Antagonist and Metabotropic Glutamate Receptor 2/3 Agonist in Rodents: Detailed Investigations with a Selective Allost. J. Pharmacol. Exp. Ther. 326 , 577–586. doi:10.1124/jpet.108.138107

Sattler, R., Tymianski, M., 2001. Molecular Mechanisms of Glutamate Receptor-Mediated Excitotoxic Neuronal Cell Death. Mol. Neurobiol. 24, 107–130. doi:10.1385/MN:24:1-3:107

Scheerer, P., Park, J.H., Hildebrand, P.W., Kim, Y.J., Krauss, N., Choe, H.-W., Hofmann, K.P., Ernst, O.P., 2008. Crystal structure of opsin in its G-protein-interacting conformation. Nature 455, 497–502. doi:10.1038/nature07330

Schiefer, J., Sprünken, A., Puls, C., Lüesse, H.-G., Milkereit, A., Milkereit, E., Johann, V., Kosinski, C.M., 2004. The metabotropic glutamate receptor 5 antagonist MPEP and the mGluR2 agonist LY379268 modify disease progression in a transgenic mouse model of Huntington's disease. Brain Res. 1019, 246–254. doi:http://dx.doi.org/10.1016/j.brainres.2004.06.005

Schoepp, D., Bockaert, J., Sladeczek, F., 1990. Pharmacological and functional characteristics of metabotropic excitatory amino acid receptors. Trends Pharmacol Sci 11, 508–515.

Schoepp, D.D., Goldsworthy, J., Johnson, B.G., Salhoff, C.R., Baker, S.R., 1994. 3,5-Dihydroxyphenylglycine is a Highly Selective Agonist for Phosphoinositide-Linked Metabotropic Glutamate Receptors in the Rat Hippocampus. J. Neurochem. 63, 769–772. doi:10.1046/j.1471-4159.1994.63020769.x

Schoepp, D.D., Jane, D.E., Monn, J.A., 1999. Pharmacological agents acting

at subtypes of metabotropic glutamate receptors. Neuropharmacology. doi:10.1016/S0028-3908(99)00092-1

Schöneberg, T., Schulz, A., Biebermann, H., Hermsdorf, T., Römpler, H., Sangkuhl, K., 2004. Mutant G-protein-coupled receptors as a cause of human diseases. Pharmacol. Ther. doi:10.1016/j.pharmthera.2004.08.008

Schröder, H., Wu, D.-F., Seifert, A., Rankovic, M., Schulz, S., Höllt, V., Koch, T., 2009. Allosteric modulation of metabotropic glutamate receptor 5 affects phosphorylation, internalization, and desensitization of the μ-opioid receptor. Neuropharmacology 56, 768–778. doi:10.1016/j.neuropharm.2008.12.010

Schroeder, K.S., 1996. FLIPR: A New Instrument for Accurate, High Throughput Optical Screening. J. Biomol. Screen. 1, 75–80. doi:10.1177/108705719600100205

Selkirk, J. V., Price, G.W., Nahorski, S.R., Challiss, R.A.J., 2001. Cell type-specific differences in the coupling of recombinant mGlu1a receptors to endogenous G protein sub-populations. Neuropharmacology 40, 645–656. doi:10.1016/S0028-3908(00)00208-2

Sevastyanova, T.N., Kammermeier, P.J., 2014. Cooperative Signaling between Homodimers of Metabotropic Glutamate Receptors 1 and 5. Mol. Pharmacol. 86, 492–504. doi:10.1124/mol.114.093468

Shapiro, D.A., Kristiansen, K., Weiner, D.M., Kroeze, W.K., Roth, B.L., 2002. Evidence for a Model of Agonist-induced Activation of 5-Hydroxytryptamine 2A Serotonin Receptors That Involves the Disruption of a Strong Ionic Interaction between Helices 3 and 6. J. Biol. Chem. 277 , 11441–11449.

Sharma, S., Rodriguez, A.L., Conn, P.J., Lindsley, C.W., 2008. Synthesis and SAR of a mGluR5 allosteric partial antagonist lead: Unexpected modulation of pharmacology with slight structural modifications to a 5-

(phenylethynyl)pyrimidine scaffold. Bioorg. Med. Chem. Lett. 18, 4098–4101. doi:http://dx.doi.org/10.1016/j.bmcl.2008.05.091

Sheffler, D.J., Gregory, K.J., Rook, J.M., Conn, P.J., 2011. Allosteric Modulation of Metabotropic Glutamate Receptors. Adv. Pharmacol. 62, 37–77. doi:10.1016/B978-0-12-385952-5.00010-5

Shen, W., Slaughter, M.M., 1998. Metabotropic and ionotropic glutamate receptors regulate calcium channel currents in salamander retinal ganglion cells. J. Physiol. 510 (Pt 3, 815–28.

Shigemoto, R., Nomura, S., Ohishi, H., Sugihara, H., Nakanishi, S., Mizuno, N., 1993. Immunohistochemical localization of a metabotropic glutamate receptor, mGluR5, in the rat brain. Neurosci. Lett. 163, 53–57. doi:0304-3940(93)90227-C [pii]

Shiraishi-Yamaguchi, Y., Furuichi, T., 2007. The Homer family proteins. Genome Biol. 8, 206. doi:10.1186/gb-2007-8-2-206

Siehler, S., 2009. Regulation of RhoGEF proteins by G12/13-coupled receptors. Br. J. Pharmacol. 158, 41–49. doi:10.1111/j.1476-5381.2009.00121.x

Siehler, S., 2008. Cell-based assays in GPCR drug discovery. Biotechnol. J. doi:10.1002/biot.200800001

Silve, C., Petrel, C., Leroy, C., Bruel, H., Mallet, E., Rognan, D., Ruat, M., 2005. Delineating a Ca2+ binding pocket within the venus flytrap module of the human calcium-sensing receptor. J. Biol. Chem. 280, 37917–37923. doi:10.1074/jbc.M506263200

Simon, L., Toth, J., Molnar, L., Agoston, D. V, 2011. MRI analysis of mGluR5 and mGluR1 antagonists, MTEP and R214127 in the cerebral forebrain of awake, conscious rats. Neurosci. Lett. 505, 155–159. doi:http://dx.doi.org/10.1016/j.neulet.2011.10.010

Simon, M.I., Strathmann, M.P., Gautam, N., 1991. Diversity of G proteins in

signal transduction. Science 252, 802–8. doi:10.1126/science.1902986

Simonds, W.F., Butrynski, J.E., Gautam, N., Unson, C.G., Spiegel, A.M., 1991. G-protein beta-gamma dimers: Membrane targeting requires subunit coexpression and intact gamma C-A-A-X domain. J. Biol. Chem. 266, 5363–5366.

Sistiaga, A., Herrero, I., Conquet, F., Sánchez-Prieto, J., 1998. The metabotropic glutamate receptor 1 is not involved in the facilitation of glutamate release in cerebrocortical nerve terminals. Neuropharmacology 37, 1485–1492. doi:http://dx.doi.org/10.1016/S0028-3908(98)00129-4

Skeberdis, V.A., Lan, J.Y., Opitz, T., Zheng, X., Bennett, M.V.L., Suzanne Zukin, R., 2001. mGluR1-mediated potentiation of NMDA receptors involves a rise in intracellular calcium and activation of protein kinase C. Neuropharmacology 40, 856–865. doi:10.1016/S0028-3908(01)00005-3

Sladeczek, F., Pin, J.P., Récasens, M., Bockaert, J., Weiss, S., 1985. Glutamate stimulates inositol phosphate formation in striatal neurones. Nature 317, 717–719. doi:10.1038/317717a0

Smith, J.S., Rajagopal, S., 2016. The ß-arrestins: Multifunctional regulators of G protein-coupled receptors. J. Biol. Chem. 291, 8969–8977. doi:10.1074/jbc.R115.713313

Sondek, J., Bohm, A., Lambright, D.G., Hamm, H.E., Sigler, P.B., 1996. Crystal structure of a GA protein [beta][gamma]dimer at 2.1 A resolution. Nature 379, 369–374.

Sondek, J., Lambright, D.G., Noel, J.P., Hamm, H.E., Sigler, P.B., 1994. GTPase mechanism of Gproteins from the 1.7-A crystal structure of transducin alpha-GDP-AIF-4. Nature 372, 276–279. doi:10.1038/372276a0

Sourdet, V., Russier, M., Daoudal, G., Ankri, N., Debanne, D., 2003. Long-

term enhancement of neuronal excitability and temporal fidelity mediated by metabotropic glutamate receptor subtype 5. J. Neurosci. 23, 10238–10248. doi:23/32/10238 [pii]

Spooren, W.P.J.M., Gasparini, F., Salt, T.E., Kuhn, R., 2001. Novel allosteric antagonists shed light on mglu5 receptors and CNS disorders. Trends Pharmacol. Sci. doi:10.1016/S0165-6147(00)01694-1

Stacey, M., Lin, H.-H., Gordon, S., McKnight, A.J., 2016. LNB-TM7, a group of seven-transmembrane proteins related to family-B G-protein-coupled receptors. Trends Biochem. Sci. 25, 284–289. doi:10.1016/S0968-0004(00)01583-8

Stockton, J.M., Birdsall, N.J., Burgen, A.S., Hulme, E.C., 1983. Modification of the binding properties of muscarinic receptors by gallamine. Mol. Pharmacol. 23, 551–7.

Strader, C.D., Candelore, M.R., Hill, W.S., Sigal, I.S., Dixon, R.A.F., 1989. Identification of two serine residues involved in agonist activation of the ß-adrenergic receptor. J. Biol. Chem. 264, 13572–13578.

Sugiyama, H., Ito, I., Hirono, C., 1987. A new type of glutamate receptor linked to inositol phospholipid metabolism. Nature. doi:10.1038/325531a0

Sugiyama, Y., Kawaguchi, S.Y., Hirano, T., 2008. mGluR1-mediated facilitation of long-term potentiation at inhibitory synapses on a cerebellar Purkinje neuron. Eur. J. Neurosci. 27, 884–896. doi:10.1111/j.1460-9568.2008.06063.x

Sutherland, E.W., Wosilait, W.D., 1955. Inactivation and activation of liver phosphorylase. Nature. doi:10.1038/175169a0

Suzuki, G., Kimura, T., Satow, A., Kaneko, N., Fukuda, J., Hikichi, H., Sakai, N., Maehara, S., Kawagoe-Takaki, H., Hata, M., Azuma, T., Ito, S., Kawamoto, H., Ohta, H., 2007. Pharmacological characterization of a

new, orally active and potent allosteric metabotropic glutamate receptor 1 antagonist, 4-[1-(2-fluoropyridin-3-yl)-5-methyl-1H-1,2,3-triazol-4-yl]-N-isopropyl-N-methyl-3,6-dihydropyridine-1(2H)-carboxamide (FTIDC). J. Pharmacol. Exp. Ther. 321, 1144–53. doi:10.1124/jpet.106.116574

Swanson, C.J., Bures, M., Johnson, M.P., Linden, A.-M., Monn, J. a, Schoepp, D.D., 2005. Metabotropic glutamate receptors as novel targets for anxiety and stress disorders. Nat. Rev. Drug Discov. 4, 131–44. doi:10.1038/nrd1630

Swartz, K.J., Merritt, a, Bean, B.P., Lovinger, D.M., 1993. Protein kinase C modulates glutamate receptor inhibition of Ca2+ channels and synaptic transmission. Nature 361, 165–168. doi:10.1038/361165a0

Takagi, N., Besshoh, S., Marunouchi, T., Takeo, S., Tanonaka, K., 2012. Metabotropic Glutamate Receptor 5 Activation Enhances Tyrosine Phosphorylation of the N-methyl-D-aspartate (NMDA) Receptor and NMDA-Induced Cell Death in Hippocampal Cultured Neurons. Biol. Pharm. Bull. 35, 2224–2229. doi:10.1248/bpb.b12-00691

Takeda, S., Kadowaki, S., Haga, T., Takaesu, H., Mitaku, S., 2002. Identification of G protein-coupled receptor genes from the human genome sequence. FEBS Lett. 520, 97–101. doi:10.1016/S0014-5793(02)02775-8

Tallaksen-Greene, S.J., Kaatz, K.W., Romano, C., Albin, R.L., 1998. Localization of mGluR1a-like immunoreactivity and mGluR5-like immunoreactivity in identified populations of striatal neurons. Brain Res. 780, 210–217. doi:10.1016/S0006-8993(97)01141-4

Tanabe, Y., Masu, M., Ishii, T., Shigemoto, R., Nakanishi, S., 1992. A family of metabotropic glutamate receptors. Neuron 8, 169–179. doi:0896-6273(92)90118-W [pii]

Tang, W.J., Gilman, a G., 1991. Type-specific regulation of adenylyl cyclase by G protein beta gamma subunits. Science 254, 1500–1503.

doi:10.1126/science.1962211

Tatarczyńska, E., Kłodzińska, A., Chojnacka-Wójcik, E., Pałucha, A., Gasparini, F., Kuhn, R., Pilc, A., 2001. Potential anxiolytic- and antidepressant-like effects of MPEP, a potent, selective and systemically active mGlu5 receptor antagonist. Br. J. Pharmacol. 132, 1423–1430. doi:10.1038/sj.bjp.0703923

Tateyama, M., Abe, H., Nakata, H., Saito, O., Kubo, Y., 2004. Ligand-induced rearrangement of the dimeric metabotropic glutamate receptor 1alpha. Nat. Struct. Mol. Biol. 11, 637–642. doi:10.1038/nsmb770

Tateyama, M., Kubo, Y., 2008. Regulatory role of C-terminus in the G-protein coupling of the metabotropic glutamate receptor 1. J. Neurochem. 107, 1036–1046. doi:10.1111/j.1471-4159.2008.05672.x

Tateyama, M., Kubo, Y., 2006. Dual signaling is differentially activated by different active states of the metabotropic glutamate receptor 1alpha. Proc. Natl. Acad. Sci. U. S. A. 103, 1124–8. doi:10.1073/pnas.0505925103

Techlovská, Š., Chambers, J.N., Dvořáková, M., Petralia, R.S., Wang, Y.X., Hájková, A., Nová, A., Franková, D., Prezeau, L., Blahos, J., 2014. Metabotropic glutamate receptor 1 splice variants mGluR1a and mGluR1b combine in mGluR1a/b dimers in vivo. Neuropharmacology 86, 329–336. doi:10.1016/j.neuropharm.2014.08.011

Thomas, P., Smart, T.G., 2005. HEK293 cell line: A vehicle for the expression of recombinant proteins. J. Pharmacol. Toxicol. Methods 51, 187–200. doi:10.1016/j.vascn.2004.08.014

Towbin, H., Staehelin, T., Gordon, J., 1979. Electrophoretic transfer of proteins from polyacrylamide gels to nitrocellulose sheets: procedure and some applications. Proc. Natl. Acad. Sci. U. S. A. 76, 4350–4354.

Traynelis, S.F., Wollmuth, L.P., McBain, C.J., Menniti, F.S., Vance, K.M.,

Ogden, K.K., Hansen, K.B., Yuan, H., Myers, S.J., Dingledine, R., 2010. Glutamate Receptor Ion Channels: Structure, Regulation, and Function. Pharmacol. Rev. 62, 405–96. doi:10.1124/pr.109.002451

Tronci, V., Vronskaya, S., Montgomery, N., Mura, D., Balfour, D.J.K., 2010. The effects of the mGluR5 receptor antagonist 6-methyl-2-(phenylethynyl)- pyridine (MPEP) on behavioural responses to nicotine. Psychopharmacology (Berl). 211, 33–42. doi:10.1007/s00213-010-1868-x

Tsuchiya, D., Kunishima, N., Kamiya, N., Jingami, H., Morikawa, K., 2002. Structural views of the ligand-binding cores of a metabotropic glutamate receptor complexed with an antagonist and both glutamate and Gd3+. Proc. Natl. Acad. Sci. U. S. A. 99, 2660–5. doi:10.1073/pnas.052708599

Tsuji, Y., Shimada, Y., Takeshita, T., Kajimura, N., Nomura, S., Sekiyama, N., Otomo, J., Usukura, J., Nakanishi, S., Jingami, H., 2000. Cryptic dimer interface and domain organization of the extracellular region of metabotropic glutamate receptor subtype 1. J. Biol. Chem. 275, 28144–28151. doi:10.1074/jbc.M003226200

Turlington, M., Noetzel, M.J., Chun, A., Zhou, Y., Gogliotti, R.D., Nguyen, E.D., Gregory, K.J., Vinson, P.N., Rook, J.M., Gogi, K.K., Xiang, Z., Bridges, T.M., Daniels, J.S., Jones, C., Niswender, C.M., Meiler, J., Jeffrey Conn, P., Lindsley, C.W., Stauffer, S.R., 2013. Exploration of allosteric agonism structure-activity relationships within an acetylene series of metabotropic glutamate receptor 5 (mGlu5) positive allosteric modulators (PAMs): Discovery of 5-((3-fluorophenyl)ethynyl)- N -(3-methyloxetan-3-yl)picolinamid. J. Med. Chem. 56, 7976–7996. doi:10.1021/jm401028t

Ulas, J., Satou, T., Ivins, K.J., Kesslak, J.P., Cotman, C.W., Balázs, R., 2000. Expression of metabotropic glutamate receptor 5 is increased in astrocytes after kainate-induced epileptic seizures. Glia 30, 352–361. doi:10.1002/(SICI)1098-1136(200006)30:4<352::AID-GLIA40>3.0.CO;2-6

Um, J.W., Kaufman, A.C., Kostylev, M., Heiss, J.K., Stagi, M., Takahashi, H., Kerrisk, M.E., Vortmeyer, A., Wisniewski, T., Koleske, A.J., Gunther, E.C., Nygaard, H.B., Strittmatter, S.M., 2013. Metabotropic glutamate receptor 5 is a coreceptor for Alzheimer abeta oligomer bound to cellular prion protein. Neuron 79, 887–902. doi:10.1016/j.neuron.2013.06.036

Urizar, E., Claeysen, S., Deup??, X., Govaerts, C., Costagliola, S., Vassart, G., Pardo, L., 2005. An activation switch in the rhodopsin family of G protein-coupled receptors: The thyrotropin receptor. J. Biol. Chem. 280, 17135–17141. doi:10.1074/jbc.M414678200

Varney, M. a, Cosford, N.D., Jachec, C., Rao, S.P., Sacaan, a, Lin, F.F., Bleicher, L., Santori, E.M., Flor, P.J., Allgeier, H., Gasparini, F., Kuhn, R., Hess, S.D., Veliçelebi, G., Johnson, E.C., 1999. SIB-1757 and SIB-1893: selective, noncompetitive antagonists of metabotropic glutamate receptor type 5. J. Pharmacol. Exp. Ther. 290, 170–181.

Venkatakrishnan, a J., Deupi, X., Lebon, G., Tate, C.G., Schertler, G.F., Babu, M.M., 2013. Molecular signatures of G-protein-coupled receptors. Nature 494, 185–94. doi:10.1038/nature11896

Venter, J.C., Adams, M.D., Myers, E.W., Li, P.W., Mural, R.J., Sutton, G.G., Smith, H.O., Yandell, M., Evans, C.A., Holt, R.A., Gocayne, J.D., Amanatides, P., Ballew, R.M., Huson, D.H., Wortman, J.R., Zhang, Q., Kodira, C.D., Zheng, X.H., Chen, L., Skupski, M., Subramanian, G., Thomas, P.D., Zhang, J., Gabor Miklos, G.L., Nelson, C., Broder, S., Clark, A.G., Nadeau, J., McKusick, V.A., Zinder, N., Levine, A.J., Roberts, R.J., Simon, M., Slayman, C., Hunkapiller, M., Bolanos, R., Delcher, A.L., Dew, I., Fasulo, D., Flanigan, M., Florea, L., Halpern, A., Hannenhalli, S., Kravitz, S., Levy, S., Mobarry, C., Reinert, K., Remington, K., Abu-Threideh, J., Beasley, E., Biddick, K., Bonazzi, V., Brandon, R., Cargill, M., Chandramouliswaran, I., Charlab, R., Chaturvedi, K., Deng, Z., Di Francesco, V., Dunn, P., Eilbeck, K.,

Evangelista, C., Gabrielian, A.E., Gan, W., Ge, W., Gong, F., Gu, Z., Guan, P., Heiman, T.J., Higgins, M.E., Ji, R.R., Ke, Z., Ketchum, K.A., Lai, Z., Lei, Y., Li, Z., Li, J., Liang, Y., Lin, X., Lu, F., Merkulov, G. V, Milshina, N., Moore, H.M., Naik, A.K., Narayan, V.A., Neelam, B., Nusskern, D., Rusch, D.B., Salzberg, S., Shao, W., Shue, B., Sun, J., Wang, Z., Wang, A., Wang, X., Wang, J., Wei, M., Wides, R., Xiao, C., Yan, C., Yao, A., Ye, J., Zhan, M., Zhang, W., Zhang, H., Zhao, Q., Zheng, L., Zhong, F., Zhong, W., Zhu, S., Zhao, S., Gilbert, D., Baumhueter, S., Spier, G., Carter, C., Cravchik, A., Woodage, T., Ali, F., An, H., Awe, A., Baldwin, D., Baden, H., Barnstead, M., Barrow, I., Beeson, K., Busam, D., Carver, A., Center, A., Cheng, M.L., Curry, L., Danaher, S., Davenport, L., Desilets, R., Dietz, S., Dodson, K., Doup, L., Ferriera, S., Garg, N., Gluecksmann, A., Hart, B., Haynes, J., Haynes, C., Heiner, C., Hladun, S., Hostin, D., Houck, J., Howland, T., Ibegwam, C., Johnson, J., Kalush, F., Kline, L., Koduru, S., Love, A., Mann, F., May, D., McCawley, S., McIntosh, T., McMullen, I., Moy, M., Moy, L., Murphy, B., Nelson, K., Pfannkoch, C., Pratts, E., Puri, V., Qureshi, H., Reardon, M., Rodriguez, R., Rogers, Y.H., Romblad, D., Ruhfel, B., Scott, R., Sitter, C., Smallwood, M., Stewart, E., Strong, R., Suh, E., Thomas, R., Tint, N.N., Tse, S., Vech, C., Wang, G., Wetter, J., Williams, S., Williams, M., Windsor, S., Winn-Deen, E., Wolfe, K.H., Zaveri, J., Zaveri, K., Abril, J.F., Guigó, R., Campbell, M.J., Sjolander, K. V, Karlak, B., Kejariwal, A., Mi, H., Lazareva, B., Hatton, T., Narechania, A., Diemer, K., Muruganujan, A., Guo, N., Sato, S., Bafna, V., Istrail, S., Lippert, R., Schwartz, R., Walenz, B., Yooseph, S., Allen, D., Basu, A., Baxendale, J., Blick, L., Caminha, M., Carnes-Stine, J., Caulk, P., Chiang, Y.H., Coyne, M., Dahlke, C., Mays, A., Dombroski, M., Donnelly, M., Ely, D., Esparham, S., Fosler, C., Gire, H., Glanowski, S., Glasser, K., Glodek, A., Gorokhov, M., Graham, K., Gropman, B., Harris, M., Heil, J., Henderson, S., Hoover, J., Jennings, D., Jordan, C., Jordan, J., Kasha, J., Kagan, L., Kraft, C., Levitsky, A., Lewis, M., Liu, X., Lopez, J., Ma, D., Majoros, W., McDaniel, J., Murphy, S., Newman,

M., Nguyen, T., Nguyen, N., Nodell, M., Pan, S., Peck, J., Peterson, M., Rowe, W., Sanders, R., Scott, J., Simpson, M., Smith, T.F., Sprague, A., Stockwell, T., Turner, R., Venter, E., Wang, M., Wen, M., Wu, D., Wu, M., Xia, A., Zandieh, A., Zhu, X., Sinsheimer, R.L., Sanger, F., Seeburg, P.H., Strauss, E.C., Kobori, J.A., Siu, G., Hood, L.E., Gocayne, J.D., Martin-Gallardo, A., McCombie, W.R., Jensen, M.A., Adams, M.D., Adams, M.D., Adams, M.D., Kerlavage, A.R., Fields, C., Venter, J.C., Adams, M.D., Soares, M.B., Kerlavage, A.R., Fields, C., Venter, J.C., Polymeropoulos, M.H., Marra, M., Adams, M.D., White, O., Sanger, F., Coulson, A.R., Hong, G.F., Hill, D.F., Petersen, G.B., Mahy, B.W.J., Esposito, J.J., Venter, J.C., Fleischmann, R.D., Fraser, C.M., Bult, C.J., Tomb, J.F., Klenk, H.P., Venter, J.C., Smith, H.O., Hood, L.E., Schmitt, H., Zhao, S., Lin, X., Weber, J.L., Myers, E.W., Green, P., Pennisi, E., Venter, J.C., Adams, M.D., Marshall, E., Pennisi, E., Adams, M.D., Rubin, G.M., Myers, E.W., Collins, F.S., Sanger, F., Nicklen, S., Coulson, A.R., Prober, J.M., Myers, G., Selznick, S., Zhang, Z., Miller, W., Hattori, M., Dunham, I., Carvalho, A.B., Lazzaro, B.P., Clark, A.G., Schuler, G.D., Altschul, S.F., Gish, W., Miller, W., Myers, E.W., Lipman, D.J., Olivier, M., Chaudhari, N., Hahn, W.E., Milner, R.J., Sutcliffe, J.G., Dickson, D., Ewing, B., Green, P., Crollius, H.R., Pruitt, K.D., Katz, K.S., Sicotte, H., Maglott, D.R., Uberbacher, E.C., Xu, Y., Mural, R.J., Burge, C., Karlin, S., Mural, R.J., Salamov, A.A., Solovyev, V. V., Miklos, G.L., John, B., Francke, U., Horvath, J.E., Schwartz, S., Eichler, E.E., Bickmore, W.A., Sumner, A.T., Holmquist, G.P., Bernardi, G., Zoubak, S., Clay, O., Bernardi, G., Ohno, S., Broman, K.W., Murray, J.C., Sheffield, V.C., White, R.L., Weber, J.L., McEachern, M.J., Krauskopf, A., Blackburn, E.H., Bird, A., Gardiner-Garden, M., Frommer, M., Larsen, F., Gundersen, G., Lopez, R., Prydz, H., Cross, S.H., Bird, A., Grunau, C., Hindermann, W., Rosenthal, A., Antequera, F., Bird, A., Cross, S.H., Slavov, D., Smit, A.F., Riggs, A.D., Elliott, D.J., Makeyev, A. V., Chkheidze, A.N., Lievhaber, S.A., Pan, Y., Decker, W.K., Huq, A.H.H.M., Craigen, W.J., Nouvel, P., Goncalves, I., Duret,

L., Mouchiroud, D., Smith, T.F., Waterman, M.S., Delcher, A.L., Trask, B.J., Sharon, D., Barbazuk, W.B., McLysaght, A., Enright, A.J., Skrabanek, L., Wolfe, K.H., Burt, D.W., Skrabanek, L., Wolfe, K.H., Taillon-Miller, P., Gu, Z., Li, Q., Hillier, L., Kwok, P.Y., Taillon-Miller, P., Piernot, E.E., Kwok, P.Y., Altshuler, D., Marth, G.T., Cargill, M., Halushka, M.K., Zhang, J., Madden, T.L., Nachman, M.W., Bauer, V.L., Crowell, S.L., Aquadro, C.F., Nickerson, D.A., Jorde, L., Wang, D.G., Przeworski, M., Hudson, R.R., Rienzo, A. Di, Tavare, S., Clark, A.G., Kaessmann, H., Heissig, F., Haeseler, A. von, Paabo, S., Sonnhammer, E.L., Eddy, S.R., Durbin, R., Bateman, A., Ponting, C.P., Schultz, J., Milpetz, F., Bork, P., Goodenough, D.A., Goliger, J.A., Paul, D.L., Wilkinson, D.G., Nakamura, F., Kalb, R.G., Strittmatter, S.M., Horner, P.J., Gage, F.H., Casaccia-Bonnefil, P., Gu, C., Chao, M. V., Wang, S., Barres, B.A., Geppert, M., Sudhof, T.C., Littleton, J.T., Bellen, H.J., Maximov, A., Sudhof, T.C., Bezprozvanny, I., Lemke, G., Perrimon, N., Bernfield, M., Lindahl, U., Kusche-Gullberg, M., Kjellen, L., Hurskainen, T.L., Hirohata, S., Seldin, M.F., Apte, S.S., Black, R.A., White, J.M., Aravind, L., Dixit, V.M., Koonin, E. V., Garcia-Meunier, P., Etienne-Julan, M., Fort, P., Piechaczyk, M., Bonhomme, F., Mansur, N.R., Meyer-Siegler, K., Wurzer, J.C., Sirover, M.A., Tatton, N.A., Kenmochi, N., Chen, F.W., Ioannou, Y.A., Madsen, H.O., Poulsen, K., Dahl, O., Clark, B.F., Hjorth, J.P., Chambers, D.M., Peters, J., Abbott, C.M., Khalyfa, A., Carlson, B.M., Carlson, J.A., Wang, E., Aeschlimann, D., Thomazy, V., Munroe, P., Wu, S.M., Cheung, W.F., Frazier, D., Stafford, D.W., Furie, B., Kehoe, J.W., Bertozzi, C.R., Pawson, T., Nash, P., Velden, A.W. van der, Thomas, A.A., Fraser, C.M., Tettelin, H., Brett, D., Muller, H.J., Kern, H., Feinberg, A.P., Collins, C.A., Guthrie, C., Eddy, S.R., Wang, Q., Khillan, J., Gadue, P., Nishikura, K., Holcik, M., Sonenberg, N., Korneluk, R.G., McKinsey, T.A., Zhang, C.L., Lu, J., Olson, E.N., Capanna, E., Romanini, M.G.M., Smith, J.M., Charlesworth, D., Charlesworth, B., Morgan, M.T., Bailey, J.E., Maleszka, R., Couet, H.G. de, Miklos, G.L., Miklos, G.L., Crutchfield,

J.P., Young, K., Gell-Mann, M., Lloyd, S., Barabasi, A.L., Albert, R., Colucci-Guyon, E., Ewing, B., Green, P., Ewing, B., Hillier, L., Wendl, M.C., Green, P., Lander, E.S., Waterman, M.S., Krogh, A., Sjölander, K., Sjölander, K., Bairoch, A., Apweiler, R., Tatusov, R.L., Galperin, M.Y., Natale, D.A., Koonin, E. V., 2001. The sequence of the human genome. Science (80-.). 291, 1304–51. doi:10.1126/science.1058040

Vermeiren, C., Najimi, M., Vanhoutte, N., Tilleux, S., De Hemptinne, I., Maloteaux, J.M., Hermans, E., 2005. Acute up-regulation of glutamate uptake mediated by mGluR5a in reactive astrocytes. J. Neurochem. 94, 405–416. doi:10.1111/j.1471-4159.2005.03216.x

Vernon, A.C., Palmer, S., Datla, K.P., Zbarsky, V., Croucher, M.J., Dexter, D.T., 2005. Neuroprotective effects of metabotropic glutamate receptor ligands in a 6-hydroxydopamine rodent model of Parkinson's disease. Eur. J. Neurosci. 22, 1799–1806. doi:10.1111/j.1460-9568.2005.04362.x

Vohra, S., Taddese, B., Conner, A.C., Poyner, D.R., Hay, D.L., Barwell, J., Reeves, P.J., Upton, G.J.G., Reynolds, C.A., 2013. Similarity between class A and class B G-protein-coupled receptors exemplified through calcitonin gene-related peptide receptor modelling and mutagenesis studies. J. R. Soc. Interface 10, 20120846. doi:10.1098/rsif.2012.0846

Wall, M.A., Coleman, D.E., Lee, E., Iñiguez-Lluhi, J.A., Posner, B.A., Gilman, A.G., Sprang, S.R., 1995. The structure of the G protein heterotrimer Giα1ß1γ2. Cell 83, 1047–1058. doi:10.1016/0092-8674(95)90220-1

Warne, T., Moukhametzianov, R., Baker, J.G., Nehmé, R., Edwards, P.C., Leslie, A.G.W., Schertler, G.F.X., Tate, C.G., 2011. The structural basis for agonist and partial agonist action on a ß1-adrenergic receptor. Nature 469, 241–244. doi:10.1038/nature09746

West, R.E., Moss, J., Vaughan, M., Liu, T.Y., Liu, T.Y., 1985. Pertussis toxin-catalyzed ADP-ribosylation of transducin. J. Biol. Chem. 260,

14428–14430.

Wheatley, M., Wootten, D., Conner, M.T., Simms, J., Kendrick, R., Logan, R.T., Poyner, D.R., Barwell, J., 2012. Lifting the lid on GPCRs: The role of extracellular loops. Br. J. Pharmacol. doi:10.1111/j.1476-5381.2011.01629.x

White, J.H., Wise, A., Main, M.J., Green, A., Fraser, N.J., Disney, G.H., Barnes, A.A., Emson, P., Foord, S.M., Marshall, F.H., 1998. Heterodimerization is required for the formation of a functional GABAB receptor. Nature 396, 679–682.

Willars, G.B., 2006. Mammalian RGS proteins: Multifunctional regulators of cellular signalling. Semin. Cell Dev. Biol. doi:10.1016/j.semcdb.2006.03.005

Willars, G.B., Müller-Esterl, W., Nahorski, S.R., 1999. Receptor phosphorylation does not mediate cross talk between muscarinic M3 and bradykinin B2 receptors. Am. J. Physiol. - Cell Physiol. 277, C859–C869.

Wood, M.R., Hopkins, C.R., Brogan, J.T., Conn, P.J., Lindsley, C.W., 2011. "Molecular switches" on mGluR allosteric ligands that modulate modes of pharmacology. Biochemistry 50, 2403–2410. doi:10.1021/bi200129s

Wu, H., Wang, C., Gregory, K.J., Han, G.W., Cho, H.P., Xia, Y., Niswender, C.M., Katritch, V., Meiler, J., Cherezov, V., Conn, P.J., Stevens, R.C., 2014. Structure of a class C GPCR metabotropic glutamate receptor 1 bound to an allosteric modulator. Science 344, 58–64. doi:10.1126/science.1249489

Xie, X., Ramirez, D.R., Lasseter, H.C., Fuchs, R.A., 2010. Effects of mGluR1 Antagonism in the Dorsal Hippocampus on Drug Context-induced Reinstatement of Cocaine-seeking Behavior in Rats. Psychopharmacology (Berl). 208, 1–11. doi:10.1007/s00213-009-1700-7

Xu, F., Wu, H., Katritch, V., Han, G.W., Jacobson, K. a, Gao, Z.-G., Cherezov, V., Stevens, R.C., 2011. Structure of an Agonist-Bound Human A2A Adenosine Receptor. Science (80-.). 332, 322–327. doi:10.1126/science.1202793

Yan, K., Kalyanaraman, V., Gautam, N., 1996. Differential ability to form the G protein βγ complex among members of the β and γ subunit families. J. Biol. Chem. 271, 7141–7146. doi:10.1074/jbc.271.12.7141

Yan, Q.J., Rammal, M., Tranfaglia, M., Bauchwitz, R.P., 2005. Suppression of two major Fragile X Syndrome mouse model phenotypes by the mGluR5 antagonist MPEP. Neuropharmacology 49, 1053–1066. doi:10.1016/j.neuropharm.2005.06.004

Yanagawa, M., Yamashita, T., Shichida, Y., 2011. Comparative fluorescence resonance energy transfer analysis of metabotropic glutamate receptors: Implications about the dimeric arrangement and rearrangement upon ligand bindings. J. Biol. Chem. 286, 22971–22981. doi:10.1074/jbc.M110.206870

Yin, S., Noetzel, M.J., Johnson, K. a, Zamorano, R., Jalan-Sakrikar, N., Gregory, K.J., Conn, P.J., Niswender, C.M., 2014. Selective actions of novel allosteric modulators reveal functional heteromers of metabotropic glutamate receptors in the CNS. J. Neurosci. 34, 79–94. doi:10.1523/JNEUROSCI.1129-13.2014

Yung-Chi, C., Prusoff, W.H., 1973. Relationship between the inhibition constant (KI) and the concentration of inhibitor which causes 50 per cent inhibition (I50) of an enzymatic reaction. Biochem. Pharmacol. 22, 3099–3108. doi:10.1016/0006-2952(73)90196-2

Zhang, Y., Rodriguez, A.L., Conn, P.J., 2005. Allosteric potentiators of metabotropic glutamate receptor subtype 5 have differential effects on different signaling pathways in cortical astrocytes. J. Pharmacol. Exp. Ther. 315, 1212–1219. doi:10.1124/jpet.105.090308

Zhao, Z., Wisnoski, D.D., O'Brien, J.A., Lemaire, W., Williams, D.L., Jacobson, M.A., Wittman, M., Ha, S.N., Schaffhauser, H., Sur, C., Pettibone, D.J., Duggan, M.E., Conn, P.J., Hartman, G.D., Lindsley, C.W., 2007. Challenges in the development of mGluR5 positive allosteric modulators: The discovery of CPPHA. Bioorganic Med. Chem. Lett. 17, 1386–1391. doi:10.1016/j.bmcl.2006.11.081

Zhou, X., Hollern, D., Liao, J., Andrechek, E., Wang, H., 2013. NMDA receptor-mediated excitotoxicity depends on the coactivation of synaptic and extrasynaptic receptors. Cell Death Dis. 4, e560. doi:10.1038/cddis.2013.82

Zhou, Y., Malosh, C., Conde-Ceide, S., Martínez-Viturro, C.M., Alcázar, J., Lavreysen, H., Mackie, C., Bridges, T.M., Daniels, J.S., Niswender, C.M., Jones, C.K., Macdonald, G.J., Steckler, T., Conn, P.J., Stauffer, S.R., Bartolomé-Nebreda, J.M., Lindsley, C.W., 2015. Further optimization of the mGlu5 PAM clinical candidate VU0409551/JNJ-46778212: Progress and challenges towards a back-up compound. Bioorg. Med. Chem. Lett. 25, 3515–3519. doi:http://dx.doi.org/10.1016/j.bmcl.2015.06.096

Zou, M.-F., Cao, J., Rodriguez, A.L., Jeffrey Conn, P., Newman, A.H., 2011. Design and synthesis of substituted N-(1,3-diphenyl-1H-pyrazol-5-yl)benzamides as positive allosteric modulators of the metabotropic glutamate receptor subtype 5. Bioorg. Med. Chem. Lett. 21, 2650–2654. doi:http://dx.doi.org/10.1016/j.bmcl.2010.12.110